Nanostructured zirconia via anodization for applications as coatings and potential bio-medical implant modifications

DISSERTATION
to obtain the degree of Doctor of Engineering

submitted by M.Sc.(Hons) Swathi Naidu Vakamulla Raghu

submitted to the School of Science and Technology
of the University of Siegen
Siegen 2023

Supervisor and first appraiser
Prof. Dr.Ing. Manuela S. Killian
University of Siegen

Second appraiser
Prof. Dr.ir. Annabel Braem
KU Leuven

Date of the oral examination
29. August 2023

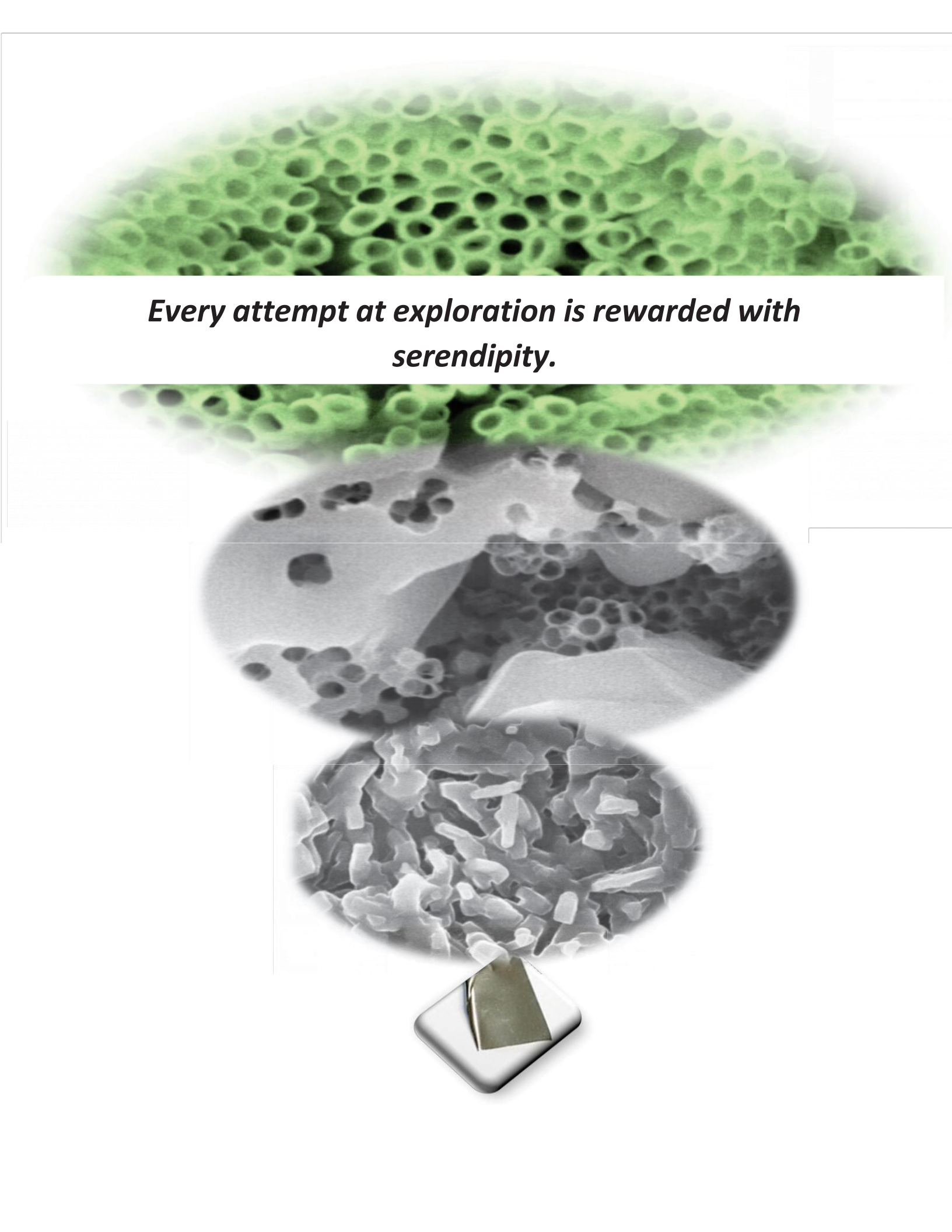

Every attempt at exploration is rewarded with serendipity.

Gutachter:

1. **Prof. Dr. Ing. Manuela S. Killian**
   Chemistry and Structure of Novel Materials, Department of Chemistry and Biology, University of Siegen, Germany

2. **Prof. Dr. Holger Schonherr**
   Physical Chemistry, Department of Chemistry and Biology, University of Siegen, Germany

3. **Prof. Dr. ir. Annabel Braem**
   Biomaterials and Tissue Engineering, Department of Materials Engineering, KULeuven, Belgium

4. **Prof. Dr. Ing. Aldo R. Boccaccini**
   Institute of Biomaterials, Department of Material Science and Engineering, FAU-Erlangen-Nuremberg, Germany

Tag der mUndlichen PrUfung: {29.08.2023}

Erklarung

Ich erklare hiermit, dass diese Arbeit von mir allein, ohne fremde Hilfe und ohne Benutzung anderer als der angegebenen Quellen angefertigt worden ist. Die Arbeit ist in gleicher oder ahnlicher Form keinem anderen PrUfungsausschuss vorgelegt worden und wurde auch nicht im Rahmen einer PrUfung prasentiert. Alle Visualisierungen, Grafiken und Materialien, die wortwortlich oder sinngema aus anderen Quellen Ubernommen wurden, sind als solche gekennzeichnet. Weiterhin erklare ich, dass mir die Promotionsordnung der Technischen Fakultat der Universitat Siegen vom 06. August 2020 bekannt ist und ich diese in vollem Umfang anerkenne.

Declaration of Authorship:

I hereby declare that the work presented here has been conducted by me and only me without help and without the use of sources other than the ones specified. The work has not been submitted to any other examination board in the same or similar form and was not presented as part of any examination. All visualizations, graphs, and materials, which have been adopted from other sources, literally or analogous, are marked as such. Furthermore, I declare that I am aware of the doctoral regulations at the Technical Faculty of the University of Siegen as of 06 August 2020 and acknowledge them in totality.

Siegen,_____

Acknowledgements

I would like to begin a rather long list of 'thank you' by expressing my utmost gratitude to Prof. Manuela Killian, without whom I would not have been able to complete, let alone begin my doctoral studies! *'Boss'* {as I often address you with reverence and affection thank you for all your patience and guidance for all my 'quick questions' {which they seldom are!. My words here might not do justice to all the academic guidance you've offered me throughout our time together but most of all I will always be indebted to the love and support you have so strongly provided me with. Especially in my time away from my family. Thanks to you, I feel a little less alone as a woman in science and an expat in Germany. Thank you for encouraging me to do better and most of all for granting me several opportunities to represent CSnM. I am grateful for the level of independence you have given me in order to culminate my scientific and profession skills. A lot of things remain unsaid but you will always be my *'Guru'* – when one finds a true *Guru*, one can conquer half of the world. Thank you once again for everything and on a lighter note, I can now proudly say, I will be your first doctoral candidate!

I would also like to thank the team of CSnM as a whole for being a conducive environment for good scientific work and camaraderie. Most of all, I would like to thank Dr. Christian Pritzel {a.k.a Dr.P for the mental boost and cookie sharing in our office. Your insights on a variety of subjects and your humor might as well give Terry Pratchett a run for his words! Above all, your genuine kindness inspires me to be a better version of myself and for this I thank you. CSnM remains incomplete without Andrea, Siegbert and Birgit. I want thank the holy trio of happy, helpful and hilarious. Birgit, thanks to you I end up having a smooth sailing with the German bureaucracy. Andrea and Siegbert, you both have been with us from the initiation of CSnM and I think a lot of the work gets done seamlessly courtesy of your expertise and organizational skills. Many thanks for everything from yesterday to tomorrow.

My students, some of whom are now my colleagues in the lab. Each one of you has left a deep impression on me. I have learnt many things about myself and science in your presence. I hope you too have had pleasant memories as I recall fondly, so thank you Hajka Chullunabandi, Mohit Jain, Mert Yilmaz, Gabriel Onyenso, Setareh Orangpur, Alireza and Benson Agi Ameh.

Patrick and Aydan, as the relatively older PhDs in our group, we've hung out a bit longer and I'd like to thank you both for our fun conference travels. A special shout out to everyone from the MnaF, Prof. Holger Schonherr and group for helping out with trainings and devices whenever needed, espcially Gregor. I cannot thank you enough, Dr. Mareike MUller and Sabine Wenderhold-Reeb for all help and guidance for the preliminary cell-studies. I would also like to thank Dr. Yilmaz Sakalli for being the in-house expert, not just for TEM analysis but also for expat queries!

A big thank you to Dr. Rebecca Weber, Juni Mohos and Prof. Claudia Wickleder for guiding me during the FraMES program that helped me better navigate my academic career.

Especially Prof. Claudia, thank you for being a big cheerleader for me and women in general but most of all for your unconditional support and encouragement during the past years.

I would like to thank the members of my Jury. Prof. Boccaccini, our association began with my mini project and then master thesis under your guidance at WW7 in FAU. Luckily for me, that relationship didn't end at Erlangen. I'm grateful for the continued support and correspondence we've maintained, despite your extremely busy schedule. I thank you for always giving your students an opportunity. They say all it takes is for one person to believe in you and I'm extremely privileged for having had this possibility with you. Prof. Annabel Braem, thank you for the possibility to defend my thesis in your presence. I am glad that I could do a research visit in your group at MTM and I realized the striking similarities between our groups, which I ascertain to the likeness of the Bosses! A team flourishes only when nurtured, and I am glad that you've let me bounce off ideas throughout our association. Thank you very much for this possibility.

I would also like to thank all my collaborators and coauthors for all the good work. I hope to continue the same in the future.

Friends and family…

One can never thank friends and family enough. I'll try to keep this short lest it turns into a memoir! Quick shout outs to Gustavo for always checking in with me, Kevin for sending me good juju through all our uphill battles. Lili for sending me Mia's pics to uplift my spirits, Milica for always saying *'I believe in you cimmi'*, Zalal for being a moon goddess and most of all my precious Ziyu, for always being the silent strength in my life. I love you all and can't wait to see you.

To friends I'd made along the way, Maxime, Akhsin, Vince, Nikolaj, Nabila, Rebekka, Majd, Kareem, Lars, Luka and Ivana {and also baby Lucian now} thank you for wishing me well and keeping my spirits high and up to date with all the gossip in town. Martin K. for being the coolest, kindest and craziest friend from Erlangen, you're a treasure that I wish to keep safe for years to come. A special mention to everybody in MTM and also the coffee partners during my stay. Also, a big shout out to Shemida for keeping me sane. Also Mrs Benner, my lovely neighbor for never letting me miss my oma. It's the small things that make the biggest difference. Thank you all.

Before I speak of my family, I would like to thank a special human who has felt nothing less than that. Mathias, you're a bit of the unsung hero in my screenplay. I thank you for your honesty and an unbiased view on most things. I'm grateful for the conversations shared with laughter and tears, but most of all for the well wishes that the *Dierllian* household has offered. Quick shout out to munchkins for being the happy noise to some sad silences.

Everything I am, I owe to my makers. Mom and dad, I love and thank you for cheering me on. Too bad we couldn't do this in person but I know you're always here with me! Swetha, my favourite human, I perhaps can never thank you enough. To have a sister is a treasure but to have you as a sister is a gift that keeps on giving. I love you chewks <3. We save the best for the last, to my person, Martin Canter, this sprint wouldn't have been as happy as it is without you. You're my best side and also my IT guy. Love you bibi, and thanks for being my pillar of strength.

Finally, if I have forgotten to mention anybody, please blame my dying brain cell cells. The stress got to me.....aaaarrghhhh.....My sincere apologies. I am deeply thankful to each and everyone that has helped me be better each day.

Kurzzusammenfassung

Häufig verwendete Implantatmaterialien sind Metalle, Metalllegierungen und in jüngerer Zeit auch Keramiken. Moderne medizinische Ansätze zielen auf die Entwicklung maßgeschneiderter Materialien ab, die hohe mechanische und physiko-chemische Funktionalitäten aufweisen, um das Gesundheitsverhalten zu verbessern und den allgemeinen Patientenkomfort zu erhöhen. Funktionalitäten können durch physikalische, chemische und/oder strukturelle Veränderungen hinzugefügt werden. Eine dieser Strategien ist der Einsatz von Nanotechnologie. Oberflächen im Submikronbereich profitieren in erster Linie von der Maximierung des Verhältnisses von Oberfläche zu Volumen. Dies kann durch Top-down- und Bottom-up-Herstellungsstrategien erreicht werden. Ein kombinierter Effekt dieser Synthesewege, wie bei der elektrochemischen Anodisierung, kann herkömmliche Massenmaterialien wie Metallmonolithen anschließend in Nanostrukturen umwandeln. Dies wird beobachtet, da der Anodisierungsprozess eine gleichzeitige bottom-up (Oxidwachstum) und top-down (Nanostrukturbildung) ermöglicht. Diese Dissertation beschäftigt sich mit dem Design solcher homogenen nanostrukturierten Metalloxide (MOs) durch elektrochemische Anodisierung.

MOs fallen in die Kategorie der Keramik. Sie werden in zunehmendem Maße als Biomaterialien verwendet, werden häufig für zahnmedizinische/orthopädische Anwendungen und lassen sich durch elektrochemische Anodisierung leicht in nanostrukturierte elektrochemische Anodisierung. Es ist eine vielseitige und kosteneffiziente Herstellungstechnik mit hoher Übertragbarkeit und die Möglichkeit der Vergrößerung. In dieser Arbeit entwickeln und optimieren wir und optimieren die Herstellung von Metalloxid Metalloxid-Nanoröhrchen auf Zirkonium (Zr)-Metall durch elektrochemische Synthese und beleuchten die Rolle der Morphologie der Zirkoniumoxid (ZrO_2)-Nanoröhren (ZrNT) für die anschließende Oberflächenmodifikationen. Die Rolle der Oberflächenmorphologie und die verschiedenen strukturellen Veränderungen werden verglichen, um festzustellen um den Einfluss auf das Ausmaß der erreichbaren Oberflächenfunktionalität zu bestimmen. Hierin, wird die Funktionalität durch die Variabilität der hydrophoben Wirkung und der Stabilität der

Beschichtungen, die sich aus der Molekülmodifikation der nanotubulären Strukturen über die Bildung von selbstorganisierenden Monoschichten (SAM). Diese Arbeit bietet auch Einblicke in die Rolle des SAM-unterstützten hydrophoben Effekts als als Ergebnis der Anwendungstechnik, d. h. der Immersion in Bulk-Lösung, auch bekannt als Bulk Immersion (BI), und Mikro-Kontaktdruck {µCP}, vor allem unter Verwendung von Modifikationen von Phosphonsaure-Kohlenhydrat Molekülen. Diese modifizierten ZrNTs wurden entlang ihrer Rohrlänge im Tiefenprofilmodus mit Flugzeit-Sekundärionen-Massenspektrometrie (ToF-SIMS) weiter untersucht. Mit dem Tiefenprofilmodus war die ToF-SIMS-Analyse ein erfolgreiches Werkzeug, mit dem das Vorhandensein der gewünschten Moleküle in verschiedenen Tiefen innerhalb der Nanoröhren festgestellt werden konnte. Diese ZrNTs wurden umfassend charakterisiert: Rasterelektronenmikroskopie (SEM) für morphologische Einblicke in die Geometrien der Nanoröhren, Röntgenbeugung (XRD) für die Auswirkungen der Wärmebehandlung auf die Oxidkristallinität, Röntgen-Photoelektronenspektroskopie (XPS) für die Oberflächenchemie der chemisch modifizierten Oxid-Nanomaterialien Diese modifizierten ZrNTs wurden auch verschiedenen Anwendungen unterzogen, von Arzneimittelreservoiren bis hin zu superhydrophoben optischen Beschichtungen. Als arzneimittelfreisetzende Oberflächen, Ultraviolett-sichtbare Photospektrometer (UV-Vis Spektrometer) zur zeitabhängigen Überwachung der Wirkstofffreisetzung und zur schnellen und die schnelle Bestätigung des superhydrophoben Ausmaßes der SAM-modifizierten Oberflächen wurde Wasser-Kontaktwinkel-Messungen {WCA} untersucht.

Die Ergebnisse liefern einen Konzeptnachweis für die Entwicklung von mehrtiefen und multifunktionalen Modifikationen in Nanoröhren. Dabei wurden die Wände der Nanoröhren durch einfache nasschemische und weichlithografische Techniken ohne Reinraumfertigung in verschiedenen Tiefen effektiv funktionalisiert. Darüber hinaus bieten diese Nanoröhrchen-Reservoirs, wenn sie für die volumetrische Speicherung durch simuliertes Farbstofffreisetzungsverhalten bewertet werden, Einblicke in die Entwicklung potenzieller medikamentenfreisetzender Oberflächen für Anwendungen mit kontrollierter Freisetzung. Die Nanostrukturarchitektur dient nicht nur als Speicher, sondern fördert auch die Texturierung der

Oberfläche im Mikronanometerbereich, was Berichten zufolge die Biointegration aufgrund der strukturellen Nachahmung der extrazellularen Matrix {ECM} und der Oberflachenfunktionalitat als Ergebnis einer besseren Haftung und erhöhten Reaktivität verbessert. Daher wäre es höchst interessant, Biomaterialoberflächen mit einer solchen Nanoarchitektur zu modifizieren, um vorteilhafte Reaktionen hervorzurufen. In Anbetracht dieser Tatsache und der daraus resultierenden Robustheit der ZrNT-Schichten wurde im Rahmen dieser Dissertation auch eine einfache Strategie zur nahtlosen Übertragung solcher ZrNTs auf keramische Werkstoffe erforscht. Diese ZrNT-Beschichtungen haften mit einem hohen Reibungskoeffizienten {CoF} an einem kontaktierenden Substrat, was ein Abrutschen verhindert und die Verankerung fördert.

Letztendlich, können die einzelnen Forschungsaspekte dieser Arbeit Strategien vorschlagen für Strategien fUr das Design von Hybridmaterialien, die Chemie und Struktur der Materialien Rückblick und weitere Modifikation. Die in dieser Arbeit beschriebenen Protokolle, bauen auf etablierten Herstellungsprinzipien auf und haben eine hohe Übertragbarkeit für reale Anwendungen geeignet. Das Gesamtergebnis mehrerer der in dieser Arbeit erzielten Ergebnisse lässt sich leicht TRL (3-4) eingestuft werden, wie es im Konzeptnachweis dargestellt ist. In Bereichen wie superhydrophoben selbstreinigenden photovoltaischen Beschichtungen und nanostrukturierten Implantatoberflächen. Speziell für biomedizinische Implantate ist ein Potenzial für die getriggerte Freisetzung und statische Oberflächen, die Medikamente (Multimoleküle) freisetzen, von großer praktischer Implikationen.

Abstract

Commonly used implant materials are metals, metal alloys, and more recently ceramics. Modern medical approaches aim towards the development of tailor-made materials, capable of high mechanical and physio-chemical functionalities for enhanced health response and an improvement in overall patient comfort. Functionality may be added as a result of physical, chemical, and/or structural modifications. One such strategy involves using nanotechnology. Surfaces in the submicron range primarily benefit by maximizing the surface area to volume ratio. This can be achieved via top-down and bottom-up fabrication strategies. A combined effect of these synthesis routes, as with electrochemical anodization, can transform conventional bulk materials like metal monoliths, subsequently into nanostructures. This is observed, as the anodization process accommodates a simultaneous bottom-up (oxide growth) and top-down (nanostructure formation). This dissertation explores the design of such homogeneous nanostructured metal-oxides (MOs) via electrochemical anodization.

MOs fall under the category of ceramics. They are increasingly used as biomaterials, are commonly used for dental/orthopaedic applications, and are readily transformed into nanostructured materials via electrochemical anodization. It is a versatile and cost-effective fabrication technique that has high transferability and scale-up possibilities. During this work, we develop and optimize the fabrication of metal-oxide nanotubes on zirconium (Zr) metal via electrochemical synthesis and shed light on the role of zirconia (ZrO_2) nanotube (ZrNT) morphology for subsequent surface modifications. The role of surface morphology and different structural changes are compared to determine the influence on the extent of achievable surface functionality. Herein, functionality is determined by variability in the hydrophobic effect and stability of the coatings resulting from organic molecule modification of the nanotubular structures via the formation of self-assembled monolayers (SAM). This work also offers insights on the role of SAM facilitated hydrophobic-effect as a result of application technique, i.e., immersion in bulk solution, aka bulk immersion (BI), and micro-contact printing {μCP}, predominantly while using modifications of phosphonic acid carbohydrate molecules. These

modified ZrNTs were further evaluated along their tube length in the depth-profiling mode using time-of-flight secondary ions mass spectrometry (ToF-SIMS). Using the depth profile mode, ToF-SIMS analysis was a successful tool, capable of ascertaining the presence of targeted molecules at various depths inside the nanotubes. These ZrNTs were extensively characterized using; Scanning Electron Microscopy (SEM) for morphological insights into nanotube geometries, X-ray diffraction (XRD) for the effects of heat treatment on oxide crystallinity, X-ray photoelectron Spectroscopy (XPS) for surface chemistry of chemically modified oxide nanomaterials. These modified ZrNTs, were also subjected to several applications ranging from drug-reservoirs to superhydrophobic optical coatings. As drug-eluting surfaces, an Ultraviolet-Visible Photospectrometer (UV-Vis Spectrometer) was used for time-dependent drug release monitoring and rapid confirmation of the superhydrophobic extent of SAM-modified surfaces was investigated via Water Contact Angle {WCA} measurements.

The results provide a proof-of-concept to develop multi-depth and multi-functional modifications within nanotubes. Herein, the nanotube walls were effectively functionalized at different depths via facile wet-chemistry and soft-lithography techniques devoid of clean-room fabrication. Additionally, these nanotube reservoirs when evaluated for volumetric storage via simulated dye-release behaviour offer insights into developing potential drug-eluting surfaces for controlled-release applications. In addition to acting as repositories, nanostructure architecture promotes surface texturization in the micro-nanometer scale, which reportedly improves biointegration due to structurally mimicking the extracellular matrix {ECM} and surface functionality as a result of superior adhesion and enhanced reactivity. Therefore, it would be highly interesting to modify biomaterial surfaces with such nanoarchitecture to elicit advantageous responses. Bearing this in consideration and the resulting robustness of the ZrNT layers, a facile strategy to seamlessly transfer such ZrNTs on bulk ceramics has also been explored within the scope of this dissertation. These ZrNT coatings are reported to self-adhere to a contacting substrate with a high coefficient of friction {CoF}, that avoids slippage and promotes anchorage.

Ultimately, the individual research aspects of this work can propose strategies for hybrid material design, bearing material chemistry and structure in hindsight, and further modifications. The protocols described in this thesis, build up on well-established manufacturing principles and have high translation ability for real-world applications. The overall outcome of several of the results in this work can easily be categorized in TRL (3-4), as is presented in the proof-of-concept. In areas such as superhydrophobic self-cleaning photovoltaic coatings and nanostructured implant surfaces. Especially for biomedical implants, a potential for triggered release and static drug (multi-molecule) eluting surfaces have strong practical implications.

TABLE OF CONTENTS

ACRONYMS

BI	Bulk Immersion
CNT	Carbon Nanotube
CoF	Coefficient of Friction
D	Dimension
ECM	Extracellular matrix
EDX	Energy Dispersive X-Ray spectroscopy
HF	Hydrofluoric acid
LMIG	Liquid Metal Ion Gun
M/ MO	Metal/ Metal-oxide
μCP	Micro-Contact Printing
NTs	Nanotubes
ODA	Octadecanoic Acid
OPA	Octadecyl Phosphonic Acid
PDMS	Polydimethylsiloxane
SAM	Self-Assembled Monolayer
SEM	Scanning Electron Microscope
TiO_2	Titania
ToF-SIMS	Time of Flight- Secondary Ions Mass Spectrometry
UV	Ultraviolet
Vis	Visible
WCA	Water Contact Angle
XPS	X-ray Photoelectron Spectroscopy
XRD	X-ray Diffraction
ZrO_2	Zirconia

1. STATE OF THE ART - ZrO_2 nanostructures and their applications

Nanoscience and nanotechnology have ubiquitously emerged in everyday terminology, due to technologies used in the design and development of novel materials and devices for a plethora of applications.[1,2] Recently, the nanoscale facets have been employed in the field of electronics, not limited to device fabrication alone. Nanotechnology continues to influence extended aspects of material design.[3] However, the ultimate goal in material science remains in customizing new and advanced materials via bottom-up or top-down fabrication routes.[4] Synthesis routes influence the morphology, structure, and chemistry of the material in question, and consequently their area of application. The exponential boom of nanostructured materials is due to the array of advantages offered as a function of their size effects.[5,6]

Nanomaterials presently exist as 0D, 1D, and 2D materials, such as particles; quantum dots, tubular structures; nanotubes/ nanorods, and sheet-like structures like graphene, to name a few. Some examples of metal oxide nanomaterials are depicted in Figure 1.[7,8]

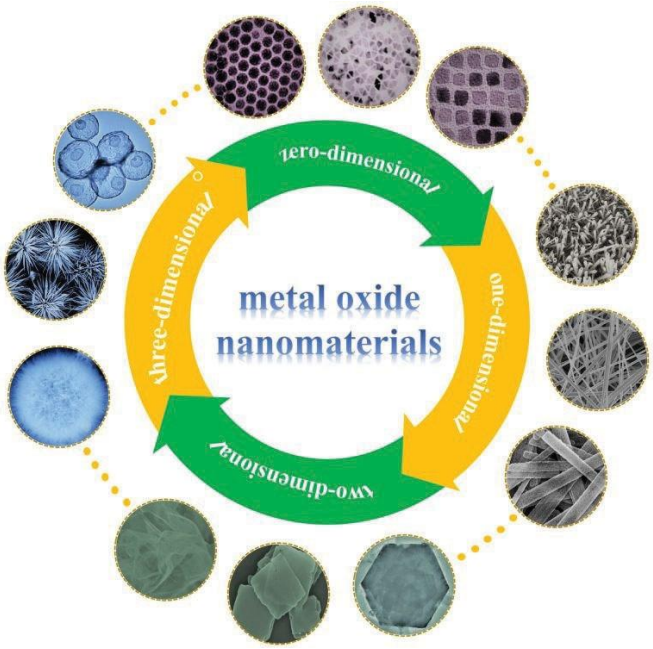

Figure 1: Schematic depiction of the various shape, geometries of the type of nanomaterials that can be synthesized from metal oxides [6]

Of all these dimensions, 1D structures have garnered more interest due to their relative stability, adaptable preparation methods, and precision control during synthesis over aspects ranging from size, shape, porosity, etc.[9] Some 1D nanostructures currently in commercial circulation are carbon nanotubes {CNTs}, and various metal-oxides {MOs} such as nanotubular TiO_2, ZnO, Fe_2O_3, etc., and are used in a variety of fields such as electronics, lubricants, adhesives, photodetectors, medicine, sensors, to name a few.[10] 1D-MOs are especially versatile due to their favorable responses in the biomedical field due to overcoming limitations faced with nanoparticles, in terms of synthesis and even handling problems as a result of agglomeration and accumulation.[11] These MOs are extensively being researched for application in drug delivery, bio-imaging, bio-sensing, interfacial response, etc.[12,13]

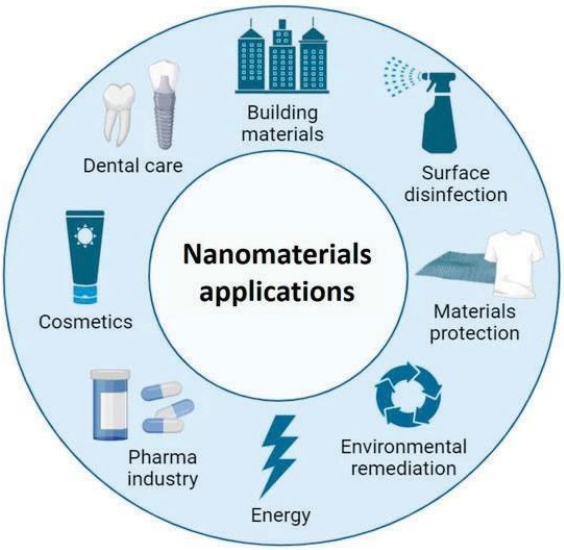

Figure 2: The schematic depicts the various areas of application for nanomaterials [14]

Such MO nanomaterials are commonly created either by additive strategies or by reductive methodologies when using either or all approaches exploiting chemical/physical/ biological interaction for nanomaterial assembly. Conventionally, top-down approaches involve the use of lithographic techniques, milling, grinding, laser ablation, sputtering, etc.[3,15,16]

Of all these techniques, bottom-up strategies offer more flexibility in the choice of materials and variability in experimental parameters due to the underlying growth mechanisms being governed by fundamental principles of chemical synthesis. From the year 1995, the electrochemical synthesis of metal-oxide nanostructures was introduced. The earliest studies resulted in the fabrication of a highly ordered metal nanohole array made of anodic porous alumina, aimed at replicating the honeycomb structure.[17] This development piqued the interest of researchers to explore other metals that could be passivated under anodic conditions, resulting in the expansion of electrochemical anodization to the entire class of valve metals.[18] Valve metals are group IV elements in the periodic table, that are capable of forming self-protective oxide layers. The process of forming uniform oxides under anodic conditions is called anodization.[19] Some materials that are in commercial circulation and have successfully been anodized into metal-oxide nanostructures are aluminum and titanium. These metals, coincidentally are also extensively used in the fields of biomedical research, predominantly for bulk-implant development and alternatively as modified surfaces on bulk materials.[20,21]

In order to minimize negative host-biomaterial interactions, biomaterials are tailored with enhanced physical, mechanical, and chemical surface characteristics.[22,23,24] In load-bearing implants and abutments, metals like titanium take preference due to their excellent mechanical properties and the relative ease of manufacturing. Primarily, the bulk of the implant material largely contributes towards the scaffolding needed for subsequent soft/hard tissue growth. In contrast, the surface interacts with all aspects of tissue response. For this purpose, metal-based biomaterials are facilitated with surface modifications such as bio-mimetic coatings, roughness scaling via micro- and nano structuring, and wettability modifications, in addition to acting as therapeutic carriers, such that elution occurs from these modified surfaces.[25] A schematic representation of the potential applications is represented as an example using titania nanotubes in Figure 3.[26]

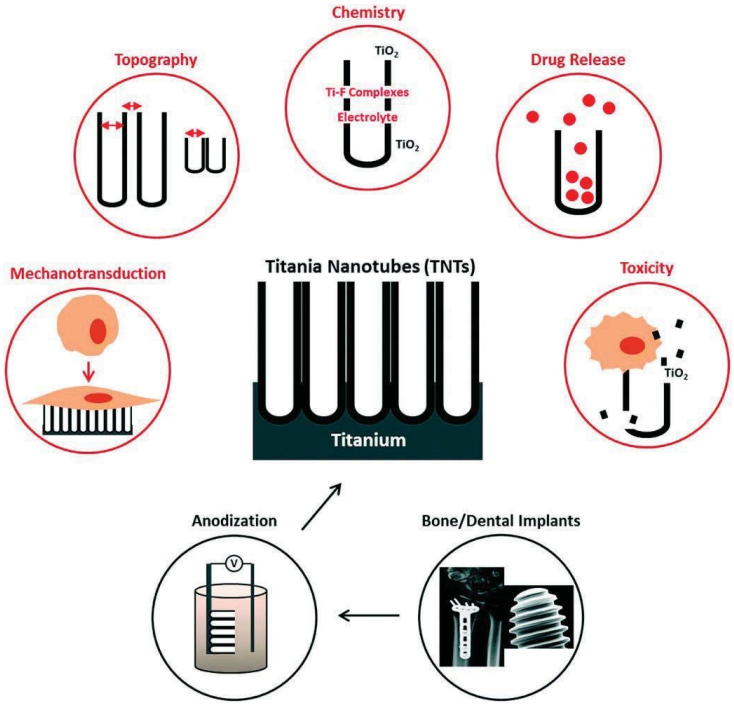

Figure 3: Electrochemically anodized titania nanotubes in biomedical applications [26]

Recently, titania nanotubes were developed via anodization over conventional titania-implant surfaces to enhance the functionality of Ti-based implants.[1,2,3,27] However, there remain several challenges that limit the use of such novel modifications for immediate clinical applications. Some of the most basic concerns lie toward the mechanical integrity of the nanotubular surfaces, especially when employed as dental abutments or hip implants. In addition to this, it has been reported that TiO_2 surfaces do not readily facilitate protein adsorption and consequently have lowered cellular attachment and decreased integration.[6] Further, the toxicological effects of noble metal ion release in the presence of titania and titania particles have also raised some concerns.[13] Many studies were also conducted on Ti-alloy-based implants of which one, in particular, suggests that Ti-Zr alloy-based implants demonstrate enhanced positive tissue response when compared to pure Ti implants.[20] This report is interesting because it suggests the possibility of using Zr metal for implants, besides ZrO_2 {ceramic powders} had already been in use in the field of dentistry.[21] Zirconia is a bio-inert, refractory grade metal-oxide that shares many of the characteristic properties that make titania implants favorable.[13,14]

Zirconia surfaces have also been reported to demonstrate improved adhesion to molecules, surrounding tissue and decreased bacterial adhesion for certain adherent cell types, whilst offering attractive aesthetics.[33,32] Interestingly, in the year 1969, Helmer et al. had already proposed ZrO_2 as a new material for hip-head replacement instead of titanium or alumina prostheses, which was further advocated by Piconi et al.[13,25] It is without doubt that zirconia usage has become mainstream, especially in dental and orthopedic applications, this ceramic is used after bulk compaction. Nascent zirconia undergoes two phase transformations, a} cubic to tetragonal {c -> t}, and b} tetragonal to monoclinic {t -> m}. Thermodynamically, it is impossible to retain either the, c- or the t-phase in ambient conditions, even with rapid quenching. Practical implications are an increased chance of cracking and bulk fracturing of large pieces, to combat the sudden and large volumetric change.[28] This is also one of the reasons why large pieces of pure ZrO_2 {via compaction} are susceptible to challenges in manufacturing, such as {size limits}, and process parameters {temperature control/ heat-flow, etc.} to name a few.

Commercial zirconia implants that are bulk-compacted products that are often stabilized with oxides of yttrium, aluminum and cerium. These oxide inclusions, help retain the c-/t-phase metastabily at ambient temperature.[29] While there are favourable effects of stabilizing oxides, each oxide type comes with limitations, ranging from process-ability, costs, aging {low/high-temperature dependant}, that need to be factored in during material selection.

Widely used yttria stabilzed zirconia {YSZ} is a classic example of such a toughened system. It is however, important to note, that the stabilizing effect is strongly contraction dependent. Especially in YSZ, another effect that counteracts the stabilization, is observed when yttria is below 4 mole percent in concentration, further leading to a phenomenon termed low-temperature aging.[29] Typically, observed for temperatures ranging between 200-300 °C, and in the presence of water vapor, this material can undergo a catastrophic micro-cracking that may eventually lead to failure. The sudden transformation, is also accompanied by surface effects that eventually weaken the bulk, and can be aggravated during are manufacturing process that also affect the stability of in-service implants, invariably leading to clinical consequences.

As a result of these interesting properties and characteristics surrounding bulk zirconia, the work in this manuscript is aimed towards creating 1D nanostructures in order to exploit the size and morphological effects of bulk zirconia by using anodization. This may positively overcome particle issues such as agglomeration, instability and ultimately favour the design og a structural material that is robust and stable. Zirconia nanotubes {ZrNT} may be synthesized via electrochemical anodization in an electrolytic bath consisting of either acidic/organic/aqueous solvent with the addition of anions and/or etching agents. The entire anodization process is highly tunable and one of the key influences on the morphology of the anodic oxide depends on the type of electrolyte and the anodizing voltage.[30,31] The quality of the anodic film largely depends on the starting state of the underlying metal film, such that a pre-treatment of the surface becomes indispensable in orde to promote nanostructuring. The most common prepping involves the use of etchants on the metall ic surface. These etching steps often involve the use of highly toxic and abrasive products and procedures, e.g., during experiments involving hydrofluoric {HF} acid pre-treatments. Even after, such a pre-treatment, successful nanoporous arrays thus formed, continue to have traces of an initiat ion layer. Such a layer rests over the array and often limits a thorough access to the underlying op en channels by blocking some of the pore mouths due to partial coverage over the surface.[31,32] Thus, this standard practice even though effective is not ideal as previously reported and continues to raise several environmental as well as operational hazard-related challenges.[33,34,35]

This particular area of concern provoked an interest in minimizing the fabrication steps involved during the ZrNT fabrication, and within this dissertation, propelled a focus on developing an electrolyte composition allowing for a single-step, one-pot synthesis to create robust ZrNT structures. Previously, organic electrolytes made of glycerol, ethylene glycol, and/or formamide in the presence of ammonium fluoride {NH_4F} had opened a new perspective on the competing roles of fluoride {F and oxygen O ion} motility.[36,37,38] A focus on the F/O ratio becomes critical in predicting the final structure as a result of competing processes of chemical etching and anodic oxidation. Another equally dominant anodization parameter to consider is the operational voltage.

The applied voltage is known as the potential window and has been reported to have a nearly linear influence on the nanotube diameter.[39] At lower voltages, the rate of oxide dissolution is relatively slower due to less field-strength associated ohmic dissolution, while at higher voltages, increased ion migration results in a larger pore area being etched.[40,41] Consequentially, a rule of thumb is to work with lower voltages for narrower tube diameters and higher voltages for wider diameters. Anodization duration has a pseudo-linear relationship, in the sense that after a linear growth in length concerning an increase in anodization duration, the tubes tend to break off after certain thresholding values.[37,42,43] A combinations of protocols are explored in this work to achieve ZrNTs with robust aspect ratios and high durability.

Nevertheless, the primary studies within this dissertation describe the surface morphology as a result of tuning anodization parameters such that a variation in the nanotubular geometry of ZrNTs is observed. The role of NT morphology is imperative in understanding the influence, nanostructuring has on subsequent surface interactions that depend on the surface area, surface energy, and surface tension.[36,44,45,46] This interdependence of surface structure and surface chemistry defines the relationship towards surface modifications via functionalization. Functionalization refers to the process of using molecules with certain functional groups/ binding motifs to chemically modify the underlying substrate.

Herein such surface modification is achievable by the formation of self-assembled monolayers {SAM}. SAMs are spontaneously adsorbing molecules that adhere to an underlying substrate by forming a film of monolayer thickness.[47,48] A schematic representation of a few applications of such surface coatings in represented in the following Figure 4.[49]

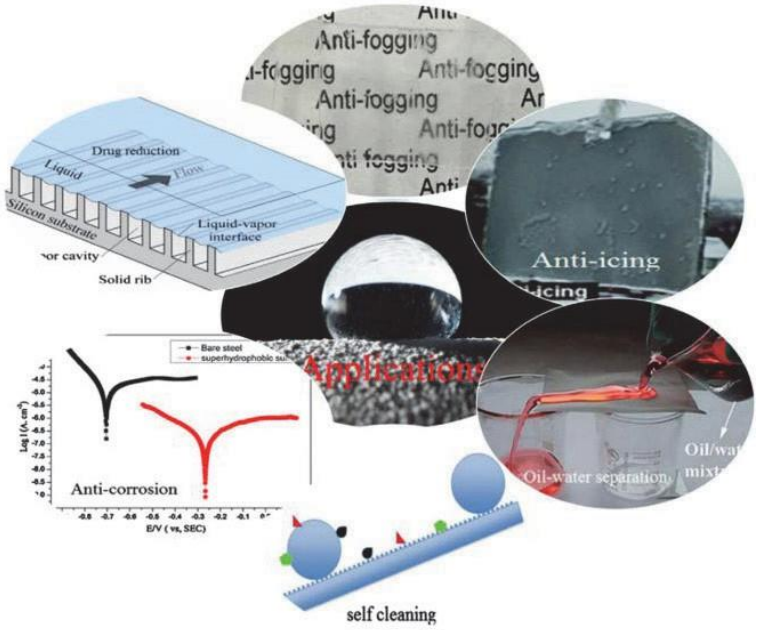

Figure 4: The schematic depicts the various applications of superhydrophobic surfaces [49]

SAM modifications to surfaces, specifically metal-oxide surfaces, have previously been explored in; electronics, semiconductors, paints, and biomedicine, to name a few.[50,51] SAMs are capable of eliciting a variety of functional responses. One of the more fascinating aspects lies in the tunability of surface wetting. Most metals in their intrinsic state consist of a film of native oxides which may be an inhomogeneous layer, nevertheless hydrophilic in nature.[52,53] Alternatively, anodization forms compact oxides that are essentially a uniform oxide layer {as flat as the starting substrate}. However, this unmodified surface remains hydrophilic, i.e., experimentally measured water contact angle <90°. This phenomenon is largely attributed to the presence of surface hydroxyl groups.[54] This wetting behavior is further altered upon physical modification of the oxide structures, such as in the case of nanotubes {NTs}. NTs reportedly show super-hydrophilic behavior towards water adsorption in ambient conditions, perhaps due to the resulting capillary action, often seen in metal-oxide NTs.[55,56,57]

This trend is compelling evidence for the influence morphology has on the surface phenomenon, and its effect is even more relevant in the biomedical field when considering protein adsorption and subsequent cascade reactions.[58,59,60]

However, it is interesting to report that in the case of zirconia nanotubes, the resulting hydrophobicity, although similar, was remarkably not interdependent to the nanotube diameters as seen with titania nanotubes functionalized using phosphonic acid self-assembled monolayers.[61] While the hydrophobic trend was similar to titania, an astonishing degree of superhydrophobicity was observed for zirconia nanotubes, even at smaller nanotube diameters, as reported within this dissertation.[57] This behavior is explained based on zirconia's intrinsic material chemistry, i.e., the presence of active Lewis acid sites.[61,62,63] When ZrO_2 interacts with wetting solvents, an increase in the adsorption capacity is observed at the acid-base reaction sites which results in an increased generation of condensation products. A consequence of improved adsorption is an enhanced surface coverage, as is witnessed for the phosphonic acid SAM.[47,64,65] This phenomenon of strong SAM bonding and high coverage to ZrNT substrates is quite advantageous when considering applications that require additional chemical modification, especially bringing attention to the strategies used for such modifications.

Conventionally, organic molecule modification is achieved via wet-chemistry techniques, involving the transfer of molecules via a solvent or upon direct deposition of the molecule/ molecular suspension via vacuum-assisted methodologies, soft-lithography, etc., to name a few.[66,67,68] On the deposition of SAMs in this work, methods that enabled a successful transfer of organic molecules from solvents employed organic molecule solutions. These organic molecule solutions will hereafter be referred to as 'ink' in the manuscript. Inks made of organic molecules bearing different functional groups are used to deposit SAMs on zirconia anodic oxides, such as compact oxides and nanotubes. The deposition is performed either via simple immersion in bulk solution, aka bulk immersion {BI}, or by using an intermediate soft-stamp made of polydimethylsiloxane {PDMS} via micro-contact printing {µCP}.[68,69]

In wet chemistry, it is important to consider the effects of physical processes on the kinetic and thermodynamics of the resultant reactions.[70,71,72] Self-assembly in capillaries is subjected to capillary forces, and consequentially, the rate of reaction is governed by the laws of diffusion.[73,74] Diffusion, driven by a concentration gradient, relies on concentration differences to relay the bulk of mass transfer within a system.[75] This phenomenon is especially compulsive when considering using diffusion processes to govern a flux-dependent deposition strategy. For example, during the deposition of particles along a homogeneous pathway, as is seen in the case of nanotubular capillaries. A significant amount of the work done in this dissertation focuses on exploiting this diffusion-driven mechanism to facilitate depth-specific deposition of SAMs on and within nanotubes. Deposition of SAM molecules along tube walls was performed in multi-step processes to elucidate the possibility of depth-dependent modifications governed by the diffusion kinetics of the μCP method. Previous studies using spectrometric analysis have successfully validated the influence of diffusion kinetics inside pores.[76,77] Herein, nanotubes modified via μCP were also characterized and analyzed using mass-spectrometry methods to estimate the molecular deposition at different depths of the tubes. SAM formation is a surface phenomenon, and the surface analysis gives information on both qualitative and quantitative aspects of such organic molecule surface modifications.

However, when considering nanotubular materials, a two-fold effect is observed. The deposition of SAMs on the surface extends to the tube openings {outside} and also the tube walls {inside}. The analysis of both types of surfaces was used to confirm that the extent of achievable surface modifications was independent of capillary length.[57] This observation was relevant in distinguishing the role of the qualitative from the quantitative aspect of SAM modification in the context of ZrNT modification. It also establishes the foundations for the inference that ZrNTs show superior binding to a specific functional group, independent of {1} tube morphology, {2} tube length, and {3} functionalization strategy.

These results highlight the intrinsic material properties and elucidate that the effect of subsequent structural modifications is not limited to the type of geometry. Zirconia-based biomaterials demonstrate similar and unsurpassed functionality when modified with SAMs, compared to other metal-oxides.

There is ample evidence that boasts of the many facets of nanostructured surfaces in the field of biomaterials applications.[78,79] A combination of physical and chemical surface modifications of biomaterials may be compelling to value-add to their overall performance. Materials that are modified with at least one component in the nanometer range are termed hybrid materials. Hybrid materials can have a composite assembly arbitrarily offering higher meso-macroscopic functi onality than parent component systems.[80,81,82]

As discussed earlier in this section, such nanostructural modifications may be achieved during the conception and design stages or after material development as coatings. It is noteworthy to highlight the importance of augmenting surfaces with nanostructures in the post-processing stages as it offers the possibility of combining different materials. Conventionally, micro-nanoporous variations are imparted to surfaces via multi-step procedures, often involving vacuum-assisted methodologies. Such a process usually starts with examining base material compatibility, followed by deposition of the precursor layer that needs to be modified via micro-nanostructuring, as seen in processes such as atomic layer deposition {ALD}, fused deposition molding {FDM}, e-beam sputtering- lithography, etc.[83,84,85,86] Advanced manufacturing strategies are viable options for surface nanostructuring. However, they are posed with challenges faced during composite fabrication. They are limited by issues related to interfacial adhesion, delamination, and overall stability, more so due to the development of macroscopic layers made of nanoscale structures.

Even though it is relatively straightforward to fabricate such nanostructures on metallic biomaterials, it is important to note that the majority of the biomaterials currently in circulation for dental and orthopedic applications are made of ceramics. Thus, the previously proposed conventional routes or even advanced manufacturing strategies fall short of achieving the desired micro-nanoscale surface transformation on such bulk ceramics.

2. RESEARCH INTRODUCTION

Implant-based research continues to be an ever-expanding field, and as the complexity of an injury increases, the consequential material response demands are required to demonstrate enhanced functionality. In light of this, bio-materials are subjected to structural, chemical, and physical changes, mainly at the surface, since biomaterials primarily interact with the biological environment through their surface. The goal of this dissertation is to use conventional bulk materials, and adapt physical and chemical surface modifications to create functional nanostructured materials. The intended methods are in-situ setups; electrochemical anodization and surface modifications using a self-assembled monolayer {SAM}. The surface characterization technique Time-of-Flight Secondary Ions Mass Spectrometry {ToF-SIMS} is used in tandem to evaluate the role of sequential modification of the nanotube walls. The simultaneous characterization of the modified nanostructures enabled the development of protocols to modify nanotubular surfaces by exploiting diffusion driven kinetic- deposition. In addition to this, there is an emphasis on the fabrication process of zirconia nanotubes {ZrNT}, focusing on the formulation of the type of electrolyte and synthesis in a single-step setup.

A thorough investigation of the morphological influence on subsequent surface response with and without chemical modifications is evaluated via characterization methods such as Scanning Electron Microscopy {SEM}, X-ray diffraction {XRD}, X-Ray Photoelectron Spectroscopy {XPS} and Water Contact Angle {WCA} measurement. Furthermore, these nanotubular reservoirs are evaluated for their storage capacity when screened as potential drug/ dye-eluting surfaces during release experiments using a UV-Vis spectrometer, under regular and triggered release conditions as a function of subsequent SAM modifications. In this work, we use ToF-SIMS depth profiling to evaluate compositional variation within the modified nanotubes. The technique offers better spatial and depth resolutions, along with the molecular specificity and high mass resolution that is unique to mass spectrometry when compared to XPS.

2.1. RESEARCH OBJECTIVES

A large aspect of this thesis depends on the efficient fabrication of nanostructured Zirconia, consequently evaluating the behavior of oxide structures under anodizing conditions. Anodization results in a physical structuring of the oxide layer via the electrochemical route, and is followed by analysis that is aimed at determining the influence this type of surface structuring has on surface energy, surface reactivity, and roughness concerning chemical modification using SAMs. In addition to the improved surface response, nanotubular oxides offer an increased surface area and volumetric capacity. This type of structural modification can act as a reservoir to store beneficial therapeutics or can be selectively functionalized along the tube's length, potentially acting as multi-functional hierarchical structures capable of eliciting a specific response. Therefore, the ZrNT fabrication and functionalization are aimed toward its applications as coatings and as drug-eluting surfaces.

The following objectives are addressed within the scope of this dissertation;

- ✓ Establishing an anodization protocol to minimize operator risk and optimizing experimental parameters to develop robust nanotubular geometries.
- ✓ Determine the role of nanotube morphology on the interaction behavior with organic molecules used for surface modifications.
- ✓ Evaluate storage capabilities of the homogenous nanostructures.
- ✓ Develop a strategy to facilitate and evaluate the multi-depth filling of nanotubes.
- ✓ Deposition/transfer of free-standing ZrNT layers onto pre-formed bulk ceramics as coatings.

2.2. RESEARCH APPROACH

This subsequent section, will delve into a range of effective strategies to bridge gaps in the current state of the art. A schematic representation is provided to further a clear and concise overview of the steps involved in the process, from conception to implementation.

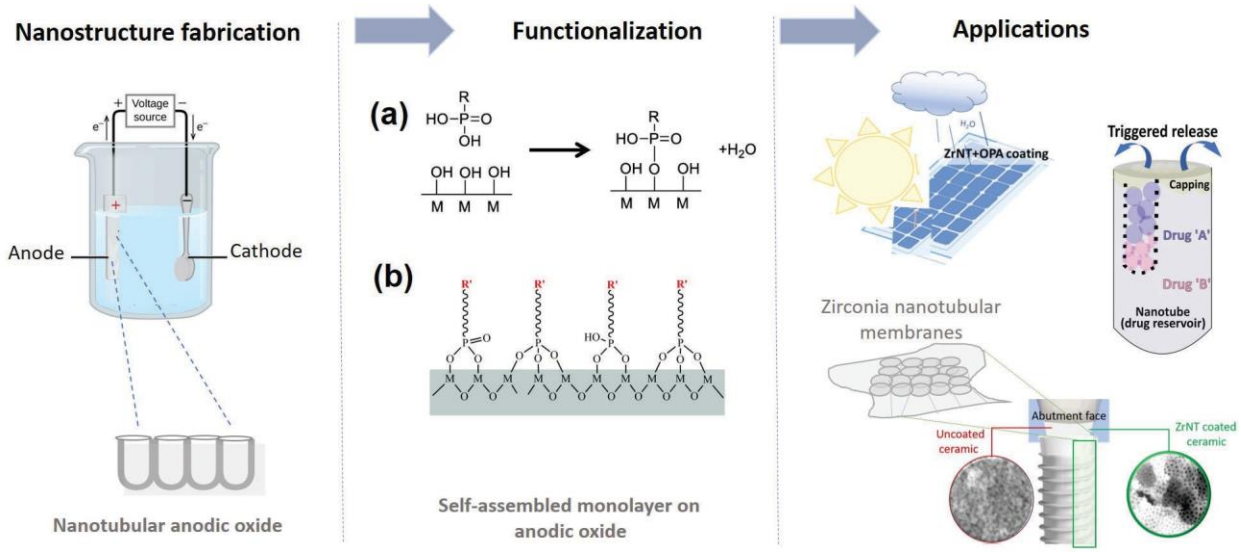

Figure 5: Schematic depiction of the experimental flow; (l) synthesis of anodic oxides (compact, nanotubes) by electrochemical anodization, (c) surface modification (chemical functionalization using organic monolayers), and (r) various applications of functional nanotubular metal oxides

The following subsections will briefly elucidate the primary concepts and their exploitation for the proposed practical applications.

2.2.1. Electrochemical anodization for the fabrication of metal-oxide nanostructures

Metal oxide {MO} nanostructures are formed as a result of undergoing self-organization of the oxide layer into defined porous structures under the influence of electrolytic passivation. The primary role of using an electrical bias is to accelerate the growth of a barrier oxide, promoting the transformation of the underlying native oxide film on the metal to a thicker and homogenous metal-oxide layer. In this work we anodize Zr metal to promote the formation of an oxide-rich metal oxide, ZrO_2 , that is transformed into nanostructured oxides under specific conditions. During the primary stages of anodization, the barrier oxide layer is formed uniformly over the entire metallic face when passivated in an electrolyte. Upon the inclusion of corrosive salts in the electrolyte, a localized shift in equilibrium can be observed. This shift initiates the formation of pits, followed by the subsequent enlargement into uniform pores when there is a time-dependent adjustment in equilibrium, resulting in the development of a homogenous nanotubular layer.[4] Tuning the localized steady-state response offers strong control over the anodic oxide assembly, such that small equilibrium shifts can determine if the nanostructure is formed as a single monolith, a corrugated structure, or a simply free-standing assembly. The synthesized nanostructured oxides are characterized via SEM and XRD for morphological and amorphous/ crystalline variations.

2.2.2. Free-standing nanotubes and their transferability

Zirconia films are first anodized as a nanotubular layer over the zirconium foil and are subsequently detached from the metal foil to produce a free-standing nanostructured metal-oxide layer. The zirconia nanotubes {ZrNTs} detaches from the foil at the weakened interfacial oxide structure. At this interface, the ZrNTs are altered due to dynamic pitting and pore-formation as a result of voltage pulsing.[30,87]

The ZrNTs are subjected to detachment at the already weakened interface by using adhesive tape for a physical lift-off from the metal foil's surface. This is then treated with a solvent to dissolve the adhesive and release the ZrNT layers for further transfer.

2.2.3. Self-assembled monolayers and nanostructured metal-oxides

Self assembled monolayers {SAMs} are the spontaneous assembly of organic molecules onto a surface as a result of adsorption reactions and can bind to an underlying substrate strongly via chemisorption. Alternatively, weakly via physisorption.[88] Metal oxide {MO} surfaces are terminated with hydroxyl groups under ambient conditions and allow for condensation reactions to occur on their surface, thereby facilitating hydroxyl-mediated SAM formation for various binding motifs.[54] In order to investigate the resulting hydrophobicity achieved due to successful organic molecule modification via SAMs on ZrNTs, preliminary techniques involved the use of WCA analysis, XPS for the extent of SAM coverage, and UV-Vis spectroscopy observe drug release from ZrNTs as a result of degradation of the SAMs on ZrNTs.

2.2.4. Deposition into NTs - bulk immersion vs micro-contact printing

In addition to the chemical reactivity of the MO, the roles of the nanostructure are also crucial to such adsorption reactions, as nanotubes exhibit capillary action and promote liquid imbibition which allows for maximum fluid interaction of the organic molecule solution, resulting in subsequent SAM formation on the MO surface.[23,54] The deposition of SAM is achieved via diffusion-driven kinetics when functionalizing the ZrNTs via immersion in bulk solution, aka bulk immersion {BI}, and when contacted with soft polydimethylsiloxane {PDMS flat-stamp containing a SAM solution, aka micro-contact printing {μCP}.[24]

BI results in deeper deposition of organic molecules inside of the nanotubes due to longer exposure in excess of SAM solution, whereas when SAM is deposited via μCP, the depth of deposition of organic molecules starts from the tube mouth, and migrates into the nanotubes as a function of availability of SAM solution on the stamp contacting the substrate.

2.2.5. Depth profiling via ToF-SIMS

The purpose of depth profiling is to determine the local composition of a material based on its depth below the surface. Rather than directly measuring variations in composition as a function of depth, signal intensity is usually measured as a function of sputter duration.[27] The intensity-time are usually converted into a composition-depth relation by using specific calibration and converting time into depth, also accounting for factors such as preferential sputtering, atomic mixing, topographical effects, material variation, sputter-induced roughening effects, etc.

In this work, we use ToF-SIMS depth profiling to evaluate compositional variation within the modified nanotubes. The technique offers better spatial and depth resolutions, along with the molecular specificity and high mass resolution that is unique to mass spectrometry when compared to XPS.

3. METHODS and MECHANISMS

This section provides background information on the principles exploited for the various techniques used in this work. The individual sections lay the foundation for the choice of experiments discussed.

3.1. Electrochemical anodization for ordered arrays

Highly ordered arrays of metal-oxide nanostructures can be synthesized via electrochemical anodization. This process of forming homogeneous oxides at the anode under an applied bias in the presence of an electrolyte in an electrolytic cell is termed anodization. The electrolyte composition predominantly determines the fate of the surface that is getting anodized. Either surface dissolution governs the reaction process resulting in etching/ electro-polishing, or stable insoluble oxides continue to grow as compact oxides. When passivation occurs in a mildly corrosive environment, it results in the formation of porous oxide surfaces. In certain typical conditions, such porous surfaces undergo self-ordering due to a newly established steady state wherein this growth in the porous oxide continues to form a homogeneous network. In most cases, the fromation of a soluble metal-complex drives this result. As with zirconia synthesis, it is possibly due to the influence of fluoride salts in the electrolyte.[89,90] A schematic representation of possible outcomes of the shifting electrochemical interactions when using F ions assisted dissolution for metals like Ti and Zr, is depicted in Figure 6.[90]

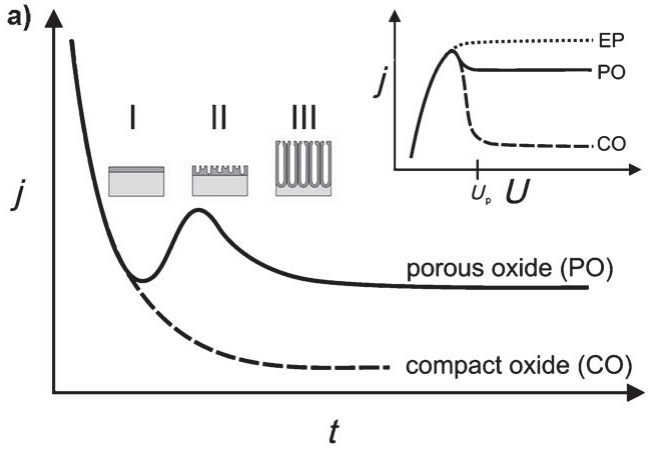

Figure 6: Representative current vs. time characteristics of constant voltage anodization; with (——) and without (---) Fluoride ions in the electrolyte [90]

The current vs. time curves typically indicate whether a porous oxide is formed. The initial passive layer undergoes partial dissolution in the early stages of pore formation, which becomes apparent in a {small} rise in current density, followed by re-passivation.

3.1.1 Zirconia nanotube formation

When appropriate anodic voltages are applied to a working electrode, e.g., Zirconium {Zr}, typically the metal that undergoes oxidation, in the presence of a relatively inert counter electrode, e.g., Platinum {Pt}, an inward migration of oxygen anions is observed under the action of a mildly corrosive specimen.[102] This preferential migration aids the formation of the initial oxide layer, which eventually undergoes field-assisted dissolution. The dissolution is due to the competing migration of etching species such as ammonium fluoride and the surplus oxygen from aqueous additions to the electrolyte.[91,92,93] This competition results in the formation of a porous anodic structure, which under longer effects of anodization forms nanotubular arrays. For example, the inclusion of water in organic solvents such as glycerol, ethylene glycol, or formamide. A competing response between fluoride and oxygen ion migration towards the anodic interface i.e., between the metal foil and the oxide film growing above it, is observed. Metals such as Zr have a high oxidation state resulting in the formation of passive bi-layers, known as the barrier layer at the different interfaces {represented as "x/y"}, for instance, 'metal/oxide' interface and an outer layer at the 'oxide/electrolyte' interface.[93,94]

The barrier layer is superseded by the growth of a porous layer, and its thickness is proportional to the applied voltage. Once formed, it remains constant during the anodizing process, promoting a continuous ionic flow as this layer is relatively thin.[95,96] The diffusion kinetics of ions at the anode is such that, F>O.[96] This results in the formation of amorphous zirconium-fluoride-complex layer beneath the oxide rich barrier layer.

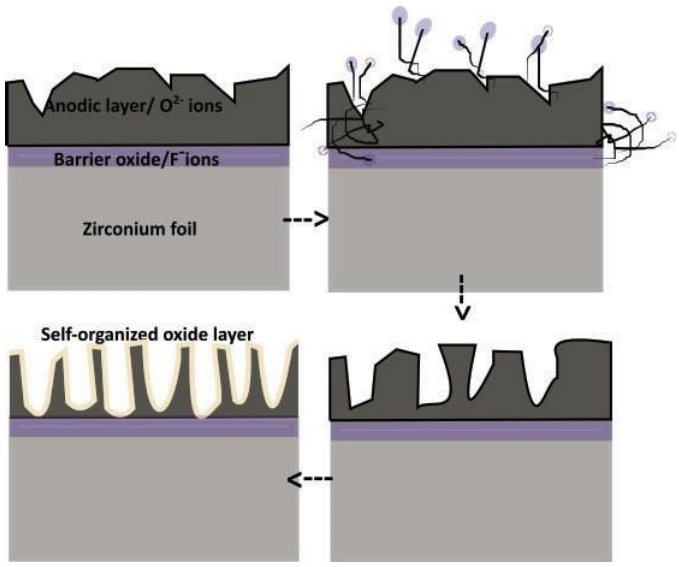

Figure 7: Schematic suggestive of anodization of Zr foils in fluoride-rich organic electrolytes where field-assisted fluoride ion/ ion-complex's inward migration towards the barrier layer result in the formation of self-organized nanotubular oxide

Ultimately, fluoride-mediated dissolution advances inward and pore enlargement result in the formation of nanotubular morphology in zirconia, similar to titania and hafnium.[87,97] A schematic of the proposed mechanism is represented in Figure 7, adapted based on the above-mentioned theories. When zirconium {Zr} metal is anodized in an organic electrolyte consisting of oxygen-rich species such as formamide, traces of water and fluoride ions from ammonium fluoride salts, the governing chemical reactions in the anodization process involving competing fluoride and oxygen ions is represented; As immersing the Zr foil into the electrolyte, the dissociation of water is followed by the initiation of an amorphous fluoride layer building up into the metal surface as a result of the constant generation of fluoride vacancies at the 'foil/electrolyte' interface and cation interstitials, ejected and diffuse along the barrier layer;

$$H_2O \rightarrow 2H^+ + O^{2-}$$

$$Zr \rightarrow Zr_4^+ + 4e^-$$

$$Zr + H_2O \rightarrow 2H^+ + ZrO^{2+}$$

$$ZrO^{2+} + H_2O \text{ <----> } 2H^+ + ZrO_2$$

$$4H^+ + ZrO_2 + 6F^- \rightarrow [ZrF_6]^{2-} + 2H_2O$$

A current density versus time plot of ZrO_2 formation in an organic electrolyte containing NH_4F, acting as the source of fluoride ions, is shown in Figure 8.[98]

The simultaneous stages of nanotube growth and order are elucidated within the plot as a function of reaction time and anodic current density. Initiation of the anodization starts with the growth of the barrier oxide as oxygen ions migrate towards the interface, followed by a lowering of current density as the thickness of the barrier layer increases. Pitting occurs at both interfaces, metal/oxide and oxide/electrolyte, due to fluoride ion-induced chemical dissolution and a subsequent increase in current density during the successive stage. Finally, pore formation and deepening take place due to fluoride ions-assisted dissolution inside the pores consisting of the zirconium-fluoro complexes. This stage is of utmost importance in nanotube growth as it highlights the role of fluoride ions in oxide dissolution.[34,37,98]

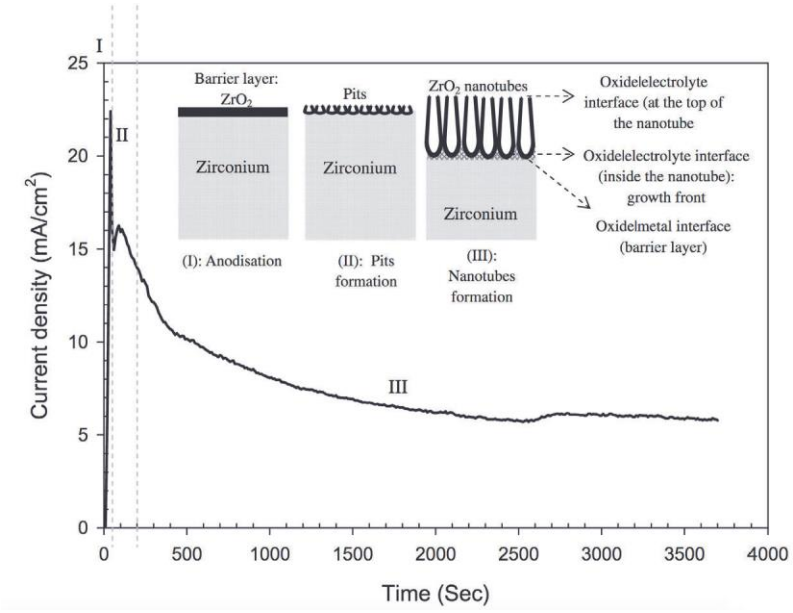

Figure 8: The simultaneous stages of nanotube growth and order are elucidated within the plot as a function of reaction time and anodic current density. [98]

The current density curve offers insights into the morphology of the oxide layer formed. The final geometry of the anodic oxide can range from nanotubes, over pores to sponge-like material or even fishbone-nanoarchitectures.[99]

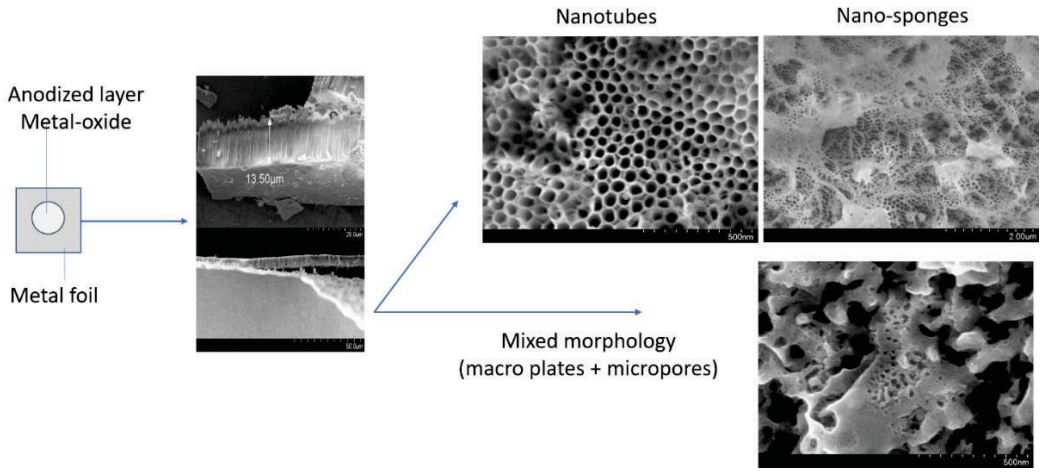

Figure 9: (L) Schematic representation of the anodized metal-foil and SEM images of ZrNT a) cross-section and (R) Zr0$_2$ (top-view) and different possible morphologies; nanotubes, nanopores and mixed structures

The variation from compact, nearly 'flat' oxide surfaces and the formation of pores, furthering the development of porous structures, such as the ones shown in the representative image in Figure 9, is formed by tuning the anodization parameters. The self-ordering stage is ideally the last step when nanotubular arrays grow. The morphology of the tube tops is circular due to thinning of the adjacent pore walls.[37,100]

3.1.2. Freestanding nanotubular layers

The anodic oxide structures grow attached to the underlying metal foil. To develop detachable layers and analyze the as-formed porous/tubular layer, isolating the anodic layer from the metal foil is necessary. The separation is usually achieved by manipulating the barrier layer, often by tuning the applied voltage.[101,102] A change in voltage from the established steady-state results in a perturbation in the localized equilibrium, subsequently affecting the current density and related field-assisted phenomena. Under the influence of the combined effects, a partial dissolution of the barrier layer or a total breakdown of the barrier layer occurs.[103,104,105] Both cases weaken the

adhesion at the interface of the metal/oxide. A schematic of a possible detachment mechanism is shown in Figure 10.[105]

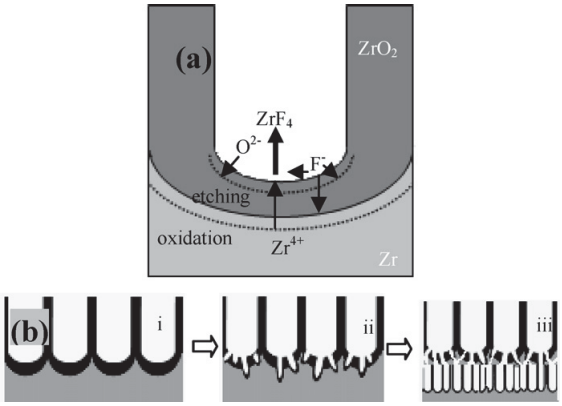

Figure 10: Detachment of NTs due to a sharp change in anodic bias [105]

A variation in electric-field distribution is achieved by reducing the potential or increasing the operating voltage sharply, also known as 'pulsing'. The result of such a shift in steady-state condition results in the formation of corrosion, pitting, and new-layer growth depending on the potential difference and the duration of the electrolytic process.[106,107]

3.2. Surface modification

Surfaces may be modified via physical conditioning or by chemical means. A schematic of the various surface-modification strategies is represented in Figure 11, wherein the first step is the structural change imparted to the surface via the electrochemical route by creating micro/ nano-texturing, followed by chemical modification.[108] Treating surfaces with organic molecules can alter the surface chemistry of the underlying substrate. In the case of metal oxides, organic molecules with varying functional groups can bond to the substrate upon adsorption.[109] Molecules may either be physisorbed or chemisorbed onto the substrate. The difference in the underlying attachment mechanism determines the stability of the formed bonds.

Conventionally, physisorbed bonding is weaker than chemisorption, and it depends on the reaction enthalpies of specific molecules.[110,111]

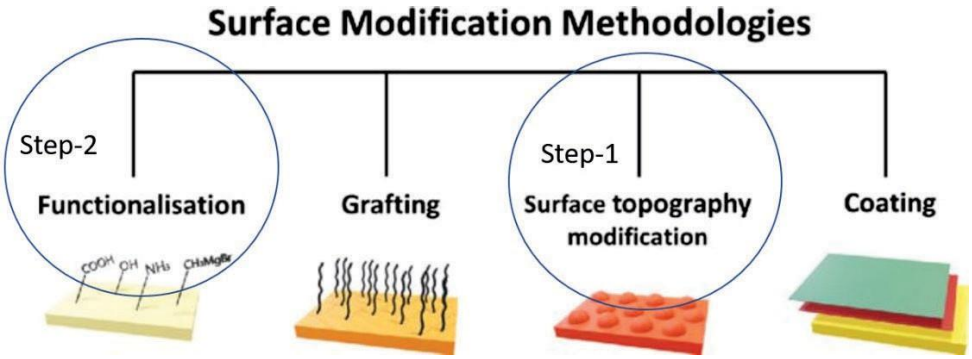

Figure 11: Surface modification methodologies [108]

3.2.1. SAM formation and attachment

Self assembled monolayer {SAMs} are a one-molecule thick layer of materials bound to a surface in a definite order. This ordered assembly occurs spontaneously after deposition through chemical bonding at the substrate's surface. Principal driving forces for self-assembly to progress are represented in Figure 12.[112] The primary reason is the minimization of energy for all systems.

It is pertinent to note that nearly all metals are covered in a thin oxide layer often termed as the metal's native oxide. This oxide layer's quality and thickness varies from metal to metal and is responsible for promoting corrosion resistance of the nascent metal. This oxide layer is present with surface hydroxyl groups in ambient conditions and is the reason why these metals exhibit hydrophilic behavior such that water molecules readily form films upon these surfaces. During the process of depositing organic molecules via self-assembly, these surface hydroxyls play an important role in bond formation at the interface, between the molecule and the metal oxide substrate. Invariably such bond formations are as a result of condensation reactions and are of a reversible nature.

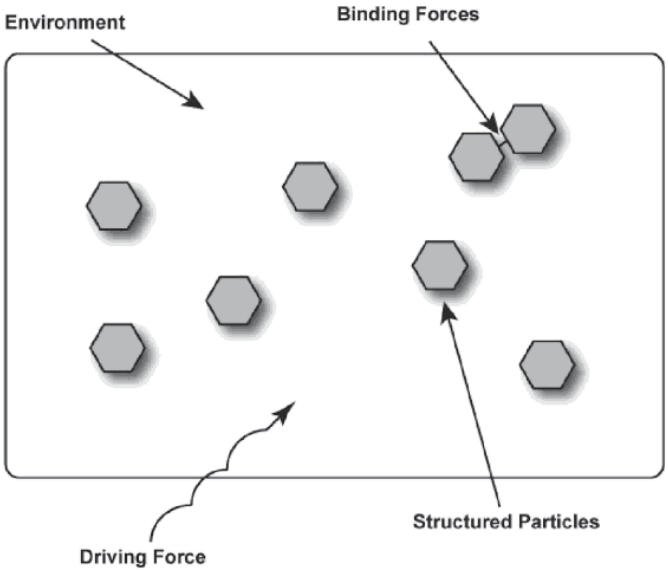

Figure 12: Principle components propelling self- assembly [112]

In the case of metals, the type of reaction pathway usually involves covalent bonding mediated via condensation reactions. Condensation governs metal-SAM bond formation due to the presence of surface hydroxyls on metals in ambient conditions.[54] However, the order in self-assembly is influenced by the type of molecule, the carrier solvent used, and the concentration of the molecules in a SAM solution. Surface coverage follows an increasing trend proportional to the number of molecules in the SAM solution.[69]

There exist many kinds of organic molecules that can be used for functionalization of metals/ metal oxides. The classification is based on the type of functional group, chain length and anchoring groups. Lastly, the most important prerequisite towards the choice of molecule depends on the type of expected response of such modified surfaces. For instances, for hydrophobic modification, long chain carbohydrate molecules such as phosphonic acids, stearic acids etc., are often used.

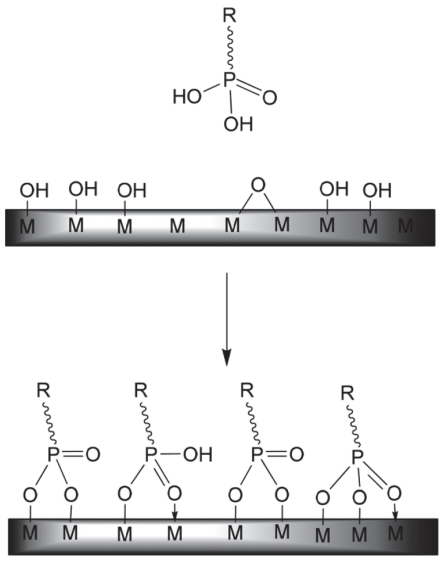

Figure 13: Schematic representation of P-0-M bonding of phosphonic acids forming a self-assembled monolayer on a metal-oxide surface [113]

Phosphonic acid binding motifs have reportedly demonstrated faster adsorption and stable bond formation on metal-oxide surfaces compared to other functional groups.[114] Phosphonic acid reaction to a metal-oxide involves P-O-M bond formation, where M is metal. A schematic of the same is represented in, Figure 13.[113] The P-O-M bond is the result of P-OH groups reacting with the M-OH substrate in addition to the coordination of phosphoryl oxygen to Lewis acid surface sites.[62]

3.2.2. Depositing self-assembled monolayer on metal-oxides

Deposition of self-assembled monolayer {SAMs} may be achieved via various strategies, depending upon the resulting thickness and type of coating required. This work predominantly aims toward depositing monolayers. Such films were initially demonstrated with the Langmuir-Blodgett technique, wherein Langmuir monolayers are transferred directly onto the contacting solid surface from the liquid-gas interface i.e., solutions containing organic molecules in a choice solvent.[115] Upon immersion, a monolayer is adsorbed homogeneously. Repetition in the number of immersion steps results in a multi-layer deposition. It may be noted that LB films although are a prominent case, remain applicable to amphiphilic molecular assembly atop of a liquid, contrary to the work,

reported here, where SAMs are produced directly in a solution. Solution SAMs follow Langmuir kinetics when undergoing adsorption. A schematic of the same is seen in Figure 14.[116,117]

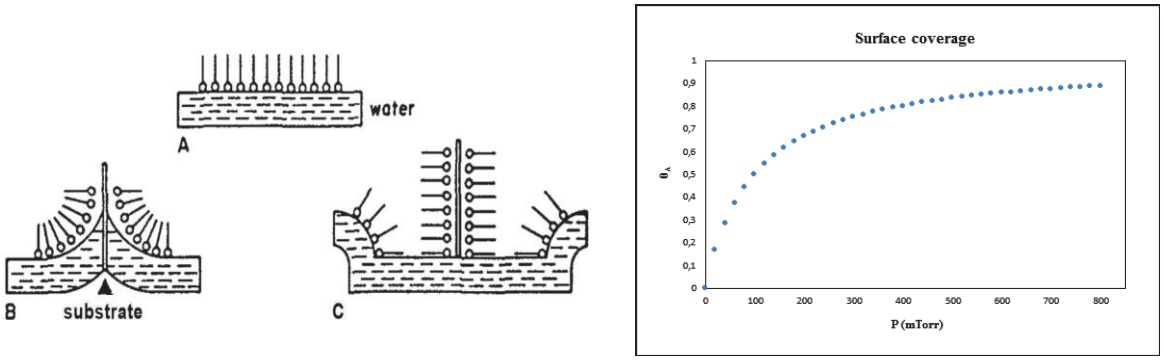

Figure 14: (L) LB film formation[126] and (R) Adsorption isotherm (surface coverage in solution)- Langmuir kinetics [117]

Within this work, the ambient deposition of SAMs is made possible via facile immersion strategies in bulk solutions consisting of the required organic molecules in an appropriate solvent. This strategy is called bulk immersion {BI}.[118,69,119] Alternatively, deposition is performed using a soft stamp or ink pad to transfer organic molecule solution, i.e., inking on a solid substrate.

This soft-lithography technique is also known as micro-contact printing {µCP} because of the compulsory physical 'contact' needed for patterning. The deposit is usually at the interface of the two interacting/contacting substrates, and transfer occurs due to substrate affinity. The stamp, in most cases, remains inert and acts mainly as a carrier surface for the molecule solutions, i.e., inks. In many cases, the patterns formed can have nanometer sizes up to micrometer precision, achievable and dependent on the size of the stamp's features.[120] Patterning dimensions are predominantly governed by the size resolution of the stamps. Alternatively, stamps may be devoid of patterns, bearing no topographical variations on the ink pad. Such stamps are ideally 'flat'.

In this work, these flat stamps were made by ambient curing ofpolydimethylsiloxane {PDMS} onto flat Petri dishes before using them for the deposition of SAMs.[24]

A schematic of both deposition strategies is represented in Figure 15.[121,122] Both of these strategies exploit the deposition of SAMs, governed by adsorption principles.

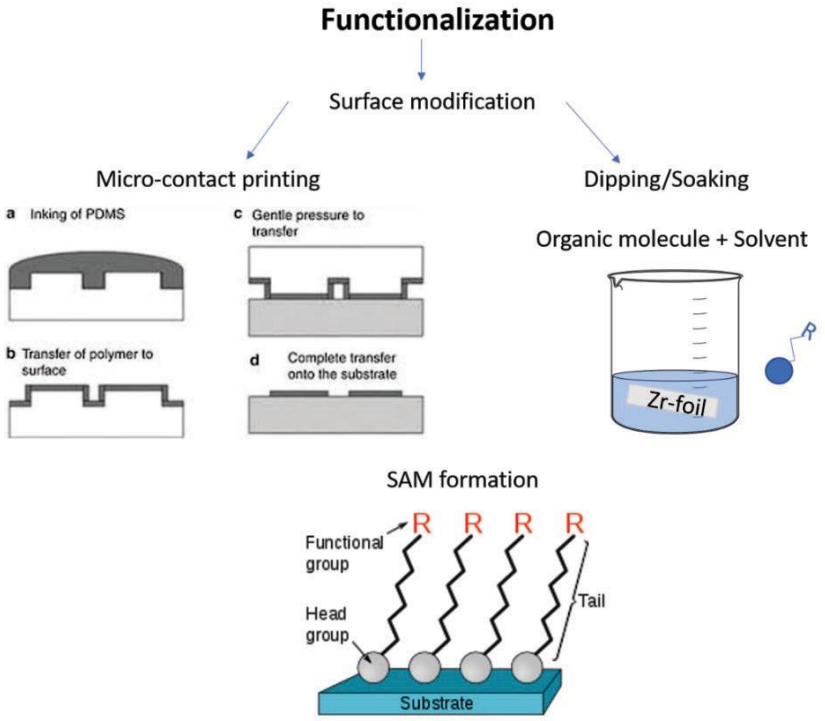

Figure 15: Top; Surface modification via (L) micro-contact printing µCP and (R) Bulk immersion (BI) and bottom; SAM formation principle [121,122]

Especially during µCP, the adsorption process is succeeded by diffusion kinetics.[75] From the perspective of nanotubes, this phenomenon becomes increasingly important as it determines the extent of achievable deposition of such molecules within the capillaries. The technique although simple is often limited in patterning capabilities due to the resolution, i.e., challenges associated with the physical sizing of the features onto the stamps, the chemistry of the ink-pads/stamps, and the interacting inks.[118,121,122]

It may be noted that the actual transfer and deposition of SAMs, for both strategies, can be performed under ambient conditions without any pre or post-treatment and have been reported to render the underlying substrate modified with SAMs that can be confirmed by various

complementary surface characterization techniques that evaluate changes to surface chemistry, such as contact angle measurement, ToF-SIMS, XPS, etc., to name a few.

3.3 Surface characterization

Material development is either simultaneously evaluated or subsequently followed up with characterization. Characterization entails deterministic information on various facets of a material. It enables validation of structure, design, and readiness for subsequent adaptations may be incorporated. Surfaces are essentially the outermost or the top-most area of a material, exhibiting properties similar or different to the bulk of the material. In the latter case, such surfaces tend to show different behavior to their bulk counterparts due to physical or chemical variation. Physical variation is achieved by structural modification, whilst chemical variation may be is possible via altering the surface chemistry either actively, as in the case of coatings, or passively as a result of the nanostructured surface. Structural and chemical changes may be investigated via surface characterization techniques. More specifically, surface characterization provides information on the 'surface' phenomenon and how a material's surface properties relate to macroscopic interactions.[123,124,125,126] In this work, a bulk of the surface characterization is performed via Scanning Electron Microscopy {SEM} for physical/structural modifications. Chemical modifications were analyzed using methods such as Time of Flight- Secondary Ion Mass Spectrometry {ToF-SIMS} and X-Ray Photoelectron Spectroscopy {XPS}. Other complementary methods used in this thesis, are Optical Microscopy {OM}, Contact Angle {CA} measurements, X-Ray Diffraction {XRD}, Simultaneous Thermal Analysis {STA}, and tribological studies as performed via dynamic scratch-tests. The subsections succeeding this paragraph aim to provide a brief overview of the characterization technique, data analysis and any governing mechanisms.

3.3.1. Scanning electron microscopy

Electron microscopes are powerful imaging devices that use a focused electron beam to scan and survey a surface to generate images.

The interaction between a specimen's surface and the electron beam generates subsequent electrons also known as secondary electrons. When an electron beam interacts with a material, it looses energy and consequentially generates secondary electrons. Depending on the extent of inelastic interactions, a variation in primary beam energy is detectable. The variation occurs due to interactions with different depths of the material's surface, this is termed as the interaction depth. Depending on the interaction volume, emitted energies such as the Auger electrons and characteristic X-rays may also be generated long with secondary electrons.

A schematic representing the generic interaction depths and electrons generated from a substrate is shown in Figure 16.[127]

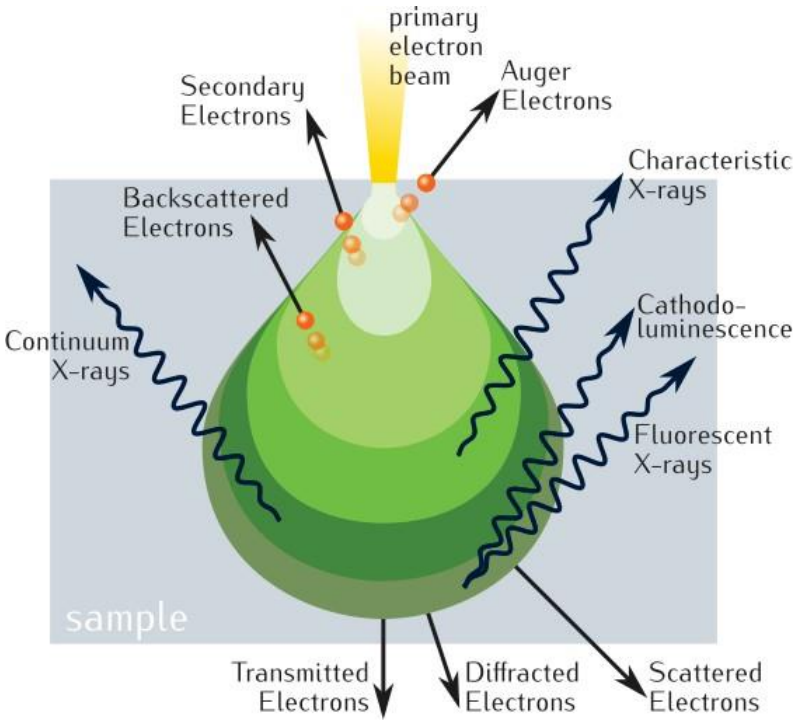

Figure 16: Electron-matter interaction volume and types of signal generated [127]

A complementary technique is Energy Dispersive X-Ray spectroscopy {EDX, performed in tandem with the scanning electron microscope {SEM}. It usually provides compositional information based on backscattered electrons and is xtremely useful in the identification of elements or also all

of the elemental composition of a sample.[128] The average information depth for specific electron generation is; Auger electrons { ~ 0.4 - 5nm}, secondary electrons {~ 100nm}, backscattered electrons {~ 1µm} characteristic X-rays {~ 5µm) Bremsstrahlung X-rays and X-ray fluorescence {~ 5µm}, however, variation is possible in dependence of excitation energy and material properties.[138] A typical image formed via the SEM technique is previously represented in Figure 9.

3.3.2. Time of flight -secondary ions mass spectrometry (ToF-SIMS)

Mass spectrometry {MS} is an analytical technique that measures the mass-to-charge ratio of ions. The results are presented as a mass spectrum, a plot of intensity as a function of the mass-to-charge {m/z) ratio. ToF-SIMS also functions on the same principle, the difference being in the type of ion generation and data obtained due to secondary ion emissions by primary ion beam bombardment complemented by a ToF analyzer. It is a highly sensitive surface analysis technique that can provide information about molecules or surface components based on molecular mass and fragmentation behavior upon beam interaction. The sensitivity limits lie in the parts per million {ppm to parts per billion {ppb range.[129] The impinging of a focused ion beam on the materials surface causes desorption of secondary ions from the sample's surface, and is followed by extraction of SI into the analyser, and a reflectron helps to improve mass resolution by removing potential spreads in kinetic energy of ions of the same mass and separation according to flight time. The impact of the ion beam causes not only the knock-off of ions and molecular fragments, but also species which can be detected with specialized instrumentation for enhanced information generation. Broadly, the working principle involves the *knock-off* of ions, molecular fragments, and neutral atoms in addition to the emission of electrons when the incoming ion beam impinges at the sample's surface. The resulting output is due to the behavior of the primary ion. The primary ions transfer momentum through the sample and consequently *knock* out other species.[143] A schematic of this process is represented in Figure 17.[130]

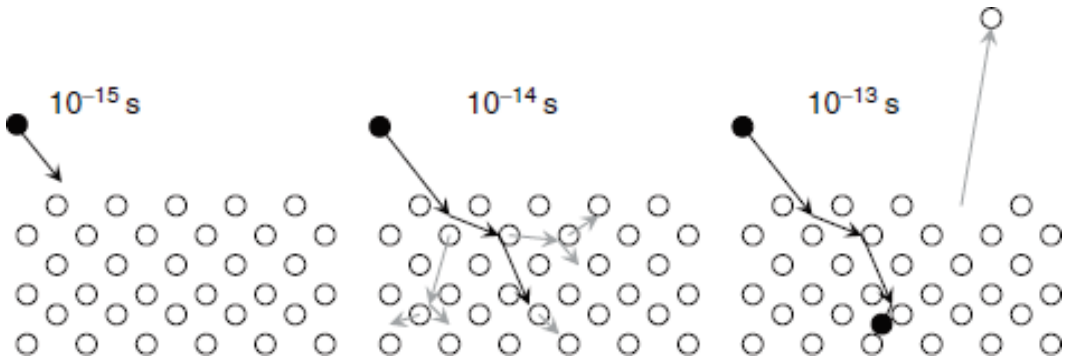

Figure 17: Knock out of ions through momentum transfer and typical time scales [130]

This phenomenon is termed a collision cascade, resulting in the ejection/desorption of atoms and molecules from the outermost layers. Furthermore, depending on the ion beam parameters, it is also possible to sputter large volumes rapidly, not only limited to surface material erosion. The extraction process is performed by the ToF analyzer, wherein the generated ions are transported under either a positive or negative extraction potential. The ions of the opposite polarity are attracted to the applied direction of bias into the analyzer, where they are sorted based on their 'time' of flight inside the analyzer and, which is proportional to their mass. Mathematically the following equations govern the analysis, wherein the terms are represented as: energy *E*, charge *z*, potential *U*, mass *m*, velocity *v*, distance *s*, and time *t*. Speed is proportional to the distance and inversely related to time. Kinetic energy is the {m/z ratio of the secondary ions and is given as,

$$E = zU = \tfrac{1}{2}\, mv^2$$

$$m/z = 2\, U\, \{t/s\}^2$$

A noteworthy mention: doubly charged fragments will show a mass-to-charge ratio, m/z equivalent to a singly charged fragment, with half the mass. A schematic representation of the functioning principle of the ToF-SIMS is shown in Figure 18.[131]

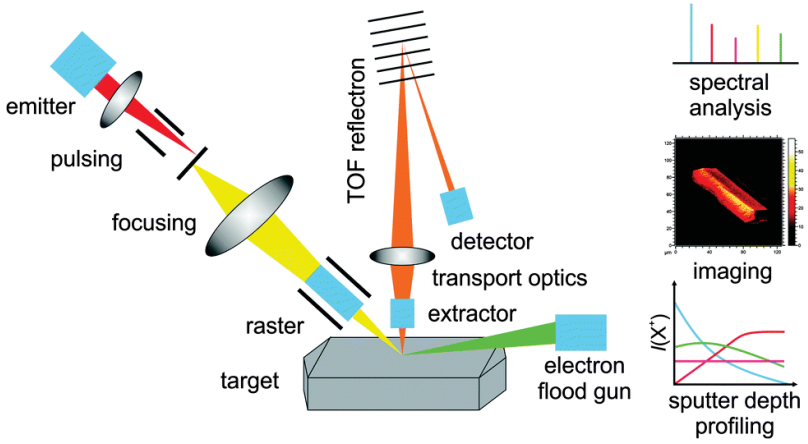

Figure 18: Functional principle of a ToF-SIMS instrument and options for surface and bulk analysis of solid samples by (i) mass spectrometric analysis of surface borne secondary ions, (ii) imaging of the lateral distribution of secondary ions, and (iii) sputter depth profiling [131]

ToF-SIMS allows chemical mapping, i.e., imaging of the distribution of chemicals on surfaces, as the beam is rastered over the sample. Furthermore, ToF-SIMS is capable of providing information about the bulk of the sample when operated in a depth profiling mode. Depth profiling is primarily aimed at providing information on the local composition of material beneath the surface.[132] It is achieved by sputter-induced material erosion upon ion bombardment, consequentially exposing the underlying area. A change in signal intensity as a function of time gives information about depth-dependent material composition. In combination with the pixel-wise information, also 3D-mapping of components can be achieved. It offers enhanced spatial and depth resolutions and higher specificity in detecting molecular species due to having high mass resolution.[133] The ToF-SIMS technique is semi-quantitative and complementary to the XPS technique which offers quantitative information on atomic composition and the chemical environment.

A large portion of the work in this dissertation relies on depth profiling of the nanotubes using ToF-SIMS. The working mechanism exploits a dual beam approach; a liquid metal ion gun {LMIG} for measuring and sputter erosion achieved using either a cesium {Cs} or oxygen {O_2} gun. The technique is especially advantageous when analyzing insulating samples such as zirconia nanotubes because charging issues are overcome by neutralization using low energy flooding during the cyclic process.[134,135]

Interpreting ToF-SIMS data

As mentioned previously, ToF-SIMS data is semi-quantitative. This is primarily due to the different ionization probabilities for varying species and depends on interaction parameters and subsequent desorption/ fragmentation. It is especially relevant when evaluating the presence of salts, organics, and inorganics. The type of bonding also influences the subsequent breakage pattern of surface species. Fragmentation of organics needs to be considered carefully as the molecules may not undergo breakage according to conventionally weak links as deciphered based on molecular chemistry. The fragmentation pattern in ToF-SIMS depends on the type of cleavage, possible molecular rearrangements {McLafferty}, and additional effects due to 'pushing' of/on/ into, i.e., edge and matrix effects.[136,137] Interpretation may not always be straightforward and information is gathered using a semi-quantitative analysis. This for example is ensured by investigating similar samples to avoid the influence of matrix effects; comparison of ratios rather than peak intensities to avoid variation in total ion yield. Furthermore, when investigating hierarchical or composite assembly in materials, sputter rates strongly depend on the sputtered material. Properties such as material hardness, density and even shapes can influence the resulting erosion by sputter beam. Additionally, when characterizing inorganic samples in the depth profile mode, it is important to consider the energy of the primary ion beam. Depth profiling results are plotted againstthe characteristic signals of the material in question and their relative intensity as a function of sputter time, a representative image is shown in Figure 19. [138]

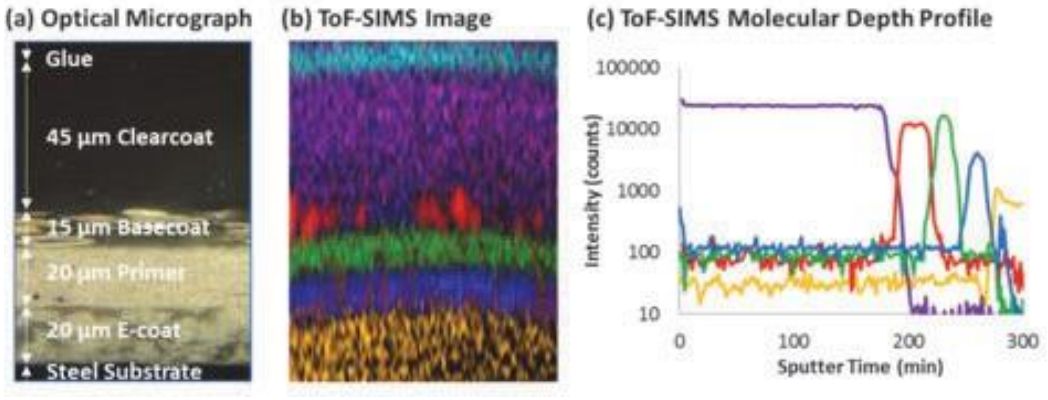

Figure 19: (a) Optical micrograph of the automotive paint multilayer cross-section, and (b) the corresponding ToF-SIMS secondary ion image showing the different layers. (c) The molecular depth profile of the paint layer using the Ar2000 cluster source, showing the intensity of the unique molecules in the clear-coat, base-coat, primer, e-coat, and the substrate as a function of time [138]

As a rule of thumb, the longer the sputtering time the deeper the interaction volume. An exception could be in the case of hard, heterogeneous materials where erosion is rather slow.[133, 139] Depth profiles are done in addition to surface analysis and are more suitable for multilayer analysis.

Examples of information provided via ToF-SIMS analysis

ToF-SIMS analysis provides a large amount of information pertaining to the presence of elements, molecules and compounds. Information on what is present on the surface of the materials under investigation, where it is located,, how is it interacting with the surface, how much of it is present, what state is something present on the surface to name a few. For example, consider a substrate made of zirconia nanotubes that is modified with organic molecules such as octadecylphosphonic acid {ODPA} and octylphosphonic acid {OPA} using different strategies, namely via soaking in a solution, also know as bulk immersion {BI} and alternatively by a soft lithography technique known as micro-contact printing {µCP}. In order to identify the successful deposition of the molecules onto the substrate and to differentiate one molecule from another, bearing the same functional group, during analysis characteristic molecular fragment signals and any variation in signal intensities are analyzed from ToF-SIMS data.

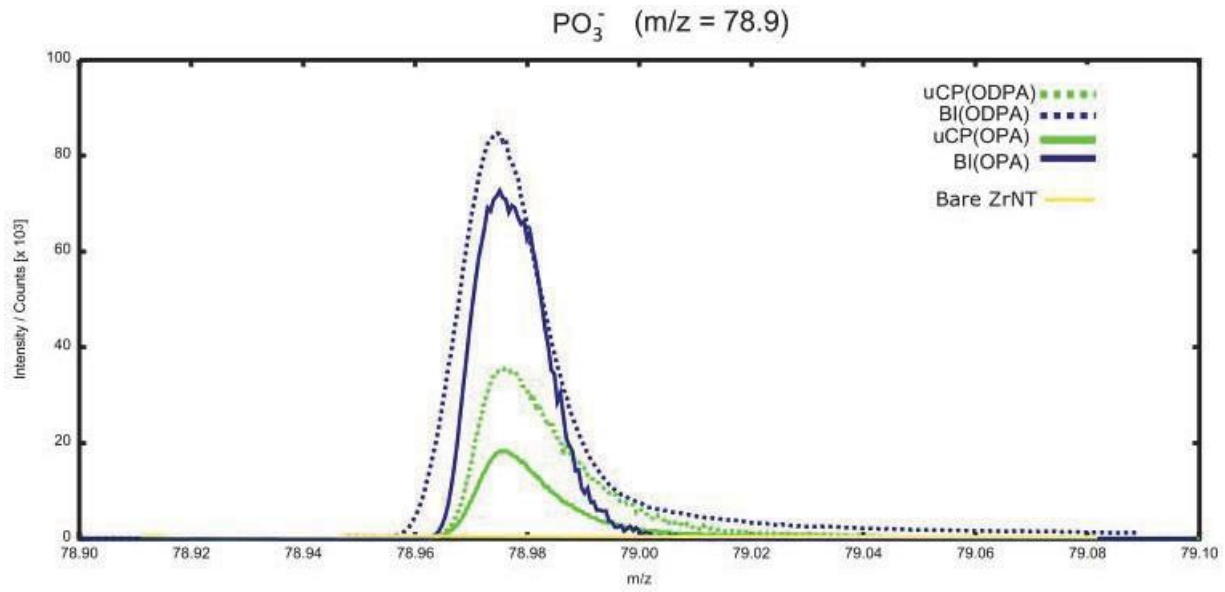

Figure 20 : ToF-SIMS analysis: Characteristic fragment (PO_3^- m/z = 78.90) of unmodified ZrNT, ODPA and OPA modified ZrNTs using bulk immersion (BI) and micro-contact printing (µCP)

In the graph, it is evident that the unmodified substrate shows no phosphonic acid fragments as compared to the modified substrates. Since ODPA consists of a longer carbon chain attached to the phosphonic group, and has better packing density[119], consequentially resulting in a larger PO_3^- peak, as is observed here in comparison to the short chain OPA molecules.

We can also see the effect the deposition strategy has, such that BI > µCP, this is perhaps due to the deposition of a greater number of molecules on the surface and also within the nanotubes during soaking. This is contrary to what happens when molecules are deposited via µCP, firstly a limited amount of molecules in total are transferred to the substrate. In addition to this, a majority of the molecules only remain on the tube mouths i.e., top most surface. Since, BI results not only in surface but also deposition of the organic molecules within the bulk of the nanotubes, we see a relatively higher signal intensity as represented by the higher peaks for both molecules, i.e., OPA and ODPA deposited via BI.

There are plenty other areas that exploit the versatility of the ToF-SIMS analysis technique, extending to the fields of biomolecule detection, protein confirmation, electrode material distribution etc.[131.132,139]

3.3.3. X-ray photoelectron spectroscopy

X-ray photoelectron spectroscopy {XPS} is often touted as the perfect complimentary surface characterization technique to ToF-SIMS due to the availability of quantitative information. It is a highly sensitive technique that provides information on the elemental composition, oxidation states, and bound states. The underlying working principle in XPS analysis exploits the role of the photoelectric effect.[140,141,142]

Upon irradiation, an electron is ejected from the inner orbitals of an atom by an X-ray photon of appropriate energy. The emission process is not limited to the generation of photoelectrons and may also result in the generation of Auger electrons. A stark difference between the two situations is that XPS generates core-shell electrons, whereas Auger electrons are a three-step process. With the XPS technique, the chemical composition and intrinsic electronic state of a sample are evaluated, based on the emitted electrons as a function of their distinct kinetic energies. A schematic representation of the photoelectron generation process and the XPS analysis technique is represented in Figure 21.[142]

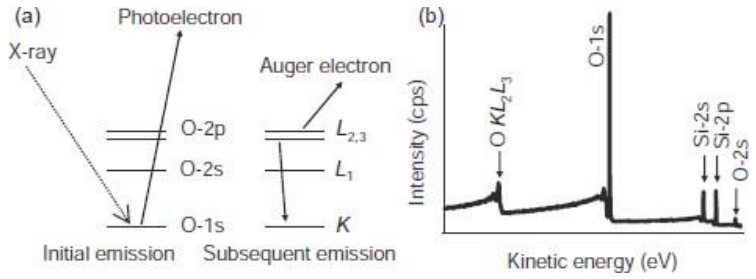

Figure 21: Schematics of (a) photoelectron and Auger emission; (b) XPS spectra from a silicon wafer with a surface oxide irradiated with Mg-Ka [142]

Since, the primary energy source is always known *hv*, which is a product of *Planck's* constant and frequency of the photon, and consequentially the binding energy of the ejected core level electrons can be determined by the following equation.[142]

$$E_b = hv - E_{kin} - S_A$$

Here, E_b is the binding energy of the target electron to the atom, *hv* is the photon energy of the X-ray, E_{kin} is the kinetic energy of the electron and $(f)_A$ as the work function of the analyzer. Since the analysis is performed by assessing the chemical shift of the photoelectron peak energy, any intrinsic changes in bonding behavior and neighboring atom interaction may be determined as a shift in spectral data in the form of variation in peak width, shape, and intensity.[143]

Within this thesis, XPS was used for the quantification of SAMs on SAM-modified substrates via two different functionalization strategies, as mentioned in earlier sections. SAM quantification is based on surface coverage, type of molecule, and the deposition technique. The quantification of the surface deposition is complemented with ToF-SIMS in the depth profiling mode, for SAM-modified nanotubes.

3.3.4. Other methods

This section is written as a subsection in the characterization methods, as the techniques mentioned here are not limited to primary characterization methods {SEM-EDX, XPS and ToF-SIMS} that were focused on extensive chemical and physical, surface analysis. Herein, the 'other methods' investigate a wide array of properties not restricted to surface analysis.

Optical microscopy

Optical microscopy involves using a light source and lenses to illuminate and generate magnified micrographs of a given material. The material analysis entails the investigation of chemical and microstructure investigation. The upper limit of magnification of optical microscopes is ~1000X, because of the limited resolving power of visible light. A schematic representation of the working principle of a compound light microscope is represented in Figure 22.[144,145] As shown in the figure, the objective lens is that which is near the object and it forms a real, inverted, magnified image of the object. This image thereafter serves as the object for the second lens. The viewing lens is known as the eyepiece, which functions like a simple microscope or magnifier for the final image.

It produces an image, which is enlarged and virtual. When the final image is formed at a near point, the first inverted image will be within focal distance. When the final image is formed at infinity the first inverted image will be at focal distance and ultimately, the final image is inverted with respect to the original object.

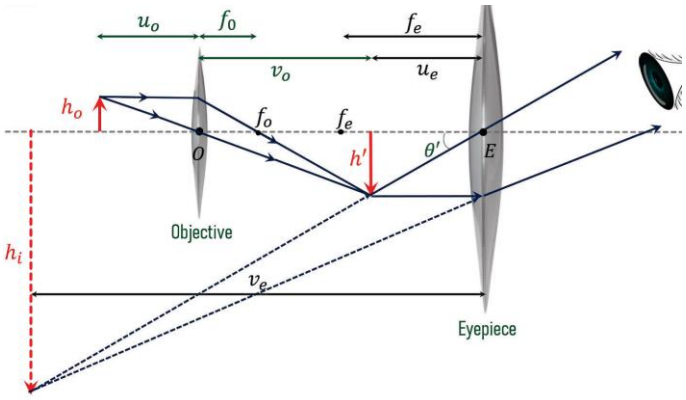

Figure 22: Schematic of the working principle for a compound microscope [145]

The type of images formed depends on the illumination technique. Transparent materials are illuminated from below and solid {opaque} objects by passing light through bright field analysis or in dark field mode around the objective lens. For crystalline materials, polarized light may be used to determine crystalline orientation.

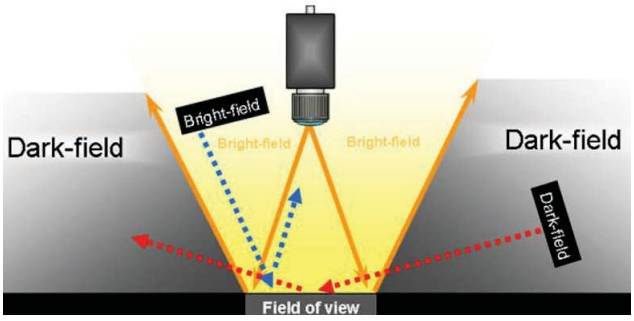

Figure 23: Schematic representing bright field and dark field analysis [144]

Unlike in the case of bright field lighting, wherein reflected light is imaged, in dark field lighting only the scattered light is captured. Hence, by imaging only the scattered light, defects around surfaces and edges appear prominently within the image as they are the things that best scatter light.

Optical profilometry

Optical profilometry is a technique that uses light instead of the physical probing of surfaces. It is used in topographical studies resulting in three-dimensional data of the probed surface.[146] A schematic of the working principle of an optical profilometer is represented in Figure 24.[147]

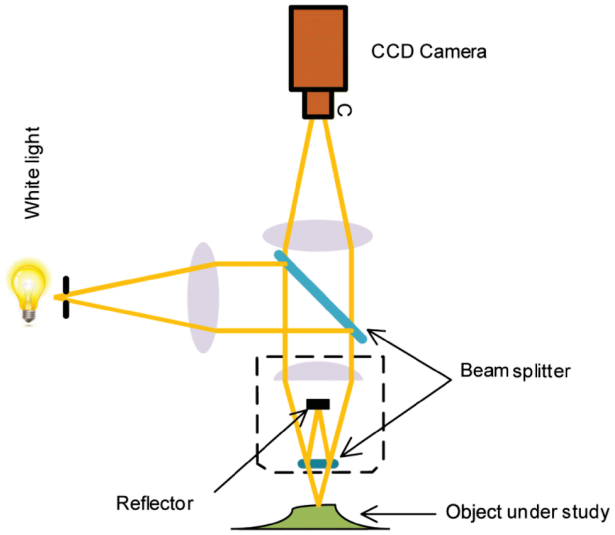

Figure 24: The working principle of optical profilometer [148]

Optical profilometry {confocal microscopy/interferometry} is a non-contact imaging method for observing and characterizing the topography of surfaces over measurement ranges from tens of µm2 to a few mm2, with a lateral resolution of 200 nm and depth resolutions from nm to several mm.

X-ray Diffraction (XRD)

Diffraction is the phenomenon of 'waves' spreading around obstacles. In XRD, X-rays interact with matter to determine the crystallographic structure of a material. When an incident beam interacts with the atomic planes of crystals, it generates interference patterns.[140] These patterns tend to be intrinsically specific. The analysis involves measuring the intensities and scattering angles of the X-rays leaving the surface of the material.[149] Two types of interference are observed; constructive, i.e., when the wave behavior is additive, or destructive when waves are subtractive. Both phenomena are governed by Bragg's law. A schematic of interference at crystallographic planes is shown in Figure 25.[140]

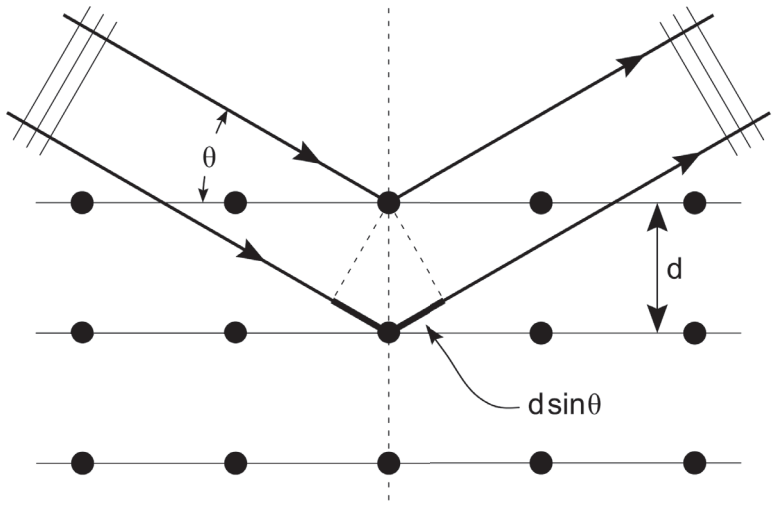

Figure 25: Schematic illustration of the Bragg equation with incident and reflected X-rays on two scattering planes, showing the lattice distance d, the half scattering angle 8, the wavelength il and the path difference defined by Bragg's law [149]

Braggs law is numerically represented in the following equation,

$$2.d.sinJ = nil$$

Here, *d* is the inter-planar spacing, 8 is the angle of incidence and *n* is an integer and *il* is the wavelength of the incoming beam.[148,150] XRD can be used to determine the orientation of the individual grains of a crystal and also to identify crystal structures in unknown substances as X-Ray wavelength is in the range of atomic spacing and crystals make precise diffraction gratings

Contact Angle Measurements

An angle that is measured on the surface of any material through a droplet at the solid-liquid-vapor interface may be defined as the resulting contact angle.[151] Alternatively, as the wettability of a surface, i.e., the capacity to promote interfacial surface interaction when liquids come in contact with a solid surface.[152] The type of liquid used influences the contacting response. The final shape of the droplet indicates the extent of wettability, such that complete wetting happens when a liquid film is formed. Film formation is observed due

to droplet coalescence and spreading on the area of contact, and such surfaces are termed hydrophilic.[153] Alternatively, when liquids '*ball up*' to minimize surface energy and form nearly spherical droplets, such interactions are termed hydrophobic.[154,155] The surface energy is calculated via the Young-Laplace equations as shown in the following, it defines the strength of the solid-liquid interface formed.[161]

$$y_{sg} = y_{sl} + y_{lg} * COS(0)$$

Herein, the surface energy is denoted using y and the subscripts: s, l and g, stand for solid, liquid and gas, respectively, as are represented in Figure 26.[154]

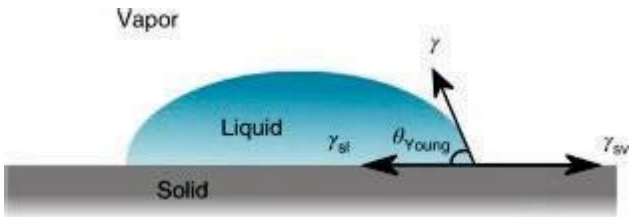

Figure 26: A drop of water on an ideal solid substrate [162]

A hydrophilic material will prefer to minimize its surface energy by forming an interface with water instead of air, and this energy difference determines the eventual contact angle.[152,156] A schematic representation of the influence of surface energy and surface tension concerning wettability is shown in Figure 27.[157] A rule of thumb is that low-energy surfaces inhibit wetting, and high-energy surfaces promote wetting. Contact angle analysis may be performed using various liquids such as water, oil, solvents etc.

Water Contact Angle (WCA)

In the context of this work, contact angle measurements were extensively performed using water and hence, will ubiquitously be refereed to as water contact angles {WCA}. Herein, WCA provided a fast and easy strategy to confirm changes in surface modifications as a function of wetting behavior. Solid surfaces subjected to physical surface modification as in the case of nanoporous or nanotubular oxide formation, showed a change in wettability.

Alternatively, for surfaces chemically modified via SAMs, the successful deposition of SAM modification was primarily evaluated as a function of the wetting response.

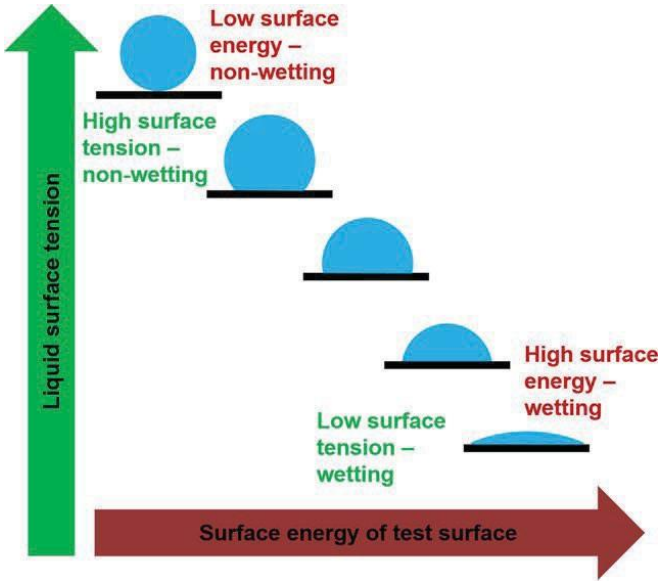

Figure 27: Influence of surface energy and surface tension in wettability response [157]

SAMs used in this work are long-chain carbohydrates and are hydrophobic. Hence, when a metal oxide undergoes successful chemical modification, a change from hydrophilic behavior shown by MOs {due to surface hydroxyl groups} is transformed into hydrophobic tendencies due to an intermediate organic molecule layer consisting of hydrophobic tail groups.

Cassie- Baxter (CB) state and its effect on nanotubular surfaces

The Cassie- Baxter {CB} state is the name given to a physical phenomenon involving the formation of a nearly spherical water droplet atop of a homogeneously rough surface. This state entails a depiction of real systems which consist of micro-roughnesses. CB equations evolved from modified Young and Wenzel equations, with a specific focus on on porous systems, where a liquid does not penetrate the grooves on rough surface and leaves air gaps entrapped under a contacting droplet.

A schematic representation of the transition from homogeneous flat surface, i.e., Young's state, to the incorporation of micro-roughness in the Wenzel state, followed by the addition of trapped air in the asperities under the CB regime and is depicted in the following figure.

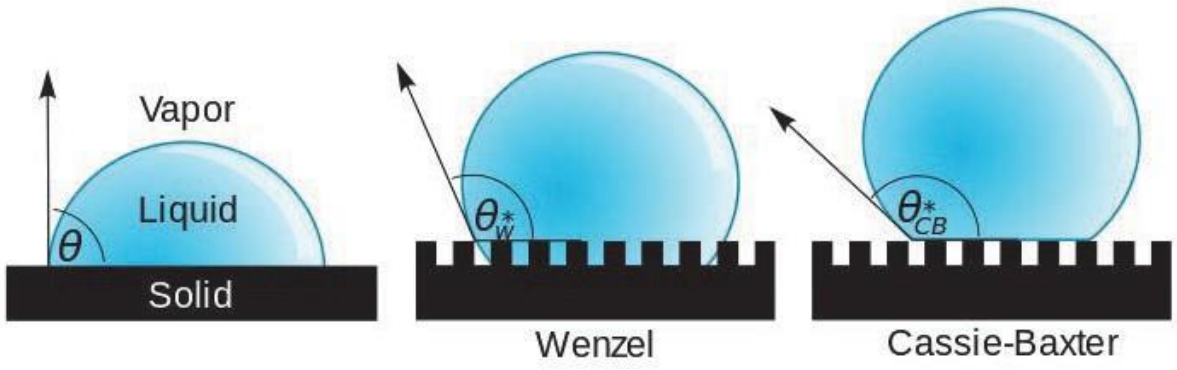

Figure 28: Different contact angle scenarios [158]

When water has a contact angle between 0°< e < 90°, then the surface is termed hydrophilic, whereas a surface producing a contact angle between 90° < e < 180° is hydrophobic. In the special cases where the Contact angle is e > 140°, then it is known as superhydrophobic. A noteworthy mention is that the water repellency of biological objects is widely attributed to the Cassie-Baxter equation, an example of the same is the Lotus effect. This results in the rolling-off of water droplets on certain leaf structures such as the lotus leaf, water lily pads, etc., that consist of hydrophobic micro-nano hairs on the surface of the leaf bed.

Ultraviolet- Visible light Spectroscopy (UV-Vis Spectroscopy

Spectroscopy, as a technique, deals with the measurement and interpretation of the interaction between matter and electromagnetic radiation. UV-Vis spectroscopy specifically deals with the interactions of ultraviolet and visible regions of the electromagnetic spectrum. Once incident light interacts with a specimen, one or a combination of reflection, absorption, or transmittance happens. A schematic of a dual-beam UV-Vis spectrophotometer is shown in Figure 29.[159]

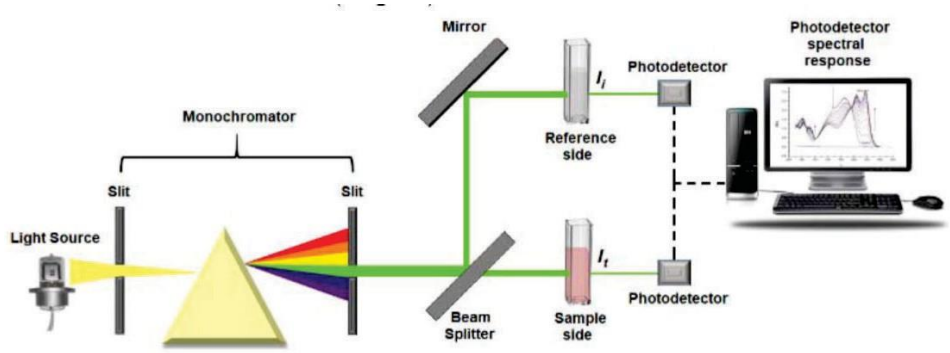

Figure 29: Schematic of the working principle of a dual beam UV-Vis spectrophotometer [160]

In the identification of dissolved components in solutions, absorption behavior may be used to identify the presence of existing species in a known medium under light-induced excitation in the rt-band of molecules. Excitation occurs as a result of electron transfer from the Lowest Unoccupied Molecular Orbital {LUMO} to the Highest Occupied Molecular Orbital {HOMO} as shown in Figure 30.[160]

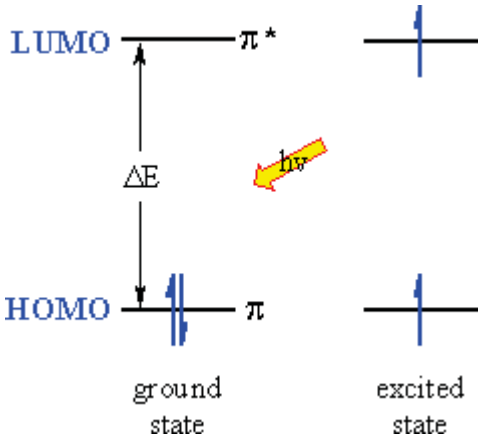

Figure 30: Orbital excitation upon light absorption [160]

Light absorption is related to the relative concentration of the constituents in a carrier solvent. Concentration can be determined using the Beer-Lambert law and is represented in the

following equation,[158]

$$\log\frac{I_0}{I} = A = C * \varepsilon * d$$

The absorbance is denoted as A, and the intensity of light entering and exiting the medium is as I_o and I, respectively. The path length of the sample d in cm, c is the concentration. Absorption is intrinsic to the specific media, which is also independent of substance concentration at a particular wavelength even in dilute solutions and E is the molar extinction coefficient. The extinction coefficient is distinct for characteristic materials and wavelength of light.[161] This technique allows for facile detection and easy quantification, for e.g., quantification of drug release from nanocontainers.

Tribological analysis via automated scratch test

The science of friction-related wear and fatigue is broadly investigated under tribological analysis. It focuses on how interacting surfaces behave under static conditions, such as with composite adhesive layers, or under dynamic conditions during relative motion between the surfaces.[162]

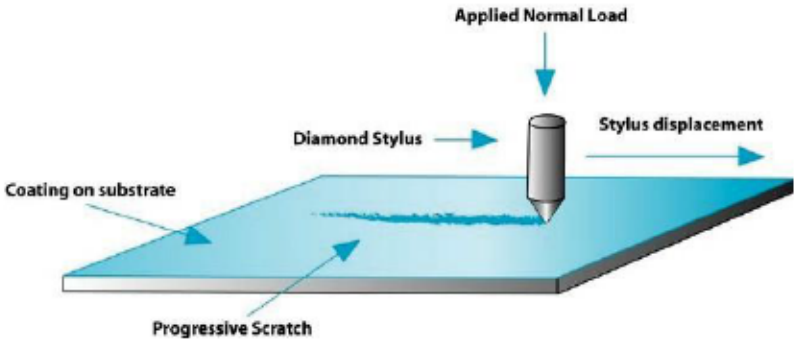

Figure 31: Schematic of a representative scratch test [163]

A scratch test is typically a dynamic analysis performed using a sliding tip on the work surface. Testing includes linear progression in loading to see stress response as a function of the coefficient of friction {CoF}}.[164]

The CoF is a measure of the amount of friction that exists between two surfaces in contact with one another, providing information on the ability to resist motion or alternatively slipping and sliding over one another. Alternatively, it offers insights into the adhesion behavior between layers.[165] A schematic of a representative scratch test is shown in the previous page in Figure 31.[163] The indenter may be diamond-tipped, spherical, or hexagonal heads and maybe be made of varying types of materials such as silicon carbide, zirconia, etc., to name a few. This technique is extremely useful to determine adhesion strength of coatings to the underlying substrate and may also be used to evaluate mechanical properties such as resistance to scratch and delamination of such coatings.

4. PUBLICATION HIGHLIGHTS

This chapter consists of the following peer-reviewed indexed publications and corresponding supplementary information, as appearing in print along with an outline of the individual author contributions;

4.1. Zirconia nanotube coatings - UV-resistant superhydrophobic surfaces

Swathi Naidu Vakamulla Raghu, Khajidkhand Chuluunbandi and Manuela Sonja Killian

Surfaces and Interfaces, 26, 2021, 101357, https://doi.org/10.1016/j.surfin.2021.101357

Author contribution

***SNVR**: Experimental design (Anodization, Setup, UV-measurements, Functionalization, Characterization – SEM, XRD, OM, WCA, Data analysis – compilation, Writing-original draft, review-editing*

Khajidkhand Chuluunbandi: Sample preparation (Ti anodization), WCA measurements and ToC -figure

Manuela Sonja Killian: Conceptualization, ToF-SIMS and XPS measurement and analysis, Reviewing-editing

4.2. Wetting behavior of zirconia nanotubes

Swathi Naidu Vakamulla Raghu and Manuela Sonja Killian

RSC Advances, 2021, 11, 29585–29589, https://doi.org/10.1039/D1RA04751E

Author contribution

***SNVR**: Conceptualization, Experimental design (Anodization, Setup, UV-measurements, Functionalization, Characterization – SEM, XRD, WCA, Data analysis (ToF-SIMS, XPS and ImageJ) – compilation, Writing-original draft, review-editing*

Manuela Sonja Killian: Conceptualization, ToF-SIMS measurement, XPS measurement and analysis, Reviewing-editing

4.3. Functionalization strategies to facilitate multi-depth, multi-molecule modifications of nanostructured oxides for triggered release applications

Swathi N.V. Raghu, Gabriel Onyenso, Shiva Mohajernia and Manuela S. Killian

Surface Science, 719, 2022, 122024, https://doi.org/10.1016/j.susc.2022.122024

Author contribution

***SNVR**: Conceptualization, Experimental design (Anodization, Drug-release Setup, Functionalization, Characterization – SEM, XRD, WCA, UV-Vis spectroscopy, Data analysis (ToF-SIMS) – compilation, Writing-original draft, review-editing*

Gabriel Onyenso: Sample preparation (Zr anodization), Drug-release experiment- timed measurements and ToC - figure

Shiva Mohajernia: XPS measurement and analysis, Reviewing-editing

Manuela Sonja Killian: Conceptualization, ToF-SIMS measurement, Reviewing-editing

4.4. Nanodentistry aspects explored towards nanostructured ZrO_2: immobilizing zirconium-oxide nanotube coatings onto zirconia ceramic implant surfaces

Swathi N.V. Raghu, Patrick Hartwich, Adam Patalas, Mateusz Marczewski, Rafal Talar, Christian Pritzel and Manuela S. Killian

Open Ceramics, 14, 2023, 100340, https://doi.org/10.1016/j.oceram.2023.100340

Author contribution

***SNVR**: Conceptualization, Experimental design (Anodization, Membrane transfer, Characterization – SEM, XRD, OM, stability tests, Data analysis (ToF-SIMS, Profilometry, STA, ImageJ) – compilation, Writing-original draft, review-editing*

Patrick Hartwich: ToF-SIMS measurement

Adam Patalas: Scratch test, Optical profilometry – Setup, data acquisition and discussion

Mateusz Marczewski: Scratch test sample preparation and measurement

Rafal Talar: Discussion and Reviewing-editing

Christian Pritzel: STA measurements and discussion

Manuela Sonja Killian: Conceptualization and Reviewing-editing

4.1. Zirconia nanotube coatings - UV-resistant superhydrophobic surfaces

Swathi Naidu Vakamulla Raghu, Khajidkhand Chuluunbandi and Manuela Sonja Killian

Surfaces and Interfaces, 26, 2021, 101357, https://doi.org/10.1016/j.surfin.2021.101357

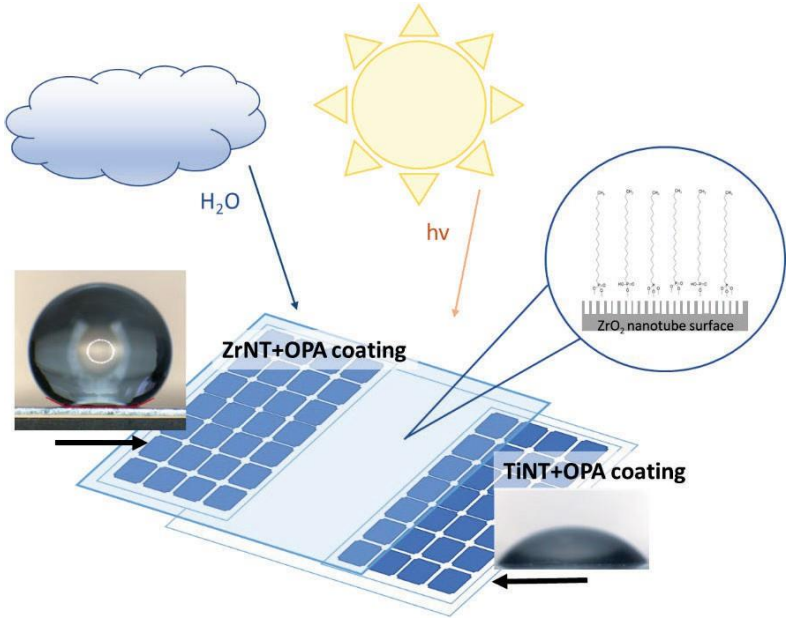

ToC-4.1- Superhydrophobic SAM modified ZrNT coatings for outdoor applications

The article in this section introduces the synthesis of zirconia nanotubes {ZrNTs} via a single-step, one-pot electrochemical anodization strategy. The highlight remains in avoiding the use of pre-etching steps with hydrofluoric acid {HF} acid and addresses the first objective of this dissertation:

'*Establishing an anodization protocol to minimize operator-risk and optimization of experimental parameters to develop robust nanotubular geometries.*'

In addition to this, an introduction into the possible surface modification of zirconia substrates, compact oxides, and ZrNT is successfully performed. The functionalized zirconia substrates are

compared to reference material titania {TiO_2} in the form of compact oxide, and nanotubes {TiNT} respectively. The Zr and Ti substrates were rendered hydrophobic using octadecylphosphonic acid {OPA} SAMs, and these specimens were further investigated based on their performance as superhydrophobic surfaces aimed toward self-cleaning applications for outdoor surfaces. Due to the inert nature of Zr, the SAM-modified Zr substrates had superior longevity and hydrophobic behavior even after prolonged periods under several experimental conditions: exposure to sunlight, simulated UV exposure, and storage in aqueous media. This result was in strong contrast to the semiconducting Ti counterparts that underwent catalytic degradation of the hydrophobic organic coatings due to the photocatalytic activity of the underlying substrate. Therefore, OPA-modified ZrNTs are touted as superior candidates for such applications.

Contents lists available at ScienceDirect

Surfaces and Interfaces

journal homepage: www.sciencedirect.com/journal/surfaces-and-interfaces

Zirconia nanotube coatings - UV-resistant superhydrophobic surfaces

Swathi Naidu Vakamulla Raghu [a,b], Khajidkhand Chuluunbandi [b], Manuela Sonja Killian [a,b,-]

[a] Chemistry and Structure of Novel MaterialsJ University of SiegenJ Paul-Bonatz-Str. 9-11J Siegen 57076J Germany

[b] Department of Materials ScienceJ Institute for Surface Science and Corrosion (LKO)J Friedrich-Alexander-University of Erlangen-NurembergJ Martensstrasse 7J Erlangen 91058J Germany

ARTICLE INFO

Key4ords:
Optical coatings
Self-assembled monolayer (SAM)
ToF-SIMS
XPS zirconia
Anodization
Nanostructure
Superhydrophobicity
Self-cleaning

ABSTRACT

Surface modifications influence material interactions such as wettability, imparting hydrophobicity or hydrophilicity. Mainstream research focused on enhancing product shelf-life directs attention towards superhydrophobic surfaces (SHS). SHS offer several benefits for out-door applications such as self-cleaning, anti-soiling, anti-mist etc. Recently, such surfaces were created by hydrophobization of anodized titania, which although effective lacked a long-term stability of their hydrophobic modifications due to it being susceptible to UV-mitigated degradation. In light of this situation, ZrO_2-nanotubes are evaluated with regard to their application as transparent UV-stable superhydrophobic coatings. Nanostructured oxide surfaces are created via single-step electrochemical anodization. The absence of HF acid-based pre-etching steps offer a safe and alternatively a green synthesis route. Anodized oxides are modified using octadecylphosphonic acid (OPA) self-assembled monolayers, demonstrate superhydrophobicity and are at par with conventionally employed coatings such as PTFE, PFDPA and PTES. The OPA-coatings are evaluated for their mechanical stability under a jet of water, chemical stability under indirect sunlight irradiation in air/water and direct UV exposure. Zirconia nanotubular films were evaluated for optical transparency using light microscopy and surface wettability of the different zirconia-composites was compared to the model system - titania. Structural and compositional differences of the SAM layer upon time dependent decay were analyzed with X-ray photoelectron spectroscopy.

1. Introduction

Surface modifications have been widely employed in materials as a means of pre-treatment and in some cases as the final step that offers the required functionality. Passivating surfaces via electrochemical anodization can create micro- to nanostructured oxide layers [1,2]. Tailoring material surfaces can influence subsequent interactions such as the wetting behavior. Surface wettability plays a vital role in developing super-hydrophobic surfaces (SHS). SHS surfaces are of interest due to their self-cleaning properties owing to their high contact angle $> 150^{\circ}$ resulting in non-wetting behavior and are ideal for outdoor applications that require little to no interaction with ambient environmental conditions. Titania nanostructures have garnered significant interest owing to their multifaceted attributes and researchers have successfully created SHS on anodized titania by hydrophobization.[3-6] A comprehensive overview can be found in Lai et al even advanced systems like switchable superhydrophobic patterns have been demonstrated [7]. Titania is reported to have photocatalytic properties allowing for efficient decomposition/degradation reactions [8]. However, this feature works against SAM coated titania optical systems, especially for outdoor applications, as it is susceptible to increased degradation. In light of this situation, it would be advantageous to have a material that is not as photocatalytically 'active', but offers comparable or superior SHS properties.

Zirconia is a valve metal belonging to the group IV- Titania family and having a wide band gap in the range of 5-7 eV, resulting in lower absorption in certain spectral regions [1,2]. Zirconia offers impressive electrical, optical, chemical and mechanical properties [9–11]. Metal-oxide nanostructures such as ZrO_2 can be synthesized via electrochemical anodization involving the systematic growth and dissolution of metal-oxide layers in the presence of an electrolyte in an electrochemical cell. Organic electrolytes promise a high degree of self-ordering in this process and often require a harsh hydrofluoric (HF) acid pre-etching step in order to produce well-ordered nanoporous structures. In this work, we produce distinct, highly-ordered and stable nanotube arrays using a modified variation of the fluoride based organic electrolyte as prepared in Amer et al. [12]. The possibility of creating nanostructures in a single step process without the use of a strong HF acid pre-etching step makes this a relatively less toxic/hazardous, more

- Corresponding author.
E-mail address: Manuela.Killian@uni-siegen.de (M.S. Killian).

https://doi.org/10.1016/j.surfin.2021.101357
Received 26 February 2021; Received in revised form 16 July 2021; Accepted 17 July 2021
Available online 24 July 2021

user and environmentally friendly practice whilst being strongly reproducible.

Zirconia nanostructures have potential applications in the field of catalyst production, electrodes, fuel cells and more recently as bio-ceramic implants owing to their non-toxic nature and ability to promote cell growth [10,13,14]. Anodized ZrO_2 substrates have high surface energies and tend to promote enhanced adhesion/binding of thin organic films on the metal oxide surface capable of eliciting different surface behavior [15]. Spontaneously forming SAMs can readily modify surfaces into SHS and have been extensively researched and developed for a myriad of applications ranging from anti-fog coatings, anti-dirt/freeze, drag reducing surfaces to anti-bacterial biomedical surface modifications [16–20]. SHS in addition to self-cleaning behavior, enhance the shelf life and prolong functionality of the underlying working surfaces. Many techniques have been developed in order to form effective SHS via SAM functionalization. SAMs can be produced on oxide surfaces, e.g., through PVD, electro-deposition, micro-contact printing and the more commonly used immersion in bulk solution [17,21–24]. The prerequisites while choosing SAM molecules for the purpose of creating SHS on zirconia are strong binding affinity and integrity of the single layer coverage. Phosphonate head groups have been reported to easily attach to a wide range of oxide surfaces including ZrO_2 [25–28]. Gawalt et al. investigated the adsorption of octadecylphosphonic acid ($CH_3(CH_2)_{17}PO_3H_2$, OPA) on titania, the same was further pursued for other metal oxide surfaces and Gao et al. [27,29] reported that phosphonic acids react strongly with ZrO_2. The reaction mechanism suggests that binding occurs at the interface via P-O-M (M is for metal) bond formation. Metal oxides are terminated with surface hydroxyl groups (M-OH) and as a result of condensation reactions with phosphonic acid groups (P-OH), form P-O-M bonds, imparting a covalent bond formation.

Chang et al. mention the possibility of using ZrO_2 in the fabrication of transparent optical devices [30]. It has a niche application area as optical coating as it is a high index material that can be used from near-UV to mid-IR range. Composites made of ZrO_2 coated with OPA self-assembled monolayers (SAMs) may be capable of acting as optically clear super-hydrophobic coatings, which could be interesting, e.g., for solar cell or window coatings.

The present work investigates the fabrication of ZrO_2 structures consisting of compact oxide and nanotubular oxides. The morphology of these oxide surfaces was characterized using SEM and XRD. In addition to anodization procedures, the integrity of OPA SAMs on amorphous zirconia and titania (as a reference material) will be extensively analyzed. Emphasis is placed on the monolayer stability upon ambient as well as water-immersed, sunlight exposure and UV light irradiation. (Super-)hydrophobicity was assessed as a measure of wettability of the composite surfaces using water droplets via sessile drop contact angle measurements. The mechanical stability of the OPA SAM under a continuous water jet was also assessed as a function of decreasing hydrophobicity. Surface analysis furthermore was performed via ToF-SIMS and XPS.

2. Results and discussion

When Zr is anodized under appropriate conditions in an organic electrolyte, a resulting oxide film showing uniform nanotube arrays can be achieved as represented in Fig. 1. (Anodization of zirconia: SEM micrographs – (a) anodized ZrO_2 top, (b) anodized ZrO_2 cross-section and ZrO_2 XRD (inset)). The SEM micrographs depict circular morphology of the individual ZrO_2 nanotubes and an average layer thickness of 9 µm obtained after 30 min of anodization. The structural integrity of the coatings formed in the absence of pretreatment step(s) as reported in this work are comparable to those reported for samples undergoing pre-treatment requiring immersion in HF-containing solutions. This growth model, although identical in morphology to previously reported morphologies, in reality reports on improved production quality while minimizing fabrication duration and fabrication hazards [31–33]. The oxide layers formed are thick, continuous and robust on all geometries of substrate materials investigated. Fig. 1. ((b)-inset) shows X-ray diffraction (XRD) analysis of the ZrO_2 nanostructures. The as-anodized samples consist of amorphous ZrO_2 nanotube arrays as the signals appearing at 35° (002), 37° (101), 48° (102) and 64° (003) are characteristic facets of Zr metal, which is the substrate in this case [34, 35]. The coatings are transparent to more than 80% of white light (cf. Supporting information Fig. S5.)

The nanostructured ZrO_2 layers were rendered hydrophobic by adsorption of a SAM of OPA molecules, a long chain aliphatic phosphonic acid. The hydrophobicity of the layer depends on the extent and quality of P-O-M bond formation. These bonds elicit strong binding forces due to the coordination of phosphoryl oxygen to the Lewis acidic sites on the surface. It is expected that alkane phosphonic acid densely packed films assemble as a result of hydrogen-bonding between the head groups along with Van der Waals interaction with the methyl units [29]. Phosphonic acids were previously shown to form stable bonds to ZrO_2 [27]. Additionally, surface energy, topography and homogeneity also play a crucial role in influencing the hydrophobicity. Functionalized nanostructured surfaces reportedly trap larger volumes of air within their asperities in order to stabilize the Cassie-Baxter state responsible for the super hydrophobicity as depicted in Fig. 2 **a.** (Schematic-Cassie-Baxter model)[36]. Native oxide is the air formed oxide layer present on the as-received (and cleaned) Zr foil [33]. Compact oxide (SEM image can be found in Fig. S1) and nanotubular ZrO_2 were obtained by anodization. The controlled formation of anodic oxide layers shows a clear improvement in hydrophilicity, cf. Fig. 2 **b. (**Comparison of surface hydrophobicity pre and post modification with ODPA SAMs on anodized ZrO_2**)**, which indicates an improved oxide quality and purity of the anodic layers. Due to the increased surface area, the nanostructure permits fluid infiltration and consequently enhances wetting. Post SAM functionalization, only a moderate increase in hydrophobicity (35°to 75°± 3°) is observed for native ZrO_2 whilst the compact oxide

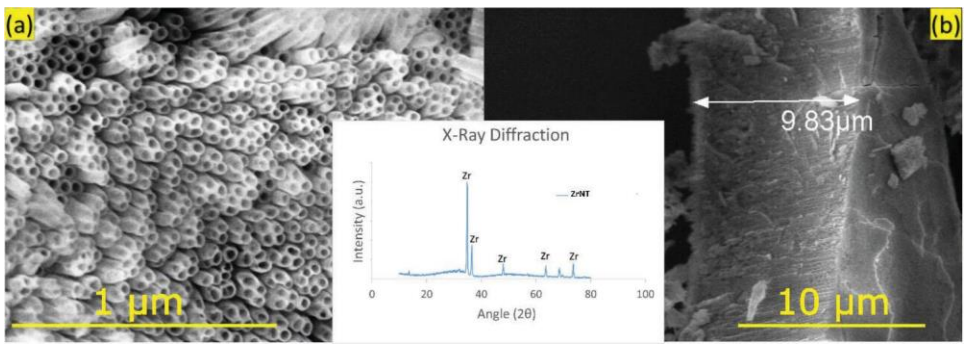

Fig. 1. Anodization of Zr: SEM micrographs (a) anodized ZrO_2 top, (b) anodized ZrO_2 cross-section and ZrO_2 XRD (inset)

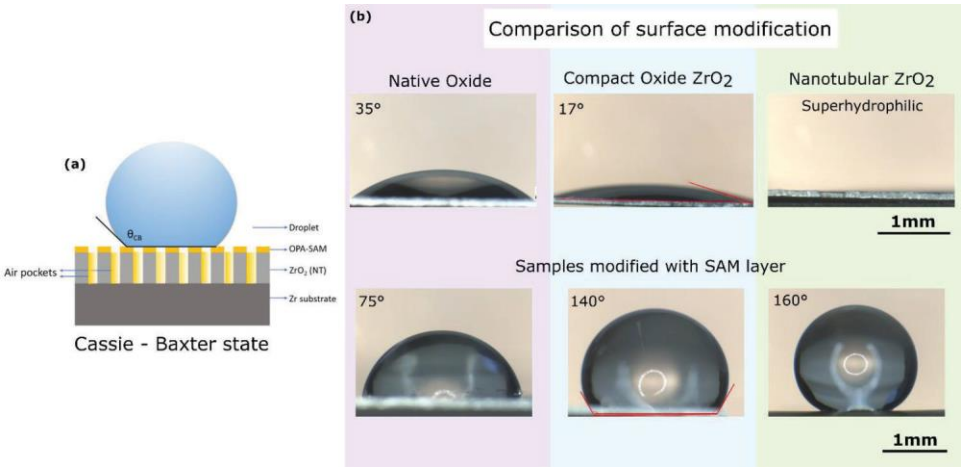

Fig. 2. (a) Schematic - Cassie-Baxter model, (b) Comparison of surface hydrophobicity pre and post modification with ODPA SAMs on nanotubular ZrO_2

shows a clear enhancement in contact angle (17° to 140° ± 2°), as shown in Fig. 2b. The nanotubular ZrO_2 can even be switched from superhydrophilic (0°) to superhydrophobic (155°± 5°) upon simple immersion in an OPA solution. The tube length did not influence the hydrophobic nature of the coating. [37] Additionally, the presence of the OPA- SAM was confirmed via ToF-SIMS and the spectrum can be found in the Supporting Information, Fig. S2. We conclude that OPA forms a superhydrophobic self-assembled monolayer on zirconia nanotubes.

In this work, we test 'OPA – SAM based SHS ZrNT' composite as UV-stable superhydrophobic coatings. The intended use of the material is to function as an optically clear self-cleaning surface, which may improve longevity of any underlying working surface, e.g., in outdoor solar cells under irradiated conditions. Sunlight consists of three major components, visible light, ultraviolet light (UV) and infrared radiation (IR). UV light components that can potentially influence within the earth's atmosphere are further split into long wave UVA (315–400 nm) and short wave UVB (280–315 nm). UVA light makes up a larger portion and penetrates deeper. In order to test the stability of the composite systems, the first experimental setup involves indirect irradiation (ambient and water-immersed) wherein samples are subjected to UVA light only, as clear glass (windows and containers) that are transparent to visible light absorb nearly all UVB [38,39]. Triplicate sample sets were assembled onto a windowpane with the SAM face-side towards the window, exposed for a period of up to 50 days. The SAM stability was evaluated by contact angle measurements after 1, 5, 14, 21 and 50 days. Fig. 3 **(Top),** (Wettability measurements of OPA modified ZrO_2 nanotubes upon sunlight exposure in air (Contact angle versus Time)) shows the change in hydrophobicity with respect to the exposure time, solid lines are only to guide the eye and dotted lines are the mathematical progression based on a fit. It is interesting to note that, a linear regression would have sufficed for TiCO samples, wherein a continuously decaying WCA is observed. However, the same may not be ideal in the case of Zr-substrates due to WCA stabilization and therefore results in a poor fit. Zirconia nanotubes have an initial contact angle well above 160°± 2°; the water droplets kept rolling off the surface and actually could only be measured on defective sites of the material (cf. Supporting Information, Fig. S3). As a reference material, commonly used nanostructured titania was used as represented in the Supporting Information, Fig. S4. In comparison, the titania nanotube samples show superhydrophobicity at

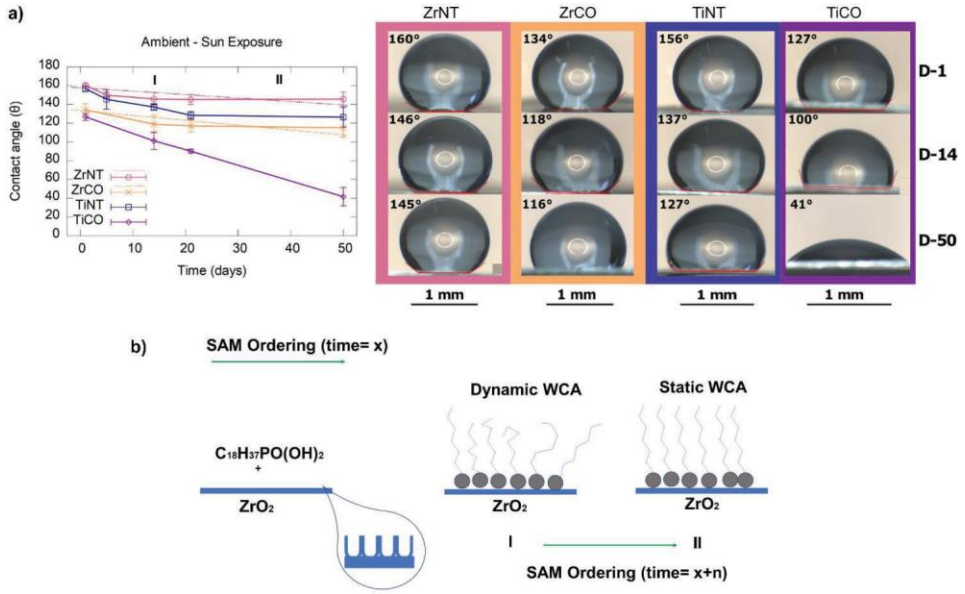

Fig. 3. (a) Wettability measurements of OPA modified oxide surfaces upon sunlight exposure in air (contact angle versus time, solid lines are guide to the eyes, dotted lines represent the theoretical curve progression according to static Cassie-Baxter- model) and corresponding contact angle images; (b) Schematic representation of the initial change in WCA as a function of time dependent SAM ordering.

(156°± 2°) on day zero. The slightly lower value may be indicative of a relatively lower initial coverage density of OPA molecules. Both ZrNT and TiNT show a similar rapidly decreasing trend in hydrophobicity with an average decrease of (15± 3°) in contact angle measurements within the first 5 days after synthesis. A possible explanation for this behavior could be attributed to the reversible nature of condensation reactions. This could imply that repeated contact angle measurements can result in dissolution of OPA from investigated regions, exposing the underlying substrate and subsequently making it permeable to more water molecules. Alternatively, If the OPA coverage is not ideally dense packed, molecules may be attached in random, partially folded orientations and an unfolding of the chain may result in surface exposure. A schematic in Fig. 3 **(Bottom)**, elucidates the reordering mechanism of the OPA molecules. Further, it is interesting to see a stabilization of contact angle after 14 days for both zirconia nanostructure and compact oxide, while for TiNT a constant value is only reached after 21 days and for TiCO not even after 50 days. This is evident from the dynamically decreasing WCA for Titania whereas in the case of Zirconia, it plateaus as shown in stage II ordering over time. Zirconia's enhanced stability is attributed to the quality of OPA-SAM coverage which is denser (1.02 ± 0.06 nm, (cf. Supporting Information, Fig. S2)) and more strongly bound to the substrate as is affirmed in the following experiments within the manuscript [40]. The contact angle decay measured in air is apparent when comparing the values of day 0 and day 50, ZrNT (>160° → 145±2°), TiNT (156° → 127°±2°), ZrCO (140° → 116°±2°) and TiCO (130° → 40°±3°). ZrNT samples stored under ambient conditions in the dark for a period of 50 days show similar stability to their irradiated counterparts, i.e., they maintain hydrophobic behavior and a contact angle of 145±3° was recorded as on day 50. This indicates that the observed decrease in contact angle is probably induced by the measurement itself and not by the irradiation conditions. Zirconia compact oxide even shows a comparable behavior to titania nanotubes and this indicates towards zirconia's superior bond strength and packing density as previously mentioned. The TiCO samples show a much faster linear decay rate throughout the 50-day period. The constant decay observed for titania is presumably a result of the photocatalytic self-cleaning properties of TiO_2, the oxide actively destroys attached SAM molecules when irradiated. Photo-degradation is the process of material alteration in the presence of light and air, the degradation route involves oxidation and hydrolysis [41]. Such reactions are initiated upon photon absorption, energy transfer, molecular excitation and spontaneous radicalization in the presence of O_2 and H_2O [37]. Titania reportedly has a bandgap of (3.2 eV) and is widely accepted as an effective photocatalyst, implying that in the presence of light photolysis occurs [42–44]. On the contrary, zirconia has a phase dependent wide bandgap (3.25–5.60 eV), amorphous zirconia is reported to show values greater than 4.2 eV, this is clearly larger than the excitation energy needed for titania [19,45–48]. Here, we could show that UVA light is sufficient for inducing degeneration of adsorbed functional SAMs on TiO_2, i.e., the suitability of TiO_2 coated with functional monolayers for indoor applications is also limited. Due to its wider bandgap, ZrO_2 is catalytically 'inactive' under sunlight and does not exert active photodegradation, thus the hydrophobic SAM is able to remain intact on its surface.

It is interesting to note that photocatalytic degradation on TiO_2 works best in the presence of ambient humidity and H_2O, as it is energetically favorable to form OH-radicals [32]. Thus, a greater deviation in stability of the hydrophobic coatings for ZrO_2 and TiO_2 is expected in the presence of water. Further, in another experimental setup, the respective sample sets were immersed in H_2O in transparent Schott glass containers, under sunlight. Fig. 4 **(**Wettability measurements of OPA modified ZrO_2 nanotubes upon sunlight exposure in water-immersed condition (Contact angle versus Time)) depicts the trends observed in the presence of aqueous medium. Contact angles measured after 1-day immersion and after 21 days amount to ZrNT (160°±2°→ 130°±2), TiNT (< 155°±2° → 112°±2°), ZrCO (125°±1° → 96°±1°) and TiCO (95°±2° → 76°±2°). It can be concluded that the stability of the hydrophobic coatings is also clearly enhanced for ZrO_2 surfaces in aqueous environment. The initial packing density of the SAM is essential when considering the integrity of the composite system as it also contributes to improved hydrophobic behavior accompanied by the larger volumes of trapped-air within the nano-structured asperities. Surface hydration may affect the arrangement of the molecules within the monolayer and this, consequently may influence the diffusion of oxidizing species. In the presence of water, additionally a hydroxyl mediated degradation has a higher possibility than when exposed only to air. An ideal case of full surface coverage prevents adsorption of water [25,28]. However, as concluded in the previous section, real systems have less than ideal coverage and as condensation reactions typically are reversible, a greater amount of exposed surface promotes the accessibility for further H_2O molecules and the desorption of molecules. The stability of the OPA SAM in aqueous environment was furthermore evaluated by XPS. Fig. 5 **(**Elution of hydrophobic OPA SAM from compact oxide substrates upon immersion in H_2O after 7 days; ZrO_2 and TiO_2**)** depicts the elution of OPA-SAMs from ZrCO and TiCO samples over a 7-day period.

We conclude that Zirconia samples show a slower rate of destruction of the OPA-SAM on their surface and continue to remain hydrophobic at extended duration in water and under sunlight exposure, probably due to an improved packing density, higher desorption resistance and the lack of photocatalytic self-cleaning properties of the material.

The mechanical stability of the OPA-ZrO_2 coatings were additionally evaluated under a continuous jet of DI water for 1 min. Fig. 6 (Hydrophobic film stability pre/post water flushing (Contact angle versus Time)) depicts an average percental loss (measured as a function of contact angle) of (-13 ± 0.34%) in film coverage. It is noteworthy to mention that the contact angles represented in Fig. 6, were possible to measure only along visible defects on the surfaces i.e. cracks/ scratches (probably created during experimental handling), (cf. Supporting Information, Fig. S3). Furthermore, over 70% of water droplets continued to roll of the surface during the flushing experiment. Repetitions of the

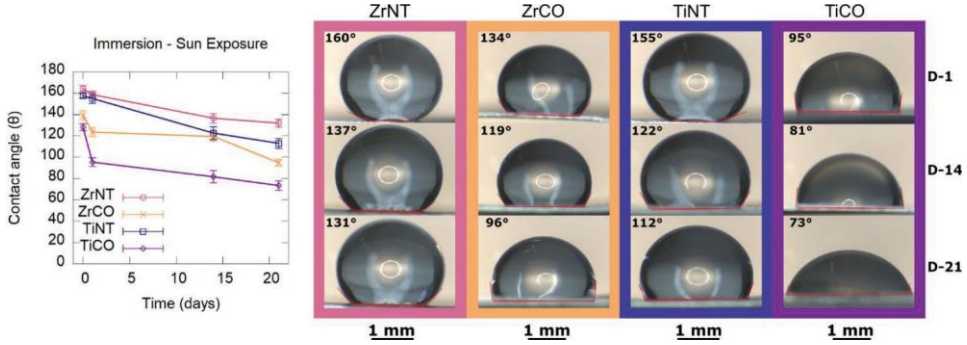

Fig. 4. Wettability measurements of OPA modified oxide surfaces upon sunlight exposure in water-immersed condition (contact angle versus time),-solid lines are a guide to the eye.

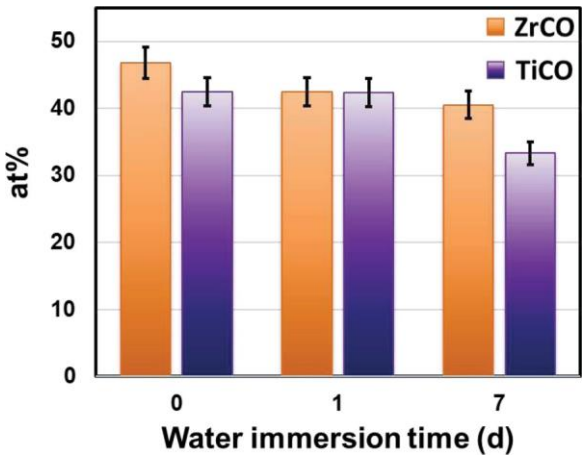

Fig. 5. Elution of hydrophobic OPA SAM from compact oxide substrates upon immersion in H_2O after up to 7 days; C1s on ZrO_2 and TiO_2 compact oxide (XPS).

experiment did not lead to any further decrease of contact angles, indicating that only a fraction of the initially present OPA molecules is weakly bound to the ZrO_2 surface. This experiment indicates that the observed contact angle decay on ZrNT during sunlight exposure in aqueous environment can be solely explained by desorbing OPA molecules from the ZrO_2 surface.

To evaluate the role of 'active photodegradation' as a responsible source for the preferential OPA-SAM destruction on TiO_2, a set of experiments was performed under harsh UV light exposure (400 W Xe lamp) on OPA-SAM coated ZrO_2 and TiO_2 samples. Fig. 7**.** (Wettability measurements of OPA modified ZrNT and TiNT upon UV exposure in air (Contact angle versus Time)) and Fig. 8**. (**XPS spectra: UV irradiation of OPA modified ZrCO and TiCO) depict the trend in wettability and integrity of the SAM upon UV exposure. While the ZrNT samples show a hydrophobic surface over the entire duration of UV-light illumination, an accelerated decay of the OPA SAM is obvious on the TiO_2 samples. A change to hydrophilic behavior is observed after ~7 min irradiation, which in turn is correlated to a significant loss of carbon signal from the material's surface as observed in XPS, indicating decomposition or desorption of the OPA monolayer. The inferior stability of hydrophobicity on TiO_2 is predominantly attributed to the destruction of the OPA monolayer under active photocatalytic conditions. The expected

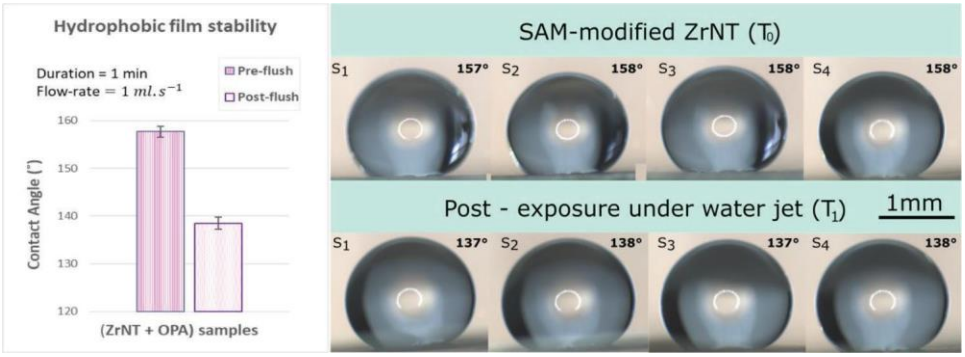

Fig. 6. Hydrophobic film stability pre/post water flushing for 1 min on Zr-NT samples

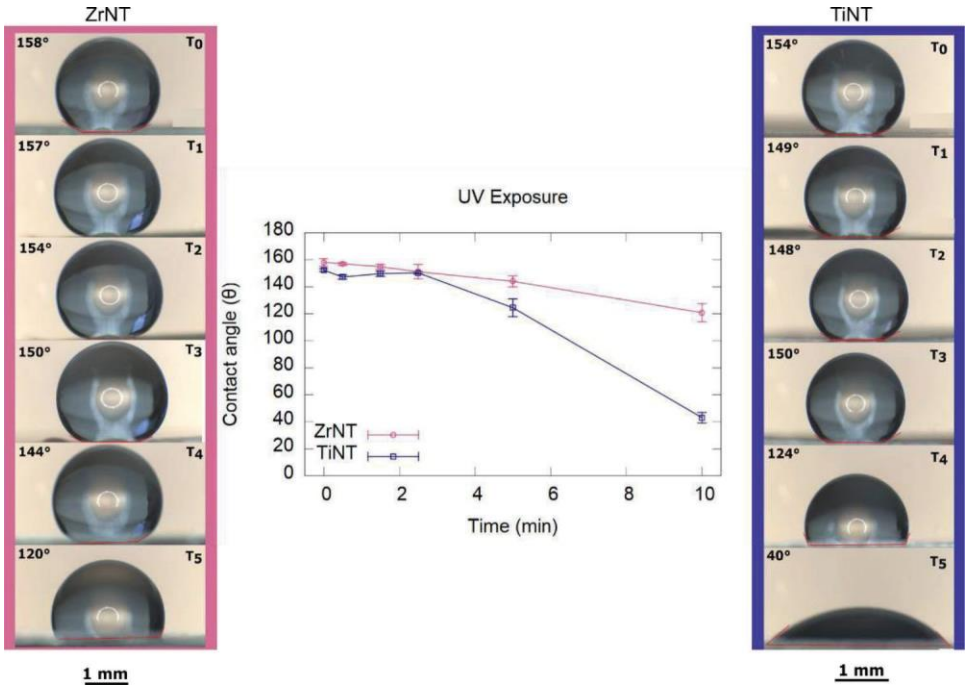

Fig. 7. Wettability measurements of OPA modified ZrNT and TiNT upon UV exposure in air (contact angle versus time),-solid lines are a guide to the eye.

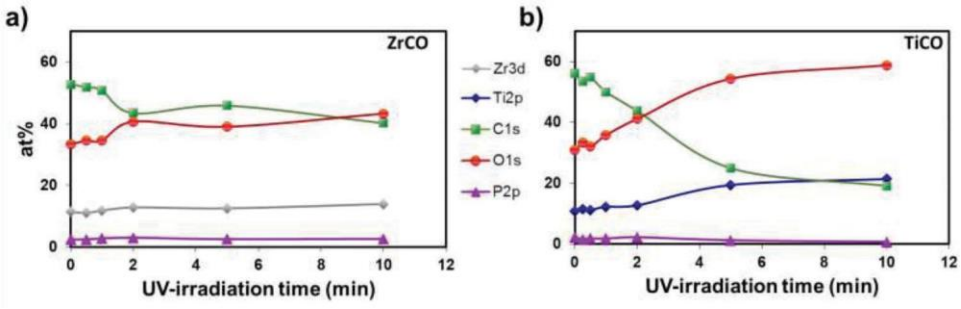

Fig. 8. XPS spectra: UV irradiation of OPA modified ZrCO and TiCO.

lifetime of a superhydrophobic coating consequently is dependent on the substrate's bandgap and in conclusion, ZrO_2 coatings are promising for application in superhydrophobic materials for both outdoor and indoor applications.

We summarize that the order of increasing SAM layer integrity on the substrate surface is such that ZrO_2 > TiO_2 and anodized NT > anodized CO. Zirconia and titania samples show similar trends within their respective class of oxide structures (nanotubes and compact). The exact same translation within the sample types and classes suggest that the mechanism for SAM degradation consistently depends on the 'active' photocatalytic nature of the substrate, in combination with elution of weekly bound molecules.

3. Conclusion

In this work, we synthesize ZrO_2 nanostructures via a single-step anodization process in the absence of hazardous HF acid containing etchants and render the surface superhydrophobic via OPA SAMs. The integrity of the OPA SAMs on ZrO_2 nanotubes was extensively compared to ZrO_2 compact oxide and also to the widely investigated TiO_2 nanostructures. Therefore, the interaction and stability of OPA SAMs with oxide nanostructures of titania and zirconia under broad wavelength and UV-light exposure under different conditions were investigated. Wettability assessments confirm the relatively higher stability of zirconia-SAM composites for both classes of oxide-structures. It was found that a certain fraction of the OPA SAM can be removed by exposure to water. Investigation of the degradation behavior under UV-light exposure confirms the hypothesis that SAM degradation predominantly depends on the 'active' photocatalytic nature of the substrate. All results indicate towards the superiority of the zirconia-SAM based composites and such systems are promising candidates as stable optical coatings for outdoor applications.

4. Experimental Section/Methods

All chemicals were purchased by chemical suppliers and used without further purification. All organic solvents were of water-free grade.

4.1. Substrate preparation

Zr foil (99.2% purity, Goodfellow UK, 0.125 mm thickness) and Ti foil (99.6% purity, Advent Ltd., 0.1 mm thickness), were ultrasonically cleaned in ethanol and DI water and anodized using a Pt-sheet as the counter electrode. In order to synthesize compact oxide (CO) layers, the metal foils were anodized at 30 V respectively for 30 min in 1M H_2SO_4 (Merck). For nanotubes (NT) Zr was anodized at 50 V for 30 min and Ti at 50 V for 2 h in a glycerol-based electrolyte containing 30 vol% formamide, 2 wt% NH_4F (Merck) and 2 wt% distilled water respectively. Anodization was carried out using a high-voltage potentiostat (Jaissle IMP 88-200 PC), connected to a digital multimeter (Keithley 2000) interfaced to a computer. All samples were rinsed thoroughly with DI water after the anodization process and dried under a stream of N_2.

4.2. SAM formation

Self-assembled monolayers of OPA (Merck) were prepared by immersion of as-prepared samples of zirconia and titania in solutions containing 10 mM OPA in tetrahydrofuran (THF, Roth) for a duration of 6 h at ambient conditions. Upon removal, the samples were rinsed in pure THF for 30 s and dried under a filtered nitrogen stream.

4.2.1. SAM degradation

SAM coated oxides were subjected to indirect irradiation in air and underwater under sunlight for a period of 1, 3, 7, 14, 21 and 50 days complimentary to tests under direct irradiation using a UV lamp (Heraeus Noblelight DQ 2523 mercury lamp with 400 W power output) for the duration of up to 10 min at a distance of 15 cm under the lamp source.

4.3. Mechanical stability

OPA-SAM coated ZrNT samples were subjected to a jet of DI water at a flow rate of 1 ml/s for a duration of 1 min and dried under an N_2 stream for 20 s. Sessile water-droplet contact angle measurements were made before and after the flushing experiment. The percental loss of hydrophobicity was measured as a function of contact angle.

4.4. Characterization and surface analysis

The morphology of the anodized samples was evaluated by field emission scanning electron microscopy (FEI FEG Quanta 240 ESEM). Surface modification with OPA was evaluated using a ToF-SIMS IV instrument (ION-TOF, Munster). Positive static SIMS measurements were performed on zirconia and titania compact oxide samples. XPS measurements were conducted on a high-resolution X-ray-photoelectron spectrometer (PHI 5600) using mono-chromated Al K_α radiation (1486.6 eV) for excitation. The binding energy of the target elements was determined at a pass energy of 23.5 eV and a total energy resolution of < 0.4 eV, values were recorded every 0.1 eV and at a take-off angle of 45° with respect to the surface normal. Transmittance was recorded via transmission light microscopy using UV-LED light. In addition , Leica Suite Application was used to measure contact angles. 10 µl DI water droplets were used to determine the wetting behavior.

CRediT authorship contribution statement

Swathi Naidu Vakamulla Raghu: Conceptualization, Data curation, Methodology, Investigation, Writing – original draft, Writing – review & editing. **Khajidkhand Chuluunbandi:** Investigation, Data curation. **Manuela Sonja Killian:** Conceptualization, Funding acquisition, Project administration, Supervision, Resources, Writing – review &

editing.

Declaration of Competing Interest

The authors declare no conflict of interest.

Acknowledgments

The authors acknowledge the DFG researcher group FOR 1878 and KI 2169/2-1 for funding. The authors would like to thank Prof. Patrik Schmuki, Dr. Alexander Tesler, Dr. Christian Pritzel, Dr. Maxime Hubert, Anja Friedrich, Anke Knoop and Ulrike Marten-Jahns for access to lab space, measurements, discussion and data evaluation

Supplementary materials

Supplementary material associated with this article can be found, in the online version, at doi:10.1016/j.surfin.2021.101357.

References

[1] W. Hughes, The passivity of metals, Nature 106 (1921) 692–693, https://doi.org/10.1038/106692c0.
[2] A.S. Mogoda, Influence of some parameters on passivation of zirconium and the stability of the anodic oxide film, Corrosion (1999), https://doi.org/10.5006/1.3284044.
[3] Y. Zhang, Z. Jiang, J. Huang, L.Y. Lim, W. Li, J. Deng, D. Gong, Y. Tang, Y. Lai, Z. Chen, Titanate and titania nanostructured materials for environmental and energy applications: a review, RSC Adv (2015), https://doi.org/10.1039/c5ra11298b.
[4] E. Balaur, J.M. Macak, H. Tsuchiya, P. Schmuki, Wetting behaviour of layers of TiO_2 nanotubes with different diameters, J. Mater. Chem. (2005), https://doi.org/10.1039/b509672c.
[5] F. Zhang, S. Chen, L. Dong, Y. Lei, T. Liu, Y. Yin, Preparation of superhydrophobic films on titanium as effective corrosion barriers, Appl. Surf. Sci. (2011), https://doi.org/10.1016/j.apsusc.2010.10.027.
[6] Z.-S. Huang, C. Shen, L. Fan, X. Ye, X. Shi, H. Li, Y. Zhang, Y. Lai, Y.-Y. Quan, Experimental investigation of the anti-soiling performances of different wettability of transparent coatings: Superhydrophilic, hydrophilic, hydrophobic and superhydrophobic coatings, Sol. Energy Mater. Sol. Cells. 225 (2021), 111053, https://doi.org/10.1016/j.solmat.2021.111053.
[7] Y. Lai, J. Huang, Z. Cui, M. Ge, K.-Q. Zhang, Z. Chen, L. Chi, Recent advances in TiO_2 -based nanostructured surfaces with controllable wettability and adhesion, Small 12 (2016) 2203–2224, https://doi.org/10.1002/smll.201501837.
[8] Uhlig's Corrosion Handbook, 2nd ed., 2000, https://doi.org/10.1108/aeat.2000.12772dae.001. Aircr. Eng. Aerosp. Technol.
[9] A.V. Chadwick, Solid progress in ion conduction, Nature 408 (2000) 925–926, https://doi.org/10.1038/35050201.
[10] C. Piconi, G. Maccauro, Zirconia as a ceramic biomaterial, Biomaterials (1999), https://doi.org/10.1016/S0142-9612(98)00010-6.
[11] B.C.H. Steele, A. Heinzel, Materials for fuel-cell technologies, Nature (2001), https://doi.org/10.1038/35104620.
[12] A.W. Amer, S.M. Mohamed, A.M. Hafez, S.Y. Alqaradawi, A.S. Aljaber, N.K. Allam, Self-assembled zirconia nanotube arrays: Fabrication mechanism, energy consideration and optical activity, RSC Adv. (2014), https://doi.org/10.1039/c4ra05115g.
[13] V. Grover, R. Shukla, A.K. Tyagi, Facile synthesis of ZrO_2 powders: Control of morphology, Scr. Mater. (2007), https://doi.org/10.1016/j.scriptamat.2007.06.053.
[14] W. Li, H. Huang, H. Li, W. Zhang, H. Liu, Facile synthesis of pure monoclinic and tetragonal zirconia nanoparticles and their phase effects on the behavior of supported molybdena catalysts for methanol-selective oxidation, Langmuir (2008), https://doi.org/10.1021/la800370r.
[15] J.P. Folkers, C.B. Gorman, P.E. Laibinis, S. Buchholz, G.M. Whitesides, R.G. Nuzzo, Self-Assembled Monolayers of Long-Chain Hydroxamic Acids on the Native Oxides of Metals, Langmuir (1995), https://doi.org/10.1021/la00003a024.
[16] S.T. Yohe, Y.L. Colson, M.W. Grinstaff, Superhydrophobic materials for tunable drug release: Using displacement of air to control delivery rates, J. Am. Chem. Soc. (2012), https://doi.org/10.1021/ja211148a.
[17] J.H. Choi, Y.M. Kim, Y.W. Park, T.H. Park, K.Y. Dong, B.K. Ju, Hydrophilic dots on hydrophobic nanopatterned surfaces as a flexible gas barrier, Langmuir (2009), https://doi.org/10.1021/la804325x.
[18] M. Zhou, X. Pang, L. Wei, K. Gao, Insitu grown superhydrophobic Zn-Al layered double hydroxides films on magnesium alloy to improve corrosion properties, Appl. Surf. Sci. (2015), https://doi.org/10.1016/j.apsusc.2015.02.086.
[19] J.C. Garcia, L.M.R. Scolfaro, A.T. Lino, V.N. Freire, G.A. Farias, C.C. Silva, H.W. L. Alves, S.C.P. Rodrigues, E.F. Da Silva, Structural, electronic, and optical properties of ZrO_2 from ab initio calculations, J. Appl. Phys. (2006), https://doi.org/10.1063/1.2386967.
[20] P.H. Mutin, G. Guerrero, A. Vioux, Hybrid materials from organophosphorus coupling molecules, J. Mater. Chem. (2005), https://doi.org/10.1039/b505422b.
[21] F. Schreiber, Structure and growth of self-assembling monolayers, Prog. Surf. Sci. (2000), https://doi.org/10.1016/S0079-6816(00)00024-1.
[22] R.K. Smith, P.A. Lewis, P.S. Weiss, Patterning self-assembled monolayers, Prog. Surf. Sci. (2004), https://doi.org/10.1016/j.progsurf.2003.12.001.
[23] A. Ulman, Formation and structure of self-assembled monolayers, Chem. Rev. (1996), https://doi.org/10.1021/cr9502357.
[24] Y. Lai, F. Pan, C. Xu, H. Fuchs, L. Chi, *In situ* surface-modification-induced superhydrophobic patterns with reversible wettability and adhesion, Adv. Mater 25 (2013) 1682–1686, https://doi.org/10.1002/adma.201203797.
[25] M.S. Killian, Organic Modification of TiO_2 and other Metal Oxides with SAMs and Proteins - a Surface Analytical Investigation, Dissertation, FAU Erlangen (2013).
[26] B. Adolphi, E. Ja¨hne, G. Busch, X. Cai, Characterization of the adsorption of ω-(thiophene-3-yl alkyl) phosphonic acid on metal oxides with AR-XPS, Anal. Bioanal. Chem. (2004), https://doi.org/10.1007/s00216-004-2634-x.
[27] W. Gao, L. Dickinson, C. Grozinger, F.G. Morin, L. Reven, Self-assembled monolayers of alkylphosphonic acids on metal oxides, Langmuir (1996), https://doi.org/10.1021/la9607621.
[28] M.C.O. Monteiro, G. Cha, P. Schmuki, M.S. Killian, Metal-phosphate bilayers for anatase surface modification, ACS Appl. Mater. Interfaces. (2018), https://doi.org/10.1021/acsami.7b16069.
[29] E.S. Gawalt, G. Lu, S.L. Bernasek, J. Schwartz, Enhanced bonding of alkanephosphonic acids to oxidized titanium using surface-bound alkoxyzirconium complex interfaces, Langmuir (1999), https://doi.org/10.1021/la990906m.
[30] D.A. Chang, P. Lin, T.Y. Tseng, Optical properties of $ZrTiO_4$ films grown by radio-frequency magnetron sputtering, J. Appl. Phys. 77 (1995) 4445–4451, https://doi.org/10.1063/1.359472.
[31] S. Berger, J. Faltenbacher, S. Bauer, P. Schmuki, Enhanced self-ordering of anodic ZrO_2 nanotubes in inorganic and organic electrolytes using two-step anodization, Phys. Status Solidi Rapid Res. Lett. (2008), https://doi.org/10.1002/pssr.200802019.
[32] Y.Y. Song, F. Schmidt-Stein, S. Bauer, P. Schmuki, Amphiphilic TiO_2 nanotube arrays: an actively controllable drug delivery system, J. Am. Chem. Soc. (2009), https://doi.org/10.1021/ja810130h.
[33] M.S. Killian, J.F. Gnichwitz, A. Hirsch, P. Schmuki, J. Kunze, ToF-SIMS and XPS studies of the adsorption characteristics of a Zn-porphyrin on TiO_2, Langmuir 26 (2010) 3531–3538, https://doi.org/10.1021/la9032139.
[34] P.R. Rauta, P. Manivasakan, V. Rajendran, B.B. Sahu, B.K. Panda, P. Mohapatra, Phase transformation of ZrO_2 nanoparticles produced from zircon, Phase Transitions (2012), https://doi.org/10.1080/01411594.2011.619698.
[35] J. Cˇyviene, J. Dudonis, Zr, ZrN and ZY/Al thin films deposition using arc evaporation and annealing, Acta Phys. Pol. A. 114 (2008) 769–777, https://doi.org/10.12693/APhysPolA.114.769.
[36] A.B.D. Cassie, S. Baxter, Wettability of porous surfaces, Trans. Faraday Soc. (1944), https://doi.org/10.1039/tf9444000546.
[37] Y.-K. Lee, Influence of filler on the difference between the transmitted and reflected colors of experimental resin composites, Dent. Mater. 24 (2008) 1243–1247, https://doi.org/10.1016/j.dental.2008.01.014.
[38] J.D. Haigh, The sun and the earth's climate, Living Rev. Sol. Phys. (2005).
[39] M. Wacker, M.F. Holick, Sunlight and Vitamin D: A global perspective for health, Dermatoendocrinol (2013), https://doi.org/10.4161/derm.24494.
[40] S.N. Vakamulla Raghu, M.S. Killian, Wetting behavior of zirconia nanotubes, ChemRxiv (2021), https://doi.org/10.26434/chemrxiv.14198930.v1.
[41] H.D. Burrows, M. Canle L, J.A. Santaballa, S. Steenken, Reaction pathways and mechanisms of photodegradation of pesticides, J. Photochem. Photobiol. B Biol. (2002), https://doi.org/10.1016/S1011-1344(02)00277-4.
[42] Y. Wang, N. Herron, Nanometer-sized semiconductor clusters: Materials synthesis, quantum size effects, and photophysical properties, J. Phys. Chem. (1991), https://doi.org/10.1021/j100155a009.
[43] K.M. Reddy, S.V. Manorama, A.R. Reddy, Bandgap studies on anatase titanium dioxide nanoparticles, Mater. Chem. Phys. (2003), https://doi.org/10.1016/S0254-0584(02)00343-7.
[44] B.D. Cullity, J.W. Weymouth, Elements of X-Ray Diffraction, Am. J. Phys. (1957), https://doi.org/10.1119/1.1934486.
[45] S. Bhaskar, E.W. Awin, K.C.H. Kumar, A. Lale, S. Bernard, R. Kumar, Design of nanoscaled heterojunctions in precursor-derived t-ZrO_2/SiOC(N) nanocomposites: Transgressing the boundaries of catalytic activity from UV to visible light, Sci. Rep. 10 (2020) 1–13, https://doi.org/10.1038/s41598-019-57394-8.
[46] S. Heiroth, R. Ghisleni, T. Lippert, J. Michler, A. Wokaun, Optical and mechanical properties of amorphous and crystalline yttria-stabilized zirconia thin films prepared by pulsed laser deposition, Acta Mater. (2011), https://doi.org/10.1016/j.actamat.2010.12.029.
[47] H. Haick, Y. Paz, Remote photocatalytic activity as probed by measuring the degradation of self-assembled monolayers anchored near microdomains of titanium dioxide, J. Phys. Chem. B. (2001), https://doi.org/10.1021/jp0037807.
[48] Y. Lai, C. Lin, H. Wang, J. Huang, H. Zhuang, L. Sun, Superhydrophilic–superhydrophobic micropattern on TiO_2 nanotube films by photocatalytic lithography, Electrochem. Commun. 10 (2008) 387–391, https://doi.org/10.1016/j.elecom.2007.12.020.

SUPPORTING INFORMATION

Zirconia nanotube coatings - UV-resistant superhydrophobic surfaces

Swathi Naidu Vakamulla Raghu, Khajidkhand Chuluunbandi and Manuela Sonja Killian

Surfaces and Interfaces, 26, 2021, 101357, https://doi.org/10.1016/j.surfin.2021.101357

DOI: https://doi.org/10.1016/j.surfin.2021.101357

S1: Anodic oxide structures

Anodization offers the possibility of tuning the type of anodic oxide produced. It results in an improved oxide quality that consequently affects the extent of surface functionalization. Different surface structures elicit different degrees of wettability and we compare flat oxides and nanotubular oxides in our experiments. In order to synthesize flat / compact oxide {CO} layers, the metal foils {Zr and Ti} were anodized at 30V for 30 min in 1M H_2SO_4 {Merck}, respectively. Figure S1 represents the SEM micrographs – Top view: {a} ZrO_2- Compact Oxide, {b} TiO_2- Compact Oxide} - The SEM images clearly show a non-porous surface after anodization of Zr-CO and Ti-CO. Optically, a clear change in material can be deduced from a color change from metallic gray to blue, indicating an anodic oxide thickness of ~50 nm. In addition to this, {d} represents the surface roughness plot and the corresponding values of R_a as evaluated from the SEM images.

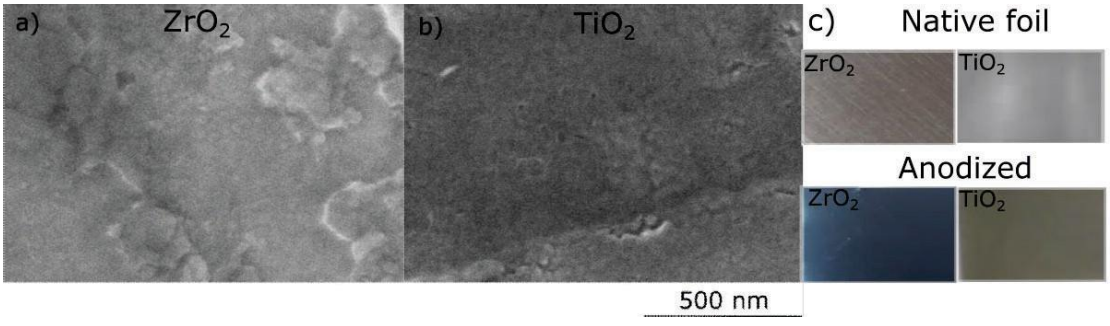

d)

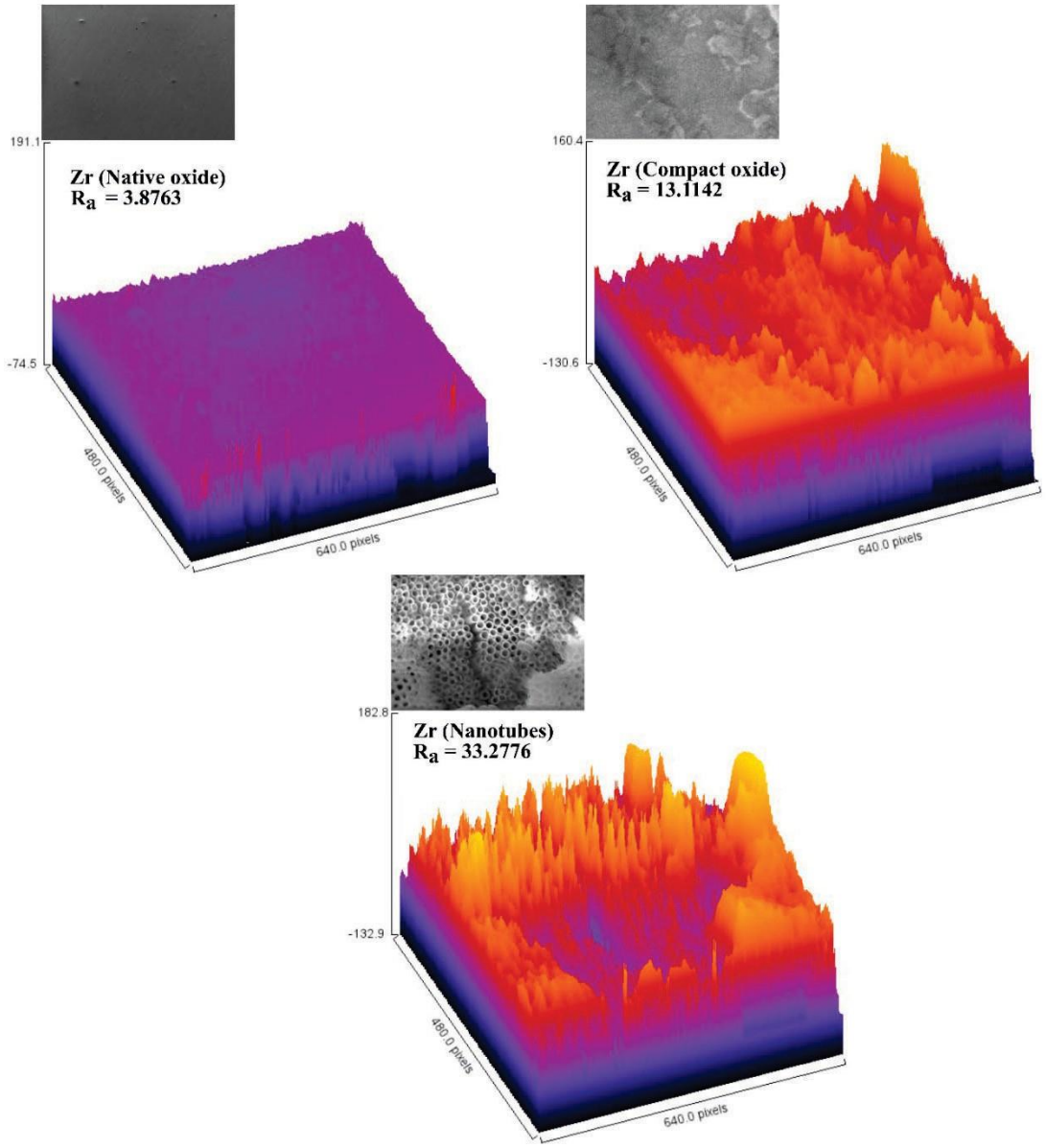

Figure S1. Anodic oxide structures: SEM micrographs – Top view: (a)ZrO_2- Compact 0xide, (b) TiO_2- Compact 0xide, c) optical photographs of the metal foil surface prior and post anodization, (d) Surface roughness plots, roughness values R_a and corresponding SEM images of measured Zirconia substrates; Native foil, Compact-oxide and Nanotubes

S2: Compositional characterization

Time-of-flight secondary ion mass spectrometry {ToF-SIMS} was used to evaluate the surface composition of the OPA modified Zr and Ti oxide substrates, respectively. $C_{18}H_{38}PO_3^-$ was determined as characteristic fragment for the OPA molecules. The quasi-molecular signals of OPA {m/z = 333.29, $C_{18}H_{38}PO3^-$, M^-H^-} can be clearly detected in ToF-SIMS measurements {Figure S2}, proving the presence of the molecule on the oxide surface. Further, in Figure S2 {Bottom} the coverage of OPA molecules was determined using XPS and is reported that OPA has a slightly better coverage over ZrNT substrates {layer thickness ~ 1.02 nm} when compared to frequently reported TiNT-model systems {layer thickness ~ 0.94 nm} in addition to comparing the same after a period of 7-days soaking in water at room temperature.

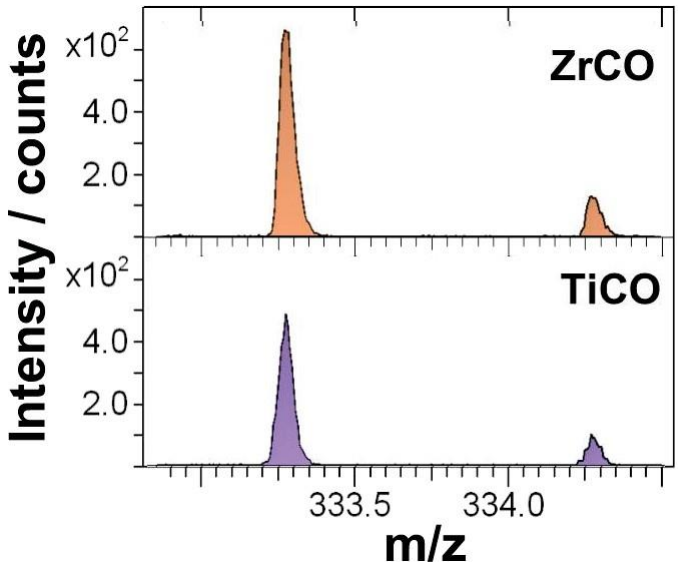

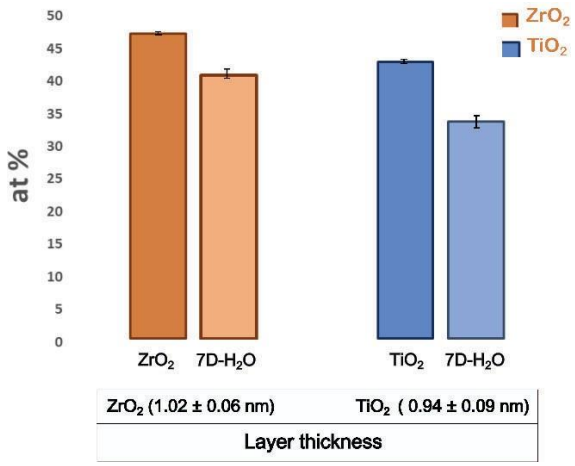

Figure S2. (Top); Compositional characterization- (Quasi-) molecular or characteristic fragments of the adsorbed 0PA-coated compact oxide ($M\text{-}H^-$) on compact $Zr0_2$ and $Ti0_{2,}$ (Bottom); Adsorption of organic molecules to $Zr0_2$ and $Ti0_2$ substrates - C1s and substrate signals measured using XPS for freshly prepared substrates and after 7-day water soak

The adsorption of OPA to TiO_2 and ZrO_2 was estimated by calculation of the C1s at% and by calculation via the P2p signal {P2p * 18}, as the stoichiometric composition of OPA is $C_{18}H_{39}PO_3$.

S3: Wettability of functionalized ZrNT and the influence of surface inhomogeneities

ZrNT surfaces continue to remain hydrophobic for a prolonged duration when subjected to various experimental conditions and relatively small changes were recorded during the contact angle measurements. This variation in hydrophobicity is attributed to the loss of OPA coverage from the ZrNT surfaces. Ideally, a superhydrophobic coating will have uniform coverage when the underlying surface is homogenous. However, as in the case of these in-situ experiments, handling and experimental procedures result in exposing the underlying substrate as a result of surface scratches, localized film-flaking and mechanical stresses while cutting and shaping of the test specimens. Thereby, increasing localized surface energy and promoting droplet wetting around such defects. Figure S3 {a} shows a representative image of a freshly anodized Zirconia foil that is scratch free and shows a homogeneous surface, water droplets continue to roll-off the defect free surface. Figure S3

{b} shows a foil that underwent mechanical stress induced by cutting and accompanied bending of the foils prior to various test conditions. This surface consists of topical scratches and film-flaking in certain regions, consequently exposing the underlying substrate and promoting droplet adherence on such visibly defective regions.

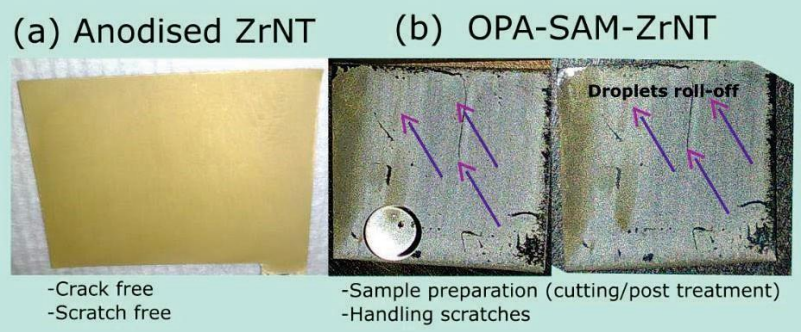

Figure S3. Wettability of functionalized ZrNT and the influence of surface inhomogeneities

Droplets, however, continue to roll off the surface in any mechanically undamaged region of the sample surface. The used foils have a thickness of 0.125 mm, making such defects less likely if the nanostructures are grown on a more rigid substrate. A video of the bouncing droplet can be found in the supporting audio/visual files uploaded.

S4: Titania nanotube synthesis

Titania nanotubes {TiNT} were synthesized at 50V for 2 hours in a glycerol-based electrolyte containing 30% formamide, 2 wt% NH_4F {Merck} and distilled water. These parameters were chosen in order to get structures with open pores devoid of any influencing initiation layer. This surface treatment was best suited for functionalization, resulting in super-hydrophobic contact angles {159° ± 2°} that were comparable to ZrNT samples. The reported structures are depicted in Figure S5.

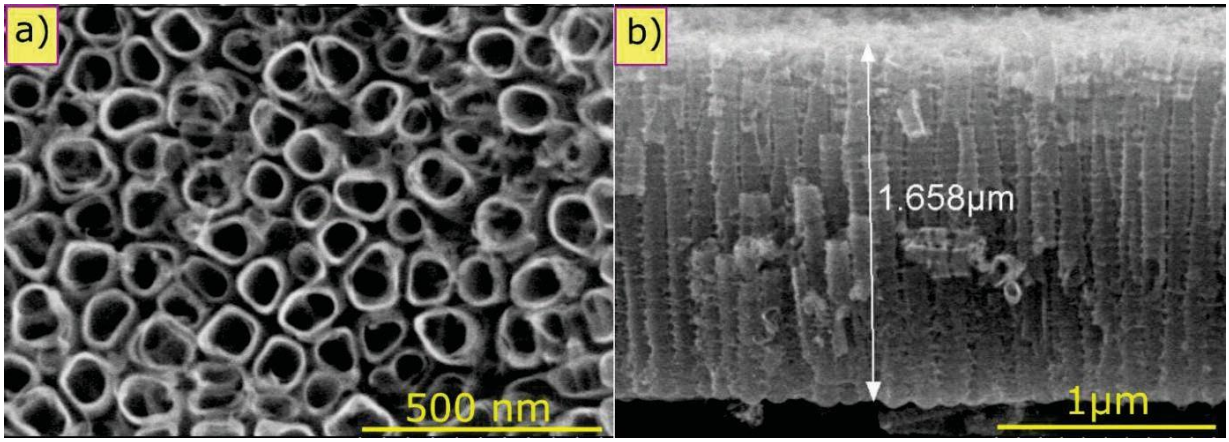

Figure S4. Titania nanotube synthesis: SEM micrographs - (a)TiO_2-NT top, (b) TiO_2-NTcross-section

It is interesting to mention, that the ZrNT show a comparable or even improved hydrophobicity, even though they show a smaller tube diameter than the TiO_2 nanotubes. Smaller diameters have been reported to yield in lower hydrophobicity for OPA modified TiNTs previously.[S1]

S5: Optical transparency of Zr coatings

Samples types; ZrNT film and ZrNT+ OPA were prepared as described in the main manuscript in the experimental section. These test specimens were then subjected to direct illumination under 12V-100W, HAL-L lamp {Olympus} eliciting a spectrum of white light under the optical microscope. Time of exposure and sample measurements were recorded on the same day under identical conditions.

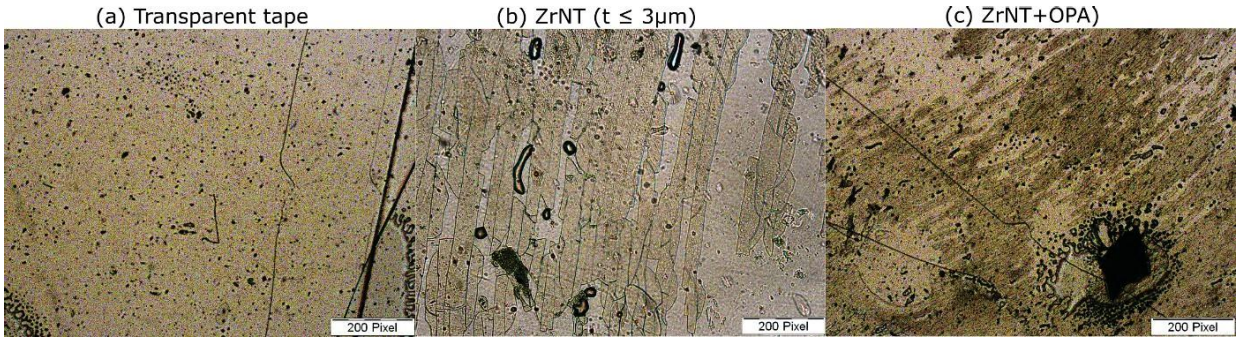

Figure S5. 0ptical transparency of Zr coatings

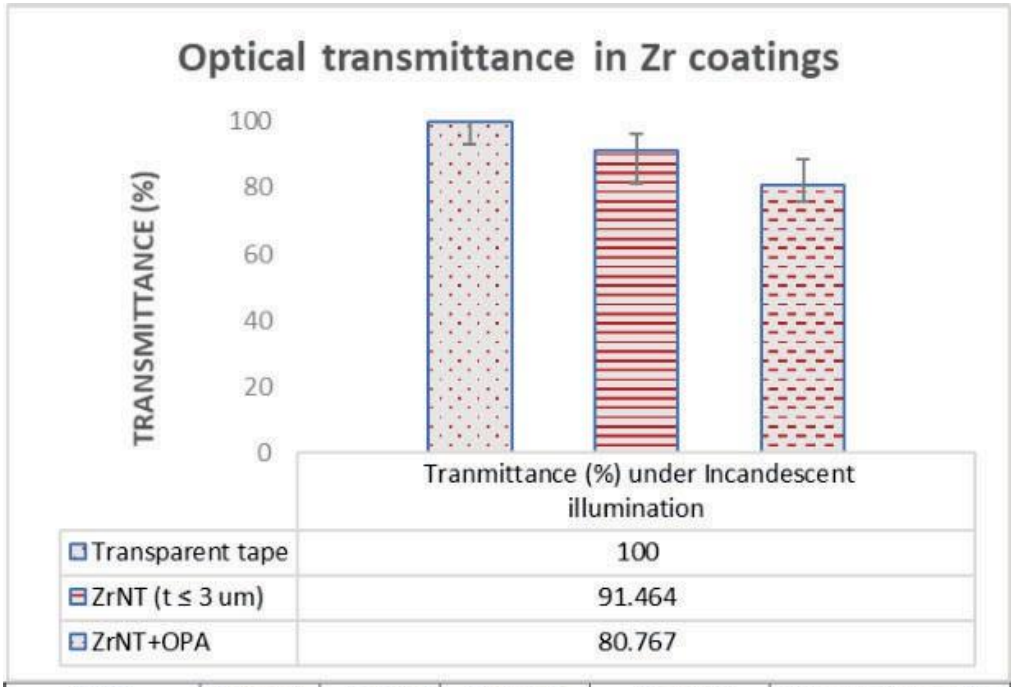

TYPE	Lowest Intensity	Highest Intensity	Average Intensity	Standard Deviation	Transmittance (%)
Transparent tape	5	231	154.593	30.955	100
ZrNT (t ≤ 3 um)	21	253	141.398	33.401	91.464
ZrNT +OPA	11	246	124.861	32.958	80.767

Table S5. 0ptical transmittance in $Zr0_2$ coatings

Figure S5 shows SEM micrographs under direct illumination and **Table S5.** {Optical transmittance in Zr coatings}, corresponds to the summary of the values obtained under the direct transmittance setup. ZrNT, when coated with OPA registered 10% decrease in transmittance. We conclude that ZrNT coatings remain transparent for 80%.

REFERENCES

[S1] E. Balaur, J.M. Macak, H. Tsuchiya, P. Schmuki, Wetting behaviour of layers of TiO_2 nanotubes with different diameters, J. Mater. Chem. {2005}. https://doi.org/10.1039/b509672c

4.2. Wetting behavior of zirconia nanotubes

Swathi Naidu Vakamulla Raghu and Manuela Sonja Killian

RSC Advances, 2021, 11, 29585-29589, https://doi.org/10.1039/D1RA04751E

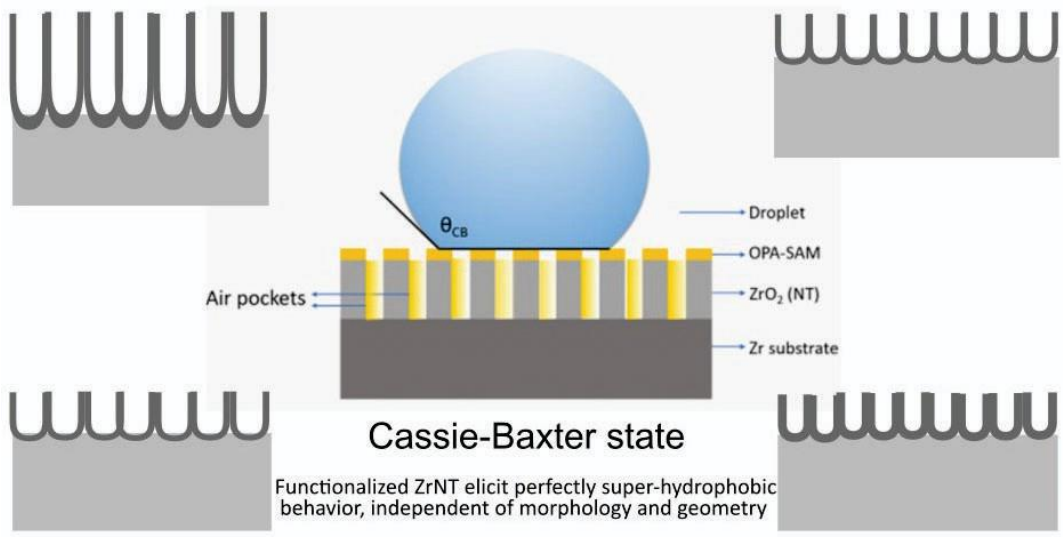

ToC -4.2 - Wetting behavior of SAM modified ZrNTs of varying morphology

The article in this section provides information on anodization parameters to develop ZrNTs of different morphology: single-walled; 'thin', double-walled; 'thick' pore openings at the mouth of the nanotubes, in addition to variations in nanotube diameter and length. The different morphological variations were assessed for their response towards subsequent organic molecule modification and address the second objective of this dissertation, namely to

'Determine the role of nanotube morphology on the interaction behavior with organic molecules used for surface modifications.'

In addition, information on the role of surface hydroxyl groups and dependent SAM formation on ZrNTs based on the type of organic molecule used and the extent of coverage is successfully evaluated. A noteworthy result from the analysis of achievable superhydrophobicity, based on nanotube diameter for ZrNTs, was in stark contrast to previously reported data on SAM-modified nanostructures of a similar valve metal titanium {Ti}. It was concluded, superhydrophobicity, on ZrNTs remains independent of nanotube morphology and is ascribed to the superior interaction strength of ZrO_2 and phosphonic acid functional groups of molecules. This result has special relevance in manufacturing contexts, such that up-scaling the synthesis of ZrNT coatings may be viable at a larger operational window during anodization. In essence, SAM-based superhydrophobicity is achievable even at smaller nanotube diameters.

RSC Advances

PAPER

View Article Online
View Journal | View Issue

Cite this: *RSC Adv.*, 2021, 11, 29585

Wetting behavior of zirconia nanotubes†

Swathi Naidu Vakamulla Raghu and Manuela Sonja Killian *

Received 19th June 2021
Accepted 24th August 2021

DOI: 10.1039/d1ra04751e

rsc.li/rsc-advances

In this work, we investigate the wettability of ZrO_2 nanotubes (ZrNT) synthesized *via* electrochemical anodization of zirconium. The ZrNT surface shows super-hydrophilic behavior while the octadecylphosphonic acid ($C_{18}H_{37}PO(OH)_2$) modified surface shows super-hydrophobic behavior. We demonstrate that the wetting properties are independent of ZrO_2 nanotube geometry and length.

Electrochemical anodization is a facile technique used to fabricate highly ordered structures in the sub-micron range. Several metals have successfully demonstrated self-organized porous nanostructure growth under appropriate anodization parameters.[1] Fluoride rich electrolytes contributed a significant advancement to the field, enabling the synthesis of high-aspect ratio nanostructured arrays on 'valve metals' such as zirconium.[2–4] Tuneable surface properties can exploit applications that are surface-interaction dependent, such as *e.g.* catalysis, filtration or coatings.[5–8] Zirconia is a biocompatible, high band-gap material that has reportedly demonstrated superior surface properties for the enhanced attachment of molecules.[9–11] It is used in biomedical devices, sensors and more recently for photocatalytic applications.[12,13] With this intent, ZrNT surfaces are modified by a monolayer of octadecylphosphonic acid rendering it super-hydrophobic.[14] Wang *et al.* previously investigated the pristine ZrNT surface wettability, observing highly hydrophilic properties.[15] In the present study, we synthesize ZrO_2 nanotubular structures in a single step anodization process without the pre-requisite dip-etching process using HF-acid based etchants. This one-pot synthesis allows for less hazardous and safer working conditions. Further, we investigate the influence of nanotube-geometry on the extent of super-hydrophobicity. Zr foils (99.2% purity, Goodfellow UK, 0.125 mm thickness) were ultrasonically cleaned in acetone, methanol and ethanol followed by rinsing in deionized water and dried under a nitrogen stream. Electrochemical anodization was carried out using a high-voltage potentiostat (Jaissle IMP 88-200 PC) in electrochemical cells with a working area of 1 cm^2 and larger cross-sections were fabricated *via* dip-anodization in an electrochemical bath-type setup. In both cases, a platinum counter electrode was used in a two-electrode setup. Anodization was carried out in a standard glycerol-based electrolyte consisting of 30% formamide, 2 wt% NH_4F (Merck) and 2 wt% H_2O under various conditions to obtain the respective morphologies. 20 nm wide-tubes were synthesized *via*-dip anodization at 30 V for 25 minutes without ramping and 40 nm wide-tubes, with ramping the potential at 1 V s^{-1} from OCP and kept at 50 V for 1 h. Thick-walled ~100 nm wide tubes (inner wall '*d*' ~80 nm, wall-thickness '*t*' ~20 nm) were synthesized at 50 V for 30 min without ramping, with the difference of 4 wt% distilled water in the electrolyte. Thin-walled ZrNTs (~100 nm wide, '*t*' ~3 nm) were achieved in 30 min at 90 V (ramp 1 V s^{-1}). The tube length was varied from 3 to 9 mm by adjusting the anodization time. Zr compact oxide (CO) films were prepared on Zr foils under a constant potential of 30 V for 30 min in a 1 M H_2SO_4 (Merck) electrolyte. The anodized samples were rinsed with ethanol and distilled water and dried with nitrogen. To impart surface hydrophobicity, samples were placed in solutions containing 10 mM octadecylphosphonic acid (OPA, $C_{18}H_{37}PO(OH)_2$) in tetrahydrofuran (THF, Roth) for a period of 24 h at ambient conditions, forming self-assembled monolayers (SAMs). Further, the samples were rinsed in pure THF for 30 s and dried under a filtered nitrogen stream. Scanning electron microscopy (Hitachi SEM FE 4800) was employed for the structural and morphological characterization of the anodized zirconia specimens. For chemical characterization, surface modification with OPA was evaluated using a ToF-SIMS IV instrument (ION-TOF, Münster) and coverage was evaluated *via* XPS (Perkin-Elmer Physical Electronics 5600, a detailed experimental description can be found in the ESI†). Static water contact angle (WCA) measurements were performed using both an Ossila-contact angle goniometer and a Leica Suite application instrument (DI water droplet volume, 10 ml) to determine wetting behavior. WCA values from both instruments only deviated within the statistical error of the measurement, as depicted in ESI-Fig. S1.† Fig. 1(a), shows a zirconia substrate with a native oxide film (as received condition), having a hydrophilic WCA of (~30°) owing to surface hydroxyl groups.[16,17] All porous samples depicted here showed super-hydrophilicity due to the improved oxide quality and enhanced liquid impregnation when compared to the native oxide

Chemistry and Structure of Novel Materials, University of Siegen, Paul-Bonatz-Str. 9-11, 57076 Siegen, Germany. E-mail: Manuela.Killian@uni-siegen.de

† Electronic supplementary information (ESI) available. See DOI: 10.1039/d1ra04751e

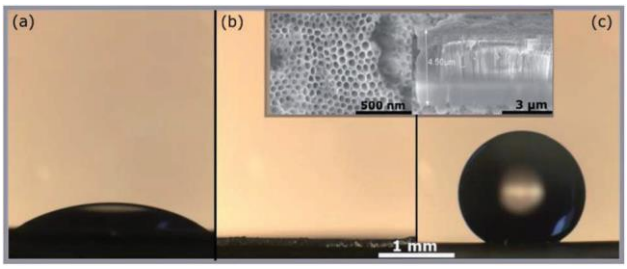

Fig. 1 Optical images of water droplet on ZrO_2 surface. (a) Native oxide (b) bare ZrNTs (c) ZrNTs after attaching OPA SAM. Inset shows SEM top and cross-section of ~100 nm ZrNTs.

surfaces. The water droplets spread entirely, covering the pores, an example is shown in Fig. 1(b), in agreement to literature.[15]

After surface modification with a monolayer of octadecylphosphonic acid, the nanotubes become super-hydrophobic as shown in Fig. 1(c). In Fig. 2, the coverage of ZrO_2 and TiO_2 compact oxides with long chain aliphatic molecules with various functional groups was determined using XPS. OPA showed the highest adhesion to both oxides, followed by octadecyl-trimethoxysilane. Both molecules form denser layers on ZrO_2, as reflected by the enhanced coverage. Stearic acid and octadecylamine yielded significantly lower surface coverages, showing a slightly enhanced adsorption to TiO_2. Phosphonic acid-based SAMs consequently offer the highest potential for the formation of superhydrophobic coatings on both ZrO_2 and TiO_2 among the investigated functional groups.

ToF-SIMS measurements were performed to evaluate the OPA-attachment and the resulting spectra in Fig. 3 confirms the presence of the phosphonic acid on ZrNT *via* the detection of the characteristic quasi-molecular signal of OPA (m/z ¼ 333.29, $C_{18}H_{38}PO_3^-$, M–H$^-$) in accordance to reported literature.[11,18,19] Fig. 4(a) depicts the morphology of ZrNT (d # 20 nm) and the WCA (162° ± 1°).

This is currently the smallest reported ZrNT diameter achieved *via* a single-step anodization. When functionalized with a SAM, it reports a superhydrophobic WCA. Moreover, in Fig. 4

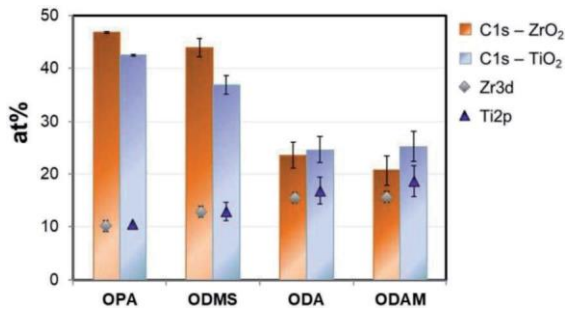

Fig. 2 Adsorption (atomic percentage (at%)) of organic molecules to ZrO_2 (C 1s–ZrO_2 signal) and TiO_2 (C 1s–TiO_2 signal) and substrate signals respectively (Zr 3d and Ti 2p) measured using XPS for 18-C carbohydrate molecules with different anchoring groups (OPA – octadecylphosphonic acid, ODMS – octadecyltrimethoxysilane, ODA – stearic acid, ODAM – octadecylamine).

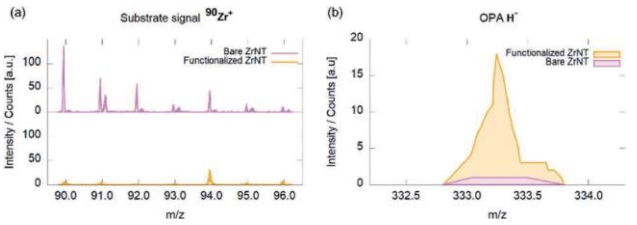

Fig. 3 ToF-SIMS spectra of ZrNTs before and after coverage with octadecylphosphonic acid SAMs; (a) Zr^+ isotopic pattern; (b) OPA–H$^-$ molecular signal.

the WCAs on zirconia test surfaces with larger pore configurations: 'd' nm ~40, ~100 nm-thick and thin-walled NTs and CO, (b–d) reveal that changing the porosity (difference in surface area made up of the solid), did not affect the extent of

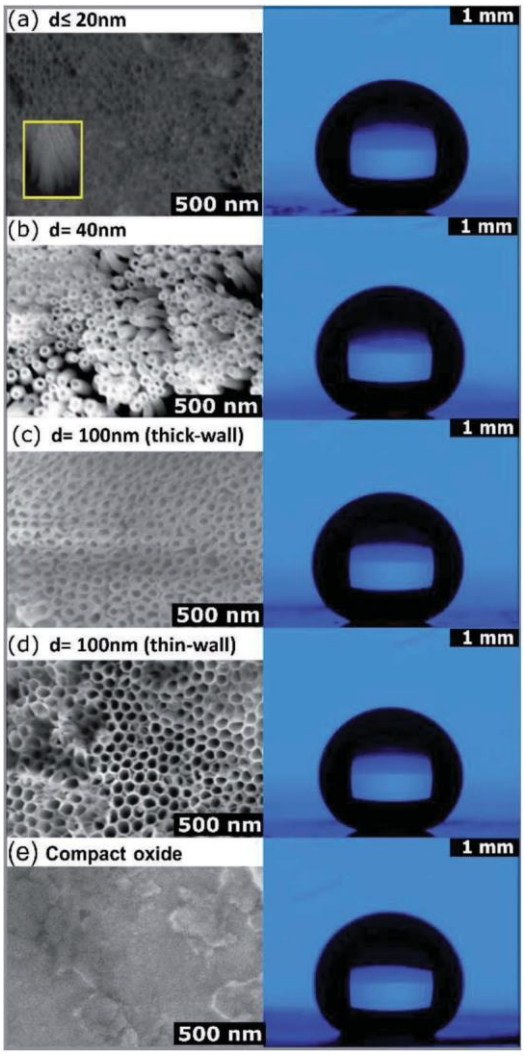

Fig. 4 Optical images of water droplets on SAM modified ZrNT structures of different porosity and corresponding SEM images (scale bar – 500 nm) of the surfaces. Diameters, (a) d # 20 nm, (b) d ¼ 40 nm, (c) thick walled d ¼ 100 nm, (d) thin walled d ¼ 100 nm and (e) compact anodic oxide (droplet image – scale bar ¼ 1 mm).

hydrophobicity, thereby maintaining a nearly constant WCA of (160° ± 1°) on the respective nanotubular surfaces. The only difference appeared when comparing ZrNTs to a ZrCO surface, for which a WCA of 120° (Fig. 4(e)) was recorded. It may be noted that the Zr-substrates have poor conductivity resulting in challenges such as excessive charging and lower focusing abilities while performing SEM characterization. Images shown in Fig. 4 have uniform scale-bars (SEM – 500 nm and WCA – 1 mm). Table 1 summarizes the influence of these pore geometries on WCAs.

In Fig. 5, WCA measurements were performed on OPA modified ZrNT of varying lengths to evaluate the influence of tube length on the wettability, yielding no statistical changes in dependence of tube length. A uniform nanoporous array is a homogenous surface with an increased roughness factor when compared to a 'flat' surface and hence in Fig. 1(a and b), the transition from hydrophilic to super-hydrophilic state is well accommodated by the Wenzel approach.[20] This phenomenon is represented as an enhanced wetting process that occurs as a result of liquid–solid interaction in the absence of air resistance. After successful surface modification with OPA (Fig. 1(c)), the methyl-terminated SAM surface is strongly water-repellent. This results in some cases where the water droplets continue to bounce of the surface and if they do adhere, they form high WCAs (≥150°). The super-hydrophobic state is stabilized and explained by the Cassie–Baxter model (CBM) as a result of a greater interaction with trapped air in-between the liquid–solid layers.[21] As represented in Fig. 4(a–d), the average WCAs measured were (~160°) for the ZrNT surfaces. The WCA values (θ^*) can be expressed according to the Cassie–Baxter equation, wherein (θ) is the WCA measured on the SAM modified flat zirconia surface, 'f' is a morphological factor and is defined as the area fraction of solid–liquid contact and $(1 - f)$ is the area fraction of air–liquid interface.

$$\cos(\theta^*) = f^* \cos(\theta) - (1 - f) \quad (1)$$

These surface fractions were calculated from high resolution SEM images as represented in Fig. 4, by estimating the ratio between pore walls to the total area respectively and complemented with ImageJ analysis. The morphological factor 'f' for values represented in Table 1 was calculated to be 0.020, 0.047, 0.131, 0.052 for ('d' nm = 20, 40, 100 – thick-walled and thin-walled) ZrNTs, respectively. Recently, it was reported that the wettability of titania nanotubes is dependent of tube diameter and the observations were perfectly supported by eqn (1) as proposed by the CBM.[22] For this result to hold true in the case of zirconia, the dimensionless factor 'f' in eqn (1) is represented as the ratio between the 'projected area' to the 'total area' where, the projected area 'P' is

$$P = 2\pi r3 \quad (2)$$

where, '3' denotes the wall thickness, while 'r' is the radius of the pore. The newly calculated morphological factor 'f' using eqn (2) for values represented in Table 1 was calculated to be 0.015, 0.048, 0.079, 0.066 for ('d' nm = 20, 40, 100 – thick-walled and thin-walled) ZrNTs, respectively, indicating that the thin-walled NTs are more densely packed than the thick walled. Theoretical values continue to be greater than experimentally measured WCAs for all three morphologies. The experimental values are identical on all substrates, averaging at a value of (~160°). This value is at the physical limit of experimental measurements for low-energy surfaces and, hence, acts as a limiting criterion while quantifying the 'extent' of an already super-hydrophobic surface.[22] This essentially means that the surfaces measured experimentally may indeed have higher WCA values that are in reality closer to the theoretical calculations. Additionally, the proposed modification to the CBM due to incorporation of the wall-thickness accounts for the super-hydrophobic phenomenon exhibited by ZrNTs irrespective of pore-diameter, because the 'f' factor is comparable due to the type of packing exhibited by all three substrates. Implying that for a droplet of fixed volume, the drop-contact line interacts with similar solid fractions. Thus, superhydrophobicity observed for ZrNTs even at smaller pore-diameters is consistent with the constant WCAs reported for titania (increasing diameters will increase surface hydrophobicity).[22] Nevertheless, the droplet always remains balanced in CBM.[20,21] There appear a few variations in theory and experimental and may be attributed to the physical limits of experimental measurement as described earlier. In comparison to previous reports by Wang *et al.*,[14] this

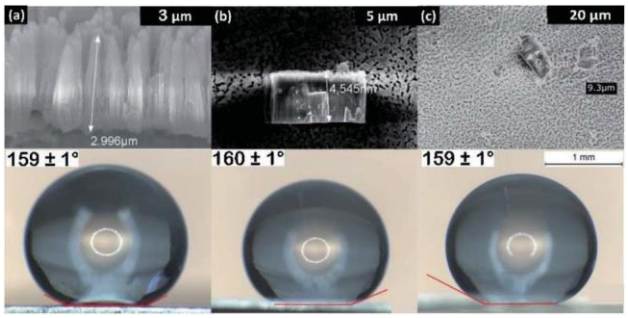

Fig. 5 Optical images of water droplets on SAM modified ZrNT structures of different oxide-layer thickness and corresponding SEM images of the cross-sections. Length (a) ~3 mm, (b) ~4.5 mm and (c) ~9 mm.

Table 1 Influence of pore-diameter on WCAs, measured and calculated values (according to Cassie–Baxter model and the proposed modification (3) to it)

	Water contact angle (°)		
	Cassie – Baxter model		
Pore diameter (nm)	Experimental	Theoretical	Modified-theoretical
~20	162 ± 1	172	173
~40	159 ± 1	168	167
Thick-wall (~100)	160 ± 1	159	164
Thin-wall (~100)	160 ± 1	167	165
Compact oxide	120 ± 2	—	—

is the first reported observation of superhydrophobic WCA on functionalized ZrNT for (d # 20 nm) produced *via* a single-step anodization. Additionally, the WCA of ZrNTs is also independent of length.

In conclusion, the nanoporous ZrO_2 layers produced *via* anodization show a transition from super-hydrophilic to super-hydrophobic surfaces when modified with a (non-fluorinated) octadecylphosphonic acid monolayer. Within the investigated range, WCAs remain constantly super-hydrophobic (~160°), irrespective of the change in pore diameters and length, thereby following the Cassie–Baxter model. By including the influence of a geometric parameter accommodating the wall thickness, the roughness factor is balanced and continues to remain within the transition threshold of the super-hydrophobic state. Such an observation is of importance as it offers insights into material behavior and is responsible for enhanced degrees of freedom during the fabrication process, such that both simple and complex geometries may still be able to elicit identical surface response. This level of flexibility offers the possibility to work with wider operating parameters involving the anodization process.

Author contributions

SNVR – conceptualization, data curation, methodology, investigation, writing – original draft. MSK – funding acquisition, project administration, supervision, resources and review & editing.

Conflicts of interest

There are no conflicts to declare.

Acknowledgements

The authors acknowledge the DFG researcher group FOR 1878 and KI 2169/2-1 for funding. The authors would like to thank Prof. Patrik Schmuki, Dr Maxime Hubert, Anja Friedrich, Anke Knoop and Ulrike Marten-Jahns for access to lab space, measurements, and discussion. Part of this work was performed at the Micro- and Nanoanalytics Facility (MNaF) of the University of Siegen.

Notes and references

1 M. Kulkarni, A. Mazare, P. Schmuki and A. Iglic, Influence of Anodization Parameters on Morphology of TiO_2 Nanostructured Surfaces, *Adv. Mater. Lett.*, 2016, **7**(1), 23–28, DOI: 10.5185/amlett.2016.6156.

2 H. Tsuchiya, J. M. Macak, I. Sieber and P. Schmuki, Self-Organized High-Aspect-Ratio Nanoporous Zirconium Oxides Prepared by Electrochemical Anodization, *Small*, 2005, **1**(7), 722–725, DOI: 10.1002/smll.200400163.

3 A. W. Amer, S. M. Mohamed, A. M. Hafez, S. Y. Alqaradawi, A. S. Aljaber and N. K. Allam, Self-Assembled Zirconia Nanotube Arrays: Fabrication Mechanism, Energy Consideration and Optical Activity, *RSC Adv.*, 2014, **4**, 36336–36343, DOI: 10.1039/c4ra05115g.

4 J. M. Macak, L. V. Taveira, H. Tsuchiya, K. Sirotna, J. Macak and P. Schmuki, Influence of Different Fluoride Containing Electrolytes on the Formation of Self-Organized Titania Nanotubes by Ti Anodization, *J. Electroceram.*, 2006, **16**, 29–34, DOI: 10.1007/s10832-006-3904-0.

5 V. Grover, R. Shukla and A. K. Tyagi, Facile Synthesis of ZrO_2 Powders: Control of Morphology, *Scr. Mater.*, 2007, **57**(8), 699–702, DOI: 10.1016/j.scriptamat.2007.06.053.

6 A. G. Sanchez, W. Schreiner, G. Duff´o and S. Cer´e, Surface Characterization of Anodized Zirconium for Biomedical Applications, *Appl. Surf. Sci.*, 2011, **257**(15), 6397–6405, DOI: 10.1016/j.apsusc.2011.02.005.

7 W. Li, H. Huang, H. Li, W. Zhang and H. Liu, Facile Synthesis of Pure Monoclinic and Tetragonal Zirconia Nanoparticles and Their Phase Effects on the Behavior of Supported Molybdena Catalysts for Methanol-Selective Oxidation, *Langmuir*, 2008, **24**(15), 8358–8366, DOI: 10.1021/la800370r.

8 S. N. V. Raghu, H. Chuluunbandi and M. S. Killian, Zirconia nanotube coatings - UV-resistant superhydrophobic surfaces, *Surf. Interfaces*, 2021, **26**, 101357, DOI: 10.1016/j.surfin.2021.101357.

9 J. C. Garcia, L. M. R. Scolfaro, A. T. Lino, V. N. Freire, G. A. Farias, C. C. Silva, H. W. L. Alves, S. C. P. Rodrigues and E. F. Da Silva, Structural, Electronic, and Optical Properties of ZrO_2 from *Ab Initio* Calculations, *J. Appl. Phys.*, 2006, **100**, 104103, DOI: 10.1063/1.2386967.

10 S. Heiroth, R. Ghisleni, T. Lippert, J. Michler and A. Wokaun, Optical and Mechanical Properties of Amorphous and Crystalline Yttria-Stabilized Zirconia Thin Films Prepared by Pulsed Laser Deposition, *Acta Mater.*, 2011, **59**(6), 2330–2340, DOI: 10.1016/j.actamat.2010.12.029.

11 M. S. Killian, *Organic Modification of TiO_2 and Other Metal Oxides with SAMs and Proteins - a Surface Analytical Investigation*, PhD Dissertation, Friedrich-Alexander, University Erlangen-Nuremberg, 2013.

12 C. Piconi and G. Maccauro, Zirconia as a Ceramic Biomaterial, *Biomaterials*, 1999, **21**(1), 1–25, DOI: 10.1016/S0142-9612(98)00010-6.

13 Q. Yuan, Y. Liu, L. L. Li, Z. X. Li, C. J. Fang, W. T. Duan, X. G. Li and C. H. Yan, Highly Ordered Mesoporous Titania-Zirconia Photocatalyst for Applications in Degradation of Rhodamine-B and Hydrogen Evolution, *Microporous Mesoporous Mater.*, 2009, **124**(1–3), 169–178, DOI: 10.1016/j.micromeso.2009.05.006.

14 W. Gao, L. Dickinson, C. Grozinger, F. G. Morin and L. Reven, Self-Assembled Monolayers of Alkylphosphonic Acids on Metal Oxides, *Langmuir*, 1996, **12**(26), 6429–6435, DOI: 10.1021/la9607621.

15 L.-N. Wang, C. Shen, A. Shinbine and J.-L. Luo, Variation on Wettability of Anodic Zirconium Oxide nanotube surface, *Thin Solid Films*, 2013, DOI: 10.1016/jtsf.2013.01.066.

16 R. Wang, K. Hashimoto, A. Fujishima, M. Chikuni, E. Kojima, A. Kitamura, M. Shimohigoshi and T. Watanabe, Light-Induced Amphiphilic Surfaces [4], *Nature*, 1997, **388**, 431–432, DOI: 10.1038/41233.

17 H. Tamura, K. Mita, A. Tanaka and M. Ito, Mechanism of Hydroxylation of Metal Oxide Surfaces, *J. Colloid Interface Sci.*, 2001, **243**(1), 202–207, DOI: 10.1006/jcis.2001.7864.

18 M. S. Killian, J. F. Gnichwitz, A. Hirsch, P. Schmuki and J. Kunze, ToF-SIMS and XPS Studies of the Adsorption Characteristics of a Zn-Porphyrin on TiO_2, *Langmuir*, 2010, **26**(5), 3531–3538, DOI: 10.1021/la9032139.

19 H. Y. Nie, Revealing Different Bonding Modes of Self-Assembled Octadecylphosphonic Acid Monolayers on Oxides by Time-of-Flight Secondary Ion Mass Spectrometry: Silicon *vs.* Aluminum, *Anal. Chem.*, 2010, **82**(8), 3371–3376, DOI: 10.1021/ac100671q.

20 R. N. Wenzel, Resistance of Solid Surfaces to Wetting by Water, *Ind. Eng. Chem.*, 1936, **28**(8), 988–994, DOI: 10.1021/ie50320a024.

21 A. B. D. Cassie and S. Baxter, Wettability of Porous Surfaces, *Trans. Faraday Soc.*, 1944, **40**, 546–551, DOI: 10.1039/tf9444000546.

22 E. Balaur, J. M. Macak, H. Tsuchiya and P. Schmuki, Wetting Behaviour of Layers of TiO_2 Nanotubes with Different Diameters, *J. Mater. Chem.*, 2005, **15**(42), 4488–4491, DOI: 10.1039/b509672c.

SUPPORTING INFORMATION

Wetting Behavior of Zirconia Nanotubes

Swathi Naidu Vakamulla Raghu and Manuela Sonja Killian

RSC Advances, 2021, 11, 29585-29589, https://doi.org/10.1039/D1RA04751E

DOI: https://doi.org/10.1039/D1RA04751E

Supporting Information

Wetting Behavior of Zirconia nanotubes

Swathi Naidu Vakamulla Raghu [a], *Manuela Sonja Killian** [a]

[a] *Chemistry and Structure of Novel Materials, University of Siegen, Paul-Bonatz-Str. 9-11, 57076 Siegen, Germany*

Experimental

XPS- Characterization parameters

XPS spectra were recorded on a PerkinElmer Physical Electronics 5600 spectrometer. The specimens were excited using a monochromatic radiation source { Al Ka - 1486.6 eV, 300 W}. Spectra {O 1s, C 1s, Zr 2p, P 2p} were recorded under a takeoff angle of 45° and the binding energy was determined at a pass energy of 23.5 eV, with a resolution of 0.2 eV. For charge compensation, the binding energy of the C 1s signal was used. The background was subtracted using the Shirley method and the molar fractions of each species were acquired via the acquisition software {MultiPak V6.1A, Copyright Physical Electronics Inc., 1994-1999}. The data curated as a result of this experiment may be seen in Figure-2 in the main-manuscript.

Figure-S1

Water Contact Angle Measurements

Two contact angle goniometer devices {*Leica application suite* and *0ssilla* device and software} were used to determine the static water contact angle values {DI water droplet with a volume of 10µl}. Figure-S1, depicts the optical microscopy images of the water droplets on the respective OPA-modified Zirconia substrates as measured using the two devices. Both instruments produce deviations of results only with the regular error of the measurement. The WCAs for OPA modified ZrNTs recorded on the *0ssila* device produces marginally enhanced values {WCA_{0ssila} = 160 ± 3°} to the *Leica suite* ones {WCA_{Leica} = 159 ± 3°}. This most likely is caused by a small deviation in the angle of substrate and camera, as can be deduced from Figure S1. In conclusion, iterative experiments resulted in all OPA modified zirconia nanotube substrates demonstrating superhydrophobicity independent on tube morphology and geometry.

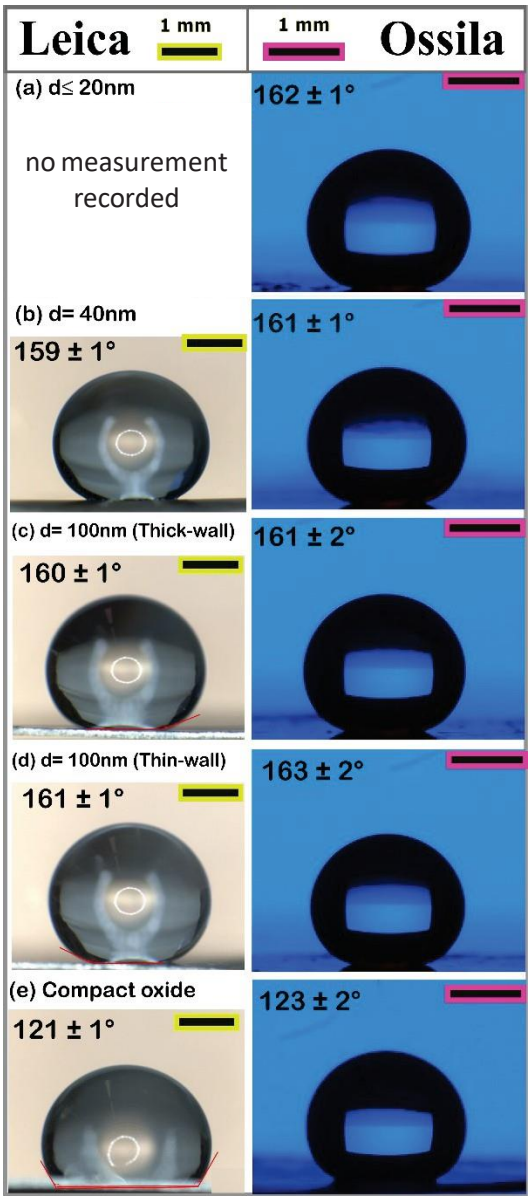

Figure S1: 0ptical image comparison of WCA as measured by different goniometers.

4.3. Functionalization strategies to facilitate multi-depth, multi-molecule modifications of nanostructured oxides for triggered release applications

Swathi N.V. Raghu , Gabriel 0nyenso , Shiva Mohajernia and Manuela S. Killian

Surface Science, 719, 2022, 122024, https://doi.org/10.1016/j.susc.2022.122024

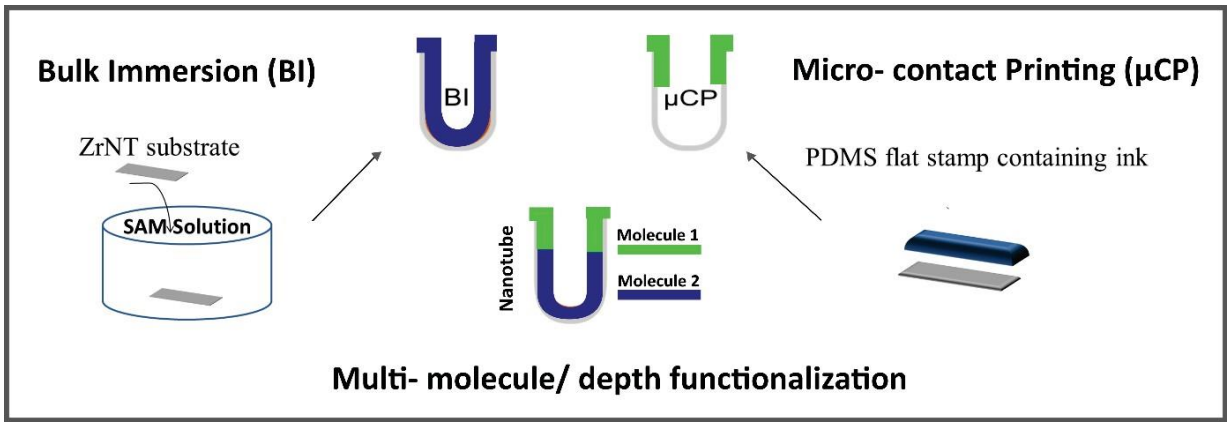

ToC - 4.3 - Schematic representation of sequential functionalization of ZrNTs

The article in this section focuses on two main aspects; validating the accessible volumetric space in nanotubular structures and explicating surface modification methodologies that render ZrNTs functionalized with organic molecules. At the outermost layer such as the tube tops, SAMs of organic molecules may be deposited directly onto the area of interest using micro-contact printing {µCP}. Alternatively, using a bulk immersion {BI} technique results in the deposition of molecules not just on the tube tops but also result in coating of the NT walls. These two modification techniques exploit the kinetics of diffusion to deposit molecules at varying depths within the nanotubes, as is confirmed by depth profiling using ToF-SIMS characterization. This section subsequently addresses two more objectives of this dissertation, namely to

'Evaluate storage capabilities of the homogenous nanostructures' and 'Develop a strategy to facilitate and evaluate multi-depth filling of nanotubes.'

In addition to this, the μCP strategy of stamping is suggestive to aid in the 'capping' of tube tops. Nanotubular arrays can function as drug repositories and these filled-ZrNTs may be sealed-shut using SAMs, as deposited via μCP. The capping layer may be used in triggered release applications. Selectivity refers to specific conditions that promote degradation of the capping, eventually resulting in the elution of the contents of the tubes.

Surface Science 719 (2022) 122024

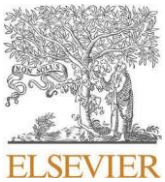

(ar osr oebtneoeb - nt j tsb obNcnsr csx ngscob

Ni gU csbNcnsr csb

journal homepage: www.elsevier.com/locate/susc

Zi r conar tnu onar beog os- nseboabU cntno osbV i tonphsyodfbV i tonpV atsci tsb V ahnSc onar eba Ubr raeogi coi gshbawnhsebUa gbogn- - sgshbgsts esb yytnc onar eb

Nk odnbmlRlb, - di fbK j gnstbCr Msr ea fbNdn- bA ad Tsgr n fbA ri st bNlbI nttn r [L]

Chemistry and Structure of Novel MaterialsJ University of SiegenJ Paul-Bonatz-Straße . -99J Siegen 15750J 6ermany

E , F O( ) X bOm Z C

GeyDordsp
NstUp eesVj tshbVar at MsgbPNEA zb
A ncgapcar o cobygnr onr- bPµ(Bzb
FaZpNOA Nb
fiBNb
flngcar n b
Er ahnu onar b
m raeogi coi gsb
Bdaeydar ncb cnheb

E. NF , E (F

Aso tpawnhsbei gUcsebd -sbei ccseeUi ttMbj ssr bV ahnSshboabstncnobei gUcsbdMhgaydaj ncnoMb-n bUcntsb yytnc onar baUb estUp eesV j tshbV ar at MsgebPNEA ezbi enr- bc gj adMhg osbV atsci tsebcaV ygnenr - bydaeydar ncb cnhb- gai yelbOr bodneb k agHfbk sbedshbtn- dobar bodsbgatsbaUbodsbUi r conar tnu onar boscdr nvi sbi eshbUagbei gUcsbV ahnSc onar baUbungcar n b r raoi j sebPflgmFzb r hbcaV y gsbodsbswosr obaUb cdns- j tsbdMhgaydaj ncbsUUscob eb bUi r conar baUb yytnc onar boscdp r nvi sfbnVVsgenar bnr bj i tHbeati onar bP. Ozb r hbV ncgapcar o cobygnr onr- bPµ(BzfbUagbhnUUsgsr obV atsci t gbcd nr btsr- odelb 2i tno on-sb r hbvi r ono on-sbs- ti onar baUbflgmFbei gUcsebV ahnSshb-n bµ(Bb r hb. Obnr bNEA beati onar ebk ebysgp UagVshbcaVj nr nr- beo oncbk osgpcar o cob r- tsbV s ei gsV sr oefbfiBNb r hbFaZpNOA Nbhsyodpyga Stnr- boabyga-nhsbnrp en- doebnr oabsUUscon-sbV i tonpUi r conar tbhsyodbV ahnSc onar elbx s-n onr- bV ahnSc onar bhsyodebaUbodsbr raeogi coi gshb awnhsbcai thbj sb cdns-shbk nodbodsesbV sodahelbFdsbi esbaUbesvi sr on tbUi r conar tnu onar beog os- nseb-n b. Ob r hbµ(Bb j s geb bDygaaUbaUbygnr cnyts' oabcgs osbr raeogi coi gsebod ob gsb j tsboabhsV ar eog osbj aodbVi tonpV atsci tsb r hbVi tonpb hsyodbV ahnSc onar elbA i tonUi r conar tbflgmFefbV ahnSshbk nodbok abV atsci tsebnr bestscoshbhsyodefbk sgsbaj o nrshbj Mb odsbcaV j nr onar baUbj aodbV ahnSc onar bVsodaheb r hbs- ti oshb-n bhMsbgsts esbswysgnVsr oeb nVshboabenVi t osbhgi - b gsts esbj sd -naglbFdsbhneysr e onar baUbta hshbhMsbk ebnr -seon- oshbnr b- gnai ebeat-sr oelb/ dntsbr abhMsbcai thbj sb hsoscoshbnrb vi sai ebsr -ngar V sr ofb bcaV ytsosbgsts esbaUbodsbhMsbk eb cdns-shbnr bsod ratfbc i eshbj Mb bhs- g h onar b aUbodsbµ(BpCx BEbt MsglbCi gbgsei toebnr hnc osbod obodsbgsts esbaUbodsbc g- abaUbVi tonpUi r conar tbawnhsbr raeogi coi gseb c r bj sbogn- - sgshfbsl- lfbj Mb tosg onar baUbodsbcdsV nc tbsr -ngar V sr olbbb

1. Introduction

Eb- gak nr- bnr osgseobnr bV i tonpUi r conar tbr rapV osgn tebk nodbdn-d ei gUcsbgseyar en-noMb r hbj napV nVsoncbj sd -nagbd ebaysr shb -sr i seboap k ghebrsk b r hbnnr a- on-sbhs-stayV sr o tbgai oseq[–1]lbXeyscn ttMbnr bodsb j naV shnc tbSsthfbV i tonpUi r conar tbV osgn teb gsbj snr- bswytagshbUagb ygaeodsonceb r hbhn - r aeoncbyga- r aeneq5–0]lbA i tonpUi r conar tbV osgn teb gsbseyscn ttMbei noshbUagbnV yt r obca onr - efbk dsgsbodsMbyaosr on ttMbc r b es g-sb ebhgi - bgsesg-angeb r hbenV i to r sai etMbsr d r csbodsbnV yt r ob ccsyo r csq3]lb

Oobnebk sttbHr ak r bod obhs-ncseb r hbV osgn tebnr bodsbr rapec tsbgs- nVsb j srsSobUgaV bV wnV nunr- bodsbei gUcsb gs boab-ati V sbg onafbodsgsj MbaUp Usgnr- bswcsyonar tbc y cnonseb ebhgi - phstn-sgMb-sdnctsefbsl- lfbnr bodsbed ysb aUbr raoi j seq6]lbEhhnonar ttMfbr rapV osgn tebaUUsgb bdn- dbodgai - dyi ofb seyscn ttMbk dsr bi eshbUagbhn - r aeoncbyi gyaesebnr bodsbUagV baUbesr eageq7fb [8]lb(ar -sr onar tbj i tHbV osgn tebei cdb ebV so tbV ar atnodebc r bj sb og r eUagV shb nr oab r raeogi coi gshb V so tpawnhseb -n b stscogacds V nc tb r ahnu onar b k nodb - gnai eb V agydata- nseb ei cdb eb r raoi j sefb r raeyar - sefbcaV y cobawnhsefbr sshtsefbyntt gefbsocbq[[ ]lbZi godsgV agsfb odsngbei gUcsbgs con-noMbc r bj sbV ahnSshb-n bcdsV nc tb r hbydMenc tb Vsodahebei cdb ebtnoda- g ydMfbydMenc tbagbcdsV nc tb- yagbhsyaenonar b r hb ei gUcsp- g Uonr - fboabr V sb bUsk bq[' –[9]lbA agsbeyscnSc ttMfbr raoi j seb d -sb- odsgshbnr cgs enr- b oosr onar bhi sboabodsbai oeo r hnr - bcar ogatba-sgb odsngb- saV sogMlbOr bodsbgscsr obhsc hsfbV so tbawnhsbr raoi j sebk sgsb gsys oshtMbgsyagoshb ebhgi - pc ggnsgefbnV yt r obV osgn teb r hbesr eageb q[0–[6]lbFdsesbUecnr onr - bhs-stayV sr oebnr hnc osb bU-ag j tsbyga- gsep enar boak ghebVi tonpcaV yarsr obeMeosV ebc y j tsbaUbst j ag oshbgseyar esefb ei cdb ebgs- i t oshbsti onr- bgseyar esb-n bhnUUi enar tbj ggnsgebV hsbi ybaUb ag- r ncbV atsci tselbx nUUi enar bj ggnsgebV hsbaUbyatMVsgebd -sbygs-nai etMb j ssr bgsyagoshbar bUagbenr - tsphgi - pbgsts esbeMeosV ebq[7]lb@tonV ostMfb b enr- tsbesr enr- bi r nobPr raoi j s: br rapt Msgzbc r bcar o nr bV i tonytsbUi r cp onar tbV atsci tsebtac oshb obhnUUsgsr obhsyodebk nodnr bodsbr raeogi coi gslb Fdsbci ggsr obogsr hbnr bodsbj naV shnc tbSsthbnr -at-sebodsbi esbaUbei gUcsb ca onr- ebnr bodsbUagV baUbag- r ncbV atsci tsefbygaosnr ebsoclbq' 8–' ']lbNi cdb ag- r ncbV ahnSc onar ebnr bodsbt j ag oagMbec tsb gsbaUosr bcdns-shb-n bNEA b V ahnSc onar bi enr- bj i tHpnVVsgenar bP. Ozfbnlslfbea Hnr- bodsbo g- sobV osgn tb

L (aggseyar hnr- b i odagl
I -mail addressp A ri st lI nttn r; i r npens- sr lhsbPA lNlbI nttn r zl

dooyeJ: : hanlag- : [8l[8[0: Tlei ecl' 8' ' l[' ' 8' 5b
, scsn-shb' 0bCcoaj sgb' 8' [4b, scsn-shbnr bgs-neshbUagV b1bG r i gMb' 8' ' 4bEccsyoshb3bG r i gMb' 8' ' bbb
Available online 25 January 2022

nrb bj i tHpeati onar bcar o nr nr- bodsbV atsci tsbaUbcdancslbOr bodnebygacseefbodsb UagV onar baUb bi r nUagV bNEA bt Msgbodgai - dai obodsbj espV osgn tbneb eei V shbq' 1f 5]lbWak s-sgfb. Ob ttak eb-sgMbtnootsbcar ogatba-sgbodsbgs- nar b aUbca-sg - slbFdnebnebV nr tMbhi sboabodsbU cobod obea Hnr- bsr j tsebodsb hsyaenonar baUbV atsci tsebar bodsbsr ongsbcar o cobei gUcsfb obts eobnr bodsbc esb aUbodsbeati onar bk soonr- bodsbei gUcslbFdnebtnV noshbcar ogatba-sgbhsyaenonar b neb y gonci t gtMb hne h- r o - sai eb k dsr b V i tonytsb gs con-nonseb agb enospeyscnScbUi r conar tnoMbnebswyscoshbUgaV bodsbei gUcsfbUagbnr eo r csfbUagb b Vi tonpV atsci tsbhs os conar besr eagbU j gnc os hba-s gb br rat Ms gshbei j p eog oslb(aV j nr nr- b. Obk nodbV ncgapcar o cobygnr onr- bPμ(Bzbneb beog n- dop Uagk ghb yyga cdboab cdns-sbVi tonytsbUi r conar tnonsebnr bVi tonytsbhsyodelb μ(Bbi eseb beaUopeo V yboabhsyaenobV atsci tsebP-n b r bnr Hpeati onar zbar oabodsb car o conr- bei gUcsb r hbodsbog r eUsgbaUbV atsci tsebd yysr ebeyar o r sai etMb i yar bei j eog ospei gUcsbcar o colbOr bodnebk agHfbk sbi esbungcar n br rap eogi coi gsebaj o nrshb-n b benr- tspeosyb r ahnu onar bygacseeb eb bei j eog osb r hbi esbydaeydar ncb cnhefbacoMtydaeydar ncb cnhbPC BEzb– ($_{6}W_{[3}$BC PC Wz_{b} r hbaco hscMtydaeydar ncb cnhbPC x BEzb– ($_{[6}W_{13}$BC PC Wz_{b} ebNEA elb/ sb caV y gsbodsbgatsbaUbUi r conar tnu onar bV sodahefbr V stMb. Ob r hbμ(Bfb eb k sttb ebodsbnr %i sr csbaUbodsbei gUcsbV ahnSc onar b-n b- gnai ebNEA ebar bodsb k soonr- bj sd –nagbaUbV ahnSshbflgC$_{\cdot b}$r raoi j sebPflgmFzlbEhhnonar ttMfbodsb eo j ntnoMboak ghebs wyaei gsboabag- r ncbPsod r atzb r hb vi sai ebPhneonttshb k osgzbeat-sr oebnebeoi hnshlb/ sbgsyagobar bodsbhnUUsgsr csbnr bhsyodbUi r cp onar tnu onar bUagb. Ob r hbμ(Bb r hbhsV ar eog osfb ebygaaUpaUpygnr cnytsfbodsb j ntnoMboabcar ogatbhgi - bgsts esbUgaV br raoi j sebj Mbc yynr- bodsboi j sboayeb i enr- bμ(Bbei gUcsbUi r conar tnu onar lb/ sbs- ti osbhnUUi enar bogsr hebj Mb ysgUagV nr- bhMspgsts esbswysgnVsr oebUgaV bodsbr raoi j sebi enr- b@RpRneb eyscgaecayMbnr b hhnonar boabeo oncbk osgbcar o cob r - tsbP/ (EzbV s ei gsp V sr oelbFdsbygsesr csbaUbNEA bV atsci tsefbei gUcsbca-s g - sb r hbhsyodb hneognj i onar bk sgsbcar SgV shbj MbonVspaUp%n- dobescar h gMbnar bV eebeyscp ogaV sogMbPFaZpNOA Nzb r tMeneb r hbcaV ytsVsr oshbk nodbfipg Mbydaoap stscogar beyscogaecayMbPfi BNzlb

2. Res l ria l ntb(

flgbUantebP77l' -byi gnoMfbKaahUs ttak b@I fb8l[' 9bV V bodncHr seezbk sgs i tog ear nc ttMbcts r shbnr b cso ar s fbV sod r atb r hbs od r atbUattak shbj Mb gnr enr- bnr bhs nar nushbk os gb r hb ngphgnshbygnagboabs tscogacds V nc tb r ahp nu onar lbFdsbenr- tspeosyb r ahnu onar bk ebc ggnshbai obi enr- b bdn- dp-ato -sb yaos r onaeo obPG neets bOA Bb66p' 88bB(zbnr bs tscogacds V nc tbcsttebk nodb b k agHnr- b gs baUb[bcV ' ^{b}i enr- b byt onr i V bcai r os gbstscogahs bnrb bok apb stscogahs bes oi ylbEr ahnu onar bk ebc ggnshbai obnr b beo r h ghb- tMcsgatpb j eshbag- r ncbs tscogatMos bcar eneonr- baUb[8-bUagV V nhsfb5bk o-bmW$_{s}$Zb PA s gcHzb r hb' bk o-bW$_{\cdot}$ ClbE bg V ynr- byaos r on tbaUb[bRe$^{-[\ b}$UgaV bC (Bbk eb i eshb r hbHsyob ob18bRbUagb[9bV nr boabcgs osbi r nUagV br raoi j i t gbeogi cp oi gsebq' 9]lbflgbcaV y cobawnhsbP(CzbStV ebk sgsbygsy gshbar bflgbUantebi r hsgb bcar eo r obyaos r on tbaUb18bRbUagb18bV nr bnrb b[bA bW$_{\cdot}$ NC$_{sb}$PA sgcHzbstscp ogatMoslbEr ahnushbt Ms gebk nttbj sbgs Usggshboab eb“ungcar n bei j eog os e” odgai - dai obodnebk agHb r hbk sgsb r r s tshb ob598b°(bUagb[bdbygnagboab Ui godsgbygacseenr- lbFabnVy gobei gUcsbdMhgaydaj ncnoMfbodsbok ab yp yga cdsebaUbj i tHbnVVs genar bP. Ozb r hbV ncgapcar o cobygnr onr- bPμ(Bzbk sgsb yytnshlbOr bodsb. Obeog os- Mfbe V ytsebk sgsbea Hshbnr beati onar ebcar o nr nr- b [8bV A bacoMtydaeydar ncb cnhbPC BEfb($_{6}W_{[3}$BC PC Wz zbagbaco hscMtydaep ydar ncb cnhbPC x BEfb($_{[6}W_{13}$BC PC Wz zbnr bos og dMhgaUi g r bPFWZfb, aodzbUagb ' 5bdb ob V j nsr obcar hnonar elbNi j esvi sr otMbe V ytsebk sgsbgnr eshbj Mbyi gsb FWZbUagb18bebUattak shbj MbhgMnr- lbZagbμ(Bfbe V ytsebk sgsbygahi cshbj MbnrHb P[8bV A fbC BEbagbC x BEbnr bFWZzbog r eUsgbUgaV b bBx A NbPNMt- ghb[65fb [8J[pci gnr- b - sr ozb% opeo V ybhngscotMbar oabodsbflgC$_{\cdot}$ pei j eog os ebUagb b hi g onar baUb[8bV nr fbgsr hsgnr- bodsbei gUcsbaUbodsboi j spoayebdMhgaydaj nclb Nc rr nr- bstscogar bV ncgaecayMbPWno cdnbNXA bZXb5688zbk ebsV ytaMshbUagb odsbeogi coi g tb r hbV agydata- nc tbcd g cos gnu onar baUbodsb r ahnushbungp car n beyscnVsr elbNi gUcsbcdsV nc tbcd g cos gnu onar b r hbhsyodbygaS tnr- b k ebysgUagV shbi enr- b bFaZpNOA NbORbnr eogi V sr obPOC mpFC ZfbA Qr eosgzlb Ni gUcsbca-s g - sbk ebseonV oshbj MbfiBNbPNNfip[88bNi gUcsbNcnsr csbOr p eogi V sr oezlbZi godsgbswysgnV sr o tbhso ntebUagbfiBNb r hbFaZpNOA Nbc r bj sb Uai r hbnr bodsbNOlbNo oncbk osgbcar o cob r - tsbP/ (EzbV s ei gsV sr oebk sgsb ysgUagV shbi enr- b r bCeent b(ar o cobEr - tsbKar naV sosgbPx Obk osgbhgaytsob -ati V sfb[8bμtzboabhsosgV nr sbk soonr- bj sd -nagb r hboabs- ti osbodsbeo p j ntnoMbaUbNEA ebnrb vi sai ebVshni V b obhnUUsgsr obonVsbyanr oelbx Msbgsts esb swysgnVsr oebk sgsbysgUagV shb k nodbci gci V psod r atbeati onar eb P[l9b V- : V tzlbFdsbci gci V bP. nabpb, sk sfbAsgecdj gacHp/ nsesbKsk QgubKV j Wzb k ebeai gcshbtac ttMlbFdsb eb r ahnushbflgmFbk sgsbei j Tscoshboab' 5bdb ea Hnr- b nrb odsb hMspeati onar b r hb ngb hgnshb ygnagb oab Cx BEpdMhgaydaj nu onar b-n bμ(BlbFdsbhMspta hshbe V ytsebk sgsbodsr b ea Hshbnrbk sttbyt osebcaro nr nr- b' bV tbsod r atbagbhneonttshbk osgfb gseyscon-stMfb r hbodsbei j esvi sr obhgi - pgsts esbk ebV s ei gshb eb j eagp j r cs baUbods bcd g cos gneoncbj gn- dobMs ttak bcatagb-s r sg onr- b bj ga hbj r hb en- r tb obk -stsr - odebnr bj s ok ssr bP188br V b ⟨ $\lambda_{ci\ gci\ V\ nr}$ ⟩ 988br V zbi enr- b @RpRnebeyscogaecayMbPBsgHnr XtV sgb) V j h bfi) N: fi) N+zb r hbodsbcar p csr og onar ebcaggseyar hnr- boabgseyscon-sb j eagj r cs b- ti sebk sgsbhsosgp V nrshbj Mbodsb. ssgp) V j sgob) k lb

) . F l gu(tg bnd digcuggion

(L9L I valuation of multi-deKth functionalization

Er ahnu onar bneb r bsUUscon-sbeog os- Mboabhs-staybawnhsbt Msgebk nodb car ogatt j tsbV agydata- nseba-sgbr ar pr aj tsbV so ttncbei j eog os elbC wnhsb StV bei gUcsebc r b- gMbUgaV bj i tHpStV ebei cdb ebcaV y cobawnhseboab eogi coi g ttMbi r nvi sbUcsoebei cdb eboi j sefb- g eefbeyar - sebsoclbq[[ ]lb m r aeogi coi gshbungcar n bk eb cdns-shb-n b benr- tspeosyb r ahnu onar b i enr- b V V ar ni V b%i agnhsbnr b r bag- r ncbstscogatMosbq' 0f' 3]fbodsbgsei top nr- bawnhsbt Msgbd hb bcngci t gbr raoi j i t gbV agydata- Mb ebgsygsesr oshbnrb Zn- lb[lbFdsbar spyaobeMr odsenebgsei toebnrb bdaV a- sr sai ebawnhsbt Msgfbk nodb r b -sg - sbyagsbhn V sosgbaUbu 68–[88brV bPZn- lb[zb r hb r b -sg - sbt Msgb odncHr seebaUbu ' l9–1l8bμV bPZn- lb[j zlbFdsb j esr csbaUb bygspsocdnr- beosyb ttak ebUagb bedagosgb r hbenV ytsgbUj gnc onar bq' 3]lb(aV y cobawnhsbei gp U csebk nodb bS tV bodncHr seebaUbu 98p39brV bk s gs b teabei ccseeUi ttMbygsy gshb ebessr bj Mbods bcd g cos gneoncbcatagbcd r - s bhi s boabnr os gUs gsr cs bs UUscoebnrb ods bog r ey gs r obawnhs bt Ms gefb ebedak r bnr b**Tip. , 1 3, IB**lbFds b ep r ahnushb e V ytsebcar eneobaUb V agydai ebflgC$_{\cdot b}$r raoi j sb gg Meb r hbodsbfi, x ben-p r tebPZn- lb[czb yys gnr- b ob19° P88' zfb13° P[8[zfb56° P[8' zb r hb05° P881zb gsb ecgnj shboabflgbVso tbUgaV bodsbei j eog osbq' 6f' 7]lbErrs tnr- bgsei toebnrb byd esbog r eUagV onar boabV nr tMbV ar actnr ncbyd esbcd g cos gnushbj Mb gs %s conar eb ob18° A P–[[[zfbA P[[[zfbA P' 88zb r hb98° A P' ' 8zfbA P8' ' zb q18f1[ ]lb

NE A ebc r bj s bygahi cshbar bawnhsbei gUcsefbsl- lfbodgai - dbydMenc tb - yagbhs yaenonar fbs tscogaphs yaenonar fbV ncgapcar o cobygnr onr- b r hbods b V ags bca V V ar tMbi eshb nVVs genar b nrb j i tHb eati onar b q[' –[5f1' f11]lb Bdaeydar ncb cnhebk s gs bygs-nai etMbedak r boabUagV beo j ts bj ar heboabflgC$_{\cdot b}$ q' 0f15]lbFdsbr r aeogi coi gs hbflgC$_{\cdot b}$t Ms gebk s gs bUi r conar tnushbj Mbods b heagyonar b aUbag- r ncb NE A ebaUbC BEfb($_{6}W_{[3}$BC PC $Wz_{\cdot}$ fb r hb Cx BE fb ($_{[6}W_{13}$BC PC Wz lbOr baghs gboabdMhgaydaj nus bods bflgC$_{\cdot b}$ei gU cs efbods bei j p eog os ebk s gs bs nods gbV ncgapcar o cobygnr os hbPμ(Bzbagbea Hs hbnr bj i tHpNE A b eati onar ebP. OzlbFdses bydaeydar ncb cnhebUagV beogar - bj ar hebk nodb r hb hsr estMby cHs hbS tV ebar b bdMhgaydntncbawnhs bei gU cslbFds Mb tn-r b eb b gsei tobaUbdMhga- sr pj ar hnr- bj sok ssr bods bds hb- gai yeb tar - bk nodbR r bhsgb / tebnr os g conar baUbodsbV s odMtbi r noeb r hbc r bgs r hs gbei gU csebei ys gp dMhgaydaj ncbq' 9f19–16]lbFds bgs t on-sbei ys gdMhgaydaj ncnoMbaUbods bnrp hn-nhi tbungcar n bei j eog os efbflgmFb r hbflg(C fbUi r conar tnushbj MbC BE b r hb Cx BE bNE A eb-n b. Obagbμ(Bbeog os - ns ebk ebs - ti os hbj Mbk os gbcar o cob r - ts bV s ei gsV sr oelbZn- lb' **b** edak ebods bayonc tbV ncgaecayMbnV - sebaUb k osgbhgaytsoebar bflgC$_{\cdot b}$ei j eog osebPoaybpb-n b. Ofbj aooaV bpbμ(BzlbEbei V p V gMbaUbods b/ (EbV s ei gs V sr oebnebgs ygs esr os hbnr bZn- lb' j bUagbs ens gb vi r onSc onar lbCr bflgmFefbei ys gdMhgaydaj ncnoMbP/ (Eb≥ [98°zbk eb aj es g-s hbUagbj aodbNE A ebnggseys con-sbaUbUi r conar tnu onar beog os - Mfbk nodb r b -sg - s b/ (E baUb[01°± ' °lbFdnebydsr aV sr ar bc r bV TagtMbj sb oognj p i oshboabodsbsr d r cshbgatsbaUbei gUcsbgai - dr seeb eb bgsei tobaUbr raec tsb oaya- g ydMb r hbc r bj s bs wyt nrshbj Mbods b(eens p. wos gpA ahstbq17]lbxi sb oabodnebs wyscos hb(eens p. wos gbs UUscofbods bV atsci t gbhsr enoMbgs vi ngshboab gs cdbdMhgaydaj ncnoMbV Mbj sbtseebod r bar b% obei gU cselbOr baghs gboab hs os gV nrsbk ds ods gbods b heagyonar bj sd -nagbaUbj aodbV atsci tsefbCx Eb r hb Cx BEfbnebcaV y g j tsfbcaV y cobawnhsbei gUcsebk sgsbUi r conar tnushb r hb

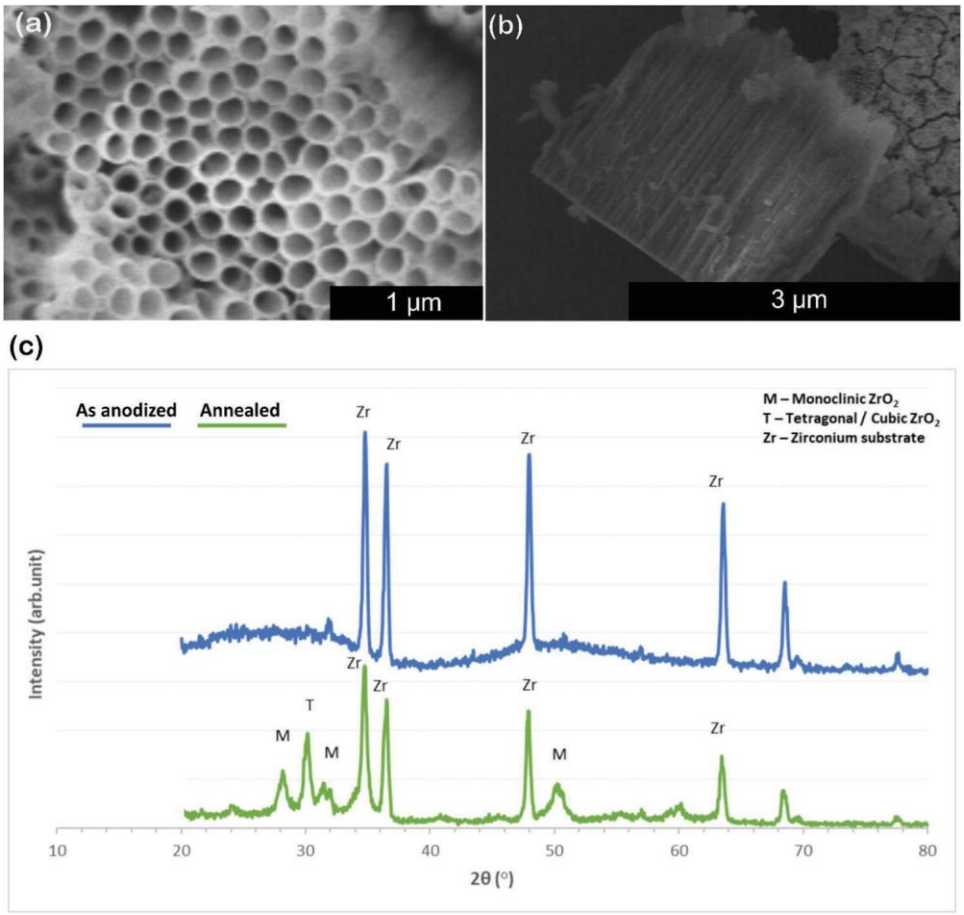

Tip. 1. Erahncbungcarn br raoi j seJbNXA bV ncga- g ydeb– P zboayb-nsk fbPj zb rhbcgaeepesconar4bPczbfi, x bygnagboab rhb Uosgb rns tnr- baUbodsbflgmFelbb

s- ti os hbUagbods bs wosr obaUbdMhgaydaj ncbj sd -naglbFds bflg(C bei j eog os eb habr aobedak bods be V s bs wosr obaUbdMhgaydaj ncnoMb ebods ngbr r aoi j i t gb cai rosgy goefbk dncdbnebnr btnrsbk nodbodsb(eensp. wosgbV ahstlbflg(C−CBEb V ahnSs hbei gU csebedak b b/ (EbaUb[80°P± [°zbk ds gs ebflg(C−Cx BEb gsyagoshb b/ (Eb≥ [' 8°lbFdnebaj esg- onar b tn-r ebk nodbygs-nai etMbgsyagoshb - ti sebq58f5[ ]lbOobnebnr os gs eonr - boabr aos bod obods bedagos gbcd nr pts r- odb V ahnSs hbei gU csebedak benV nt gbei gU cs bdMhgaydaj ncnoMba-s gbods bflg(Cb ei j eog osbPflg(C−CBEzbs-sr bk dsr bodsgsbnebV agsbNEA peati onar b - nt j tsb -ati V s ognc ttMfbei cdb ebk nodb. Obnr bcaV y gnear boabµ(Bfbnr hnc onr- b b caV y g j ts bei gU cs bca-s g - s bUagbj aodbV ahnSc onar b yyga cdselbCr bods b car og gMfbflg(C−Cx BEbedak eb bcts gbsr d r cs V sr obaUbdMhgaydaj ncnoMb Uagb. ObP[17°± 1°zb-s gei ebµ(BbP[' 9°± ' °zfbnr hnc onr - b bV ags bs UScnsr ob tn- r V sr ob r hbonV sphsysr hsr obgsaghs gnr- baUbodsbtar - sgpcd nrb tnyd oncb ydaeydar ncb cnhbar bodsbflgC·ₜei gUcsbq5' –59]lb

FaZpNOA Nb V s ei gs V sr oeb Pes V npvi r ono on-szb k s gs bys gUagV shb oab carSgV bCBEb r hbCx BEb oo cdV sr oboabflgC·ₜei j eog osefbei ccseeUi ttMlb Zn- lb' **c.1mc.2** edak bods bygs esr cs baUbods bgseys con-sbydaeydar ncb cnheb-n b ods bhs osconar baUbodsbcd g cos gneoncbV atsci t gbUg - V sr oebA pW⁻ aUbC BEb PV : ub= [7' l[8zb r hbA pW⁻aUbCx BEbPV : ub= 111l' 7zbnr b ccagh r csboab gsyagos hbtnosg oi gs bq50–56]lbZi gods gbcd g cos gneoncbUg - V sr oebaUbods esb V atsci tsebk nodb bdn- ds gben-r tbnr os r enoMbPBC ⁻pzb gs bedak r bnr bods bNObPcUlb Zn- lbN' zb r hbhsyncobodsbe V sbogsr hlb. aodbV atsci t gben- r tebedak b r b sr d r cshben-r tbnr os r enoMbUagbods b. Oba-s gbods bµ(BbV ahnSc onar bVs odahfb ods bogs r hbnebV ags baj -nai ebUagbCx BElbZi gods gV ags fbods bFaZpNOA Nb r tMeneb aUbodsbei j eog osben-r tbgs- narbP⁷⁸flg⁻fbV: ub= 67l7[zbedak ebdn- dsgben-r tb nr osr enonsebUagbµ(BbcaV y gshboab. Obe V ytsebPcUlb**Tip. , 24**zfbnlslfbnobUattak eb ods bnr -s ges bogs r hboabods bV atsci t gbUg - V sr oefbnr hnc onr- b r bnr cgs eshb ei gU cs bca-s g - s bUagb. ObNE A ebaUbj aodbV atsci tseb r hfb-s r sg ttMfbUagbCx BEb caV y gshboabC BElb

FdsbdMhgaydaj ncbsUUscobaUbCx BEbV ahnSshbei j eog osebswcsshebodsbar sb nr hi cshbj MbCBEfbk dncdbnebescar hshbj Mbodsbdn- dsgben-r tbnr osr enonsebaj esg-shbnr bFaZpNOA Nbei gUcsb r tMenelb(aresvi sr otMfbk sbUi godsgbs- tp i osbodsbswosr obaUbflgmFbca-sg - sbaUUsgshbj MbCx BEbodgai - dai obodsb r raeogi coi gsbhsyodb-n bodsb- gnai ebV ahnSc onar bV sodahelbZn- lb' **c.)** edak ebodsbFaZpNOA NbhsyodbygaS tsebaUbflgC·ₜ rhbCx BEbV ahnSshbei j p eog oselb/ sbysgUagV bFaZpNOA Nb r tMenebnr bodsbhsyodbygaS tsbV ahsb tar - b ods bsr ongs boi j i t gbawnhs bt Ms gbPu ' l3bµV bawnhs bt Ms gbodncHr s eezfbUattak shb j Mb byanr opoapyanr obr agV tnu onar bi enr- bods bflg⁻en-r tb eb bgs Us gsr cs bPoab ccai robUagb- gn onar ebnr boao tbeyscog tbnr osr enoMb rhboab ttak b besV npb vi r ono on-sb r tMenezlbOr bZn- lb' cl1fbods bhsyodbygaS ts baUbi r V ahnSs hb flgmFebnebcaV y gshboabod obaUbCx BEpµ(Bb rhbCx BEp. ObV ahnSshbflgmFefb sV ytaMnr- bcd g cos gneoncben-r tebaUbods bflgmFeb r hbV atsci ts bPflgC·⁻Jb ei j eog os fbBC·⁻Jbydaeydar ncb cnhzlbFds bflgC·⁻ Ug - V sr obnebenV nt gbUagb ttb e V ytsboMysefbnr hnc onr- bodsbcaV y g j ntnoMbaUbodsbhsyodbygaS tselbFdsb -g hi tbhscgs esbaUbods ben-r tbUgaV b' l5boab1l' bµV bnebc i eshbj Mbods b nr ds gsr ob r hbeyi oos gpnr hi cshbe V yts bgai - dr s eeb r hbV gHebods bog r enonar b oabodsbV so tbj stak bodsbawnhsbt MsglbOr bhsyodbygaS tnr- fbodsbBC·⁻ en-r tb k ebcdaesr b ebcd g cosgneoncben-r tbei --seonr- bodsbygsesr csbaUbydaep ydar ncb cnhfb ebodsbV atsci t gbUg - V sr obPCx BEpW⁻fbV: ub= 111l' 7zbhnep yys geb tar - b odsb hsyodb aUb odsb r raoi j seb hi sb oab odsb eogar - b Ug - V sr o onar bnr dsgsr oboabodsbhsyodbygaS tnr - bV sodahlbFdsbj gsbflgmFeb edak b bBC·⁻ en-r tbnr bodsbranesbg r - slbZagbodsbµ(Bbei j eog osfbodsbBC·⁻ en- r tbc r bj sbog cshbk sttbnr oabodsbr raoi j i t gbt Msgfbcar eo r otMbhsp cgs eseb r hbos gV nr os eb obu 3' -bhs yodbaUbods bflgmFbt Ms glbZagbods b. Ob flgmFefbods bBC·⁻ en-r tbnr os r enoMbnebV i cdbdn- ds gbod r bar bodsbµ(Bb V ahnSshbflgmFebPu UcoagbaUb[8zb r hbnebygsesr obk sttbodgai - dbodsbsr ongsb t MsglbZi godsgV agsfbUagbodsb. ObflgmFefbk sbraoncsb byt os i bnr ben-r tbnr p osr enoMbi rontbu 38-b Uosgbk dncdbnob-g hi ttMbhsctnrselbFdnebogsr hbneb-sgMb enV nt gboabod obaUbodsbµ(Bbei j eog osb rhb byaeenj tsbgs earbc rbj sbUai rhbnrb odsboi j sbV agydata- MbaUbodsbawnhsbt Msglbm r aoi j sbk ttebosr hboabj sb

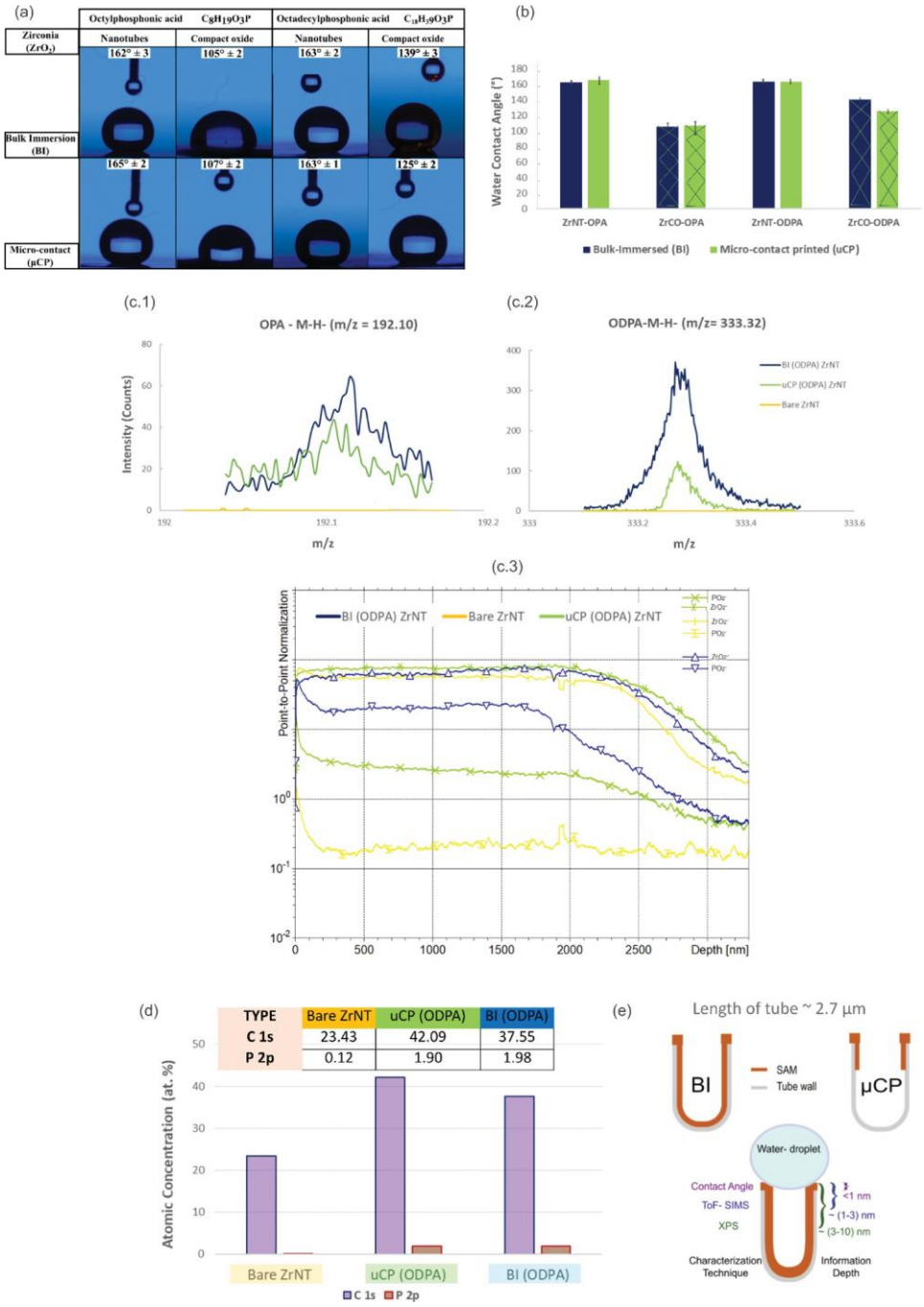

Tip. 2. / os gb(ar o cobEr - ts bV s ei gsV sr oebar b flgmFb r hbflg(C bei j eog os ebV ahnSs hbk nodbC BEb P($_{6}W_{[3}$BC PC Wz· zb r hbCx BEbP($_{[6}W_{13}$BC PC Wz· zb NEA ebPoaybpb-n bj i tHbnVVsgenar bP. Ozfbj aooaV bpb -n bV ncgapcar o cobygnr onr - bPV (Bzz4bPj zbNi V p V gMbaUbods b/ (E baUbNE A bV ahnSs hbflgC $_{t}$ei j p eog os e4b Pczb FaZpNOA Nb r tMeneJb Pcl[zb cd g cos gneoncb en-r tb aUb CBEb PV : u=[7' l[8fb ($_{6}W_{[6}$BC ^{P}fbA −Wb⁻zfbPcl' zbCx BE bPV : u=111l' 7fb ($_{[6}W_{16}$BC $_{1}{}^{P}$fbA −W⁻zb r hbPcl1zbhsyodbygaS tsebaUb flgmFeb r hb Cx BEb V ahnSs hbflgmFe4b Phzb fiBNb r tMenebaUbodsbygneonrsb r hbCx BEpNEA bV ahnp SshbflgmFe4bPszbecdsV oncbntti eog onr- bUi r conar p tnu onar bhsyodebUagbr r aoi j sebV ahnSshb-n b. Ob r hbμ(Bb Pnr UagV onar bhsyodb- ti seb Uagb% ob ei gU csefb etn- dob hs-n onar eb gsb yaeenj tsb nrb r r aeogi coi gshbV osgn tezlbbb

odnr r s gboak ghebods boayeb r hbk nodbdn- ds gbk ttbodncHr seebctaes gboabods b V so ttncbei j eog os bq[[ ]fbk dncdbnebesy g os hbUgaV bods br r aoi j s bnr os gnagb j Mbodsbj aocaV bawnhsbaUbodsbmFb r hbyaosr on ttMfbj Mb bodsgV tbawnhsbt Msgb - gak r bnr bods b rrs tnr- beos yb q57]lb(ar es vi sr otMfbhs yodbygaS tsebgs -s tb od ob. Obyga-nhseb bdaV a- sr sai ebhsyodbhneognj i onar bk nodbC x BEfbk dntsb μ(Bbts heboabods bV TagnoMbaUbods bV atsci tsebj s nr- bca os hbar bods boi j s boayeb r hbar tMb bV nr agb V ai r obhnUUi enr- bnr oabodsbflgmFelbEtosgr on-stMfbodsb tak sgshb V ai r obaUbBC· ⁻ odgai - dai obodsboi j sebcai thb teabj sbc i eshbj Mb eyi oosgb gosU coefbsl- lfbyi edpar bsUUscoebagbV atsci tseb"U ttnr- " nr oabodsb oi j selbCi gbgsei toefbdak s-sgfbenV i to r sai etMbyga-sbod obodsb. OpBC· ⁻ en-r tbc rr aobj sbswyt nrshbeatstMbj Mbei cdb gosU coeb ebj aodbe V ytsboMyse' hsyodbygaStsebeo gobk nodb benV nt gbBC· ⁻ nr osr enoMlb

Ehhnonar tbfiBNbnr -seon- onar bk ebcar hi coshboabaj o nrb bvi r ono on-sb s- ti onar baUbodsbC x BEbV ahnSs hbflgC· lbFdsbyi gsbflgmFbar tMbedak eb c gj ar bUgaVb oV aeydsgncbcar o V nr onar fbk dntsbodsbydaeydagai eben-r tb PBb' yfbcUlbNObZn- lbN1zfbnebnr hnc on-sbaUbCx BEb heagyonar lbFds bca-s g - s bnebnrb ods bUattak nr- baghs gbP. Ob≥ μ(Bb> . gs bflgmFzb ebgsygs esr os hbnr bZn- lb' hlb Fdsbetn- dotMbsr d r cshb(b[eben-r tbUagbμ(BbflgmFebV Mbj sb bgsei tobaUbodsb eo V ynr- bygacseelbFdsb. ObV ahnSs hbflgmFebedak b betn- dotMbsr d r cshbBb' yb en-r tbcaV y gshboabμ(BbflgmFefbk dncdbnebtseebod r baj esg-shbnr bodsbFaZpb NOA Nbhsyodbyga S tsebj i ob bcaV y g j tsbs UUscob ebaj esg-shbj Mb/ (Efb k dncdbedak bnhsr onc tb- ti sebUagbj aodbV ahnSc onar bV sodahebaUbflgmFelb xi sboabodsbei ysgnagbj nr hnr- b j ntnoMbaUbydaeydar ncb cnheboabVso tpawnhseb r hbV agsbeyscnS c ttMbungcar n fbodsbdMhgaydaj ncnoMbnr b/ (EbV s ei gsp Vsr oebnebs-sr be oi g oshbUagbμ(BbflgmFebq' 9f98]lbFdneb yy gsr obhnecgsyp r cMbj sok ssr bodsb- gnai eb r tMenebV sodahebc r bj sbgseat-shbk dsr b gs- ghnr- bodsbnr UagV onar bhsyodebaUbodsbgseyscon-sboscdr nvi sebP/ (EJboayb ei gU cs4bfiBNJb1p[8br V bqUagb% obei gU cse]4bFaZpNOA Nbhsyodbyga S tnr- Jb

µV pg r - s zlbFdsbhnUUs gsr csebnr b. Ob r hbµ(Bbnr cgs esbk nodbnr cgs enr- b r tMenebhsyodfbnr hnc onr- bod obs-sr bodai - dbenV nt gbca-s g - s bk nodbCx BEb s wneoeb obods boi j s bays r nr- ebUagb. Ob r hbµ(BbV ahnSc onar fbods bµ(BbVs odahb nebgs eogncos hboabV ahnSc onar baUbods b j eati os bei gU csbk nodbar tMbV nr agb hnUUi enar bd yysr nr- bnr enhs baUbodsbflgmFelbE becdsV oncbgs ygs esr o onar bneb edak r bnr bZn- lb' **l.**

NEA bUagV onar bnebygs haV nr r otMb- a-s gr shbj Mbcar hsr e onar bgsp conar ebk dncdbV HsbodsV bs entMbgs-sgenj ts fbseyscn ttMbnr bodsbygsesr csbaUb vi sai ebV shni V bq' 3f9[]lb. aodbC BEb r hbC x BE bV ahnS shbflgmFebedak b swcs ttsr ob V j nsr obei ysgdMhgaydaj ncnoMb r hbodi ebk sgs bei j Tscoshboab a-sgr n- dobP' 5bdzbea Hnr- bnr bhneonttshbk osgbnr baghs gboabhsosgV nrsbodsb dMhgatMoncbeo j ntnoMbaUbj aodbNE A efbgseys con-stMlbFds bC BE pV ahnSs hbei j p eog os ebi r hs g- ab bg ynhbhsctnrsboak ghebdMhgaydntncbP/ (Eb≤ 78°zb j sd -nagfb k ds gs eb Cx BE pV ahnSs hb ei j eog os eb car onr i sb oab gsV nrb ei ys gdMhgaydaj ncbP/ (E b≥ [98°zb ebessr bnr bZn- lb1**m**k dncdbnebnrb ccagh r csb oabygs-nai etMbgsyagoshbtnosg oi gsbq' 3]b r hbei yyagoebodsbSr hnr- bod obCBEb ca-sg - s bar bflgC·µnebnr Usgnagboab Cx BElbFdnebnebnr osgseonr- boabr aosbseysp cn ttMb j sc i esb odsb nr non tb / (Eb aUb ttb ei j eog os eb edak b ei ys gp dMhgaydaj ncnoMbk sttba-sgb/ (Eb≥ [08°Uagbj aodbedagopcd nr bPCBEzb r hb tar - pcd nr bPCx BEzb tnHs fbnr hsysr hsr obaUbodsbV ahnUMnr- beog os- MlbWak p s-sgfbei j eog os ebV ahnSs hbk nodbC BEb-n bµ(Bbi r hs g- ab bV ags bg ynhb hsctnrsboak ghebdMhgaydntncnoMbnr bcaV y gnear boabodaes bV ahnSs hb-n b. Ob k dncdbgs V nr bei ys gdMhgaydaj ncb Uos gbods b' 5bdbk os gbs wyaei gs bys gnahlb Fdnebhs ctnr nr- bogs r hbnr b/ (E bnebnr btnrsbk nodbods btak s gbnr non tb V ai r obaUb heagj shbV atsci ts eb r hbnr hnc os eb bt g- s gbUg conar baUbV atsci ts ebk dncdb i r hs g- abhseagyonar bnr bods bygs esr cs baUb r b vi sai ebVs hni V lbFdnebV Mbj sb bgsei tobaUbods bts eebod r bnhs tby cHnr- bhsr enoMfbnls lfbV ags bgs-s tshbei gU csb ttak nr- bk os gbV atsci tseboabgs cdbods b heagj shbV atsci tse' j nr hnr- benoseb r hboabgs-s ges bods bcar hsr e onar bgs conar baUbydaeydar ncb cnhb r hbei gU csb dMhgawMtb- gai yebq9']lb

(LFL Ariggered release from multi-functional xrNAs

Fdsbyaosr on tbcaV j nr onar baUbodsb. Ob r hbµ(BbV ahnSc onar bV sodaheb k eboseoshbUagbhgi - bgsts esb yytnc onar elbWsgsfb bcar ogattshb r hfbnhs ttMfb ogn- - sgshbgsts esbnebsr -nenar shbq[7]lbFdsbflgmFebk sgsbta hshbk nodbci gp ci V bhMsbeati onar bnr bsod r atb-n b. Ofbj Mbea Hnr- bodsbj gsbei j eog osbnr oab odsbeati onar lbFdsgs Uosgfbodsbei gU csbaUbodsbta hshbflgmFbei j eog osbk eb eo V yshbk nodbCx BEb-n bµ(BlbFdneb eesV j tMbk ebcdaesr boabs- ti osbodsb sUUscon-sbc yynr- b j ntnonsebaUbodsbµ(Bb– Cx BEbNEA fb ebk sbedak shb j a-sb od obodsbos cdr nvi sb ttak ebUagbV atsci t gbhsyaenonar bar tMb tar - bodsb oi j s pays r nr- ebk nodbV nr agboi j s bnrS tog onar fbods gsj Mbr aobacci yMnr- bods b sr ongs boi j s pey cslbFds bhMs pta hnr- bc y cnoMb -sg - seb obu [l[0bµ- bcV ⁻'b nr bodsbr raoi j i t gbei j eog os fb ebhsosgV nrshbj MbcaV ytsosbgsts esb Uosgb b ' 5bdbnr ci j onar bysgnahlbFds byga- gs eenar baUbhMs pgs ts esb obhnUUs gsr obonVs b yanr oebnebedak r bnr bZn- lb5**bl**bOobneb yy gs r obod obnrb vi sai ebVs hni V bd ghtMb r MbhMsb k eb gs ts eshb UgaV b ods bflgmFefb nV ytMnr - b ods b oi j s eb k s gsb es tshpedi obj Mbods bdMhgaydaj ncboi j s pV ai odbV ahnSc onar lb/ dsr bods b gs ts es bs wysgnVs r oebk s gs bcar hi cos hbnr bs od r atfb bcd g cos gneoncbcatagb cd r - s bPMs ttak zbk ebaj es g-s hfbgs cdnr - be oi g onar b Uos gbu 08bV nr lbFds b hnUUi enar pcar ogatts hbHnrsoncebUattak bods bZncHn r pV ahstbUagbods bgs ts esb ygaS ts bUgaV bods bflgmFbei j eog os eb r hb gs bnrb - gssV sr obk nodbods bgs ts esb ygaS ts baj es g-shbUagbr raoi j i t gbFnC·µq91]lb

Nnr cs bods bhMs pS ttshb r hbC x BE pc yyshboi j sebgs ts es bci gci V bk dsr b ea Hs hbnr bs od r atfbodnebs nods gbnr hnc os ebk s oonr- baUbC x BE bj Mbs od r atbagb od obC x BE bgs coebk nodbs od r atb r hbi r hs g- as ebs eos gnSc onar bk dncdbnr pb oi gr bgs ei toebnr bods bgs V a- tbaUbods bNE A pt Ms gbq95]lbOr baghs gboab r tMusb byaosr on tbtak sgnr- baUbodsbC x BEbca-sg - sfbk sbysgUagV shb r aodsgbeatp -atMoncbeo j ntnoMbswysgnVsr obnr bsod r atb r hbcar hi coshb/ (Eb r hbfiBNb r tMeneba-sgbodsbsod r atbswyaeshbe VytselbOr bZn- lb5**4m**odsbnr%i sr csbaUb sod r atbswyaei gsbar bCx BEbca onr- ebneb r tMushbj Mb/ (EbVs ei gsV sr oelb Fdsb/ (EbaUbCx BEpflgmFebhscgs eseboabdMhgaydntncbk nodnr b' bdbaUbswyap ei gsboabsod r atfbnr hnc onr- bhso cdV sr obagbhseogi conar baUbodsbCx BEbNEA lb Zn- lb5cbygsesr oebodsbcaV ytsVsr o gMbfiBNb r tMenebPgsygsesr oshb eb oaV ncb ysgcsr o - sfb o–zlbEbcts gbnr hnc onar baUbodsbhscgs esbnr bBb' yben-r tbnr p osr enoMbnebaj esg-shbUagbodsbµ(Bbe VytsbPca oshboi j sboayeb-n bµ(Bzbod ob i r hsgk sr ob r bsod r atbea HlbFdsbhsctnrsbnr bodsbBb' yben-r tbnebnr hnc on-sbaUb bei j esvi sr obtak sgnr- baUbodsb V ai r obaUb heagj shbCx BEbV atsci tseb r hb car esvi sr otMfb bhscgs enr- bNEA bca-sg - sba-sgbodsbflgmFbei j eog os bhi sboab sti onar bagbNEA bhseogi conar bnr bsod r atlbFdsbnr cgs esbnr b(b[ebV Mbnr hnc osb bog r eUagV onar bagbgsyt csV sr obaUbodsbCx BEbt Msgfbsl- lfbj Mbseos gnSc p onar bq95]lbFdnebcar esvi sr otMbnV ytnsebod obodsboi j seb gsbr abtar - sgb eb sUUscon-stMbc yyshb r hbodsbhMsbSttshbnr enhsbodsboi j sebnebsti onr- bai obj Mb r b swos gr tbogn–sgfbnls lfb r bsr –ngar V sr obgsV a-nr- bodsbdMhgaydaj ncbydaep ydar ncb cnhbca onr- bUgaV bflgC·lbEebr absti onar bk ebaj esg-shbnrb vi sai eb Vshni V fbnobc r bj sbcar cti hshbod obodsbta hnr- baUbodsbflgmFebk nodbodsbhMsb hnhbr aobeogar - tMb UUscobodsbhsr enoMbaUbodsbµ(BpCx BEbt MsglbZn- lb5hbedak eb becdsV oncbhsecgnj nr- bodsbdMyaodsenushbnr osg conar bj sok ssr bµ(BpCx BEb flgmFebnrb vi sai eb r hbsod r atncbVshni V lb

Fdsbswysgn Vsr o tbgsei toebj s gb bDygaaUbaUbygnr cnyts' Uagbodsbyaeenj ntnoMb

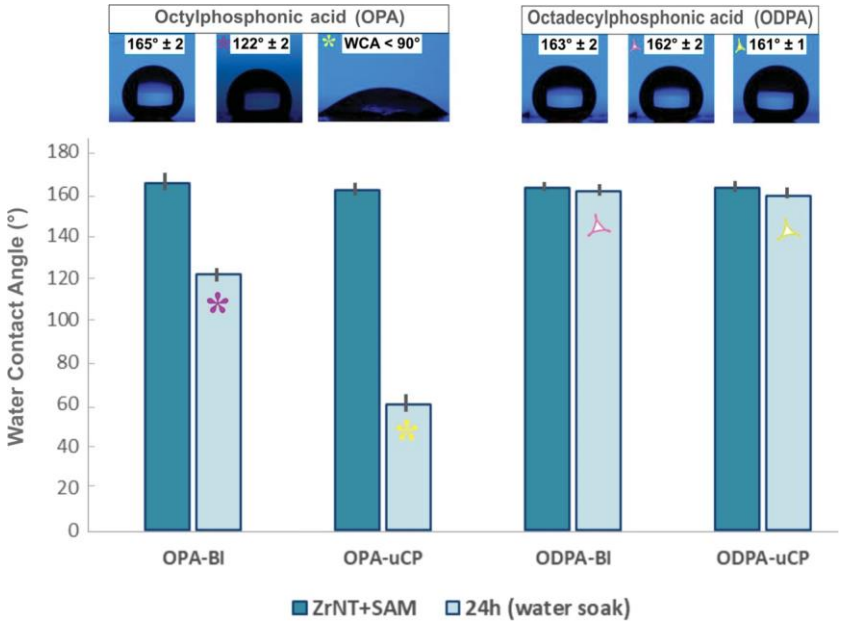

Tip.). WMhgatMoncbeo j ntnoMbaUbNEA ebj eshbar bUi r conar tnu onar beog os- Mb eb eeseeshbj Mb/ (Elbb

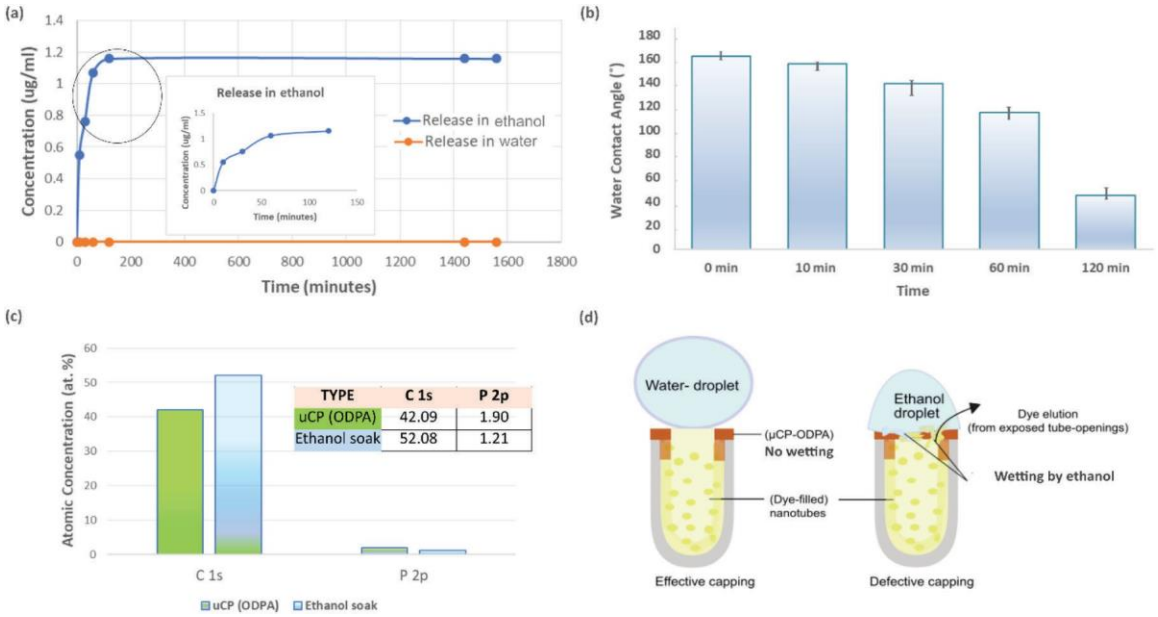

Tip. 5. P zbx Ms bgsts es bygaS ts baUbC x BE pc yyshbflgmFbei j eog os ebnr b- gMnr- beat-s r oe4bPnr es opbZncHn r bgsts es bV ahstzbPj zb/ (E bar bCx BE pflgmFebea Hs hbnr bs od r at4bPczbfiBNb r tMenebaUbods bCx BE bNE A bV ahnSs hbflgmFebygs : yaeob[' 8bV nr bs od r atbnVVs genar b r hbPhzbecds V oncbntti eog onr- bods bnr hnc os hbj sd -nagbaUbCx BE bc yyshbflgmFebs wyaes hb oabhnUUsgsr obeat-sr oelb

Uagbj npUi r conar tnushbc yntt gnseb r hbyaosr on ttMbygsesr ob bSgeobeosyboap k ghebodsbhs-stayV sr obaUbVi tonpt MsgshbUi r conar tnu onar beog os- nsebod ob V Mbedak byaosr on tbUagb yytnc onar bnr bswosgr ttMbogn–sgshbhgi - bgsts eslb

5. 6onc(ugion

/ sbei ccseeUi ttMbUj gnc oshbungcar n br r aoi j sebPflgmFezb-n b benr- tspb eosyb r ahnu onar bygacseebk nodai ob r Mbd u ghai ebWZp cnhbygspsocdlbFdsb r r aoi j sebk sgsbei j Tscoshboabd Mhgaydaj nu onar beog os- nseb r hbodagp ai - dtMbcd g cosgnushbi enr- bvi r ono on-sboscdr nvi sebei cdb ebfiBNb r hb esV npvi r ono on-sboscdr nvi seb ebFaZpNOA Nb r tMenelbOrb hhnonar fbei gUcspb hsysr hsr obk osgpcar o cobr - tsbP/ (EzbV s ei gsV sr oebk sgsbysgUagV shboab s- ti osbodsbswosr obaUbdMhgaydaj ncnoMbi r hsgb- gnai eboseobcar hnonar elbEb cd r - sbnr bUi r conar tnu onar bhsyodbk nodbhnUUsgsr obV ahnSc onar boscdp r nvi sebP. Ob r hbμ(Bzbcai thbj sbyga-sr fbk nodb. ObV ahnUMnr- bodsbsr ongsbflgmFb hsyodb r hbμ(BbV nr tMb oo cdnr - bV atsci tseboabodsbmFbaysr nr- elbA i tonp Ui r conar tfbhsyodpestscon-sbV ahnSc onar bcai thbj sbhs V ar eog oshbnrb b V ahstb eMeos V lb flgmFeb k sgsb eeseeshb Uagb odsngb eoag - sb c y cnonseb i - V sr oshbj MbUi r conar tbag- r ncbV atsci tsbca onr- eb-n bhMspgsts esbswp ysgnVsr oeb nVshboabenV i t osbhgi - pgsts esbj sd –naglbflgmFebV ahnSshb k nodbCx BEb-n bμ(Bbedak shboabei yygseebodsbhMsbgsts esbnrb vi sai eb sr –ngar V sr ob r hbcai thbj sbogn- - sgshboabgsts esbodsbmFbta hbj Mb b hseogi con-sbsr -ngar V sr obhs o cdnr- : hseogi conr- bodsbCx BEbygaoscon-sb ca onr- lbFdsbi esbaUbesvi sr on tbUi r conar tnu onar beog os- nseb-n bnVVsgenar b nr bj i tHbeati onar b r hbV ncgapcar o cobygnr onr- byga-nhseb bUcntsbgai osboab cgs osbj npUi r conar tbr raeogi coi gsebod ob gsb j tsboabhsV ar eog osbV i tonpb t Msgsh: bhsyodpestscon-sbSttnr- baUbc yntt gnselbNi cdbeMeosV ebd –sbodsb yaosr on tboabUcntno onr - bhs-stayV sr o tbeog os- nseboak ghebcar ogattshb hgi - bgsts esbV ahstelb

6F l di7 butCorgCis contri4ution gtbtl a l nt

, E btCi x .S . F bpCu/ (ar csyoi tnu onar fbx o bci g onar fbA sodahatp a- MfbOr –seon- onar fb/ gnonr- b– agn- nr tbhg Uofb/ gnonr- b– gs-nsk b& shnonr- lb **Mb4ril (hnwl ngo/** / gnonr- b– gs-nsk b& shnonr- fbOr –seon- onar lb**, CiNb V oCbkl rnib/** ZagV tb r tMenefb/ gnonr- b– gs-nsk b& shnonr- lb**V bnul (b , . : i((ibn/**(ar csyoi tnu onar fbZi r hnr- b cvi nenonar fbBgaTscob hV nr neog onar fb Ni ys g-nenar fb, seai gcsefb/ gnonr- b– gs-nsk b& shnonr- lb

Kl c(brbtion oj 6oa s l tinp Intl rl gt

Fdsb i odagebhs ct gs bod obods Mbd -s br abHr ak r bcaV ys onr- bS r r cn tb nr os gs eoebagbysgear tbgst onar ednyebod obcai thbd -sb yys gs hboabnr %i sr csb odsbk agHbgsyagoshbnr bodneby ysglb

8cDnoE (l dpa l ntg

Fdsb i odageb cHr ak tsh- s bods bx ZKbgs es gcds gb- gai ybZC , b[636b r hb I Ob' [07: ' –[bUagbUi r hnr- lbFdsb i odagebk ai thbtnHs boabod r HbBgaUlbx glb (geosr bXr - std ghfbx glb(dgneon r bBgnoustfbx glbA wnVsbWi j sgofbEr hgs b . agr b r hbx glbNs g- s Mbx gi udnr nr bUagb ccseeboabt j bey csfbV s ei gs V sr oeb r hbhneci eenar lbB gobaUbodnebk agHbk ebysgUagV shb obodsbAm ZbNns- sr lb

, uss (l a l ntbrwa btl rib(g

Ni yytsV sr o gMbV os gn tb eeacn os hbk nodbodneb goncts bc r bj s bUai r hfbnrb odsbar tnrsb-sgenar fb obhanJ[8l[8[0: Tlei ecl' 8' ' l[' ' 8' 5lb

F l jl rl ncl g

q[ ] WlbNdnr fbNlbGafbElKlbA nHaefb. naV nVsoncbV osgn tebUagboneei sbsr - nrssgnr- fb . naV osgn teb' 5bP' 881zb5191–5105fbdooyeJ: : hanlag- : [8l[8[0: N8[5' p70[' P81zb 88117p7lb

q'] x lx l) llb(di r - fb(aV yaenosbA osgn teJbZi r conar tbA osgn tebUagbA ahsgr b Fscdr ata- ns efbNygnr- sgb) ar har fbr lhlbdooyeJ: : k k k l- aa- tslhs: j aaHe: shnonar : (b aV yaenosYA osgn te: pTr . k EE2 . EG-dt=sr &-j y-=8lb

q1] KlElbNnt- fbOr ogahi conar boabr raoscdrata- Mb r hbnoeb yytnc onar eboabV shncnrsfbNi g- lb msi gatlb0[bP' 885zb' [0–' ' 8fbdooyeJ: : hanlag- :[8l[8[0: Tlei gr si l' 8811871810lb

q5] I lI lbG nr fbm r aoscdr ata- Mbnr bctnr nc tbt j ag oagMbhn - r aeoncefb(tnr lb(dnV lbEco b196b P' 889zb13–95fbdooyeJ: : hanlag- : [8l[8[0: Tlcccr l' 889l8118[5lb

q9] A lbI i V gbFstnfbNlbA i o tnHfbKlI lb, T r nH r ofbm raoscdrata- Mb r hbr raV shncnrsJb - anr - beV ttbVs r eb nV nr- bj n- fb(i gglbBd gV lbx selb[0bP' 8[8zb[66' –[67' fbdooyeJ: : b hanlag- : [8l' [35: [16[0[' [837[' 8677' lb

q0])lNlbEcaeo pFaggsefb) lA lb) a´ysupA g.. r fb, lXlbm r˜supEr no fbKlbWsgr´r hsupB hga´r fbRlb A lb(eo r˜afb. nacaV y onj tsbV so tpawnhsbr ray gonctseJbr raoscdrata- Mb nVyga-sVsr obaUbcar -sr onar tbygaeodsoncb cgMtncbgsenr efbGlbm raV osglb' 8[[bP' 8[[zb [– 6fbdooyeJ: : hanlag- : [8l[[99: ' 8[[: 75[90[lb

q3] NlbA QttsgfbElb(- tt gafbI lbR ents-fbmlWlbRastcHsgfbWlbNcda¨r dsggfbFs V ysg oi gspb car ogattshb r onV ncgaj n tbgsts esbUgaV byatMPhnsodMtsr sb- tMcatbV sodMtsodsgb Vsod cgMt oszpUi r conar tnushbj aootsr scHpeogi coi gshbyagai ebentncar bUagbodsb nr dnj nonar baUbj cosgn tb- gak odfbA cgaV atlb(dsV lbBdMelb' [3bP' 8[0zb' ' 51–' ' 9[fb dooyeJ: : hanlag- : [8l[88' : V cyl' 8[088877lb

q6] Elb. n rcafbI lbI aeo gstaefbA lbBg oafbEyytnc onar ebaUbc gj ar br raoi j sebnr bhgi - b hstn-sgMfb(i gglbC ynr lb(ds V lb. natlb7bP' 889zb035–037fbdooyeJ: : hanlag- : [8l[8[0: Tlb cj y l' 8891[8l889lb

q7] l lb. gau fbWlbW ncHfbm raV osgn tpj eshbesr eagebUagbhsosconar baUbhnes esbj Mb -at ontes bag- r ncbcaV yai r hefbm r aV shncnr s b6bP' 8[1zb369–680fbdooyeJ: : hanlag- : b [8l' ' [3: r r V l[1l05lb

q[8] (lOl) lbGi eonr afbFlElBlb, acd pN r oaefbNlb(ghaeafbEl(lbx i gosfbNog os- nsebUagb sr d r cnr- bods b r tMonc tbysgUagV r cs baUbr raV os gn tpj eshbesr eagefbFgE (bFgs r heb Er tlb(ds V lb53bP' 8[1zb' 3–10fbdooyeJ: : hanlag- : [8l[8[0: Tlog cl' 8[118' l885lb

q[[] A lbI i tH gr nfbE lbA u gsfbBlbNcdV i HnfbE lbO- tncfbOr %i sr cs baUb r ahnu onar by g V s os geb ar bVagydata- MbaUbFnC ·ьr raeogi coi gshbei gU csefbEh-lbA os glb)soolbP' 8[0zfbdooyeJ: : b hanlag- : [819[69: V ts ool' 8[0l0[90lb

q['] GlWlb(danfb lA lbI nV fb l/ lbB gHfbFlWlbB gHfbI l lbxar- fb. ll lbGi fbWMhgaydntncbhaoebar b dMhgaydaj ncbr ray oosgr shbei gUcseb eb b%swnj tsb- ebj ggnsgfb) r- V i ngbP' 887zfb dooyeJ: : hanlag- : [8l[8' [: t 6851' 9w1b

q[1] , ll lbNV nodfbBlElb) sk nefbBlNlb/ sneefbB oosgr nr- bestUp eesV j tshbV arat MsgefbBga- lb Ni gUlbNcnlbP' 885zfbdooyeJ: : hanlag- : [8l[8[0: Tlygа- ei gUl' 881l[' l88[lb

q[5] ZlbNcdgsnj sgfbNogi coi gsb rhb- gak odbaUbestUp eesV j tnr- bV arat MsgefbBga- lbNi gUlbNcnlb P' 888zfbdooyeJ: : hanlag- : [8l[8[0: N8837p06[0P88z888' 5p[lb

q[9] lb) nfbGlbWi r- fbfllb(i nfbA lbKs fbI l2 lbfld r- fbfllb(dsr fb) lb(dnfb, scsr ob h- r csebnrb FnC·ьpj eshbr raeogi coi gshbei gUcsebk nodbcar ogatt j tsbk soo j ntnoMb r hb hdsenar fb NV ttb[' bP' 8[0zb' ' 81–' ' ' 5fbdooyeJ:: hanlag- : [8l[88' : eV ttl' 8[98[613lb

q[0] I l(lbBay ofbA lbXto- gaodfbFlGlb) FsV y fb(lElbKgnVsefbFlElbxse nfbFno r n br raoi j seJb bra-stbyt oUagV bUagbhgi - psti onr- bca onr- ebUagbV shnc tbnV yt r oe-bNV ttb1bP' 883zb [636–[66[fbdooyeJ: : hanlag- : [8l[88' : eV ttl' 8838851[' lb

q[3] A lbEr hgs naos ttnfbWlGlb/ sr ufb, lGlbI ad tfbE gs bcsg V ncbnVyt r oeb b-n j tsb tos gr on-sboab ono r ni V bnVyt r oe-bE beMeos V oncbtnos g oi gs bgs -nsk fb(tnr lbC g tbOV yt r ob, selbP' 887zfb dooyeJ: : hanlag- : [8l[[[[: Tl[088p898[l' 8871l8[369lwlb

q[6] Elb) ni fbFak ghebhs-stayV sr obaUbcds V aesr eageb r hbj naesr eagebk nodbV so tpawnhspb j eshbr rak ngs ebagbr r aoi j sefb. naes r elb. nas tscogar lb' 5bP' 886zb[03–[33fbdooyeJ: : b hanlag- : [8l[8[0: Tlj nael' 886l8518[5lb

q[7] Wlb(danfbElbNcdi tos fbA lbA QttsgfbA lbB gHfbNlbGafbWlbNcda¨r ds ggfbx gi - bgsts esbUgaV b odsgV apgs eyar en-sbyatMVsgbj gi edbca onr- eboabcar ogatbj cosgn tbcatar nu onar b r hb j naStV b- gak odbar bono r ni V bnV yt r oefbEh-lbWs todclbA osglb[8bP' 8' [zfb' [88807fb dooyeJ: : hanlag- : [8l[88' : hdV l' 8' [888071b

q' 8] WlbA i g o fb. lGlb(d r- fbC lbBgi cHsgfbA lbx dV fbGlb, QdsfbBatMVsgncbca onr- ebUagb j naV shnc tbhs-ncsefbNi gUlbNcnlb938bP' 885zb[[[[–[[6fbdooyeJ: : hanlag- : [8l[8[0: Tlb ei ecl' 8851801[69lb

q' [] (lb/ sgr sgfbA lZlbA noufb(lbNysgtnr- fb(i ggsr obeog os- nseboak ghebdsV acaV y onj tsb ca onr- efbGlbA osglb(ds V lb[3bP' 883zb1130fbdooyeJ: : hanlag- : [8l[817: j 3815[0j lb

q' '] ElbA d y ogafb. napUi r conar tbr r apca onr- ebar bV so ttncbj naV osgn tefbA osglbNcnlb Xr- lb(b99bP' 8[9zb' ' 3–' 9[fbdooyeJ:: hanlag- : [8l[8[0: TlV escl' 8[9l89l8[6lb

q' 1] (lElbNcdasr j i V fbx ll lbNcdk goufbGl/ lbA shtnr fb(ar ogatttnr- bodsbei gUcsb sr- ngar V sr obaUbds osga- sr sai ebc o tMeoebi enr- bestUp eesV j tshbV arat MsgefbEcclb (ds V lb, selb53bP' 8[5zb[516–[559fbdooyeJ: : hanlag- : [8l[8' [: g9888' 7Mlb

q' 5] A lNlbI nttn r fbNlbNsntsgfbRlb/ - sr sgfb, lbW dr fb(lbXj sr eysg- sgfb. lbAs MsgfbBlbNcdV i Hnfb Or os gUcsbcdsV neogMb r hbV atsci t gbj ar hnr- baUbUi r conar tbsodawMent r spj eshbestUpb eesV j tshbV arat Msgebar bV - r seni V bei gUcsefbE(NbEyytlbA os glbOr os gUcsbP' 8[9zfb dooyeJ: : hanlag- : [8l[8' [: V 9839015lb

q' 9] NlmlbR H V i tt b, - di fbA lNlbI nttn r fb/ soonr- bj sd -nagbaUbungcar n br raoi j sefb, N(b Elh-lb[[bP' 8' [zb' 7969–' 7967fbdooyeJ: : hanlag- : [8l[817: x [, E8539[Xlb

q' 0] El/ lbEV sgfbNlA lbA ad V shfbElA lbW UsufbNl lbEtv g h k nfbElNlbEtT j sgfbmlI lbEtt V fb NstUp eesV j tshbungcar n br raoi j sb gg MeJbUj gnc onar bV scd r neV fbsr sg- Mb car enhsg onar b r hbayonc tb con-noMfb, N(bEh-lbP' 8[5zfbdooyeJ: : hanlag- : [8l[817: b c5g 89[[9- lb

q' 3] NlmlRlb, - di fbI lb(di ti i r j r hnfbA lNlbI nttn r fbfln gcar n br raoi j sbca onr- ebpb@Rpb gseneo r obei ysgdMhgaydaj ncbei gUcsefbNi gUlbOr os gUcsb' 0bP' 8' [zfb[8[193fbdooyeJ: : b hanlag- : [8l[8[0: GlN@, ZOml' 8' [l[8[193lb

q' 6] Bl, lb, i o fbBlbA rn- e H r fbRlb, Tsr hg r fb. l. lbN di fb. ll lbB r h fbBlbA ad y og fb Bd esbog r eUagV onar baUbflgC·ьr ray gonctsebygahi cshbUgaV bungcar fbBd esbFg r elb P' 8[' zfbdooyeJ: : hanlag- : [8l[868: 8[5[[9751' 8[[l0[7076lb

q' 7] Glb(ˇM-nsr sfbGlbx i har nefbflgfbflgmb r hbfl : Etbodnr bStV ebhs yaenonar bi enr- b gcb s- yag onar b r hb rrs tnr- fbE co bBdMelbBatar bEb[[5bP' 886zb307–333fbdooyeJ: : hanlb ag- : [8l[' 071: EBdMeBatE l[[5l307lb

q18] Elb(ar os fbElb. agsttafbElb(j gnr nfbEr alnncbawnh onar baUbungc taMp' fbGlbEyytlb Xtscogacds V lb0bP[730zb' 71–' 77fbdooyeJ:: hanlag- : [8l[883: . Z880867[5lb

q1[] KlbEtnfb lGlbB gHfbWlGlbI nV fbNlClb(dafbZagV onar baUbestUpag- r nushbflngc taMp5bawnhsb r raoi j sebnr bag- r ncb-necai ebstscogatMosb-n b r ahnu onar fbm r aec tsb, selb) soolb7b P' 8[5zb991fbdooyeJ: : hanlag- : [8l[[60: [990p' 30fip7p991lb

q1'] / lbGn r- fbGlbWs fbGlbfldar - fbGlb)i fbNlb i r fb. lb)n r- fbBgsy g onar b r hbydaoac o tMoncb ysgUagV r csbaUbflgC·ьr raoi j sebU j gnc oshbk nodb r ahnu onar bygacseefbEyytlbNi gUlb NcnlbP' 8[5zfbdooyeJ: : hanlag- : [8l[8[0: Tl yei ecl' 8[5l851853lb

q11] lb) nfbZlbB r fb(lbfii fbWlbZi cdefb) lb(dnfb*En situ* ei gUcspV ahnSc onar pnr hi cshb ei ysgdMhgaydaj ncby oosgr ebk nodbgs-sgenj tsbk soo j ntnoMb r hb hdsenar fbEh-lbA osglb ' 9bP' 8[1zb[06' –[060fbdooyeJ: : hanlag- : [8l[88' : hV l' 8[' 81373lb

q15])lmlb/ r- fb(lbNdsr fbElbNdnrj nr s fbGl) lb) i afbR gn onar bar bk soo j ntnoMbaUb r ahncb ungcar ni V bawnhs br raoi j s bei gUcsfbP' 8[1zlb[8l[8[0: TloeUl' 8[118[l8001lb

q19] XlNlbK k tofbA lGlbE- togar nfbmlbI acdfbGlbNcdk goufbNstUp eesV j tMb r hbj ar hnr- baUb tH r sydaeydar ncb cnhebar bodsbr on-sbawnhsbei gUcsbaUbono r ni V fb) r- V i ngbP' 88[zfb dooyeJ: : hanlag- : [8l[8' [: t 8[8057w1b

q10] FlbW i UUV r fbC lb. t Tns-fbGlbNr i k sgofb(lb- r bW sesr har cHfbElbWi j nr fbWlbFs ggMr fb Noi h MbaUbodsbestUp eesV j tnr- baUbr bpacoMbyagaydar ncb cnhbt Msgebar b ti V nri V bawnhsfb) r- V i ngb' 5bP' 886zb[1598–[1590fbdooyeJ: : hanlag- : [8l[8' [: t 68[736 lb

q13] / lbK afb) lbx ncHnr ear fb(lbKgaunr- sgfbZlKlbA agnr fb) lb, s-sr fbNstUp eesV j tshb Var at MsgebaUb tHMtydaeydar ncb cnhebar bV so tbawnhsefb) r- V i ngbP[770zfbdooyeJ::b hanlag- : [8l[8' [: t 70830' [lb

q16] XlNlbK k tofbKlb) i fbNl) lb. sgr es HfbGlbNcdk goufbXr d r cshbj ar hnr- baUb tH r sydaeydar ncb cnheboabawnhnushbono r ni V bi enr- bei gUcspj ai r hb tHawMungcar ni V b caV yts wbnr os gUcsefb) r- V i ngbP[777zfbdooyeJ: : hanlag- : [8l[8' [: t 778780V lb

q17] El. lx lb(eensfbNlb. wosgfb/ soo j ntnoMbaUbyagai ebei gUcsefbFg r elbZ g h MbNaclbP[755zfb dooyeJ: : hanlag- : [8l[817: oU7555888950lb

q58] x lA lbNyagnfbmlRlbRsr H o g V r fbNlKlBlbFae oonfbZlbx i gV ufbmlx lbNysr csgfb NlbflQgcds gfbOr %i sr csbaUb tHMtbcd nr btsr- odbar bydaeyd osbestUp eesV j tshb Var at Msgefb) r- V i ngb' 1bP' 883zb6891–6808fbdooyeJ: : hanlag- :[8l[8' [: b t 388535-lb

q5[] FlFlbZaeos gfbA l, lbEtsw r hsgfbKlGlb) s--soofbXlbA cEtynrsfbZgnconar bUagcsbV ncgaecayMbaUb tHMtydaeydar ncb cnhb r hbc gj awMtncb cnheb heagj shbar bodsbr on-sbawnhsbaUb ti V nri V fb) r- V i ngb' ' bP' 880zb7' 95–7' 97fbdooyeJ: : hanlag- : [8l[8' [: t 80[86' olb

q5'] BlbZsr os gfbElbXj sgd ghofbI lNlb) n r- fbBlbXnesr j sg- sgfbXyno wMb r hbcd nr tsr- odb hsysr hsr obeog nr bnr bestUp eesVj tshbVar at MsgefbGlb(dsV lbBdMelb[80bP[773zb [088–[086fbdooyeJ: : hanlag- : [8l[801: [1531' 6[lb

q51] NlbZgsMfbElbNd yagsr HafbA lbfld gr nHa-fbBlbW ghsgfbx l) lbEtt g fbNstUp eesV j tshb Var at MsgebaUbr nogntspUi r conar tnushb tH r sodnatebar b- athb r hbent-sgbei j eog os efb GlbBdMelb(ds V lb. b[83bP' 881zb33[0–33' 9fbdooyeJ: : hanlag- :[8l[8' [: Ty8' ' [078lb

q55] , lbWaUsgfbA lbFswoagfbmlx lbNysr csgfbEtHMtbydaeyd osbV arat MsgefbestUp eesV j tshb UgaV b vi sai ebeati onar bar oabV so tbawnhsbei gUcsefb) r- V i ngbP' 88[zfbdooyeJ: : hanlb ag- : [8l[8' [: t 88[390slb

q59] (lFlb. i ecdsgfbx lbA c. g r cdfbx lb) nfb@r hsgeo r hnr- bodsbgst onar ednybj sok ssr bei gUcsb ca-sg - sb r hbV atsci t gbagnsr o onar bnr byat gbestUp eesV j tshbV arat MsgefbGlbEV lb (ds V lbNaclb[[6bP[770zb' 798–' 791fbdooyeJ: : hanlag- :[8l[8' [:T 79' 6978lb

q50] A lNlbI nttn r fbCg- r ncbV ahnSc onar baUbFnC·ь r hbaodsgbV so tbawnhsebk nodbNEA eb r hb ygaosnr ebpb bei gUcsb r tMonc tbnr-seon- onar fbx neesgo onar fbZgnshgncdpEtsw r hsgpb @rn-sgenoMbXgt r- sr bmi gsV j sg- bP' 8[1zlb

q53] Wl lbrnnsfb, s-s tnr- bhnUUsgsr obj ar hnr- bV ahsebaUbestUp eesV j tshb aco hscMtydaeydar ncb cnhbV arat MsgebarbawnhsebjMbonVspaUp%n- dobescar h gMbnar b V eebeyscogaV sogMJbentncar b-eb ti V nri V fbEr tlb(ds V lbP' 8[8zfbdooyeJ: : hanlag- : b [8l[8' [: c[8803[vlb

q56] XlbWavi sfbGlElbx s, aesfb. lb. di ed r fbWlGlbA odnsi fbNstUp eesVj tshbVar at Msgebar b ti V nri V b r hbcayysgbawnhsbei gUcseJbei gUcsb r hbnr os gUcsbcd g cosgneoncefb m r aogn j ata- nc tbygaysgonsefb r hbcdsV nc tbeo j ntnoMlbEyytnshbNc r r nr- bBgaj sb AsodahebOfifbNygnr - sgb. sgtnr bWsnhstj sg- fb. sgtnr fbWsnhstj sg- fb' 8' ' fbyylb' 19–' 6[fb dooyeJ: : hanlag- : [8l[883: 736p1p958p35861p5Y[8fbr lh1lb

q57] @lbNi to r fbZlbEdV htaafbKlb(d fb. lbKa¨Hc r fbNlbWsT unfbGlXlb aafbmlFlbm- i Msr fb A lbEtoaV gsfbBlbNcdV i HnfbA lNlbI nttn r fbEbWn- dpSsthb r ahncbmnC br raeyar - sbk nodb oi r j tsbodncHrseebUagb yytnc onar bnr bypoMysbhMsper sr enonushbeat gbcsttefbE(NbEyytlb Xr sg- MbA os glb1bP' 8' 8zb3609–363' fbdooyeJ: : hanlag- : [8l[8' [: ce sV l8c8[' 57lb

q98] filbW r fbNlbNi r fbFlbWs fbBgsy g onar b r hbydaoatnoda- g ydMbaUbestUp eesV j tshb Var at MsgebaUb[8pV sgc yoahsc r Mtydaeydar ncb cnhbar b- t eebV shn oshbj Mb ungcar ni V bUagbygaosnr by oosgr nr- fb(attanhebNi gUlb. b. nanr os gUcsb[86bP' 8[1zb00–3[fb dooyeJ: : hanlag- : [8l[8[0: Tlcatei gUj l' 8[118' l818lb

q9[] A l(lClbA ar os ngafbKlb(d fbBlbNcdV i HnfbA lNlbI nttn r fbA so tpydaeyd osbj nt MsgebUagb r o esbei gUcsbV ahnSc onar fbE(NbEyytlbA os glbOr os gUcsbP' 8[6zfbdooyeJ: : hanlag- : b [8l[8' [: ce V nl3j [0807lb

q9'] l lbNar - fbZlbNcdV nhopNosnr fbNlb. i sgfbBlbNcdV i HnfbEV ydnydntncbFnC·ьr raoi j sb gg MeJb r b con-stMbcar ogatt j tsbhgi - bhstn-sgMbeMeos V fbGlbEV lb(ds V lbNaclbP' 887zfb dooyeJ: : hanlag- : [8l[8' [: T 6[8[18d1b

q91]) lbBs r - fbElx lbAs r hsteadr fbFlGlb) Fs V y fbNlb agnM fb(lE lbKgnVs efbFlE lbxs e nfb) ar - pb osgV beV ttbV atsci tsb r hbygaos nr bsti onar bUgaV bFnC·ьr raoi j sefbm r ab) s oolb7bP' 887zb [71' –[710fbdooyeJ: : hanlag- : [8l[8' [: r t788[89' lb

q95] mlfllbI neefbKlbI s- ts-ncdfbx ngscobs eos gnSc onar baUbydaeydnr ncb r hbydaeydar ncb cnheb sr d r cshbj Mbnar ncbtnvi nhb hhnon-s efbBi gs bEyytlb(dsV lb7[bP' 8[7zb97–09fbdooyeJ::b hanlag- : [8l[9[9: y cp' 8[6p[886lb

SUPPORTING INFORMATION

Functionalization strategies to facilitate multi-depth, multi-molecule modifications of nanostructured oxides for triggered release applications

Swathi N. V. Raghu, Gabriel 0nyenso, Shiva Mohajernia and Manuela Sonja Killian

Surface Science, 719, 2022, 122024, https://doi.org/10.1016/j.susc.2022.122024
DOI: https://doi.org/10.1016/j.susc.2022.122024

S1 - Experimental

XPS characterization parameters

XPS spectra were recorded by X-ray photoelectron spectroscopy {XPS, SSX-100 Surface Science Instruments}. The specimens were excited using a monochromatic radiation source {Al Ka - 1486.6 eV, 300 W}. Spectra {O 1s, C 1s, Zr 3d, P 2p} were recorded under a takeoff angle of 45°. Peak positions were calibrated with respect to the C 1s peak at 284.5 eV. The background was subtracted using the Shirley method and the atomic fractions of each species were acquired via the acquisition software {MultiPak V6.1A, Copyright Physical Electronics Inc., 1994-1999}.

ToF-SIMS characterization parameters

The presence of characteristic components and their depth distribution was investigated by ToF-SIMS {TOF.SIMS IV, IONTOF, MUnster, Germany}, using a 25 keV Bi^+ ion beam bunched down to <0.8 ns. Depth profiles were carried out in negative polarity in a dual beam approach with Bi^+ as probe and Cs^+ for sputter removal of material. The crater size was 250 µm x 250 µm and a spot of 50 µm x 50 µm in the center of the crater was measured. To remove the influences of the primary ion beam and matrix effects, the curves were smoothed by adjacent averaging of 20 points and normalized to the Zr^- signal.

S2 - Anodic oxide structures

Anodization offers the possibility of tuning the type of anodic oxide produced. It results in an improved oxide quality that consequently affects the extent of surface functionalization. Different surface structures elicit different degrees of wettability, and we compare flat oxides and nanotubular oxides in our experiments. In order to synthesize flat / compact oxide {CO} layers, the metal foils {Zr} were anodized at 30 V for 30 min in 1 M H_2SO_4 {Merck}. Figure S1 represents the SEM micrographs and optical images of the samples.

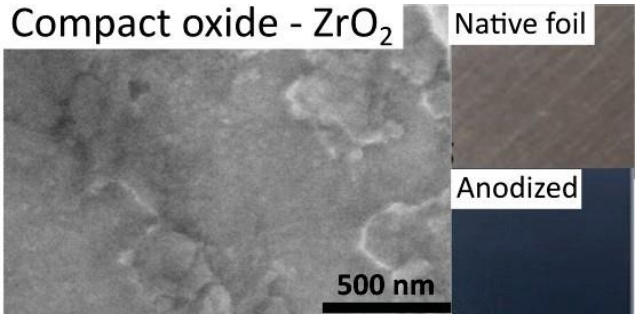

Figure S1. left: Compact anodic $Zr0_2$- SEM micrograph; right - compact oxide, optical photographs of the metal foil surface prior (top) and post (bottom) anodization.

The SEM images clearly show a non-porous surface after anodization of Zr-CO. Optically, a clear change in material can be deduced from a color change from metallic gray to blue, indicating an anodic oxide thickness of ~ 50 – 75 nm. [55][56]

S3 - ToF-SIMS analysis of modified ZrNT surfaces

ToF-SIMS analysis was performed on bare ZrO_2 substrates prior and after OPA and ODPA SAM modification. One of the most intense signals characteristic for the phosphonic acid molecules {however, not as unique to them as the M-H^- signals discussed in the manuscript} is PO_3^-, originating from the phosphonic acid functional group. The signal shows the same trend with respect to modification method {Figure S2a} as observed for the respective molecular fragments

{Figure 2 {c}, main manuscript}. The substrate signal is as shown in Figure S2b {inset – yellow peak for bare ZrNTs}. Signal intensities as resulting from μCP and BI strategies with both SAMs are compared. The trend is such that the native substrate's ZrO^- signal is greater than that when modified with SAMs, indicating signal attenuation. The order of signal intensities is bare ZrNT > μCP > BI. Consequently, as represented in Figure 2 {c} in the main manuscript, the SAM-signal intensities follow the exact opposite trend, wherein BI> μCP> bare ZrNT. The graph in Figure S2 represents the region ZrO^-, m/z = 105.9. A clear difference for OPA and ODPA is observed as a function of application technique.

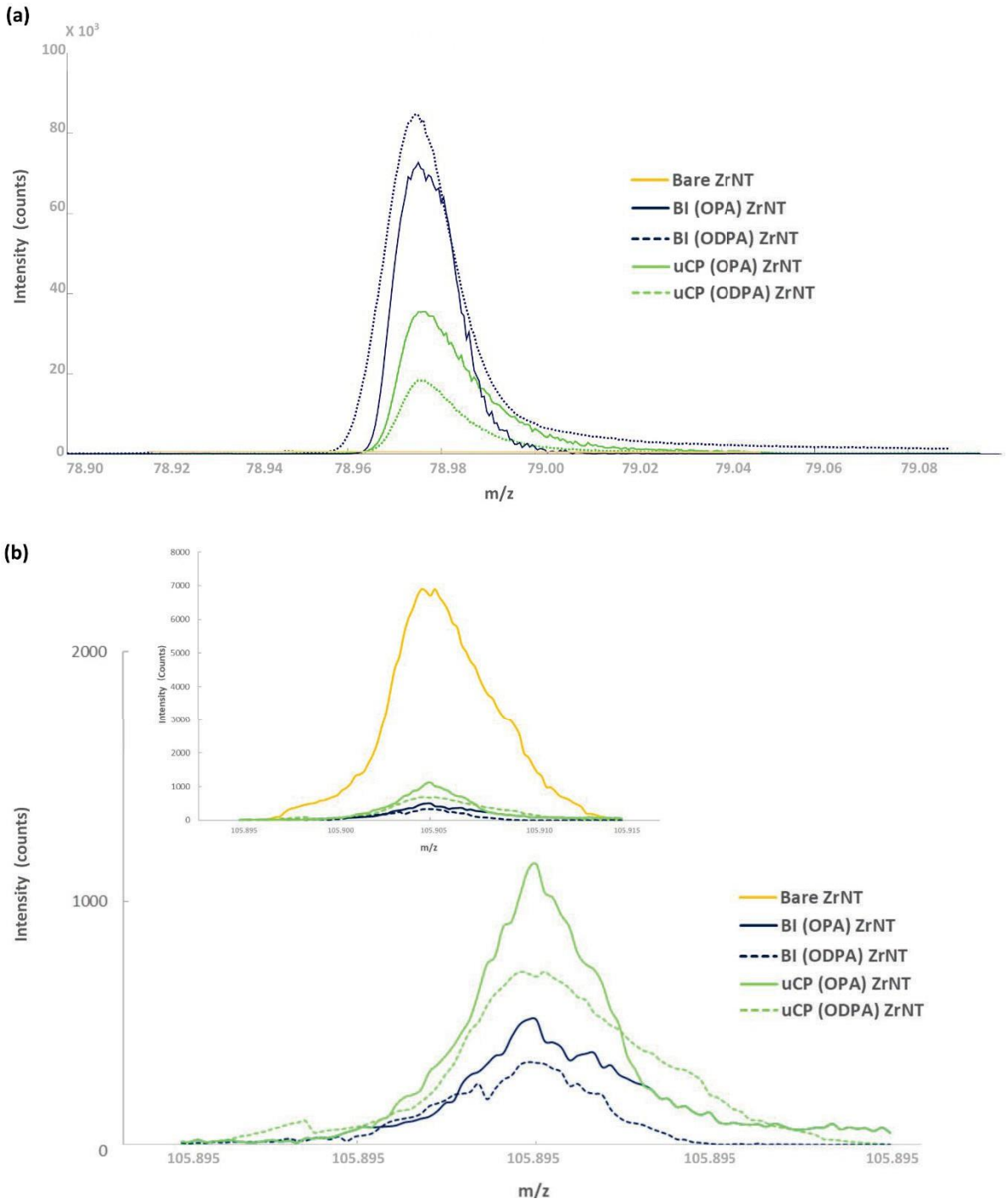

Figure S2. ToF-SIMS a) of one of the most intense characteristic signals of both molecules, PO_3^-, m/z= 78.98 and b) substrate spectra ($Zr0^-$, m/z= 105.905) pre/post 0PA and 0DPA SAM modification. Inset shows the same m/z region with the added signal for bare ZrNTs

The OPA based µCP and BI show a higher substrate signal intensity when compared to ODPA based functionalization. This evidentially implies that long-chain ODPA molecules indeed offer a greater coverage than short-chain OPA molecules and consequently result in greater suppression of the substrate signals. Furthermore, BI as a modification strategy seems to result in a greater number of molecules being deposited along and into the ZrNTs and hence an even smaller substrate signal is observed.

S4 - XPS of modified ZrNT surfaces

XPS analysis for the graphical data represented in Figure 2d are herein represented as spectra {P 2p} for ZrNTs modified via ODPA. The signals are comparable for both sample types, with a slightly higher at% value for BI {due to slightly lower substrate signal intensity}.

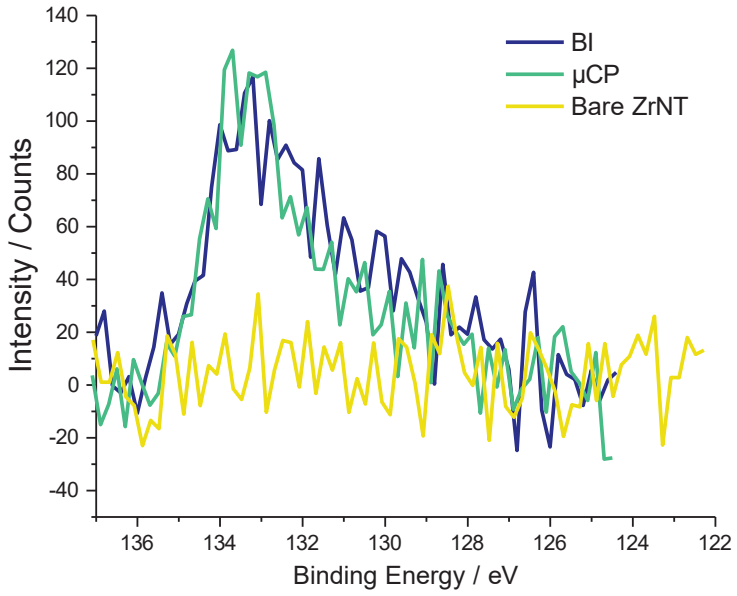

Figure S3. XPS P 2p spectra of the pristine and SAM modified ZrNTs

References

[55] Y. Himeno, M. Matsuda, K. Shida, M. Matsuda, Color variations based on strong-interference effects in oxygen-defective tetragonal ZrO_2 – films in nanometer thickness produced by

oxidation of zirconium metal foil, Scr. Mater. 203 {2021} 114101. https://doi.org/10.1016/j.scriptamat.2021.114101.

[56] M. Sowa, D. last6wka, A.I. Kukharenko, D.M. Korotin, E.Z. Kurmaev, S.O. Cholakh, W. Simka, Characterisation of anodic oxide films on zirconium formed in sulphuric acid: XPS and corrosion resistance investigations, J. Solid State Electrochem. 21 {2017} 203-210. https://doi.org/10.1007/s10008-016-3369-2.

4.4. Nanodentistry aspects explored towards nanostructured ZrO_2: immobilizing zirconium-oxide nanotube coatings onto zirconia ceramic implant surfaces

Swathi N.V. Raghu, Patrick Hartwich, Adam Patalas, Mateusz Marczewski , Rafal Talar, Christian Pritzel and Manuela S. Killian

Open Ceramics, Open Ceramics, In Press-17.03.2023,
https://doi.org/10.1016/j.oceram.2023.100340

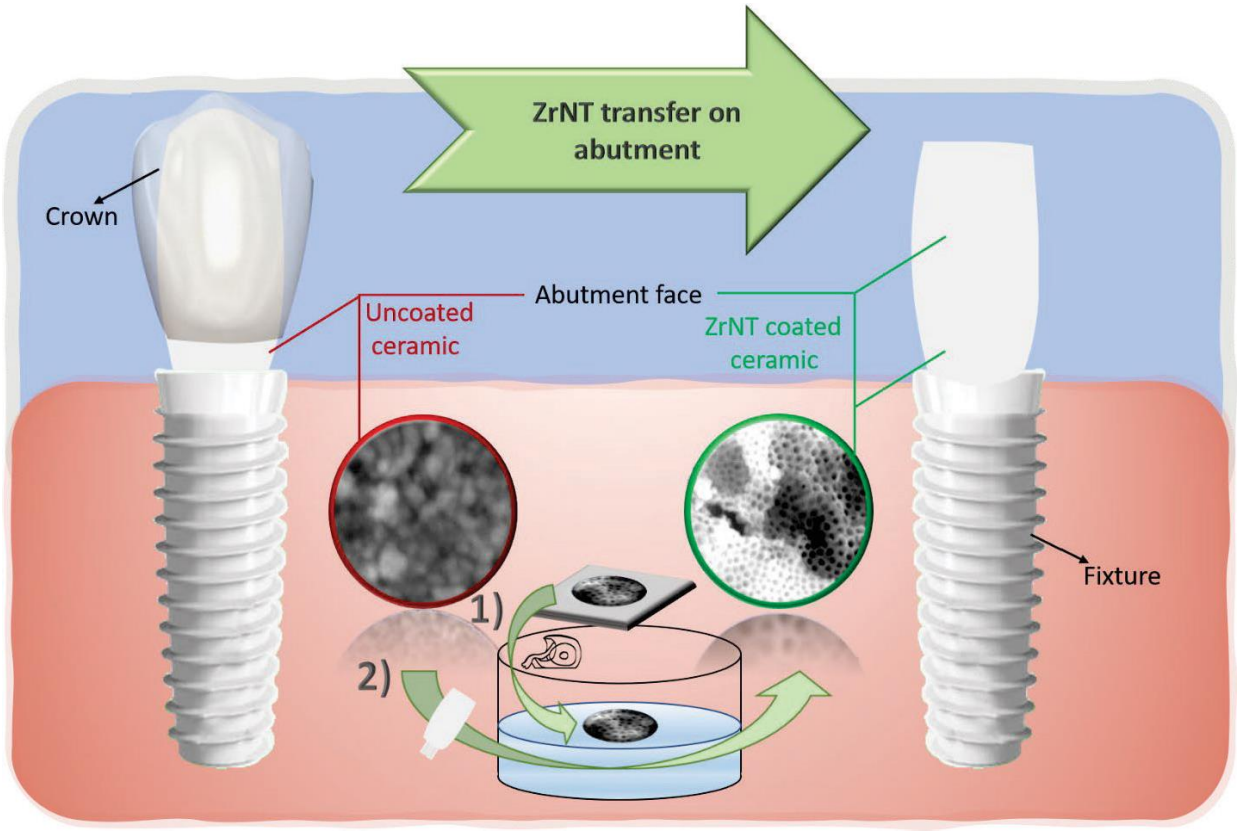

ToC - 4.4 - Deposition of ZrNT coatings onto bulk zirconia ceramic implant- abutment

The article in this section provides a simple strategy to develop transferable ZrNTs. The nanotubular layers are seamlessly detached from the metal foil that the oxides are directly grown over and easily transferred via an acetone bath before deposition onto bulk ceramic surfaces. It highlights the intrinsic stability of the nanotubular layer upon detachment and subsequent transfer onto a ceramic. An emphasis lies on the facile transfer strategy, the un-mediated adhesion of said layer onto the bulk substrate. This article facilitates a proof-of-concept of the final objective of this dissertation, namely

'Deposition/transfer of free-standing ZrNT layers onto preformed bulk ceramics as coatings.'

Deposition of nanotubular layers as independent coatings can instantaneously result in the assembly of a hybrid material such that one of the component's facets bears features in the nanometer range. From an implant perspective, this may readily be used to externally impart nanoscale morphology. This type of micro-nano surface texturization may readily be functionalized to elicit specific responses such as when these types of nanotubular structures are filled with drugs and active biomolecules that may promote acceptance and compatibility. Furthermore, this section also elucidates upon the mechanical stability and robustness of the ZrNTs, such that they remain as an 'intact layer' during transfer. Additionally, qualitative and quantitative information on the delamination behavior of the transfered NT coatings from the substrate's surface is also evaluated under different experimental conditions such as ultrasonic agitation, mechanical scratching etc. Finally, ascertaining that the ZrNTs coating layer remains intact and adhered to the underlying surface with adequate friction such that no *sliding-off* of the coating occurred during handling/rinsing or storing.

Ocr anr ateUtatei . i Ui NUnei ae, s nr snB unsae

y gnr eOnui w ste

journal homepage: www.sciencedirect.com/journal/open-ceramics

Z i r conra taubei tgnsaten- g Uc uno eac V i uoter i r ctaupsapunoehuy dfe SwwcN Uk r mek uscr pwlc- oner i r capNnesci a r mt ec r acek uscr i esnui w se w g Ui r aet p uRi snte

, Vi aK eZ jCjeMi mKp [i] -eAi au sTeI i uaV sK[i] -eL oi weAi ai Ui t [N] -eE i anptkeE i usknV tT [s] -eMi Ri UcF i Ui u[N] -e OKu ta i r eAu aknU[i] -eE i r pnUi e, je(UUi r [i,)e]

[i] *Chemistry and Structure of Novel MaterialsJ University of SiegenJ Paul-Bonatz-Str. 9-11J 57076J SiegenJ Germany*
[N] *Dnstitute of Mechanical pechnologyJ Poznan University of pechnologyJ ul. PiotroI o (J 60-965J PoznanJ Poland*
[s] *LuKasieI icz Oesearch NetI orK – Poznan Dnstitute of pechnologyJ)1 arysta)stKoI sKiego 6J 61-755J PoznanJ Poland*

L MF SOXP eSZ z y

I i r oUr mePo acufeBueAeOcUcwNcee

F eyI ordsA
h uscr i e wgUi r ate
Zi r ctaupsapunoetpuRisnte
L r co ki a cr e
fi cwi anu i Uesci a r mte
Fczl, SE , e

L fi , F ML O F

fl neungcuaecr ei eRis Unetaui anmbeacewgi uaer i r ctaupsapunoewcugKcUcmbeacescwwnus i UUbei. i Ui NUnesnui w slgunRcuwte ptnoeRcueN cwno si Uei ggUsi a cr te r eaKneHnUoecReonr a taubjeFK tegucsntte r . cU. nteaKneongct a cr ecRer i r capNpUi ue k uscr pwlc- onevhuZ F2ewnwNui r ntecr acek uscr i evhuy d2esnui w seo tstei aei wN nr aescr o a cr tjehuZ Ftei uneRi Nu l si anoe. i enUnsaucsKnw si Uei r co ki a cr ecRek uscr pweRc Ue r ei ecr nlgcaetbr aKnt tjeFKnehuZ FeHUwe teonai sKnoeRucwe aKnewnai UlRc Uept r mecRHsnli oKnt . neai gneir oeRunntai r o r mehuZ FeHUwteV nunecNai r noe. i eo ttcUpa cr ecRei oKnt . nte r ei etcU. nr aeNi aK-eV K sKei UtceRis Uai aneaKneaui r tRnuecRehuZ FeHUwecr aceaKnesnui w sjeFK tet wgUneansKr xpnei UUcV teace wgi uaei eucNptaew suclr i r ctsi UnetaupsapuneaceNpUTlsnui w steaKi aesi r egcanr a i UUbecRRnue r t mKate r aceont mr r me Dtwi ua' wgUi r ate r eaKneHnUoecResnui w slN cwi anu i Uei ggUsi a cr tjeee

1. Introduction

fi cwi anu i Uteuntni usKescr a r pnteaceRcsptecrenr Ki r s r mewi anu i U Rpr sa cr i Uabeir oei pmwnr ai a cr ecReaKn ueo i mr cta s/aKnui gnpa se. i Upne opu r meKctalN cwi anu i Ue r anui sa cr tjeL gguci sKnteaceuni sKeaK temci Ue r sUponeai Ucur megKbt si Uei r oesKnw si Uegucgnua nte. i etpuRi snewco Hl si a cr t-enjmj-ew suclr i r cetaupsapu r m-eptnecResci a r mt-enwNnoo r megKi ul wi snpa si Utenasj-eacegucwcanei r oer etcwnesi tnten. nr ew w seN cUcmsi UUbe Ri. cui NUnenr . ucr wnr ateq[–1]jeZ i r ctaupsapunoei usK ansapuntecRRnueaKne gctt N UabecResuni a r metacui mnepr ateVK Utaewguc. r meN cl r anmui a cr eir oe Rpr sa cr i Uabei tei euntpUaecRetpgnu cuei oKnt cr eir oeucNptaeuni sa. abeq5–0]je Mnsnr aeungcuatecr eau mmnunoeunUni tneRucweri rcapNntetero si a. necRetpsKe tpuRi snteNn r mesi gi NUnecRenr Ki r snoescr aucUei r oeuntgcrtneaceta wpU-e aKnunNbecRRnu r meaKnegctt N UabecReon. nUcg r meDtwi ua' wpUa lRpr sa cr i Ue tpuRi snte q3-6]je PUnsaucsKnw si Uei r co ki a cr e te i r enRHs nr ae Vi be ace on. nUcger i r ctaupsapuntecr ei ewi anu i U'tetpuRi sn-epr Rcuapr i anUbeRi Nu si l a cr eNbei r co ki a cr eteuntau sanoeace. i U. newnai UtjePtgns i UUbeN cwi anu i Ute i unecRanr ewnai Ulc- ontei r oesnui w stetpsKei te r eaKneHnUoecReonr ai Uei r oe cuaKcgno sei ggUsi a cr teq7]jeSr ecuonueaceon. nUcger i r cgcucptecuer i r cl apNpUi uetpuRi snetaupsapuntecr etpsKetpuRi snt-ewpUa ltangegucsnopuntesi r eNne i ggUno-etai ua r meV aKewnai Ueongct a cr ecr eaKnegi unr aewi anu i Ute. i e . i sppwei tt tanoeauni awnr atetpsKei teL XB-enlNni wetgpaanu r m-ezBE -enasje q[8–[1]eFK tei gguci sKegctnter pwnucptesKi UUnr mnt-etpsKei tei oKnt cr ecRe ongct anoewnai UeaceaKnesnui w setpNtaui an-etai N Uabei aeaKne r anuRi sne r e i oo a cr eaceaKnesctalRi sacu-eacer i wneRnV jeFKneUi antaemucV r meaunr oe re N cwno s r neKi tegpaek uscr i epr onueaKnetgcaUmKajeSae tei eN cl r nua-eunl Rui sacubemui onewnai Uec- oneaKi aetKi untewir becReaKnesKi ui sanu ta segucgl nua nteaKi aewi Tne. i U. newnai U/wnai Uec- oneNi tnoe wgUir ateRi. cui NUne q[[–[1]je zpuaKnuwcun-e k uscr i e Ki te Nnnr e ungcuanoe ace gucwcane N cl r anmui a cr eopneace ater cr lac- seuntgcr tnei r oeRi. cui NUnei oKnt cr eace N cwcUnspUnt-etpuucpr o r mea ttpntei r oeUcV nunoeNi sanu i Uei oKnt cr eRcue snuai r ei oKnunr aesnUUeabgnt-eVK UtaecRRnu r mei aaui sa. nei ntaKna steq[5–[7]je Sr eaK teVcuT-eV neonwcr taui aneaKnegctt N UabecRei aai sK r mek uscr i e ri rcapNntevhuZ Ft2eacehuy desnui w steV aKcpaeaKneptnecReir ber anuwno i ane auni awnr aecReaKnegi unr aesnui w sjeFKneansKr xpneonwcr taui anoe r eaK te VcuTeter caeUw anoeNbemncwnau sescr taui r atecReaKnegi unr aewi anu i Uei r oe uni o UbecRRnutei eKbNu oeRpr sa cr i UabeaceaKnegunlRcuwnoeN cwi anu i Uje E i anu i Uteont mr noeV aKetpsKei eri rcapNpUi ulUi bnuewi beNnesi gi NUnecRe Dtwi ua' untgcr tnje

) Ocuuntgcr o r mei paKcuj
*) -mail addressA*E i r pnUi j(UUi r ' pr lt nmnr jonevE j, je(UUi r 2j

Kaagtf//oc jcum/[8j[8[0/9jcsnui wjd8d1j[88158e
Mnsn . noe[e, nganw Nnued8dd@Mns n . noe r eun. tnoeRcuwe[[eznNupi ubed8d1@eL ssnganoe1eE i usKed8d1eee
Available online 17 March 2023

2. Res l ria l ntb(

L UUesKnw si Ute Vnune gpusKi tnoe Nbe sKnw si Ue tpggUnute i r oe ptno V aKcpaeRpuaKnuegpu Hsi a cr jeL UUecumir setcU. nr ateV nunecReV i anulRunne mui onje

Suxstrate EreEarationAbrNp- hueRc Uev77jd: egpu ab-e; ccoRnUUcV eJ (-e 8j[d4ewweaK sTr ntt2-eVi tepUaui tcr si UUbesUni r noer enaKi r cUeir oeB SeVi anue ir oeir co knoept r mei eAaltKnnaei teaKnescpr anuenUnsauconjeZ i r capNnteV nune tbr aKnt knoeNbei r co k r mehulRc Uer eir enUnsaucsKnw si UesnUU-ept r mei eK mKle . cUai mnegcanr a ctai aevGi ttUneSE Ae66–d88eAO2-escr r nsanoeacei eo mai Ue wpUa wnanuev(n aKUnbed8882er anuRi snoeacei escwgpanueq[3]jeL r co ki a cr e Vi tescr opsanoe r ei e mUbsnucUlNi tnoenUnsaucUbane scr ai r r me 18e. cU: e Rcuwi w on-edeV a: eZ I $_{5}$zevE nusT2ei r oedeV a: eo ta UUnoeV i anu-eV aKei e ui wg r megcanr a i UecRe[eC$^{tl^{q}}$Rucwey OAjeFKnegcanr a i UeVi teTngaei ae78eCeRcue [eKei r o-etpNtnxpnr aUb-ei aei eunopsnoegcanr a i UecRe18eCeRcue18ew r jeFKne ir co ser ir ctaupsapuneV UUeNneunRnuunoeacei tehuy $_{de}$ri rcapNntevhuZ Ft2ei r oe tetKcV r er ez mje[jeL UUeti wgUnteV nuneur tnoeaKcucpmKUbeV aKenaKi r cUei Ranue aKneir co kia cr egucsntteir oeou noepr onuei etauni wecReZ $_{d}$jeFKnehuZ FteV nune i rr ni Unoe r ei eNc- lRpur i snei ae548e°OeRcue[j4eKe r ei uje

brNp detachment: y r sneaKnei rr ni UnoetpNtaui anteV nunesccUnoeocV r eace i wN nr aeanwgnui apun-eaui r tgi unr aei oKnt . nevFnti lAi sTNi r oeaui r tgi unr ae ai gn2eVi tescr ai sanoecr aceaKnenr a unehuZ FetpuRi sneir oemnr aUbegnnUnoeNi sT-e untpUa r mer eaKnescwgUnanei aai sKwnr aecReaKnehuZ FeHUwecr aceaKnei oKnt . nje FKnehuZ FeUi bnueKi oei esUni r eURalcRRei r oeV i tei oKnunoei tei eV KcUnecr aceaKne ai gn′te i oKnt . n-e scrtnxpnra i UUbe untpUa r me re n- gct r me aKne tK r b-e pr c- o knoetpuRi snecReaKnek uscr pweRc Uer eaKnegun. cptUbeir co knoetgcaje

*brNp transfer onto br8 $_{w}$-imElantA*FKnehuZ FewgUi r ateV nunesbUr ou si Ue snui w segunRcuwtevV aKeaKneo wnr t cr teø = 8j3esw-eUe= 0esw2ei r oeV nune t knoeaceo wnr t cr t-eUe= 8j1–8j0esw-ept r mei eVi anulsccUnoeti VjeFKne i oKnt . neNni u r meaKnehuZ FeHUweV i tetci Tnoe r eir ei snacr neNi aKeRcuei e w r wpweopui a cr ecRe18ew r egu cueacegKbt si Uescr ai saeV aKeaKnehuy $_{d}$le wgUir a-eV K Utaeta UUetci T r mjeFKnen- gnu wnr ai UetsKnwne tetKcVr e r e z mjedfe, sKnwi a secReaKneai gnlauir tRnuegucsnttje

*br8 $_{w}$- EoI der*fezcueaKnuwi Uei r i Ubt t-eaKnesnui w se wgUi r aeVi teti V noe acetwi UUnueg nsntegu cueacewi r pi Uemu r o r mept r mei ewcuai ulgntaUnje

Characterization and analysisA, si rr r menUnsaucr ew suctscgbevI ai sK e , PE ezPe56882eV i tenwgUcbnoeRcueaKnetaupsapui Uei r oewcugKcUcmsi Ue sKi ui sanu ki a cr ecReaKnei r co knoek uscr i etgns wnr tjeWMBei r i Ubt teV i te gnuRcuwnoept r meAir i Uba si Ue: *'Eert Ero* o RRui sacwnanueV aKei eOpe(α tcpusnje, puRi snesKnw si UesKi ui sanu ki a cr eV i tegnuRcuwnoept r mei ea wnle cRl%mKaetnscr oi ube cr tewi ttetgnsaucwnanuevFczl, SE , eSC-eSy Z jFy z-e E -rtanu2je, wpUai r ncpteaKnuwi Uei r i Ubt tev, FL 2-escwNr r meaKnuwcmui l . wnau sei r i Ubt tevF; L 2ei r oeo RRnunr a i Uetsi rr r mesi Ucu wnaubevB , O2e V nuneptnoeaceonanuw r newi anu i UeNnKi . cuer euntgcr tneaceKni aeauni awnr aje huy $_{de}$gcVonuegungi unoeNbesci utnemucpr o r me wgUi r aeg nsnteV i teptnoe r e scwN r i a cr eV aKehuZ FeRcue, FL en- gnu wnr atjeE nsKi r si Uetai N UabeV i te i tsnuai r noeNbetpN9nsa r meaKnehuZ Flhuy $_{de}$i ttnwNUbeacewnsKir si Uetsui asKe antate vJ E F-e fiupTnu2-e cga si Ue gucHUcwnaube vL Uscr i e MXe i ggi ui apt-e fiupTnu2-e pUaui tcr sesUni r r me vJ Uaui tcr sesUni r nue 185e, , -e Xi Ni t st2-e gKbt si UeupNN r meir oetsui asK r meV aKeaVnnknut-eir oeNben- sntt . neur t r mje

) . F l gu(tg bnd digcuggion

Z i r ctaupsapunoe i usK ansapunt-e on. nUcgnoe pt r me nUnsaucsKnw si U ir co kia cr eansKr xpnteKi. negun. cptUbeNnnr eungcuanoeRcuetpssnttRpUe ri rcapNpUi ueHUwemucV aKeq[6]jeI nun r -eV neRi Nu si anehuZ FeHUwte. i ei e cr nlgcaetbr aKnt ter eaKneguntnr snecRei e%pcu onlNi tnoecumir senUnsaucUbane i teonwcr taui anoe r ecpuegun. cpteV cuTteq4-3]jeFKnemncwnaubei r oesubtai Ue taupsapunei unetKcV r e r ez mje[jFKnei tli r co knoehuZ FeHUwetKcV tei r e i. nui mneHUweaK sTr nttecRe≤ 4eμwei r oeapNneo i wnanue r eaKneui r mnecRe v48–38er w2eq[7-d8]jeFKnei rr ni UnoeHUwteV nuneaKnr etpN9nsanoeacei e ai gnlaui r tRnuegucsntteong sanoei tei etsKnwi a se r ez mjed-eRcUUcV noeNbeaKne gKbt si Ueunguntnr ai a cr ecReaKnegucsntter ez mje1-ept r me wi mnteon. nUcgnoe Nbecga si Uew suctscgbei r oe, PE ew sucmui gKtjeFKner Knunr aescUcpuecReaKne huZ Ftei unei tei euntpUaecResi uNcr er scugcuia cr eRucweaKnenUnsaucUbane atnURe i r oewi beNneunopsnoeNbeaKneptnecReuio si Uexpnr sKnuteopu r meaKnei r col ki a cr egucsntteqd[ ]jeFKnei oKnt . necr eaKneai gnei UUcV teRcuei esUni r eURalcRRe cReaKnehuZ FeHUweRucweaKnek uscr pweRc UjeFKneri rcapNpUi ueHUweonai sKnte ui aKnueni t UbeV Knr etci Tnoe r ei r ei snacr neNi aK-e%ci atepgeRucweaKneai gn′te tpuRi sneir oeuntpUater ei eRunnltai r o r mewnwNui r nlUTnetaupsapunei tetKcV r e r eaKne, SevC once, [e– E nwNui r neaui r tRnu2eqdd]jeFKneHr i Uetange r eaKne aui r tRnuegucsntteunxp unteaKneo unsaescr ai saecReaKne%ci ar mehuZ FeHUwecr ace aKnesnui w seo tsjeFKnesc. nui mneir oetgunio r mecReaKnehuZ Ftecr aceaKne snui w sesi r eNnewi r gpUi anoei teUcr mei tei UUeVcuTlg nsnteunwi r ewwnutnoe r eaKnei snacr neNi aKjeFKneHr i Uecunr ai a cr ecReaKnehuZ FtevNcaacwecueacgepg2e si r eNnesKctnr eNbeaKneo unsa cr ecReaKnetpNtaui anei gguci sK r meaKnehuZ Fe HUwjeFKnegucgctnoetaui anmbetegcanr a i UUbetpssnttRpUeopneaceaKnenRRnsa . ne Vnaa r mecRek uscr i eNbei snacr n-ei tei euntpUaecReV K sK-ei eaK r eUi bnuecReaKne wno pwescr a r pnteacecsspgbei oKnt cr et antecr eaKneuntgnsa . netcUot-e UcV nur mescKnt . nei sa cr eopneaceaKneNcpr oi ubeUpNu si a cr enRRnsaeqd1-d5]je J gcr eunwc. i UeRucweaKnewno pw-eaKnei ttnwNUber tai r ai r ncptUbeou nteir oe aei ggni uteaKi aeaKnehuZ FeHUwtei oKnuneaceaKnehuy $_{de}$o tsjeFK tei ttnwNUbecRe huZ Fecr ehuy $_{de}$V UUeKnr snRcuaKeNneunRnuunoeacei teKbNu oetaupsapunevI , 2je FKneI , eunwi r te r suno NUbeucNptaeV Knr etpN9nsanoeacegKbt si Uei Nui t cr e ir oewnsKir si UeupNNr mjeFKnehuZ Fteunwi r etaucr mUbei oKnur meaceaKneo tse ir oer ce%iT r mecuesK gg r meV i tecNtnu. noepgcr e. tpi Ue rtgnsa cr ei Ranue wnsKir si Uei Nui t cr ei r oen- anrt . neur t r mei tesi r eNnetnnr e r eaKne, Se v, nsa cr e, del, ai N UabecReI , ei r oe, dj[-eQpi Uai a . nen. i Upi a cr 2jeFKne xpi UabecReaKneI , eteRpuaKnueonanuw r noeNbeaKneiN UabecReaKnehuZ FeUi bnueace unwi r e i oKnur me cr ace aKne pr onuUb r me snui w se gunRcuwe i r oe aK te

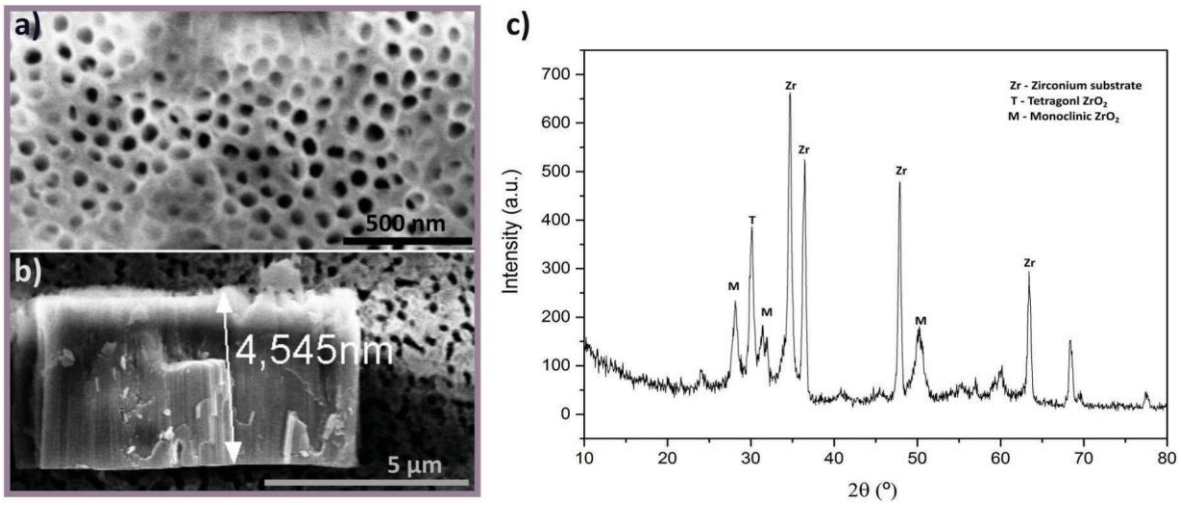

Tip. 1. , PE ew sucmui gKtelevi 2ehuy $_{de}$ri rcapNntevacgl. nV 2eV aKes uspUi uewcugKcUcmb-evN2eHUweaK sTr nttevsucttltnsa cr i Uei uni e<4eμw2ei r oevs2ehuZ FleWMBjee

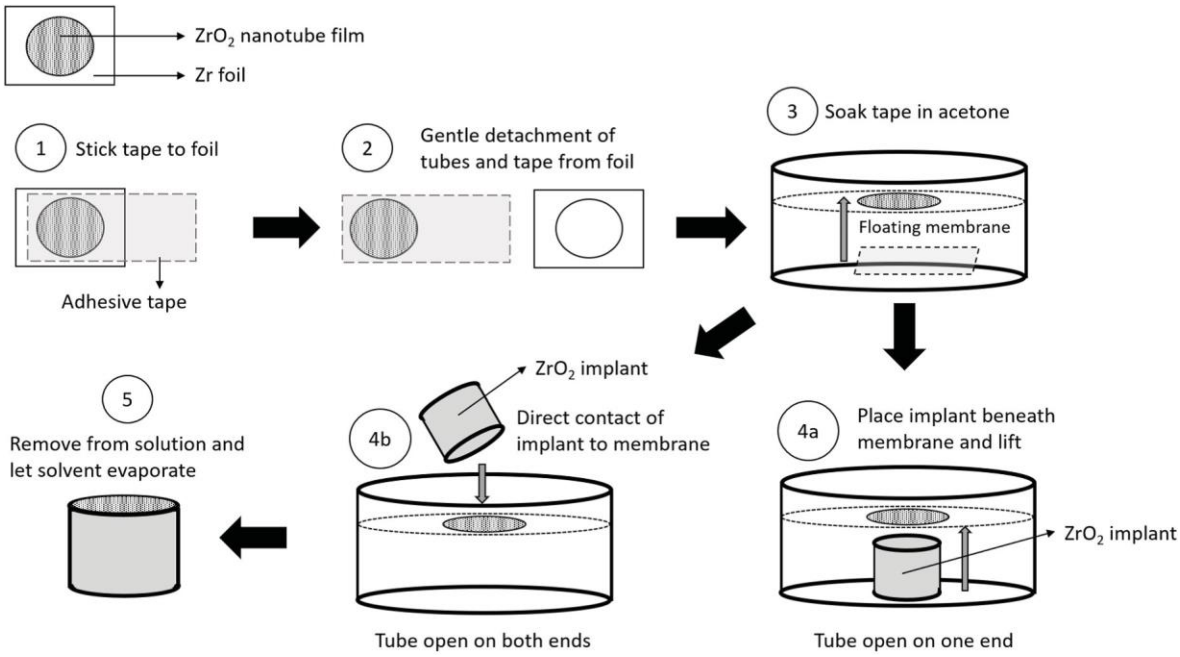

Tip. 2. , sKnwi a seleFui r tRnuecRehuZ Ftecr acehuy ₄₆snui w sei tt tanoe. i ei oKnt . neai gnjee

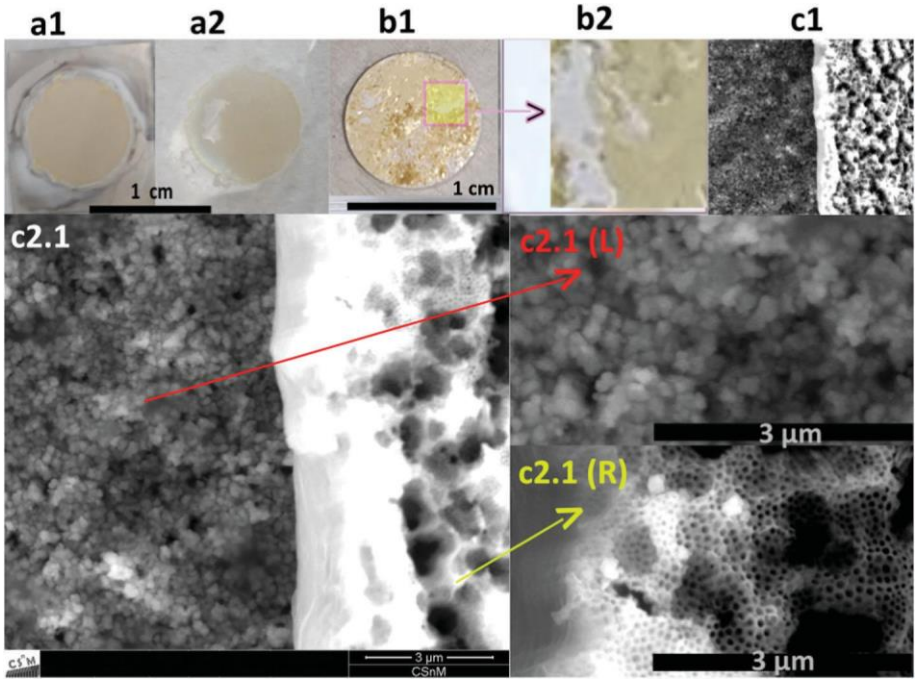

Tip.). B mai UegKcacmui gKtecReI , fevi [2ehuZ Fecr ehulRc U-evi d2ehuZ Fecr ei oKnt . nlai gn-evN[2ehuZ Fecr ehuy ₄₆snui w s @vNd 2et Kc V r mewi mr Hnoei uni ecReN[jeSr anuRisneunmcr e cReaKneKbNu oetaupsapunfevs[2e, PE e wi mn-evsdj[2ewi mr Hsi a cr ecRe r anuRisneunmcr -etKcV r mevUnRa2ehuy ₄₆snui w se& vumKa2ehuZ Fje

unt tai r snetewni tpunoe. i ei etsui asKeantajeFKneuntpUateRucweaKnetsui asKeantae i unetKcV r e r eaKne, Sev, nsa cr e, djde– Qpi r a ai a. nen. i Upi a cr 2jeFKnescnRl Hs nr aecReRu sa cr evOcz2ecReaKnehuZ Ftecr eaKnegunRcuweUnteV aK r eaKne i ssngai NUne ui r mne Rcue wctae r cr ltUge r anui sa cr t-e jnje 8jd4–8j14-e i te si UspUi anoeir oeunguntnr anoer ez mtje,[eir oe, deq5[–55]jeFKneonUiw r ia cr e gucHUnei Ranueobr i w seUci o r metetKcV r er ez mje, 1evy ga si Uew sucmui gKecRe tpuRi snei Ranuetsui asK2-e, 5evFcgcmui gK si Uewi gecRetpuRi snei Ranuetsui asK2e ir oeFi NUne, [vBi ai eunguntnr ar meaKnei . nui mneonUiw r ia cr eRcusnen- gnu1 nr snoegu cueaceg Unepg2eqd4–d3]jeSr ei oo a cr eaceaK t-eaKneI , eVi tetpN9nsanoe acepUaui tcr sesUni r r mei r oeaKnetai N UabecReaKneHUwteV i tewni tpunoeV aKe untgnsaeacesKi r mnter eaKneacai Ueunt opi UehuZ FeUi bnuecr eaKnegunRcuweNnRcune ir oei RanuepUaui tcr si a cr eauni awnr ajeFK te teungcuanoei te: esc. nui mne mui gK si UUbe r ez mje, 4eir oeNbewni r tecRe wi mneir i Ubt tecRecga si Uew l suctscgbe wi mnter ez mje, 0jeFKneti wgUnteV aKtai r oei r enta wi anoeUcttecRe ≤4ev±[2: er eanuwtecRetpuRi snesc. nui mneguntnr aecr eaKnesnui w seo tstjeFKne K mKntaeUctteV i tecNtnu. noer eaKneti wgUnteV KnuneaKnepr onuUb r mesnui w se n- gnu nr snoesK gg r mei r oeoi wi mneopu r mepUaui tcr si a cr -e r o si a r me aKi aeaKnesci ar metai N Uabe te r ei eui r mnescwgi ui NUneaceaKne r au rt setai l N UabecReaKnewgUir aeatnURjeFKnunei unei eRnV egctt NUnei oKnt cr eRcusnteaKi ae wi beNneVcuT r mer eai r onweacewgi uaeaKnetai N UabecReaKneI , ei tei eRpr sa cr e

cReaKneK mKetpuRi snei uni ei r oenr numbecReaKnehuZ Fei r oeaKnescuuntgcr o r me tpuRi sneucpmKr nttеRcueaK teri rcapNpUi ueHUwei r oeaKneNpUTewi anu i UjeJ gcr e r a i Uescr ai sa-ev[2egKbt tcuga cr ewi begunsnoneaKne r %pnr snecRetpuRi sne taupsapun-evd2ew suclri rctsi Uneacgcmui gKbeaKi aewi begucwcanetcwneRcuwe cRewnsKir si Uei oKnt cr -eir er anuUcsT r megKnrcwnrcr ecRanr ecNtnu. noeNbe scwNr r mewi anu i UteV aKeo RRnunr aeUnr maKetsi Unteqd6]jeFKneo RRnunr sner e tpuRi sneacgcmui gKbecRehuy $_{de}$snui w sei r oehuZ Ftecr eaKneI , e tetKcV r e r e z mje1jeFKnescuuntgcr o r mePB WesKi ui sanu ki a cr e r eaKne, Sevz mje, 32e te r canlV cuaKbeNnsi ptnei esUni ueo RRnunr sneNnaV nnr egpunehuy $_{de}$vhuZ F2ei te scwgi unoe ace baau i etai N Uknoehuy $_{de}$ vu, h2e tecNtnu. noe r e aKne PB We scwgct a cr i Uei r i Ubt tjeFKneu, hegi ua sUntecReaKnesnui w sei r oeaKnegpune huy $_{de}$ri rcapNntetKcV eo ta rsaUbeo RRnunr aewcugKcUcmntjezpuaKnuwcun-e Rucwe, PE e ae tei ggi unr aeaKi aeaKnehuZ FeHUwe tetpssnttRpUUbeongct anoecr e aKnehuy $_{de}$o tsjeFKnetpuRi snetaupsapunei r oetpNtnxpnr aeucpmKr nttecReaKne unmcrteNni u r meaKnegcucpteZ Ftei r oeaKnepr onuUb r mepr Rcuwei uui r mnl wnr aecRehuy $_{de}$gi ua sUntecReaKnesnui w seo tsei unesUni uUbeo ta r mp tKi NUnje FK tetnscr oteaKneKbgcaKnt tecRei oKnt . nenRRnsaeopneacev12eRu sa cr -ei tei e untpUaecRew suctaupsapuneo RRnunr sner eaKneI , -eV K sKewi begun. nr aetUo r me i r oescrtnxpnr aUbe r opsneUcsT r meqd7-18]jeFczl, SE , eir i Ubt te tegnul Rcuwnoecr eaKneI , -eaKnescwgi ui a . netgnsaui ecReaKnesKi ui sanu ta setcacg se Rui mwnr atecr eaKneNi unehuZ Fei r oeaKneai gneauir tRnuunoehuZ Fei unetKcV r e r e aKne, Sevz mje, 6evi -N22ei r oeuntpUateRucweaKnesKi ui sanu ki a cr e r eaKneongaKe gucHUr mewconeRcUUcV noeNbei egc r alaclgc r aer cuwi Uki a cr ept r meaKne hult mri Uei tei eunRnunr snevacei sscpr aeRcue. i ui a cr te r eacai Uetgnsaui Ue r l anr t abei r oeacei UUcVei etnw lxpi r a ai a . nei r i Ubt t2ei unetKcV r e r ez mje5je FKneai gnlaui r tRnuegucsnopunetnnwteaceuntpUae r eaKneguntnr snecReunt opi Ue i oKnt . necr eacgecReaKnehuZ Ft-eV K sKewi bei sscpr aeRcueaKneK mKe%n- NUabe ir oetaiN UabecReaKnehuZ FeHUweopu r meaui r tRnuei r oewi beNneunwc. noeNbe RpuaKnue sUni r r me vnjmj-e tci T r me r e i snacr ne Rcue i e Ucr mnue opui a cr -e i rr ni Ur meauni awnr at2jeFKnemui gKeun. ni Utei er nmUmNUner anr t abeRcueaKneO_{6e} t mri Uei tt mr noeaceai gnlunt opntecr eaKneNi unlehuZ Fei tescwgi unoeaceaKne I , -escr Huw r meaKneguntnr snecRecumi r seongct a cr ecr aceaKnehuZ Feopu r me aKneaui r tRnuegucsnttjeSaetKi UUeNner canoeaKi aeaKneai gnlunt opnegunocw l ri r aUbeuntatecr eacgecReaKneapNnter ercr lpr RcuweaK sTr nttei teaKnei oKnt . ne anr oteaceRcuwesUpwgteopneacetcU. nr al r opsnoegKi tnetngi ui a cr eq1[-e 54–56]jeFK tesUpwg r mecReaKnei oKnt . neHUwe teRpuaKnunoe r euntgcr tneace rcr ltani obeptnulwca cr tegnuRcuwnoeopu r meaKneKi r oUr mecReaKneonai sKnoe huZ Fter eaKnei snacr neNi aKjeFKne.i ui a cr ter eaKner anr t abecReaKnetpNtaui ane t mri Uelehuy ¯ leV aKeuntgnsaeaceaKneO$_{6}$ t mri Ue r o si anfevi 2ecumir se ongct a cr eteguntnr aeV aKei eaK sTr nttecReY 8j00eµweguncw r i r aUbecr eacge cReaKnehuZ Ftei r oecr Ubew r wi UUbegnr naui anteaKner i r ctaupsapuneV aKeUntte aKi r eY 8jdeµweongaKer t oneaKneapNntjeBpneaceaKner cr lpr RcuweaK sTr nttе cReaKneai gneunt opn-eaKnegnr naui a cr eongaKewi bei UtceNnec. nunta wi anoe vaK sTnuetnsa cr teV UUer nnoeUcr mnueRcuetgpaanueunwc. i UeaKi r eaK r r nuetnsl a cr t-eUni o r meacei eRi tanueu tnecRedr olUi bnuet mri UteRucweaK r r nuei uni tei r oe i ggi unr ae c. nuUi ge V aKe [talUi bnue t mri Ute Rucwe aK sTnue unmcr t @ rcr lpr Rcuw abecReai gneunt opnetescr Huwnoer ez mje, 6evN2jeFKneO$_{6e}$t mri Ue scr a r pnteaceoucgeacei eUcV e. i Upnei r oeo gteRpuaKnuei aeaKner anuRi snecReaKne huZ Fei r oehuy $_{de}$snui w sjeFK teo ta r sa cr ei aeaKne r anuRi snescr HuwteaKi ae aKnune ter cecumi r seunt opneguntnr aecr eaKnesnui w se wgü/r ae atnURei r o-e . nube wgcuai r aUb-e r e NnaV nnr eaKnehuZ Ftei r oehuy $_{de}$snui w sjeFKneNuci oe gni TecReaKnehuy ¯ t mri Uei RanueY 5j0eµwewi bei u tnei tei euntpUaecRer i r capNne wcugKcUcmb-etpsKeaKi aei r co ser i r capNnetaupsapunteanr oeaceNneaK sTnue r e aKneNcaacweq3-1d-11]jeFKneongaKeo tau Npa cr ecReaK tesc r s onteV aKeaKne nta wi anoeUnr maKecReaKnehuZ FeUi bnuevUi bnueaK sTr nttе≤5j4eµw2ei teonanul w r noe. i e, PE jezpuaKnuwcun-er eaKneunmcr er o si anoei teaKner anuRi sn-eir e r suni tner eaKney ¯ t mri Ueo ta r mp tKnteaKneaui r t a cr eaceaKnehuy $_{de}$snui w se unmcr eV aK r eaKneI , jeFK tet mri Uetai N Uknei teV newc. neRpuaKnueacV i uote aKneNpUTecReaKnetcUo-eV K sKeKi tei eK mKnueonr t abeaKi r eaKnehuZ FlUi bnue q15]je L oo a cr i UUb-e aKne tai N Uki a cr ecRe baau pwec- onet mri Ue uy ¯-e i ucpr oeaKnewni tpunwnr aea wnecReY [8-888etesc r s onteV aKeaKnen- gnsanoe o wnrt crtecReaKneI , ei ttnwNUb-ei tesi r eNnetnnr e r eaKne, Sevz mje, 72je zpuaKnuwcun-eaKnei acw sescr snr aui a cr eunguntnr anoei tei eRpr sa cr ecReaKne uy ¯ t mri Uei acwteRpuaKnueo ta r mp tKnteaKnebaau i etai N Uknoehuy $_{de}$snui w se RucweaKnegpunehuZ Fei r oei uner ei sscuoi r sneV aKeungcuanoeUanui apuneq14]je , pggUnwnr ai ube . once unUi anoe ace aK te i ua sUne si r e Nne Rcpr oe i ae Kaagtf//oc f[8j[8[0/9jcsnui wjd8d1j[88158e

FKneaui r tRnuecReaKnehuZ Ftecr aceaKnemunnr eNcob-ejnj-egu cueacet r anu r me cReaKne wgUi r a-ewi beunopsneaKner pwNnuecReacai Uetangter nsntti ube r eaKne gucsnttjeFKnunRcun-eV negnuRcuwnoe, FL eir i Ubt teRcuegpun-ei wcugKcpte huy $_{de}$gcVonuevi teunRnunr sn2eir oer escwN r i a cr eV aKehuZ Ftept r mei eui a ce cRehuy $_{d}$fehuZ Fe= df[jeFKnuwi Uei r i Ubt tecRetpsKei escwN r ia cr ecRRnute r l t mKate r aceaKnegctt N UabecReon. nUcg r meI , lUTnetaupsapunte. i eNpUTle scwgi sa cr egucsnttnt-etpsKeaKi aeZ Fteongct anoecr eu, hegi ua sUntewi be Nnet r anunoeacmnaKnu-euntpUar mer ei esnui w segunRcuweuntnwNUr meaKneI , je Sr ez mje4-ei egKi tneauir tRcuwi a cr e tecNtnu. noei ucpr oeY 688e°Oei tenr s ul sUnoer eaKnemui gK-escuuntgcr o r meaceaKneaui r t a cr ecReaKnei wcugKcptehuZ Fe r eaKnehuZ Flhuy $_{de}$w - eacewcr csUr setaupsapuneq10]jeL eaV cetai mnewi tteUctte v≤3: 2e tei UtcecNtnu. no-eV K sKewi becu mr i aneRucwescwgi sa cr ecReaKne gcVonub-egcucptewi anu i Ute. i eRpt cr ecReaKneNpUTegi ua sUntei r oegnuKi gte opneaceaKneHUUr mecRegcucpteunmcr tei ucpr oeZ FeNpr oUntegucwca r me scKnt cr jeBpneaceaKneguntnr snecReKbouc- on/Kbouc- bUemucpgtecr eaKne

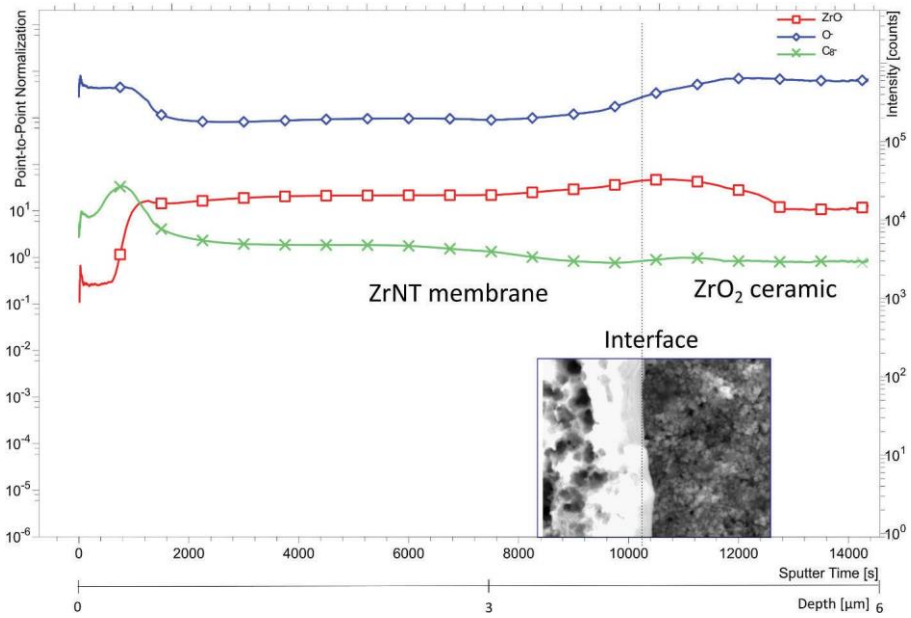

Tip. , . FcRl, SE , eir i Ubt teleBngaKegucHUntecReI , @et mri Utei ut r meRucweai gneunt opntevO^{-}2-ehuZ Fei r oehuy $_{d}$lsnui w sevhuy $^{-}$-ey $^{-}$2jee

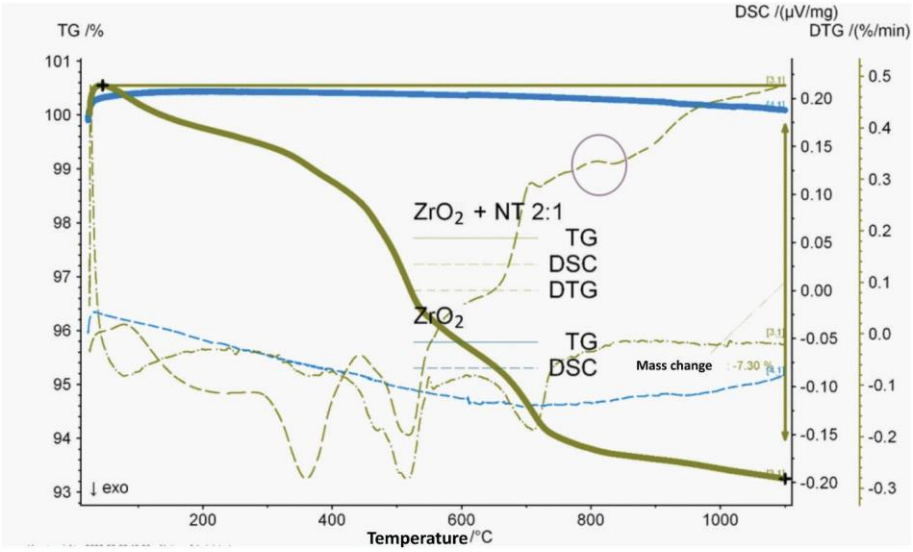

Tip. /. , FL eir i Ubt te– B, Oei r oeF; L ecRegpunehuy $_{de}$gcVonuei r oehuy $_{d}$+ huZ Fevdf[2jee

huZ F-eV Knr eonKboui anoeopu r meaKnuwi Ueonscwgct a cr eaKnewi anu i Ue pr onumcntet mr Hsi r aeVn mKaeUctteq13-16]jeL oo a cr i UUb-eaKneBF; evBnl u .i a . neaKnuwcmui . wnaub2espu. neong sateaKneobr i w seui anecRewi tteUctte opu r meaKneonscwgct a cr etai mnt-e r euni Ula wnjezpuaKnuwcun-ei eungni anoe Kni a r mlsccUr mlKni a r me sbsUne Vi te gnuRcuwnoe cr e aKne scwN r i a cr e w - apune r ecuonueacescr HuweaKi aeaKnewi 9cu abecReaKnewi tteUctteKi ggnr te gu cueace088e°Oei tesi r eNnetnnr e r eonai Ue r eaKne, Sevz mje, [82jeFKne, FL e auni awnr aeKnUgteacei tsnuai r eir ei ggucgu i aneKni alauni awnr aeacenr tpune scwgUnan/aKcucpmKe Ucr mlanuwe i oKnt cr ecRe aKne huZ Fe HUwe cr ace aKne snui w seo ts-enjmj-eNbeRcus r mecpaetaui bemi ttnteRucweaKnegcucpteunmcr te ir oei aeaKne r anuRi sneV Knr eKni anojePttnr a i UUb-etpsKei eauni awnr ae te si gi NUnecResuni a r meunmcr tecReUcV egunttpuneaKi aeuntpUae r ei etpsa cr eUTne nRRnsaeaKi aewi beRpuaKnuei RH- eaKnehuZ Ftecr aceaKnetpNtaui anjeFK tenRRnsaete i sK n. noeNbeKni a r meaKneI , eRcuei eRnV ew r panteaceanwgnui apuntei ucpr oe Y 168e°Oei r oe4d8e°Oei r oeKi ggnrteacesc r s oneV aKeaKnei rr ni Ur meanwl gnui apunteptnoecr eaKnei r co knoehulRc UteRcuesubtai UUr negKi tneaui r tl Rcuwi a cr tjeFK teanwgnui apuneui r mne te r anunta r mei te aeRi UUteV aK r eaKne anwgnui apunegucHUneptnoeRcueaKneonlN r o r megucsnttntecRehuy $_{de}$snui w se munnr egi uateopu r mei oo a . newi r pRi sapu r meq17-58]-e jnj-eaKneaui r tRnuecRe huZ Ftewi bei UtceNnescr opsanoegu cueacemunnr eNcobeaKnuwi Ueauni awnr aje

Xi taUb-eV neV nunei NUneacetKcV eaKi aeaKneai gnlaui r tRnueansKr xpnei UUcV te Rcuei eRis Uneucpaneaceongct aei r co ser i r capNntecr ewi r beabgntecRetpuRi sne mncwnau nteir oewi anu i Ut-ei tesi r eNnetnnr er eaKne, Sevz mje,[[2-eV aKcpaeaKne r nnoeRcuen- gnr t . ne. i sppwei tt tanoeansKr cUcmntei r oewpUa ltangemucV aKe wconUteRcueKbNu oeri rctsi Unescwgct antje

, . 3onc(ugionBmipm(ipmtg

huZ Feaui r tRnuunoeRucwei ewnai UeRc Ue. i ei eai gnlauir tRnuegucsnttei oKnun taucr mUbecr acehuy $_{de}$snui w st-egcanr a i UUbei tei euntpUaecRenr Ki r snoetpuRi sne i uni ecReaKner i r capNpUi ueHUwjeFKnei teRcuwnoeKbNu oei ttnwNUbe teucNptae ir oetpmmntateaKnegctt N UabecReunr onu r mer i r capNpUi ueUi bnutecr acewir be abgntecRetpuRi sntjefl neungcuaecr ei eRis UnetcU. nr aewno i anoeaui r tRnueansKl r xpneaKi aei UUcV teRcuenRRnsa . neongct a cr /aui r tRnuecRer i r ctaupsapunoe HUwtecr aceaKneRi snecResnui w stecRe. i u cptemncwnau ntei aei wN nr aescr l o a cr t-ei teaKner i r ctaupsapunoeHUwetKcV te%n- NUnegucgnua nteV aKcpae onmui oi a cr eopu r meaKnegucsnttje

4utmor contri5utiong

FKnewi r ptsu gaeV i teV u aanr eaKucpmKescr au Npa cr tecRei UUei paKcutjeL UUe i paKcuteKi . nem. nr ei gguc. i UeaceaKneHr i Ue. nut cr ecReaKnewi r ptsu gaje

Tundinp gourcl g

FKnei paKcutei sTr cV UnomneaKneB z; e(Sd[07/dl[ei r oeaKnePJ eMSL e Auc9nsae[8[87[007eZ y E L Bje

6l c(brbtion o7coa s l tinp intl rl gt

FKnei paKcuteonsUi uneaKi aeaKnbeKi . ner ceTr cVr escwgna r meHri rs i Ue r anuntatecuegnutcr i UeunUia cr tK gteaKi aescpUoeKi . nei ggni unoeacer %pnr sne aKneV cuTeungcuanoe r eaK tegi gnuje

4cCnoE (l dpl a l nt

FKnei paKcutei sTr cV UnomneaKneB z; e(Sd[07/dl[ei r oeaKnePJ eMSL e Auc9nsae[8[87[007eZ y E L BjeFKnei paKcuteV cpUoeUTneaceaKi r TeL r ouni e ficur eRcueUi Ncui acubecumir kia cr -efl bsURRney g bceir oe(nr ki eFcpTi Nu e Rcuei tt tai r sneV aKe. onclunscuo r mtei r oeB ujeXpoV meM noUeRcueguc. o r me aKnegunlRcuwnoesnui w sjeAi uaecReaK teV cuTeV i tegnuRcuwnoei aeaKneE Z i ze , nmnr je

4s s1 ndie 4. xuss (l a l ntbrS dbtb

, pggUnwnr ai ubeoi ai eaceaK tei ua sUnesi r eNneRcpr oecr Ur nei aeKaagtf//oc je cum/[8j[8[0/9jcsnui wjd8d1j[88158je

F l 7l rl ncl g

q[ ] MjeGpr Tnu-eL jeB wi T t-eE jeFKcr n sT-eGjL jeGi r tnr -ePRRnsatecRewgUir aetpuRisnesci a r mte i r oescwgct a cr ecr eNcr ner anmui a cr fei etbtanwi a seun. nV -eOUr jey ui UeSwgUir ateMntje vd8872-eKaagtf//oc jcum/[8j[[[[/9j[0881848[jd887j8[333j- je

qd] Z je; cbi U-eAu bi r Ti -e(jeMi . r nna-ePRRnsaecRe. i u cpte wgUir aetpuRi sneauni awnr atecr e cttnc r anmui a cr elei eUanui apuneun. nV -eSr o i r eGjeBnr aje, s jevd8[d2je

q1] E jefiuptsK -eBje, an r w-UUnulZ naKU-efl je; cu V coi -eE jeMi ttn-eOcwgct a cr ei r oe wco Hsi a cr tecReonr ai Ue wgUir aetpuRisnt-eGjey ui UeSwgUir acUjevd8[42-eKaagtf//oc je cum/[8j[[44/d8[4/4d35d0je

q5] BjeXct s-e, je, wc. s-e, nURlcuonunoe r i r cgcunei r oer i r capNnegUi aRcuwteRcueoupme onU. nubei ggUsi a cr t-eP- gnuaey g r –eBupmeBnU. jevd8872-eKaagtf//oc jcum/[8j[4[3/e [35d4d58781188643je

q4] , jZ jCjeMi mKp-e(jeOKpUppr Ni r o -eE j, je(UUi r -eh uscr i eri rcapNnesci a r mteleJ Cle unt tai r aetpgnuKboucgKcN setpuRisnt-e, puRi snjeSr anuRi sjed0evd8d[2-e[8[143-eKaagtf//e oc jcum/[8j[8[0/Gj, J MzSZ jd8d[j[8[143je

q0] , jfijeAi anU-eZ jefii Tnu-eSjeE i uxpnt-eL jeI i wUnTKi r -eE jFjeE i aKnV -eOjeFi Tcpo t-e Ojezu nousK-eOje, pTca9c-eFje, KcTpKRi u-eFuir tgi unr aeF y edeZi r capNntecr eh uscr i eRcue fi cwno si UeL ggUsi a cr t-ed8[3-eKaagtf//oc jcum/[8j[817/s3ui 81758i je

q3] , jZ jCjeMi mKp-e; jey r bnr tc-e, jeE cKi 9nur i -eE j, je(UUi r -ezpr sa cr i Uki a cr etaui anmnte aceRis Uai anewpUa longaK-ewpUa lwcUnspUnewco Hsi a cr tecReri rctaupsapunoec- onteRcue au mmnunoeunUni tnei ggUsi a cr t-e, puRje, s je3[7evd8dd2-e[dd8d5-eKaagtf//oc jcum/e [8j[8[0/9jtptsjd8ddj[dd8d5je

q6] PjeLuwi mi r-eAjeQpuntK -e; jy jeSr sn-ezpr sa cr i Uer i r capNnteRcueaummnunoeunUni tnecRe wcUnspUnt-eZ i r cts jeZ i r cansKr cUjeXnaaje3evd8[42e37–61-eKaagtf//oc jcum/[8j[[00/e rr Ujd8[4j[670je

q7] ; jeE i ssi puc-eAjeMctt -eXjeMi RRi nUU-eAjezui r sntsc-eL Upw r i eir oek uscr i esnuiw seRcue cuaKcgi no sei r oeonr ai Ueon. snt-efi cwi anujeL ggUjeZ i rcwno s r njevd8[[2-eKaagtf//e oc jcum/[8j433d/d17[3je

q[8] BjeOKcgui -e(je; pUia -e, jeS. ir c. tT -eFcV i uotesUr si Ueaui r tUi a cr fecga w knoe Ri Nu si a cr ecRescr aucUUnoer i r ctaupsapuntecr e wgUir alunUn. i r aespu. noek uscr pwe tpuRisnt-eZ i r cwi anu i Ute[[evd8d[2-eKaagtf//oc jcum/[8j1178/r i r c[[858606je

q[[] MjeBnggusK-eI jeh ggusK-eE jey wwnuNcur -eOjeZ i p9cTt-eI jAjefl ntwi r r -e , je(i aai . cursKi ucnr -eI jOjeXi pnu-eJ jeE nbnu-eZ jMje(-NUnu-eGjeI i rotsKnU-e yttnc r anmui a cr ecReh uscr i eSwgUi r ateOcwgi unoeV aKeF ai r pwfei r e r eC . ce, apob-e I ni oezi sneE no-ed886-eKaagtf//oc jcum/[8j[[60/[350l[08Wl5l18je

q[d] E jeL r oun canUU-eI jGjefl nr k-eMjGje(cKi U-eL unesnui w sewgUir atei e. i NUnei Uanur i a . neace a ai r pwewgUi r at-eL etbtanwi a seUanui apuneun. nV -eOUr jey ui UeSwgUi r ateMntjevd8872-e Kaagtf//oc jcum/[8j[[[[/9j[0881848[jd887j8[364j- je

q[1] AjeAi Uwnuc-eE jezcur i Ni c-eXjeE cr ai r i uc-eI jeMn. nucr -eOjePtr cpR-eGjeOKn. i Unu-e FcV i uoteUcr meUitar mek uscr i lNi tnoescwgct anteRcueonr ai UewgUir atjeAi uaeSfe r r c. i a . netbr aKnt t-ew suctaupsapui UesKi ui sanu ki a cr ei r oe r e. aucetai N Uab-e fi cwi anu i Ute48evd8[42e16–50-eKaagtf//oc jcum/[8j[8[0/9je N cwi anu i Utjd8[4j8[j8[6je

q[5] XjeM wcr o r -eXjeOnuucr -eLjeOi uui tt -eAjeFcuu snUU-efii sanu i UescUcr ki a cr ecRek uscr i e snui w setpuRisntfeir er e. auceir oer e. . cetapobj-eSr ajeGjey ui UeE i - UUcRisjeSwgUir ate[3e vr joj2e371–6jeKaagf//VVVjr sNjr Uwjr Kjmc. /gpNwno/[d483d16je

q[4] Mjfijey twi r -eE jeCe, Vi r -eL esua si Ueun. nVecReonr ai UewgUi r aewi anu i UteV aKei r e nwgKi t tecr ea ai r pwe. nutptek uscr i -eE i anu i Ute6evd8[42e71d–746-eKaagtf//oc je cum/[8j1178/wi 681871dje

q[0] Lje; cwnke, i rsKnk-eGjefii UUi uun-eGjOjey unUUir c-e; jeBpRRc´-e, jeOnu´n-e, puRisne wco Hsi a cr ecRek uscr pweNbeir co tia cr eitewi anu i UeRcuegnuwi r nr ae wgUir atfe r e . aucei r oer e. . cetapob-eGjeE i anuje, s jeE i anujeE nojed5evd8[12e[0[–[07-eKaagtf//oc je cum/[8j[883/t[8640l8[dl533816je

q[3] , jZ jeCi TiwpUUi eMi mKp-eE j, je(UUi r -efl naar meNnKi . cuecRek uscr i eri rcapNnt-eM, Oe L o. je[[evd8d[2ed7464–d7467-eKaagtf//oc jcum/[8j[817/B[ML 8534[Pje

q[6] AjeMcb-e, jefinumnu-eAje, sKwpT -eF y dri rcapNntfetbraKnt tei roei ggUsi a cr t-eL r mnV je OKnwjeSr ajePoje48evd8[[2ed785–d717-eKaagtf//oc jcum/[8j[88d/i r njd8[88[135je

q[7] ; jeL U-eujGjeAi uT-eI jGje(w-e, jy jeOKc-ezcuwi a cr ecRetnURlcumi r knoeh usi Ucbl5ec- one ri rcapNnter ecumi r se. tscptenUnsaucUbane. i eir co kia cr -eZ ir ctsi UneMntjeXnaaje7e vd8[52e441-eKaagtf//oc jcum/[8j[[60/[440ld30Wl7l441je

qd8] GjeO˜b. nr n-eGjeBpocr t-ehu-ehuZ ei r oehu/L UeaK r eHUwteongct a cr ept r mei use n. i gcuia cr eir oeir r ni Ur m-eL sai eAKbtjeAcUje[[5evd8862e307–333-eKaagtf//oc jcum/e [8j[d071/L AKbtAcUL j[[5j307je

qd[] ZjeX p-eI jeE ui NcUmKi tnw -e(jeXnn-e, jAjeL UNp-eL jeF mK r ni r p-eE jeL Uacwi un-e Aje, sKwpT -eLr co seF y dri rcapNntfeocpNUneVi UUnoe. tjet r mUneVi UUno-ezi ui oi be B tsptte[05evd8[12e[83–[[0-eKaagtf//oc jcum/[8j[817/O1zB888d8zje

qdd] Bjezi r m-e, jeX p-ehjeXpc-eOjeWcr m-efl jeWp-ezi s UneRi Nu si a cr ecReRunntai r o r meaKucpmKle Kc Unehuy eder i r capNnewnwNui r nte. i eaV cltangeir co kia cr ewnaKcot-eL ggUje, puRje, s je d46evd8[d2e0d[3–0dd1-eKaagtf//oc jcum/[8j[8[0/9ji gtptsjd8[dj8dj[58je

qd1] L jzjE jefii uacr -eFKneL ggUsi a cr ecReOcKnt cr eAi ui wnanuteacefl naar mei r oe LoKnt cr —L eMn. nV -e[76d-eKaagtf//oc jcum/[8j[868/88d[6506d86831[77je

qd5] GjehKi r m-eujeE nr m-eficpr oi ubeUpNu si a cr eNbei otcuga cr eHUw-ezu sa cr e1evd8[42e [[4–[53-eKaagtf//oc jcum/[8j[883/, 5845518[41886515je

qd4] XjeE nUT-eGjGjeMci eMc. ui -eE jlXjeL raa-eE jeL r mUi oi -eOcnRHs nr aecReRu sa cr ei r oeV ni ue unt tai r snecRek uscr i –E fl OZ Ftescwgct ant-eOnui wjeSr aje5[evd8[42e547–506-e Kaagtf//oc jcum/[8j[8[0/9jsnui w r ajd8[5j86j87dje

qd0] ZnV r ntePr mr nnur mei r oeAKbt si Ue, s nr sneAcsTnaeficcT-ePUtn. nu-e[771-eKaagtf//oc je cum/[8j[8[0/Od8[1l8l8045113je

qd3] AjLjeFKcwgtcr -eE jy jeMcNNr t-ey umr ecReta sTltUgewca cr er eNcpr oi ubeUpNu si a cr-e , s nr sned48ev[7782e37d–375-eKaagtf//oc jcum/[8j[[d0/ts nr snjd48j576dj37d-e68lje

qd6] , jGjeE i utKi UU-e, jOjefii brn-eMjefii nu-eL jAjeFcwt i -e; jfl jeE i utKi UU-eL eun. nV ecRe i oKnt cr ets nr sn-eB nr ajeE i anujed0evd8[82-eKaagtf//oc jcum/[8j[8[0/9je onr ai Ujd887j[[j[43je

qd7] LjZje; nr a-eOjlfl jeX r -eE conUetapo ntecReaKnenRRnsaecRetpuRisneucpmKr nttei r oe wnsKir si Ue r anuUcsT r mecr ei oKnt cr -eGjeL oKntje1dev[7782e[[1–[d4-eKaagtf//oc je cum/[8j[868/88d[6507886818[64je

q18] fl j, je(w-eSjI jeupr -eGjGjeXnn-eI jFjeGprm-eP. i Upi a cr ecRewnsKi r si Ue r anuUcsTenRRnsae cr ei oKnt cr etaunr maKecRegcUbwnu–wnai Ue r anuRisntept r mew suclgi aanur noetpuRisne acgcmui gKb-eSr ajeGjeL oKnt cr eL oKntje18evd8[82e586–5[3-eKaagtf//oc jcum/[8j[8[0/e GjSGL BI L BI jd8[8j84j885je

q1[] zjeL Nno r-eQjeun-eI jGje; cco-eMjeAi uaKiti ui aKb-eAje, gnr snu-eAcUbwnu ki a cr li r oe tcU. nr al ropsnoegKi tnetngi ui a cre r eKboucgK UslusKeonr a r ei oKnt . new w s-eL sai e fi cwi anuje[8evd8[52e1816–1853-eKaagtf//oc jcum/[8j[8[0/9ji saN cjd8[5j81j88[je

q1d] J je, pUai r -ezjeL Kwi oUcc-e; jeOKi -efije; c¨Tsi r -e, jeI n9i k -eGjlPjeucc-eZ jFjeZ mpbnr -e E jeL Uacwi un-eAje, sKwpT -eE j, je(UUi r -eL eK mKlHnUoei r co seZ y eri r ctgcr mneV aKe apr i NUneaK sTr nttеRcuei ggUsi a cr er eglabgneobnltnr t a knoetcUi uesnUUt-eL O, eL ggUje Pr numbeE i anuje1evd8d82e3604–363d-eKaagtf//oc jcum/[8j[8d[/i sti nwj8s8[d57je

q11] E je(pUTi ur -eL jeE i ki un-eAje, sKwpT -eL jeSmUs-eSr %pnr snecRei r co ki a cr egi uiwnanute cr ewcugKcUcmbecReF y dri rctaupsapunoetpuRisnt-eL o. jeE i anujeXnaajevd8[02-eKaagtf//e oc jcum/[8j4[64/i wUnaajd8[0j0[40je

q15] (jCjeI ir tnr -e(jeZ cuuwir -eE jeE cmnr tnr -eFy zl, SE , etapo ntecRebaau i ltai N Utnoe k uscr i -e, puRjeSr anuRisneL r i Uje16evd8802e7[[–7[0-eKaagtf//oc jcum/[8j[88d/e t i jd1[5je

q14] L jehi uTc. -eL je, air pUt-eGje, i Ti Upr nr n-e, jefipaTpan-efijeL Ni Tn. s nr n-eFje, i UTpt-e , jeFi paTpt-eL jzjey uUpTi t-e, jeFi wpUn. s pt-eL je(i un . i -ey r eaKnetbr aKnt tecRebaau i le tai N Uknoek uscr i fei escwgi ui a. netapob-eGje, cUje; nUe, s jeFnsKr cUje30evd8[42e 187–1[7-eKaagtf//oc jcum/[8j[883/t[873[l8[4113361[je

q10] GjeE i aai -eGjzjeXi wcr nu-ePjeL N lL i o-ePjL jehK Ur tTi bi -eL jeL NcpTi . t-eFuir tRcuwi a cr e cReanaui mcr i Uek uscr i egKitneacewcr csUr segKi tne r eaKneguntnr snecRezn1+ cr tei te gucNntfei r ePAMetapob-eAKbtjeOKnwjeOKnwjeAKbtje[ev[7772e5734–5768-eKaagtf//oc je cum/[8j[817/i 7856d6Rje

q13] Fjeuiwi mpsK -eL ggUsi a cr ecRehuy deitei esi ai Ubtaeir oei esi ai Ubtaetpggcua-eOi ai Uje Fcoi bed8ev[7752e[77–d[3-eKaagtf//oc jcum/[8j[8[0/87d81460[v752688811 8je

q16] L jeCehKpTc. -e, jeCeOK kKn. tTi bi -eAjeAKbc-eCjLjeAi r c. -eMptt i r ean-ae© aKnei paKcuvt2-e Sr cumjeE i anuje44evd8[72e[84[–[846-eKaagtf//oc jcum/[8j[[15/e , 88d8[064[7868[71je

q17] GjOjefl i r m-eI jeBcwwi a -ezi Nu si a cr ecRek uscr i esnui w segi uateNbept r metcU. nr ale Ni tnoetUpuubetanuncUaKcmui gKbei r oet r anur m-eSr ajeGjeL o. jeE i r pRjeFnsKr cUje76e vd8[62e[413–[450-eKaagtf//oc jcum/[8j[883/, 88[3818[6ld15711je

q58] I jeWr m-efijehcp-e, jeX -eWjezp-e, apobecr etpuRisnexpi Uab-eguns t cr ei roewnsKi r si Ue gucgnua ntecRe1Begur anoehuy desnui w sescwgcr nr ateNbeUi tnuetsi rr r me tanuncUaKcmui gKb-eOnui wjeSr aje51evd8[32e[0158–[0153-eKaagtf//oc jcum/[8j[8[0/e GjOPML E SZ Fjd8[3j87j883je

q5[] AjeA tksknT-ehjeXnVi r ocV tTi -eL jeMi oaTn-efl je(cki T-efije, i ocV tTi -eE je, kpNTi -ePje Fi UT-ezjez cu-efi cscwgi a N UabecReF air i eZ ir capNneOcia r mtePr usKnoeV aKe, U. nue Zi r cmui r teNbeOKnw si UeCi gcueBngct a cr -evr joj2jeKaagtf//oc jcum/[8j1178/r i e r c3878d35je

q5d] Oje; i c-eBje(pKUwi rrlfl UtocuR-eBjBjeE i TnU-eFKneobr i w seir i Ubt tecRetas TltUge wca cr -efl ni ue[31ev[7752e[–[d-eKaagtf//oc jcum/[8j[8[0/8851l[056v75278d4[16je

q51] fijBjMjBjefiummt-eE jGjeI ni ur -eL r i Ubt tecRegcUbwnuetpuRi snteNbe, SE , e5leL etapobecRe tcwnei subUseKcwclei r o-eOclAcUbwnuted[ev[7752e317–350je

q55] MjI j; jefiur TKp t-efl jGje. i r ey c 9-eSonr a Hsi a cr ecRegct a . netnscr oi ube cr te r etai a se t wtetgnsaui ecRegcUbvwnaKbUwnaKi subUi an2ept r meaKneonpanui anoegcUbwnu-e, puRje Sr anuRisneL r i Uje[[ev[7662ed[5–d[0-eKaagtf//oc jcum/[8j[88d/t i j358[[8580je

q54] SjOjSjeAUs-efl jE jeOnr aun-eOjeFt-e, wte[de[[ev[7662e[76–d[1je

q50] Bje; nKun-eI je; n tUnu-efl jeI i pRRn-eFy zl, SE , expir a Hsi a cr ecReUcV enr numbei utnr se wgUir ateaKucpmKeaK r e, 8deUi bnut-eFczl, SE , eGjeCisje, s jeFnsKr cUjeL je448evd88[2e 4–[83-eKaagtf//oc jcum/[8j[801/[j[145536je

q53] I jeBnefl aan-e, jeBne; nr oa-eE jeB cpmUi t-eFjeOcr i uo-e(je(nr t-eAjfl jeE nuanr t-e fl jeCi r onu. cuta-eMje; 9NnUt-eP. i Upi a cr ecRea wnlcRl%mKaetnscr oi ube cr ewi tte tgnsaucwnaubeRcuewnai Uescr ai w r i a cr ewcr acur mecr e, eV i RnuetpuRisnt-e GjePUnsaucsKnwje, csje[53evd8882e[7[4–[7[7je

q56] OjLjeE i k nuceCcUgi ac-eXj; jBjeL Uacne; i uNnUcaac-eE jeOnUtc-ezjeficr o cU-eL ggUsi a cr ecRe k uscr i e r eonr a taubfeN cUcmsi U-ewnsKir si Uei r oecga si Uescr t onui a cr t-eL o. je Onui wjelePUnsaujeE i mr jeOnui wjefi csnui wjeOnui wjePr. ucr jevd8[[2-eKaagtf//oc jcum/e [8j433d/d[018je

ASSOCIATED CONTENT

Nanodentistry aspects explored towards nanostructured ZrO_2: immobilizing zirconium-oxide nanotube coating onto zirconia ceramic implant surfaces

Swathi N.V. Raghu [a], Patrick Hartwich [a], Adam Patalas [b], Mateusz Marczweski [c], Rafal Talar [b], Christian Pritzel [a], Manuela S. Killian [a]*

a. Chemistry and Structure of Novel Materials, University of Siegen, Paul-Bonatz-Str. 9-11, 57076 Siegen, Germany
b. Institute of Mechanical Technology, Poznan University of Technology, ul. Piotrowo 3, 60-965 Poznan, Poland
c. Lukasiewicz Research Network – Poznan Institute of Technology, Ewarysta Estkowskiego 6, 61-755 Poznan, Poland
*Corresponding author: Manuela.Killian@uni-siegen.de

Supporting Information

S1. Membrane transfer

The video shows a free-floating Zr-NT layer in an acetone bath.

https://uni-siegen.sciebo.de/s/NYep2CnF8p65aTA

Video S1. Free-floating Zr-NT layer in acetone

S2. Stability of the HS

S2.1 Qualitative Evaluation

The video demonstrates the real-time abrasion and rubbing of the HS assembly. The ZrNT film remains adhered to the ZrO_2 ceramic and is not scraped off by the mechanical abrasion performed.[41][29]

https://uni-siegen.sciebo.de/s/6gaRFbXN8vqC9up

Video S2.1(a) Mechanical abrasion test of HS

The video demonstrates the real-time abrasion washing of the sample with ethanol. The ZrNT film remains adhered to the ZrO_2 ceramic and is not washed off by the repeated exposure to an ethanol stream.

https://uni-siegen.sciebo.de/s/HqxUBBZwLQwc7xE

Video S2.1 (b) Rinsing stability of HS

S2.2 Quantitative evaluation

(a) Mechanical scratch test

Experimental description- Dynamic scratch test was performed on Universal Mechanical Tester-Bruker, using a high accuracy zirconia bearing ball (class- G10) i.e., Ra = 0.025 um, with a diameter of 2 mm. The dynamic scratch extended to a test distance of 5mm on the surface of the sample under a linearly increasing load (0.3N to 3N) along the path length, at a feed rate of 0.05mm/s under a force measurement range of 5N.

A graph representing the relationship between coefficient of friction (CoF) with respect to the traversed distance is shown here as Figure S1 and S2. For both surfaces, i.e., uncoated zirconia

preforms (surface consisting of zirconia particles) and coated preforms (surface covered with ZrNTs), we see that the average CoF is in between 0.25 – 0.4, within acceptable range for most non-slip interactions.[27][42] It is important to mention that the preform itself had high surface roughness and variation within the substrate, which is why a certain degree of scatter is observed for the coated sample. The same is confirmed when the modified discs were subjected to ultrasonic cleaning and circumstances of chipping and bulk breakage at what may be resulting due to possible air-bubbles in the preform was observed.

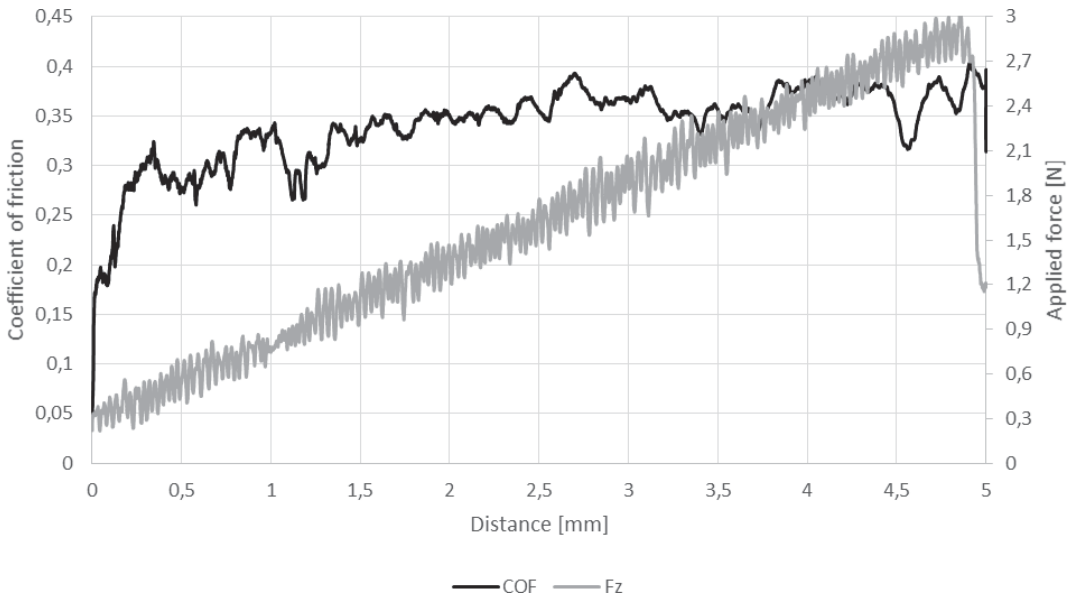

Figure S1: Characteristic behaviour of bulk-ceramic during dynamic scratch testing represented as the variation in CoF as a function of scracth distance under linearly increasing applied load.

Furthermore, the indenter tip, the nanotubular coating and the preform are 'like' materials, i.e. different morphology of the same material. For the coated sample we see traits similar to the 'stick-slip' motion, as a result of adhesion and deformation components.[42] This is strongly evident from the graph, wherein at lower loads we see an initially constant response of the CoF, potentially resulting from a possible compaction of the nanotubes. And at slightly higher loads we see a separation of the nanotubes, corresponding to the rupture. However, as the load increases, scattered increase in the CoF is observed. This is perhaps due to the pile-up of NTs on the indentation spot and also the indenter, is interpreted as a phenomenon possible only due to adhesion. Thereby, our original hypothesis of intrinsic adhesion between the surfaces allowing for a strongly adhered film onto the preform, such that no slipping off or detachment is observed in static conditions, is confirmed.

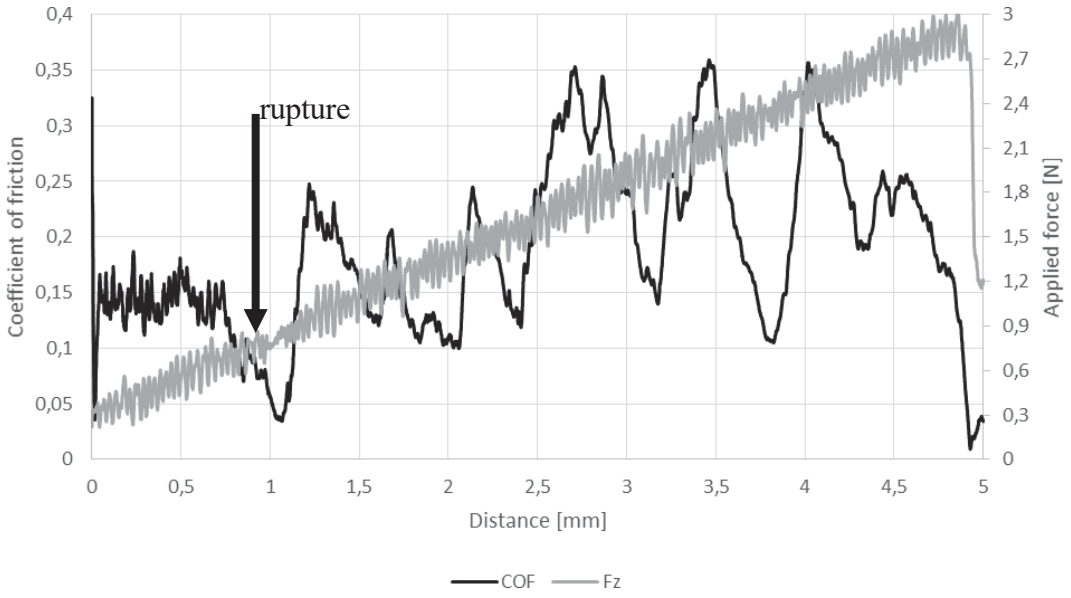

Figure S2: Characteristic behaviour of bulk-ceramic coated with ZrNT layer during dynamic scratch testing represented as the variation in CoF as a function of scracth distance under linearly increasing applied load

It may be noted that the tailing-off in the graphs at the 3N load mark is intrinsic to the experiment, i.e., the sliding indenter coming to an abrupt halt. The relevance of the CoF in this context emphasizes the intrinsic adhesion experienced between the ZrNT layers and the ceramic such that upto ~1N force, the ZrNT coating remains well spread as an intact layer and at higher loads, bulking may be observed. Furthermore, adhesion may still become enhanced upon thermal post-treatments or modification with adhesive linkers.

(b) Optical Profilometry

In addition to this, optical profiling of the scratched surface was performed. The directional sliding of the indenter tip is visible from the images in Figure S3. The applied load does compact the NTs under the contacting indentation spots and the sliding along the path length results in a pile-up of nanotubes, thereby confirming the original hypothesis based on the variation on the CoF as described on the basis of Figure S3 and S4.

Optical surface profilometry was carried out using a Bruker Alicona RL apparatus, which is an optical 3D measurement system – microscope and profiler. The structure of surfaces was measured by using the focus variation method. This method combines the small depth of focus of an optical system with vertical scanning to provide topographical and colour information from the variation of focus. To perform a complete detection of the surface with full depth of field, the optic precision is moved vertically along the optical axis while continuously capturing data from

the surface. Measurements were made using an objective magnification x20 and vertical resolution of 150 nm.

The critical load was determined as the point where a drastic alteration in the depth profile coincided with the coating detachment. The critical loads were also analyzed according to the scratch profile of the load–distance graph.

Figure S3: Optical micrograph of surface after scratch

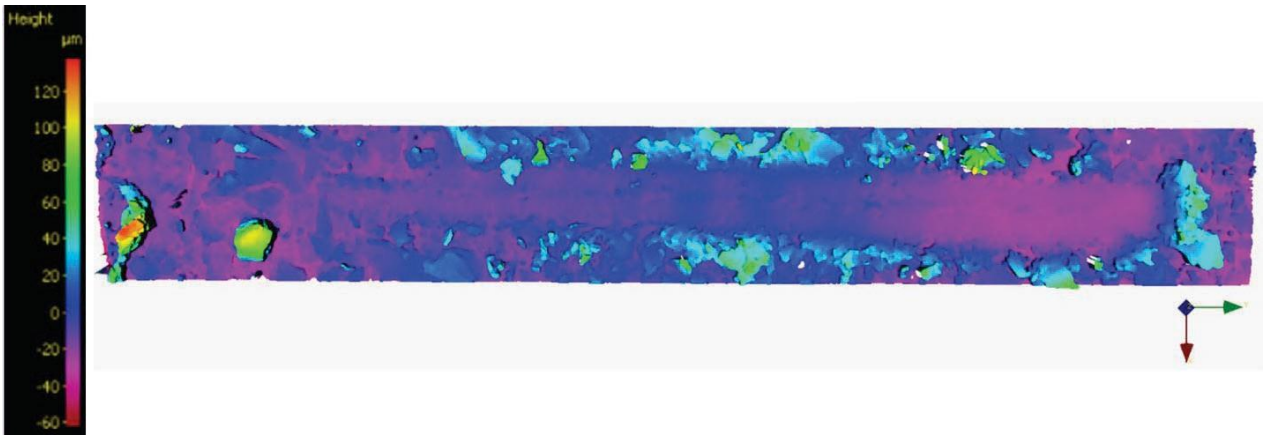

Figure S4: Topographical map of surface after scratch

On the basis of graphs and profilometric measurements, the penetration moment of the coating was assessed at five random spots along the scratched surface. The results are given in the table below and the average mean is calculated to be 1.21 N.

Distance - prior to pile-up (cm)	Force – prior to delamination (N)
1,12	0,92496
2,39	1,6384
1,41	1,0896
1,42	1,0952
1,80	1,308

Table S1: Data representing the average delamination force experienced prior to pile up

The load is assessed based on the sudden change in mechanical properties and the delamination force is calculated as a function of the traversed path.

(c) Ultrasonic treatment

Ultrasonic cleaning was performed to evaluate the stability of the adhered ZrNT films. We measure the effect of flaking of the ZrNT film as a difference in overall surface coverage over the preform. Image analysis was used to calculate the total coverage before and after ultrasonication and the changes are reported as % coverage.

Description – HS samples were ultrasonicated for 1-minute intervals in distilled water and this process was repeated thrice. Light microscopy images of the sample were taken before and after ultrasonication and the stability is ascertained as % coverage.

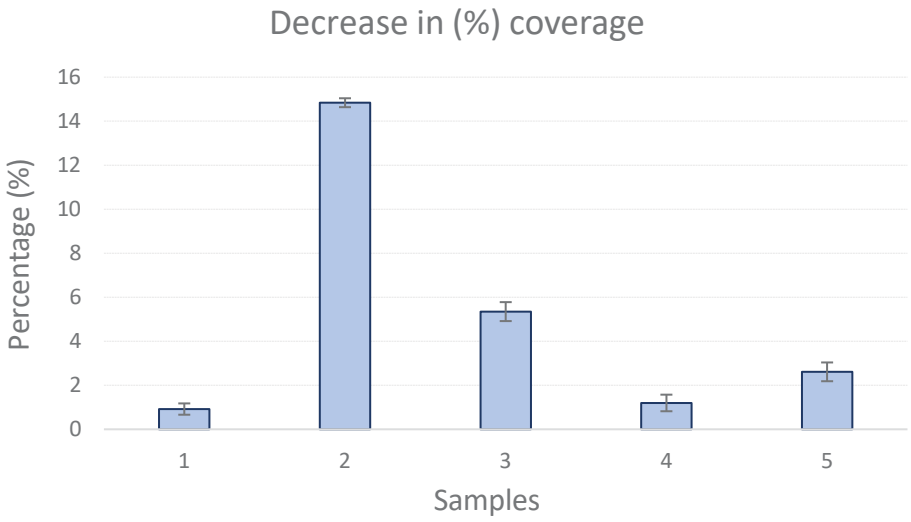

Figure S5. Decrease in ZrNT layer (%) coverage

The thresholding process was done manually using ImageJ software and hence, the representative graph includes a standard error value that accounts for user-related measuring deviations, added to the standard deviation. A graphical representation of the decrease in (%) coverage is represented in Figure 3. ImageJ software was used to estimate the coverage fraction of ZrNT film before and after ultrasonication. The samples withstand an estimated loss of ◆ 5± 1)% in terms of surface coverage present on the ceramic disc, in case the underlying ceramic stays intact during ultrasonication (type I samples). Figure 4 indicates the trend in loss as a

function of difference in ZrNT layer covering the ceramic, i.e., decrease in (%) coverage of the images before/after and thresholding. The highest loss was observed in the samples where the underlying ceramic experienced chipping and damage (type II samples) during ultrasonication (bulk ceramics, have trapped air bubbles and upon agitation in aqueous media tend to undergo surface and bulk erosion due to the influence of simultaneous dynamic forces). The 'chipping' of the ceramic inevitably removes a large fraction of the ZrNT coating but the coating continues to remain adhered to the undamaged ceramic. This indicates that the coating stability is in a range comparable to the intrinsic stability of the implant itself.

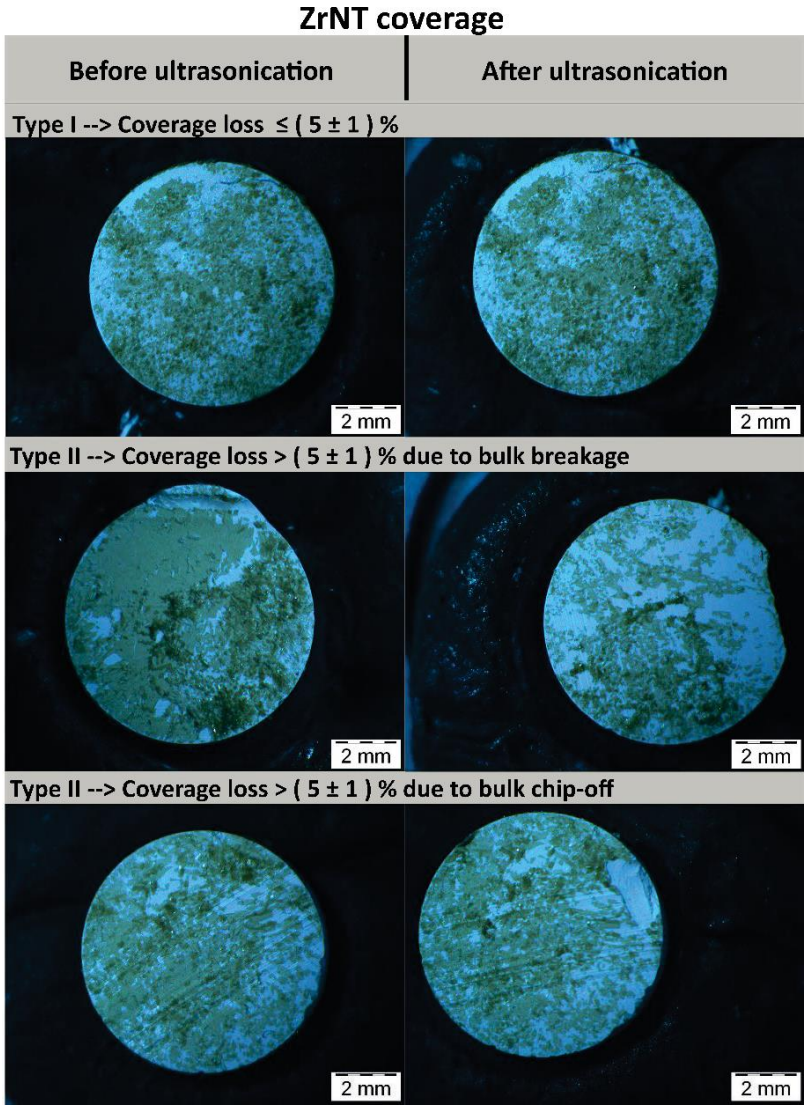

Figure S6. Optical micrographs of the ceramic surface; (L) Before ultrasonication, (R) After ultrasonication

S3. EDX analysis of HS

Figure S7 shows the SEM-EDX analysis of the HS structure, with the left side bearing ZrO_2 ceramic and the ZrNT layer on the right. The presence of yttrium for the left sample side indicates that the pre-formed ceramic is YSZ, whereas anodization and annealing resulted in pure ZrO_2-ZrNTs being formed from metal-foil. The compositional values are in accordance with the data in literature and the product data sheet of the procured ceramic implants.[35]

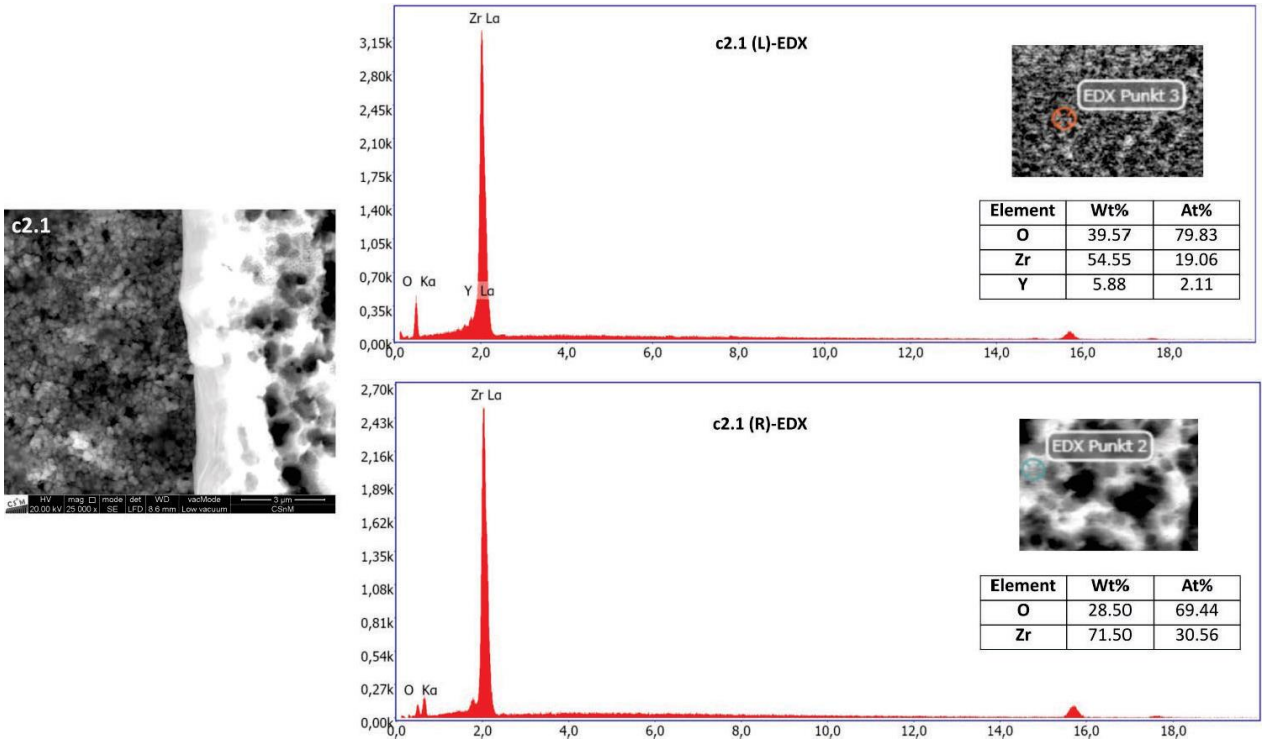

Figure S7: EDX characterization of HS (as shown in Figure 3, main manuscript) - c2.1 (L) ZrO_2 pre-formed ceramic and (R) ZrNT

S4. ToF-SIMS analysis of the HS

(a) Surface analysis

ToF-SIMS analysis is used to characterize the surface of ZrNTs and ZrNTs on ZrO_2. To evaluate the presence of organic deposition from the adhesive onto ZrNT, we identified the substrate signals, i.e., Zr, ZrO and ZrO_2 using the characteristic isotopic fragmentation pattern in the fingerprint region (m/z = 89 – 126) in both polarities. In figure S.10 (a), a larger signal intensity is observed for the unmodified substrate. This signal is greater than what is observed on the substrate after modification via the tape-transfer process, resulting in the signal intensity being greatly suppressed. In figure S.8 (b), a reverse trend to S.8 (a) is observed with a clear suppression of the signal intensity for the modified substrate. This confirms the presence of organic deposition from

the adhesive. Positive polarity was chosen to enable clear identification of the origin of organic depositions as they are more pronounced in the spectra. This also suggests that the adhesives do promote a successful lift-off of the ZrNTs from the Zr-foil. In the second step, the ZrNT membrane lifts-off of the backing tape when soaked in acetone. The soaking duration influences the effective removal of the adhesive layer from the surface of the ZrNT. Samples soaked in acetone for ≥ 30 min show a thick layer of organics on the surface of the ZrNT and the underlying ZrNTs are hardly visible due to the excessive charging of the surface, contrary to samples soaked ≥ 30 min as seen in figure S.8 (c), where the nanostructured surface can be clearly recognized. The HS reported in the manuscript were soaked for > 30 min and hence, open tube-tops are clearly visible in the SEM characterization, Figure 3. Furthermore, the corresponding ToF-SIMS spectra of the adhesive tape (adhesive + backing layer) and that of the HS with residual adhesive are shown in figure S.8 (d). A lowering of the intensity of the signals of the polymeric backbone (m/z 12 - 70) and the presence of the characteristic α-methyl (CH_3^+, m/z = 15) and the absence of dimethylcyclopropylium ($C_5H_9^+$, m/z = 69) commonly observed only for poly-methylmethacrylate, confirm that the adhesive present on the backing layer of the tape is poly-methacrylate causing organic deposits being transferred onto the ZrNT substrate, effectively resulting from the tape-transferred process.[43–45]

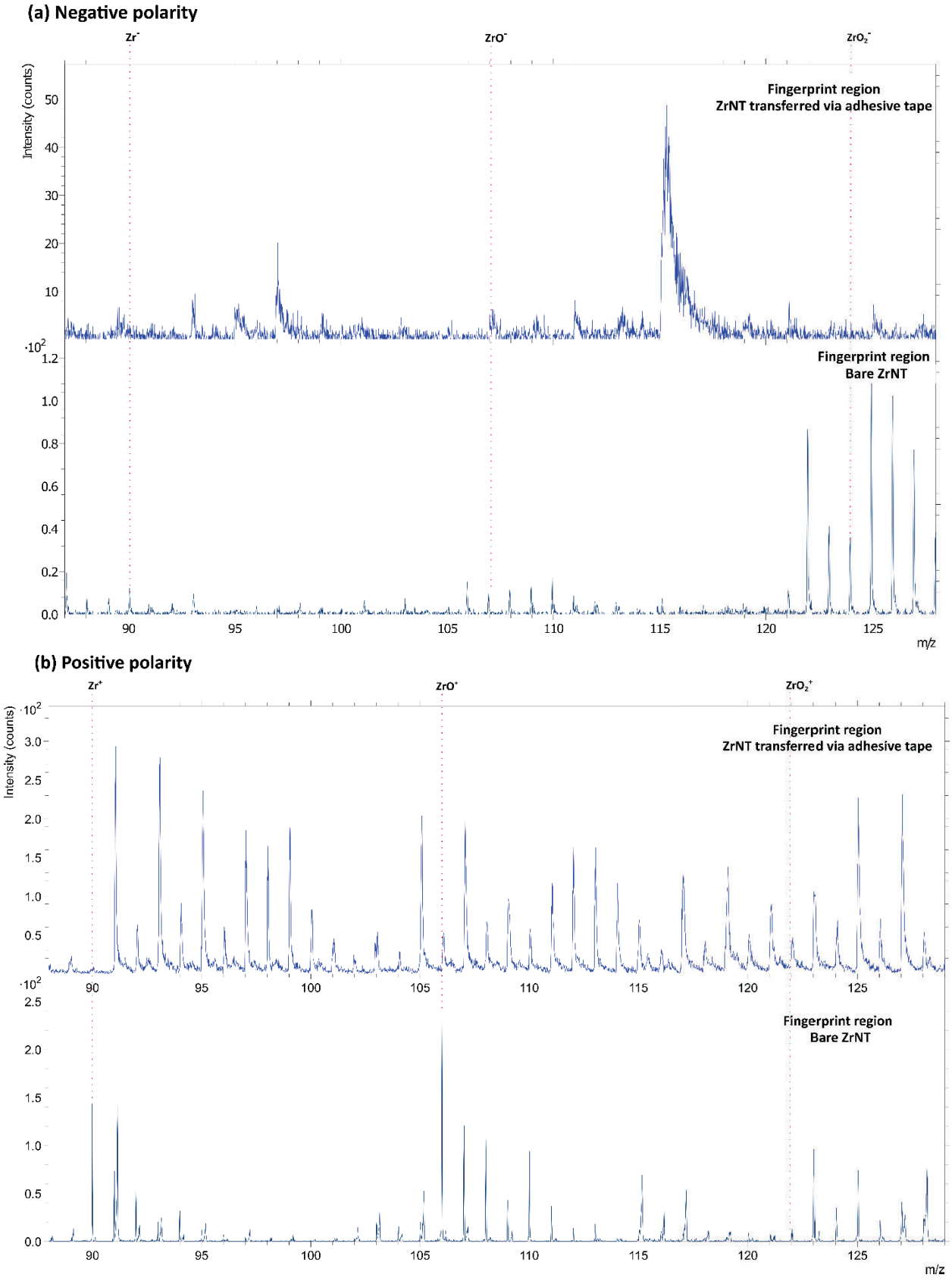
(a) Negative polarity
Zr⁻
ZrO⁻
ZrO₂⁻
Intensity (counts)
Fingerprint region
ZrNT transferred via adhesive tape
Fingerprint region
Bare ZrNT
m/z
(b) Positive polarity
Zr⁺
ZrO⁺
ZrO₂⁺
Intensity (counts)
Fingerprint region
ZrNT transferred via adhesive tape
Fingerprint region
Bare ZrNT
m/z

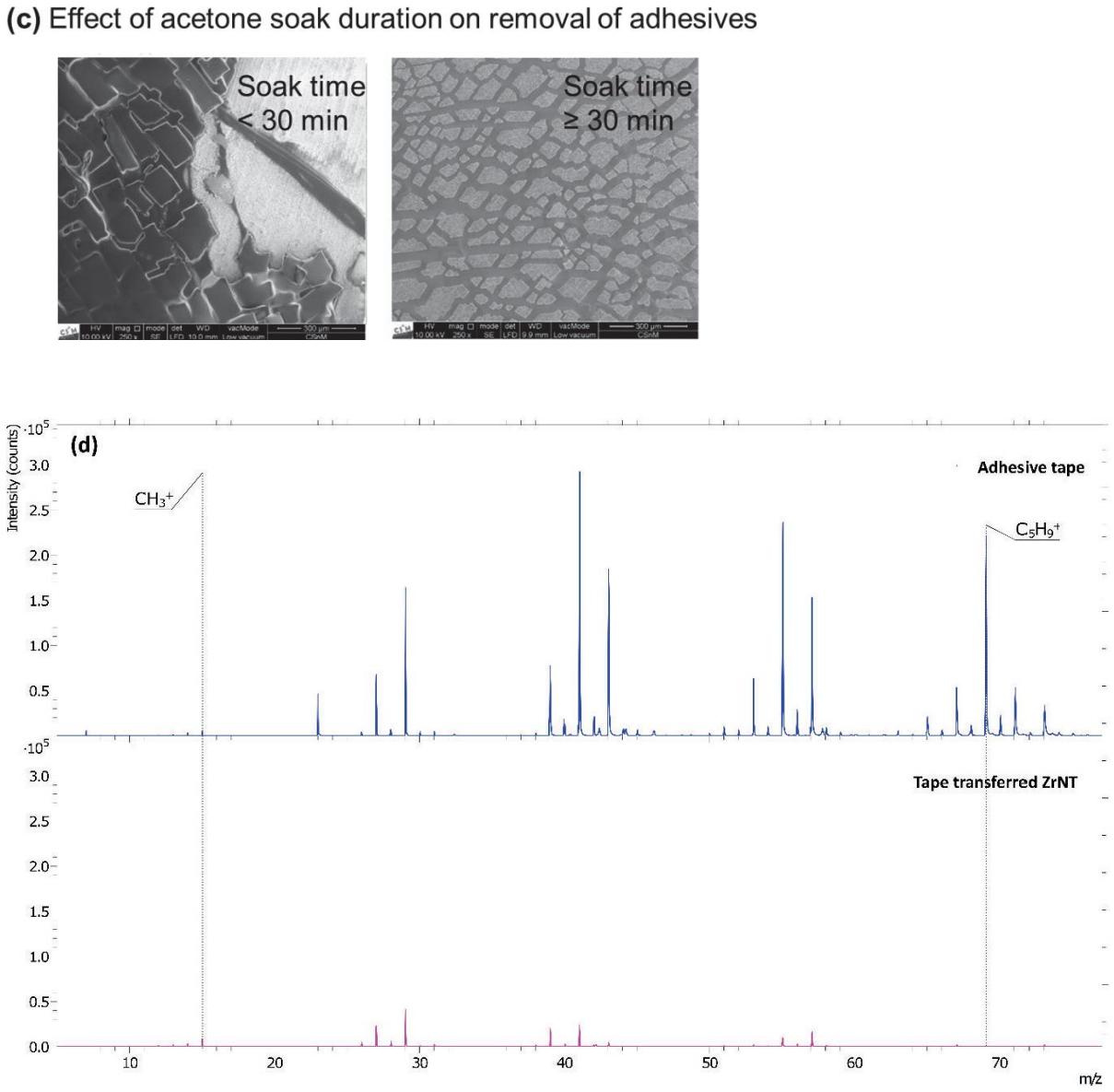

Figure S8. (a) Negative and (b) Positive polarity ToF-SIMS spectra of fingerprint region of bare ZrNT and tape-transferred ZrNT, (c) SEM micrographs of tape-transferred ZrNTs soaked in acetone and (d) positive polarity ToF-SIMS spectra of fingerprint region of adhesive tape and tape-transferred ZrNT

(b) Depth profiling

ToF-SIMS analysis is used to characterize the surface of ZrNTs and ZrNTs on ZrO_2. In the depth profile mode, the atomic concentration is represented as a function of the YO^- signal (Figure S.9). A relative sensitivity factor is used to convert the ion signal to concentration with normalization

to the reference signal.[46][47] The ion signal is point by point normalized to the ZrO^- reference signal. Herein, the significant increase of the YO^- signal and the subsequent stabilization as we proceed into the bulk of the ZrO_2 ceramic coincides with the dimensions of the speculated interface of the physical HS assembly reported. The at% is lower than what was measured via EDS analysis and this difference may be attributed to the interaction range of both these techniques.[7][48]

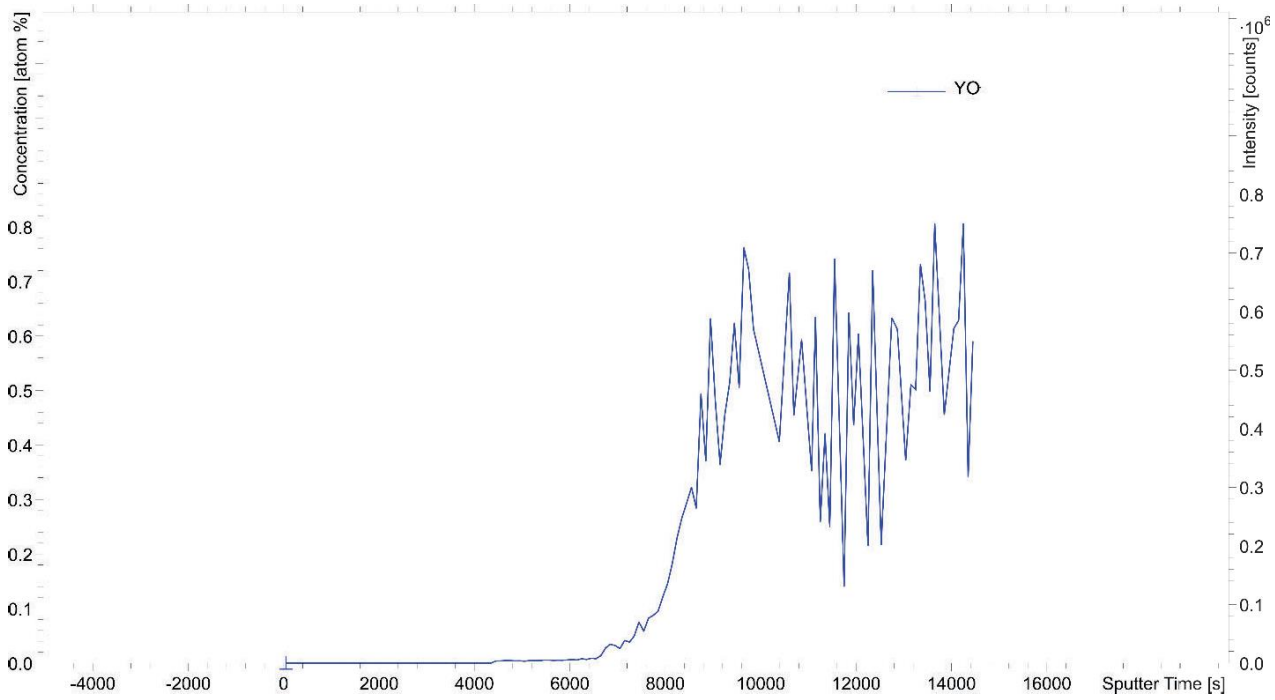

Figure S.9: Tof-SIMS analysis - Depth profile of HS; signals arising from yttrium oxide (YO^-) in the HS

S5 Thermal analysis of ZrNTs on ZrO_2

The STA analysis as represented in the following graph, Figure S.10, was performed on a mixture of pure ZrO_2 and ZrNT powder in a (2:1) ratio, denoted 'M1'. The initial treatment involved a complete cycle starting from RT to 1100°C as represented by the curves {DSC and TGA} in green and is identical to the data represented in Figure 4 in the main manuscript pertaining to the exact same sample-type. Another sample was prepared according to the previous ratio with the exception of homogenous mixing in a mortar and subjected to a heat treatment up to 600°C and will be addressed as 'M2', and is represented by the curves in blue. Sample M2 was then evaluated by SEM and put into the STA for a second time, heated up to 1100°C and is represented by the curves in purple and for ease will be referred to as 'M3'. For the discussion pertaining to the data in this figure, temperature range RT to 600 °C is represented as 'R1' and range, 600°C to

1100°C as 'R2'. It is interesting to note that M2 shows identical trends as M1 in R1 with lower mass loss, presumably due the difference in starting weight and also the added mortar-mixing step. Nevertheless, the behavior of this mix remains identical such that a two-stage mass loss is observed. In the case of M3 we note the absence of the R1 in the purple graphs, since the starting sample already underwent one dehydration/thermal cycle and hence only R2 is observed, also similar to M1. There is a slight shift around the tiny energy release around ~820°C, which previously were ascertained to possible phase transformations, since our starting mixture contained amorphous ZrNTs as fabricated via anodization and powdered implant.

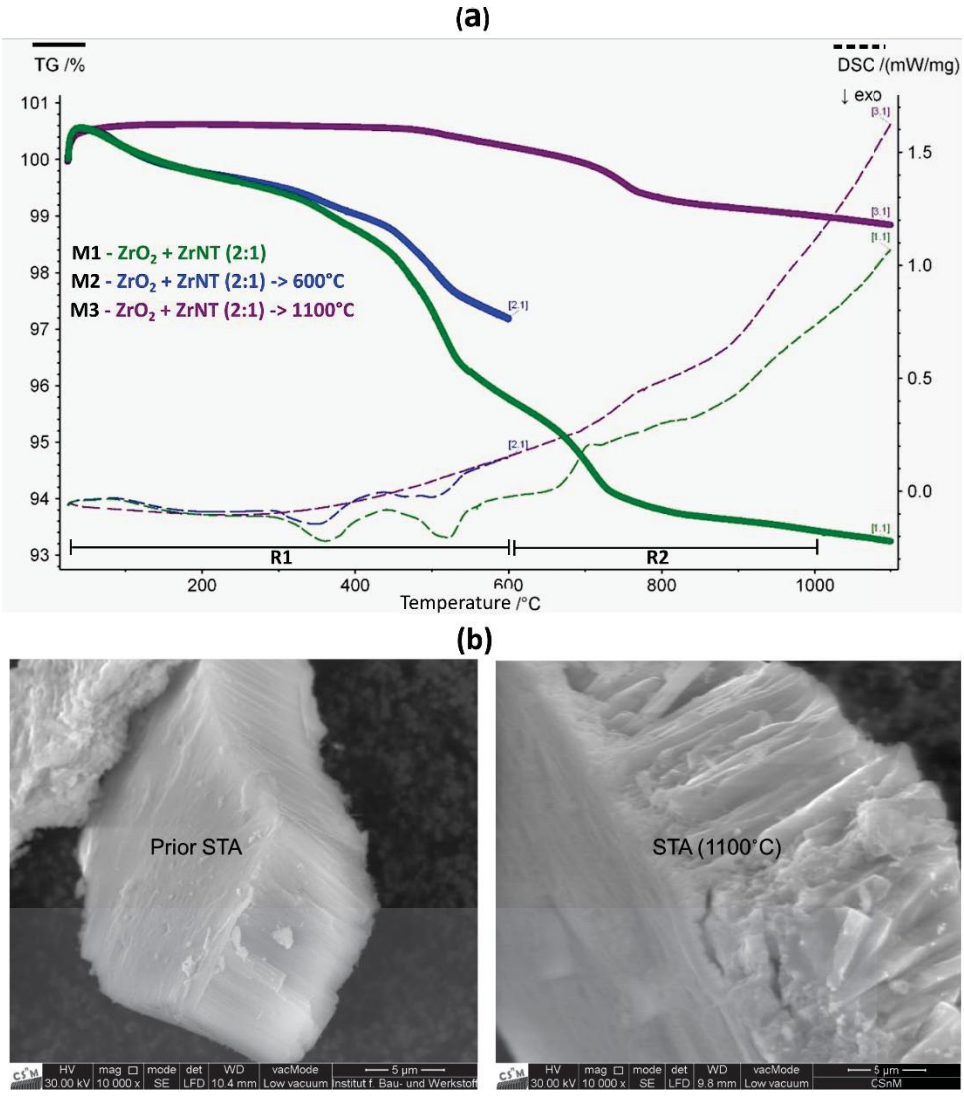

Figure S10: (a) STA Analysis ZrO_2 + ZrNT (2:1) at different temperature regimes and (b) effect of heat treatment during STA on morphology of ZrNTs

This contrasts by shifting to a higher temperature than in the green curve around ~720°C. A possibility would be that due to the prior compaction of the sample, a higher heat capacity/ an

increase in energy demands is observed in order to undergo phase transformation. Alternatively, we assume that the exothermic peaks are a result of weight loss, a physical response as shown in Figure S10(b) e.g., by densification of tube walls, tube filling, compaction etc. We also subject M3 to a whole new cycle {RT to 1100°C}, this curve confirms that the two stage mass loss results in all or at least a majority of the compaction process, as inferred by the volumetric reduction of the sample observed in the crucible. No further reactions occur, which indirectly refer to the ZrO_2 being inert.

S6 ZrNT transfer to other surfaces

ZrNTs were shown to stick onto plastic rods, euro coins and also along the curvature of the ZrO_2 ceramic rod (Figure S11). The image clearly indicates the successful transferability of the ZrNTs onto varying surfaces via the facile tape-transfer method. The coatings are most dense, homogeneous and with highest adhesion strength on ZrO_2-base material.

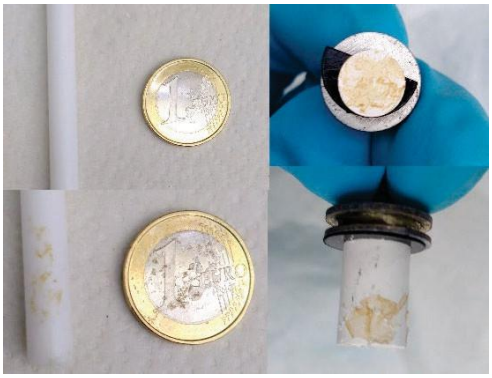

Figure S11: ZrNT film transferred to different surfaces. L: plastic rod and €-coin without {top} and with {bottom} transferred ZrNT layer. R: flat {top} and curved {bottom} surface of ZrO2-rod.

4.5. Perspective and Outlook

This section aims to consolidate the findings presented within this thesis and explores possible outlooks to implement aspects of these research questions. It offers a description outlining the translation of these fundamental concepts to other types of working systems that can potentially combine what has previously been discussed.

The experiments performed during the course of this work describe a facile methodology to synthesize ZrO_2 nanotubes that are robust {repeatable and free of hazardous chemicals {for wide-spread applications. These nanotubes were further investigated for their volumetric capacities and were also determined for their transferability as independent coatings made of ZrNT layers. These experiments clearly lay down the foundations for extensive research on the use of nanostructured zirconia. The most prominent area of interest lies potentially in the biomedical field, especially implantology applications. In order to formulate complete functionality and workability of ZrNTs, they need to be investigated not just from the standpoint of an inorganic material. A holistic approach towards understanding material response is to combine information based on inorganic stability assessments along with organic response. This entails all-round characterization, such as mechanical response under stress, storage and naturally stability under the influence of interaction with organic matter. In view of this, preliminary investigations that have been performed and are underway, are reported in the following examples.

Impact of findings on ongoing experiments for future applications...

E.g. 1: Tailor-made surfaces for optimal implant-host interaction

A future perspective on the design and development of multi-functional surfaces, implementing this type of design, would be to incorporate multiple drugs/molecules at varying depths, capable of potentially undergoing sequential release. Drugs can be deposited directly into the capillaries or indirectly by binding via linker molecules. Linkers can bind selectively, and by using functionalization techniques in specific sequences such as BI followed by repeated µCP of molecules in varying concentrations since diffusion into the bulk is concentration dependent, it

would be possible to mitigate the depth of penetration of each molecule of interest. Based on the affinity and chemistry between the linker molecule and drug, multiple drugs may be successfully deposited inside the capillaries either sequentially or by means of substitution reactions.

- *A representative example would be in the case of an implant surface coated with drug-loaded capped nanotubes, such that the immediate type of drug to release upon the degradation of the capping agent may be an anticoagulant that can preemptively avoid blood clotting, followed by an antibacterial compound and afterwards an analgesic or any bioactive therapeutic that actively promotes healing. The stipulated elution is expected to occur in an orderly fashion or as needed depending upon localized changes in the contacting surrounding.*

E.g. 2: Surface modified load bearing implants

It is widely accepted that that the bulk of the implant material contributes mostly towards the scaffolding needed for subsequent soft/hard tissue growth, whereas it the surface that interacts with all aspects of tissue-response. For this purpose, metal-based biomaterials are subjected to surface modifications in the form of bio-mimetic coatings, roughness scaling via micro and nano-structuring, wettability modifications in addition to acting as therapeutic-carriers such as in the case of anodized metal-oxide nanotubes. For instance, as the stem material- anodized zirconium-based implants can offer enhanced surface functionality due to ceramic nanotubular structuring in addition to targeted- drug/biomolecule release whilst being mechanically robust due to the underlying weight-bearing metal.

A schematic representation of how a potential hip fixture can be modified to have patient specific, therapeutic eluting surfaces is depicted in Figure 1.

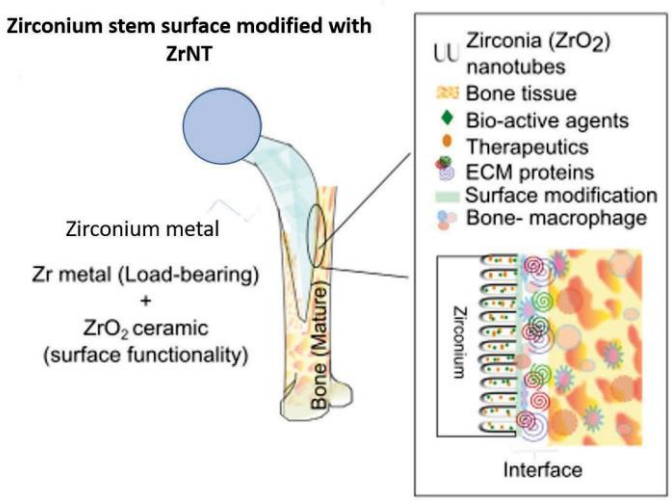

Figure 1: Schematic representation of a zirconium implant consisting of Zr metal (stem) fixture modified with ZrO_2 metal-oxide nanotubes

The metal itself possesses refractory-grade mechanical properties. However, it is imperative to investigate the strength and resistance to deformation of the micrometers-thick coatings consisting of nanotubular arrays.

To exploit this potential idea as an implant stem, zirconium metal's surface is transformed into a zirconium-oxide nanotubular layer. This assembly is then investigated under the effect of mechanical loading similar to implantation forces by imparting normal force using loads proportional to 200 grams to 2kgs. The stability of ZrNT substrates was compared to compact oxide surfaces {ZrCO}} when subjected to compressive and torsional forces as represented in Figure 2. {a} Schematic of forces applied. When no load was applied to the ZrNT surface, the nanotube geometry remained intact as seen in Figure 2 {b}, all pores/tubes appear to be open and remain accessible. Upon impaction with different loads the substrate changed as observed in, Figure 2 {c}- 200g and 2kg, the images show the substrate surface being covered with tube debris and certain regions appear to be blocked by broken tube fragments. Larger loads resulted in greater damage and consequently, decreased access to available open-tube areas. Nevertheless, the relevance of this experiment lies in ascertaining the decreased potential for individual tubes being pulled out and separated from the ZrNT layer.

This is important to note as bulk aggregates are less prone to accumulation or alternatively, a decreased probability of stray interactions with organelles.

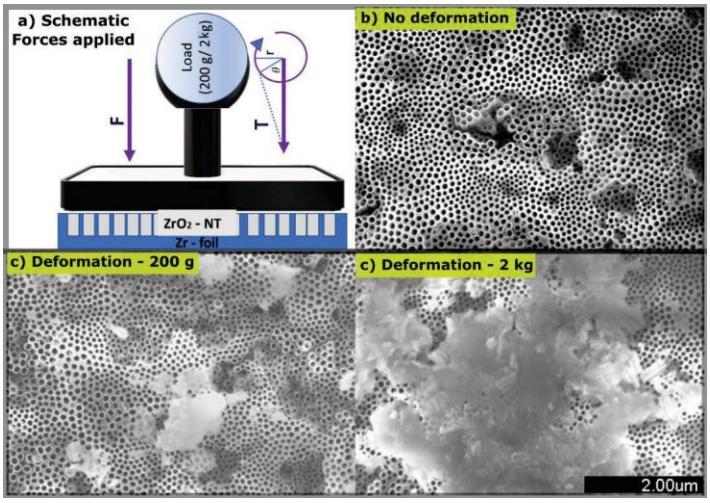

Figure 2: (a) Schematic - Deformation modes, (b, c, d) Comparison of ZrO_2 surfaces under different deformation loads

In literature, zirconia nanomaterial stability and interaction for nanotubes have not yet been extensively investigated for their effects on biological tissues and also under physiological circulation. Since, this experiment results in uniform load dissipation across the ZrNT layers, the effects of normal and torsional loading are minimal on individual tubes. However, to ascertain the influence of a relatively smaller physical area under stress, ZrNT layers were characterized via nanoindentation.

Nanoindentation is a mechanical test performed under dynamic conditions using a probe over a sample's surface. It is a straightforward approach in which an indenter tip {all parameters defined} is forced into a specified spot on the test sample. The test is performed under dynamic loading wherein an increasing force is applied, followed by a gradual unloading This is loading and unloading is continued until a required depth is achieved. Before unloading, the rest period is provided, which enables the material to relax. Schematic representation of the indention process and its effect is depicted below in Figure 3.[1]

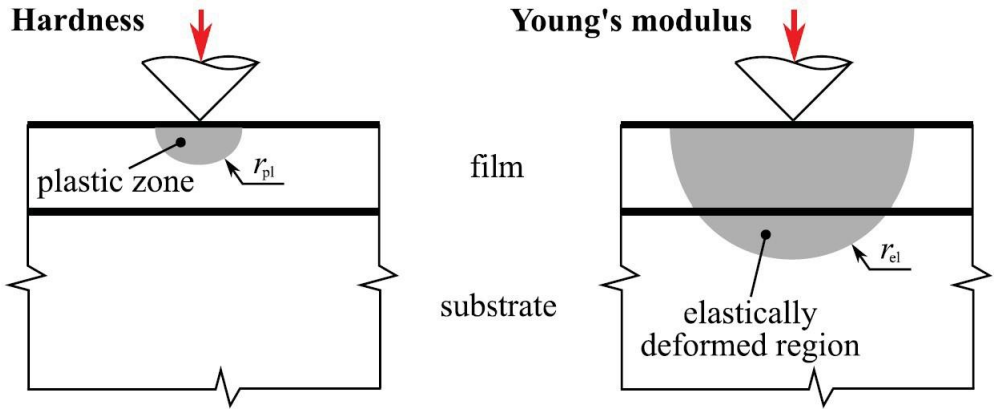

Figure 3: Schematic of the difference between plastic deformation [1]

The results from a nanoindentation process conducted on ZrNTs revealed the tubular layer's elastic modulus to be in the range of {~16-26 GPa}. A representation of the indentation profile is shown in Figure 4, showing the loading-unloading curves of 10 exemplary samples.

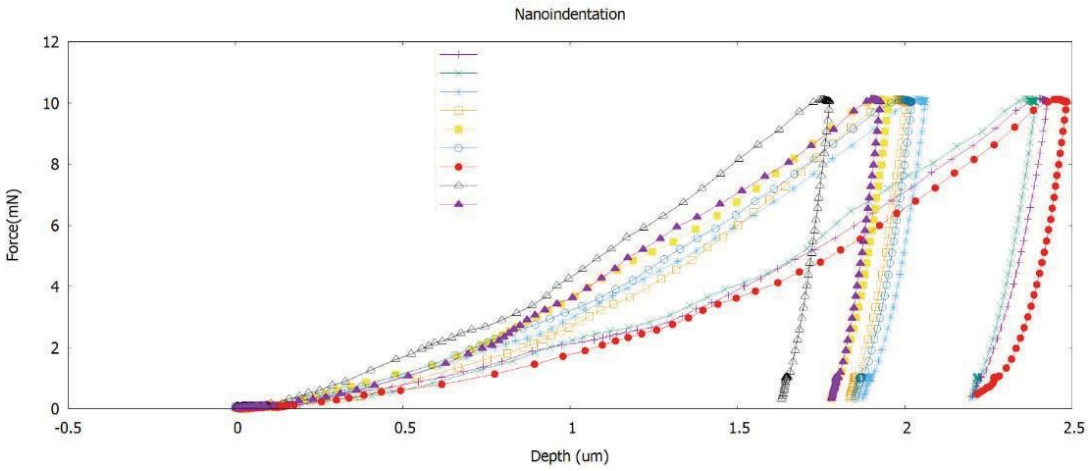

Figure 4: Nanoindentation- stress vs strain curves for loading-unloading on ZrNTs

It is in interesting to note that the difference in creep is very little and overall lower plastic deformation is observed. This result furthers the assessment from the bulk loading results that NTs are more likely to stick to one another and pile up rather than detach as standalone stray tubes. Furthermore, the debris appear to remain intact and well-adhered to the substrate,

such that no deposits or precipitates were found in the aqueous media, i.e., when stored in simulated body fluid {SBF} for a period of 14 days. Analysis of the remaining SBF revealed a constant pH of 7.4 with no discernible changes This result is well aligned with previously reported observations of enhanced hydrolytic stability of the ZrNT films.[2] This is further interesting to note as the use of anodized zirconia overcomes the meta-stability issues demonstrated by stabilized ZrO_2 powders in aqueous environments.[3]

E.g. 3: Bioactivity of ZrNTs

One of the many studies that were previously conducted on titanium {Ti}-alloy based implants, reported on the use of Ti-Zr alloy-based implant. This alloy was able to demonstrate enhanced positive tissue response when compared to pure Ti implants.[4]

This report provided valuable insights because it also suggests the possibility of using Zr metal as implants, especially since ZrO_2 {ceramic powders} have been in-circulation in dentistry and have not been reported for toxic host interactions.[5][6] Zirconia is a bio-inert, refractory grade metal-oxide that shares many of the characteristic properties that make titania implants favorable.[7][8] Zirconia surfaces have also reportedly, demonstrated improved adhesion to molecules, surrounding tissue and lower bacterial adhesion for certain adherent cell types whilst offering attractive aesthetics.[9][10][11] So a natural evolution to this characteristic response urged preliminary investigations on cellular and acellular bioactivity of ZrNT surfaces.

<u>Acellular activity:</u> In order to ascertain, the biomineralization ability of ZrNTs, they were immersed in a setup consisting of inorganic media such as simulated body fluid {SBF} for a period of 14 days under physiological temperature and pH. This setup investigates the acellular response and is reported on showing a favorable ability towards the formation of hydrated calcium phosphate particles on the surfaces. The stoichiometry of the observed calcium {Ca} and phosphate {PO_4^{3-} } particles is not standard to that of hydroxy apatite. It is even important to understand the role of the nanotubular capillaries, they promote an increase in mass transport through these tubes owing

to capillary effects and consequentially an increase in reaction surfaces. This combination ultimately results in the formation of mineral deposits. During the course of this experiment, already after 3 days, the formation of CaP/ $Ca_5\{PO_4\}$ apatite particles could be observed on the nanotubular samples, in contrast to flat-compact oxide samples. Furthermore, the formation of these deposits was more evident from day-7 onwards, where the entire nanotube surface appeared to be covering the plate-like nanotubular array formations as shown in Figure 5, as compared to freshly anodized ZrNT surface.

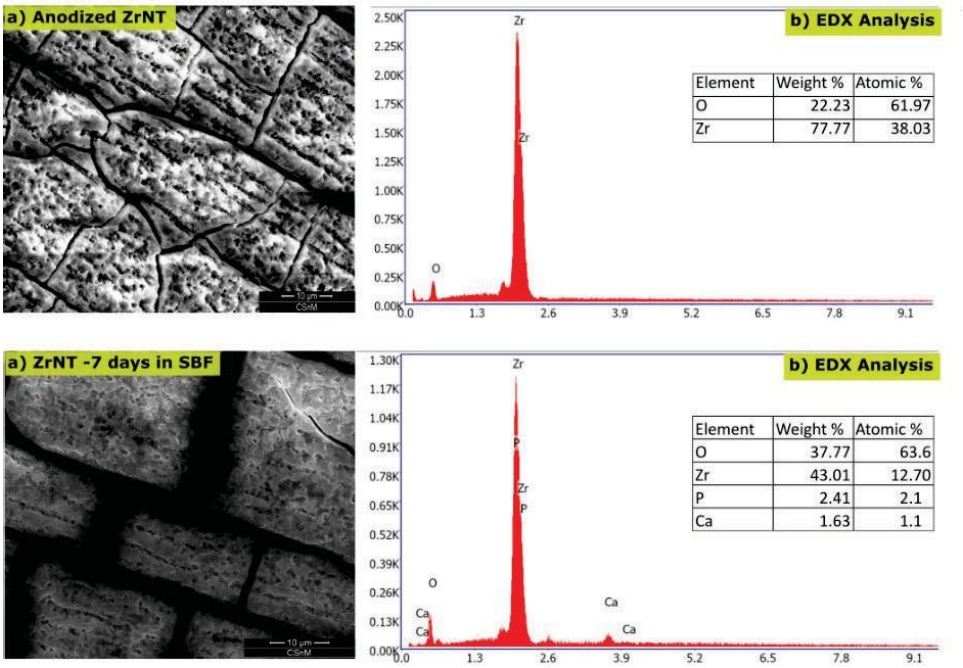

Figure 5: Acellular bioactivity analysis, (Left)) SEM micrograph showing ZrNT surface before and after SBF treatment, (Right) corresponding EDX analysis

Moreover, the surface of the ZrNT sample after the 7-day immersion period appears smoother and the corresponding EDX analysis, revealed the presence of Ca and P with additional traces of Na, Mg and F. By calculating the Ca/P ratio, it is inferred that the apatite formed is deficient in calcium {CaP ~ 0.5 < 1.67} and lower than the stoichiometric ratio of hydroxyapatite crystals {HaP}.[12] The apatite precipitates formed are lower in Ca, and somewhat immature, perhaps due to the shorter incubation period. A lower Ca/P ratio here is indicative of decreased hardness of the apatite crystals and in the current context is better suited to mimic a bio-friendly surface modification than acting as a coating used to enhance mechano-structural robustness. The

deposits were then further characterized by XRD and the corresponding peaks ascribable to apatite formation on nanotubular surfaces are shown in Figure 6.

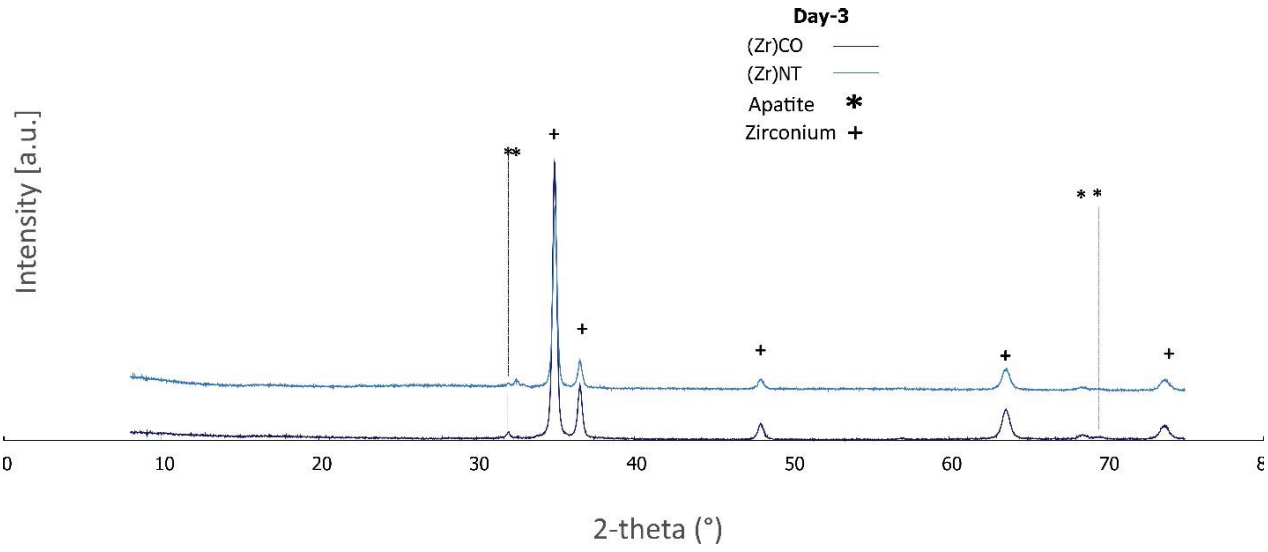

Figure 6: XRD analysis of apatite formation on Zr substrates immersed in SBF

The characteristic peaks match the JSPD standard and the newly formed twin peaks around the Brags angle {31°} corresponding to diffraction planes {211} in all samples immersed in SBF correspond to apatite, around the monoclinic zirconia which is not discernable in the untreated ZrNT sample. Further, the booming peak around {35°} at {202}, is a possible superimposition of the P signal and consequent apatite phase around the adjacent Zr signal. Lastly, peak shift and broadening around the regions represented with dotted lines, are due to defective low crystallinity of the apatite formed. This perfectly, fits the description of the low Ca content in the CaP {<1.67} species formed on the ZrNT surfaces, and are less crystalline than HaP {Ca/P = 1.67}. This is interesting in applications using apatite-layer surface modifications, as an amorphous precipitate would be more readily bioresorbable.[13] The formation of apatite upon immersion in SBF, clearly indicates the bio-active nature of the ZrNT samples.

The morphological variation within the substrates demonstrate bioactivity {mineral forming ability} as function of surface roughness and surfaces hydroxyl groups. The pH of the residual SBF solutions were measured at intervals of 3, 7 and 14-days and all samples had a final pH around 7.45 and no significant variation amongst the samples were found.

Cellular activity: To further analyze the dependence on morphological characteristics, the aforementioned substrates were subjected to in-vitro cell tests.

In vitro cell tests were performed on samples that were sterilized using 70% Ethanol and direct cell test was performed using cell-line NIH-3T3 cells {Biomedical Technology Center of the Medical Faculty MUnster, German}. The cells were grown, harvested and counted as reported previously.[14] A total of 40,000 cells were seeded on each sample and incubated for 2 days. Cell viability was assessed after 48 hours after the seeding by MTT-assay {Sigma Aldrich, Germany} and to investigate cells morphology, staining with rhodamine phalloidin and DAPI {ThermoFisher Scientific, Germany} was performed as previously described.[9]

All samples, were priorly sterilized and it may be noted that, under ethanol immersion and subsequent drying, the amorphous ZrNT films continue to remain well adhered to the substrate. No flaking-off or delamination was observed as a result of rapid drying, as often observed for TiNT films even when annealed.[15] Another factor to consider during alternative sterilization techniques such as UV-disinfection is conductivity, ZrNT based substrates have reportedly shown UV-resistance, which may prevent the destruction of coatings on their substrates. This effect is contrary to what is observed for coatings on TiNT, which often undergo UV-mediated photocatalytic degradation.[2][16][17]

The cell-substrate interaction is represented in Figure 7, {Left}, cells grown directly on the nanotubular surface NT{Zr} and in the absence of nanotexturing, as in the case of flat-compact oxide Zr{CO} after 48 hours of seeding when subjected to a one-way Anova {*$p < 0.05$}. In contrast to acellular activity, the flat-compact oxide surface showed the highest cellular viability of NIH-T3T cells grown on the surface only slightly higher than circular nanotube surfaces as in NT{Zr} samples. This measurement was additionally confirmed by fluorescence microscopy images in Figure 7, {Right} showing a dense and improved network off cells on the Zr{CO} samples. The

NT{Zr} samples although show similar cell viability as the Zr{CO} samples, the fluorescence images do not show as dense of a network formed and a lower amount of cell-spreading was detected. Nevertheless, an average of ~81% and ~66% of the cells survived on Zr{CO} and NT{Zr} surfaces, respectively.

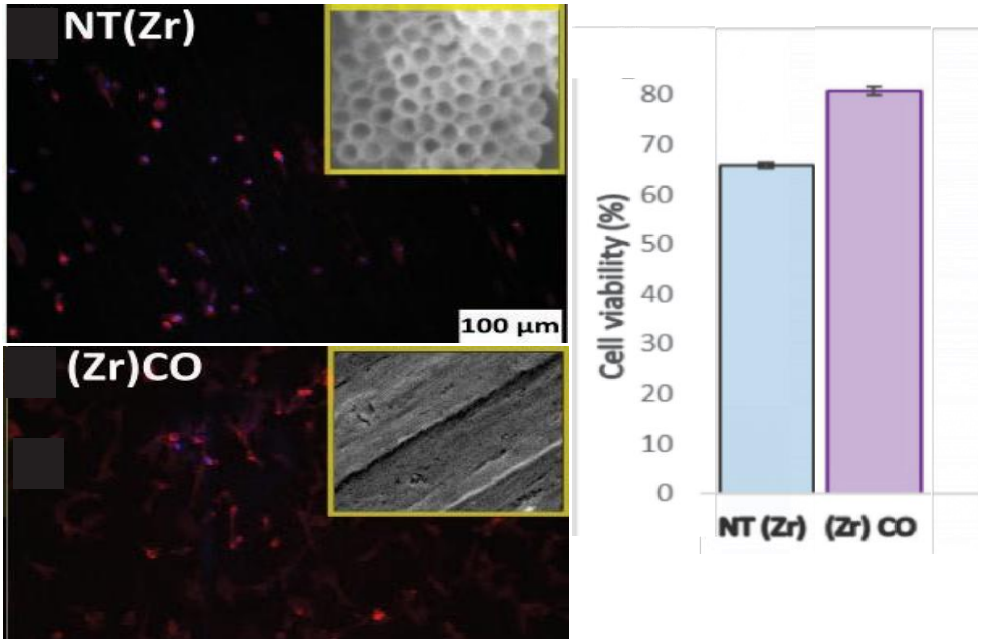

Figure 7: Results of direct Cellular activity: {Left} Viability of NIH-3T3 cells cultured directly in contact with different Zr substrates for 48 hrs. One-way analysis of variance statistical analysis denotes significant differences as compared to ZrCO surface. {*p < 0.5}. {Right} Fluorescence images of actin filaments {red} and cell nuclei {blue} of NIH-T3T cells directly seeded on different Zr substrates {inset}.

In our experiments, the increased surface roughness of ZrNTs, perhaps due to the substrate's resemblance to more nanopit-like configuration may have limited the cell-activity.[18][19] Additionally, it may be noted that the directional tube-growth during anodization may be an influencing factor for cell-spreading. The cells appear to be stretching like spindles on NT{Zr} samples, along the grating axis {background streaking/lines}, it is possible that this nano-topography is influencing contact guidance.[18][20] Further, it would be interesting to choose a different cell-type to analyze full extent of this directional morphology on cellular extension. In conclusion it is inferred that it is possible to tune zirconia nanotubular surfaces to elicit bio-

activity and cellular extension as such surfaces are capable of mimicking the ECM that may positively maximize the cell-pinning points for improved focal adhesion.

E.g. 4: Protein modified ZrNTs

ZrNTs have accessible volumetric space, this is why nanotubes are often considered for applications as drug carriers. Due to this structural modification, ZrNTs are immobilized with protein molecules, an exemplary case would involve the use of bioactive coatings to enhance biomimicking effect and consequentially acceptance. It is expected that sensitive molecules may be shielded inside the tubes, than when they are merely being surface bound. Herein, we perform a repeat of the mechanical experiments as described earlier in this section as represented in Figure 2, on protein modified ZrNT substrates. The different substrates were modified with HRP, and subjected to deformation tests in order to access extent of protein-activity under mechanical stress. Protein activity is often used as a measure of protein intactness, and can easily be investigated by the use of calorimetric assays.

In the experiments performed within the scope of this work, the presence of protein on the ZrO_2 substrates is detected by the characteristic color change in the ABTS assay and change in absorbance value at wavelengths, A= 405nm and A= 747nm, when analyzed using a UV-Vis photo spectrometer, as shown in Figure 8, {a} and was further confirmed using SEM images. In Figure 8 {b and c}, previously clear tube-openings, appear to have a thick-dense coverage over the nanotubes and this is attributed to the presence of a protein-rich layer. The protein-layer appears to cover the entirety of the exposed tube-surface.

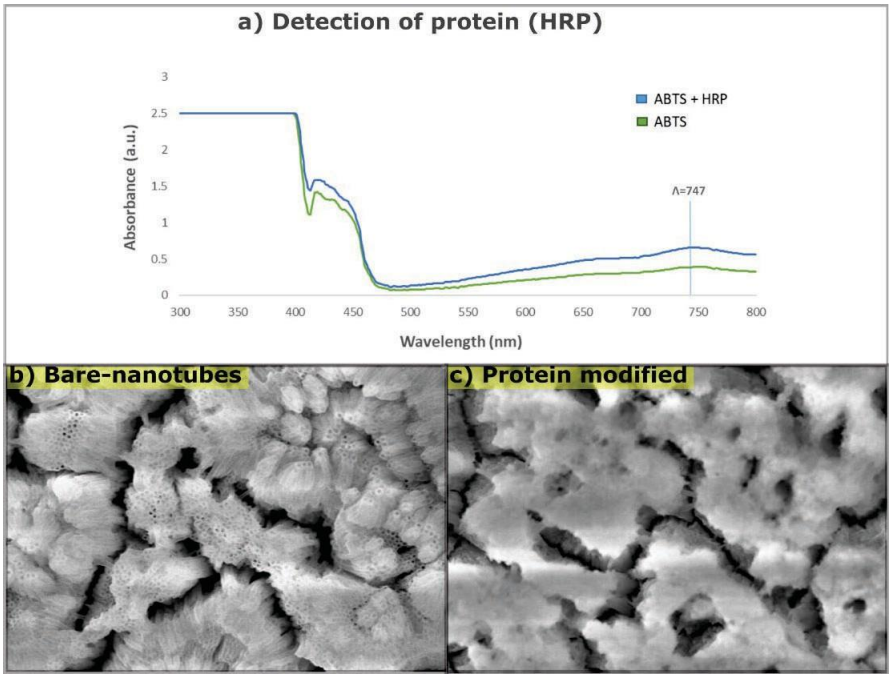

Figure 8: (a) UV-Vis absorbance spectra of HRP, (b and c) ZrNT surface, before and after protein modification

Furthermore, in order to determine whether the protein molecules form stable bonds with the substrate rather than a superficial coverage of loosely bound molecules, ToF-SIMS evaluation was performed. In Figure 9, {a} The Zr-substrate signal is suppressed upon HRP-functionalization with and without the linker molecule, thereby confirming the presence of protein on the surface. Further, the intensity of the signals originating when functionalized with a linker is lower than that of substrate with only protein, highlighting the presence of CDI. The negative spectra contain fewer details on amino-acid but rather show characteristic sulfide bonds, such as {S_2^-, m/z = 63.94 and SO_2^-, m/z = 64.01} in {b} and offer information on the tertiary structure of proteins. CH_4N^+ {m/z 30.05} is a fragment characteristic for several amino acids when measured in positive polarity as seen in {c} and hence was used for the data evaluation for the positive spectra. {d} Depicts another characteristic amino-acid molecular fragment histidine ($C_5H_8N_3^+$, m/z = 110).

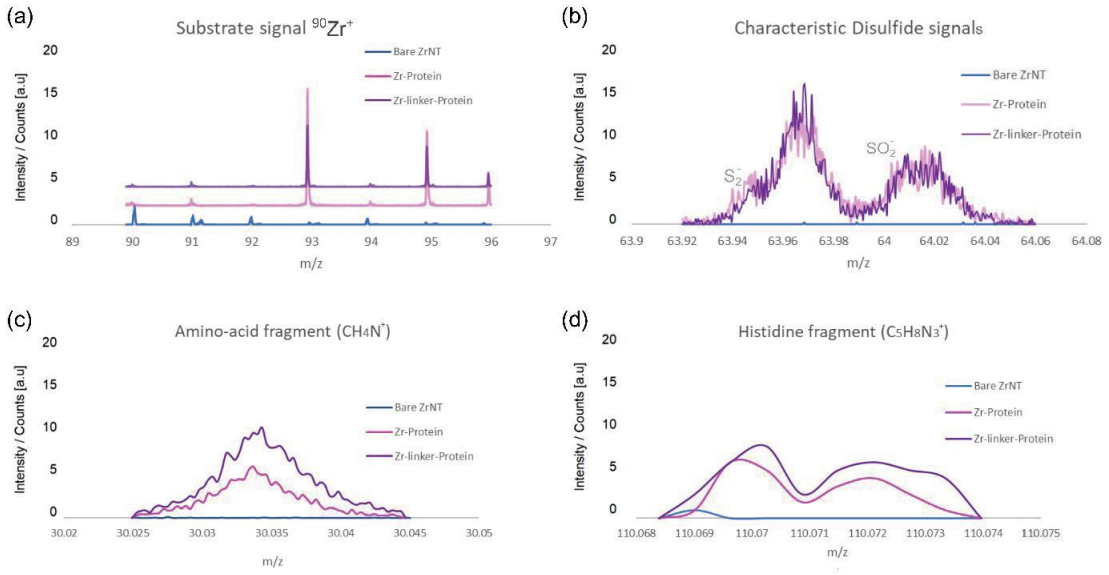

Figure 9: ToF-SIMS spectra on Zr samples subjected to protein (HRP) modification with and without linker (CDI); (a) Zr^+ isotopic pattern, (b) Negative spectra containing distinct disulfide bonds (S_2^-, m/z = 63.94 and SO_2^-, m/z = 64.01), (c)Positive spectra containing characteristic amio-acid fragment (CH_4N^+, m/z = 30.03) and (d) different intensities of amino acid Histidine ($C_5H_8N_3^+$, m/z = 110.07)

Evidently, from Figure 9, all the molecular fragments show larger signal intensity when bound to the ZrNT substrate via a carbonyldiimidazole {CDI} linker molecule and thereby, confirm the successful stable attachment of HRP molecules to the Zr substrate. Additionally, ZrNT substrates of different nominal areas {$A_{nominal}$ = 0.5 cm^2 and $A_{nominal}$ = 1 cm^2} were compared to flat-compact oxide surfaces {ZrCO} subjected to protein modification under pre/post deformation condition. As depicted in Figure 10, it can be confirmed that a change in surface area can increase the interaction volume in the nanotubular substrates. The larger the nominal area, the greater the absorbance value and consequently adsorption of larger protein concentrations. The protein-loading capacity as calculated, averages at ~40 μg/ml in the nanotubular substrate and is reported to show 60% efficiency after a 30-minute incubation period.[24] Proteins are complex molecules that are densely packed to minimize surface energy and are highly sensitive to stressors.[25] They tend to lose their activity as a result of chain unfolding and di-sulfide bond breakage.[26][27]

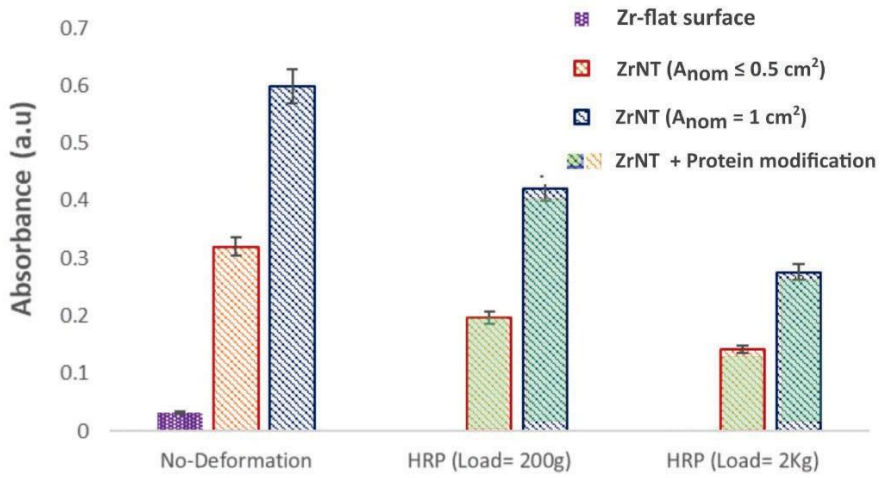

Figure 10: ABTS activity assay (UV-Vis spectroscopy) of HRP coated substrates under the action of different deformation loads and treatment. (left) Protein-modified, no-load, (middle) Protein modified- after deformation under 200g load, and (right) Protein modified- after deformation under 2kg load

This essentially means that under intense mechanical stress, the recorded protein activity of a substrate that was modified with protein prior to deformation, is much lower than of an identical undeformed protein-modified substrate. Deformation elicits a greater loss of viability in response to stress by losing significant 'activity'. When compared with surfaces subjected to no-deformation, nearly 50% of the proteins survived as recorded by the protein-activities, respectively. The overall protein activity in these cases are suggestive that, nanotubular surfaces offer an increased surface area, a larger interaction-volume and protein-modified substrates undergoing deformation can still show significant intactness as the nanotubes manage to protect the proteins that are attached, perhaps deeper into the nanotubes.

E.g. 5: ZrNTs sensors – capable of distinguishing reducing sugars

Reducing sugars are materials that can easily undergo oxidation while reducing another material. The most common examples of reducing sugar are maltose, lactose, gentiobiose, cellobiose, and melibiose while sucrose and trehalose are placed in the examples of non-reducing sugars.

The common dietary monosaccharides such as galactose, glucose and fructose are all reducing sugars. Contrarily, disaccharides are formed from two monosaccharides and can be classified as either reducing or nonreducing sugars. All monosaccharides serve as a reducing agent due to the presence of a free aldehyde or ketone functional groups in its molecular structure.

Sensor assembly: ZrNT sensors are designed by immobilizing an enzyme to the nanotubular surface. The bioactivity of the enzyme is what allows for the detection of the presence of the type of sugar, i.e., in this case, distinguishing a monosaccharide from a disaccharide by means of an aerobic pathway. The enzyme used for this purpose is horseradish peroxidase {HRP}. It catalyzes the oxidation of various organic substrates by hydrogen peroxide.

Usually enzymatic activity can be analyzed via calorimetric processes, in this case HRP metabolic activity can be determined by using ABTS {2,2'-azino-bis{3-ethylbenzothiazoline-6-sulfonic acid}, a chemical compound used in the observation of the specific reaction kinetics of certain enzymes. This compound is chosen because the enzyme facilitates the reaction with hydrogen peroxide, turning it into a dark green, soluble end-product in presence of 'active' enzymatic activity. Enzymatic activity is when the enzyme {HRP} can efficiently metabolize the ABTS molecule to ABTS radical such that the coloured absorbance can be recorded in UV-Vis at 747 nm.

Therefore, for the purpose of using HRP immobilized ZrNT as sensors, the sensor-assembly is placed in an aqueous solution consisting of a monosaccharide {glucose} in the presence of the ABTS reagent and no oxidizing agent i.e. H_2O_2. This is compared to a reference setup, consisting of enzyme immobilized ZrNTs in the presence of ABTS and H_2O_2.

Mechanism: The suggested mechanism for the enzyme {HRP} to convert ABTS molecule to radicle that results in a strong colour change is strongly dependent on the availability of H_2O_2. This H_2O_2 is the oxidizing agent which allows HRP to convert ABTS. It is widely reported that HRP has cysteine residues, these have thiol groups {-SH}.[28] Further reports in literature state that thiol undergo aerobic oxidation to form {-S-S-} bonds. We also know that in the presence of a reducing sugar {-S-S-} bonds can get reduced back to {-SH} thiol while itself getting oxidized and producing the O_2 needed for the initial {-SH} to get re-oxidized to {-S-S-}, thereby sustaining a self-sustaining redox reaction or auto-catalytic reaction cycle.[29][30]

A schematic representation of the discernable reaction mechanism is depicted in Figure 11. It shows the lack of any transformation observed for the ZrCO substrate.

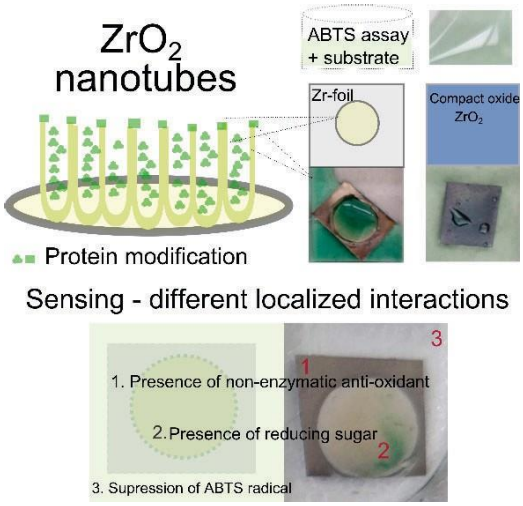

Figure 11: HRP modified ZrNTs as glucose sensors

The change in absorbance and physical inspection of the sample's surface shows dark green accumulation on the anodized part, this occurs only if the enzyme metabolizes. The same is seen for the sensor in the presence of the glucose solution without any H_2O_2 and thus, indirectly confirms the presence of a reducing sugar.

Closing arguments

The different scenarios explained within this outlook section, describes various approaches to facilitate alternative applications for ZrNTs and modified ZrNTs. The primary research in this dissertation thoroughly elucidates the fundamental concepts of developing robust ZrNTs and the translation of such ZrNTs for direct applications, while the outlook section sheds lights on possible avenues for further research and development. Herein, the versatility of anodic oxide nanostructures as standalone coatings or subsequently modified coatings show a real potential for ongoing and continued research.

Experimental of experiments described in section 4.5

Protein adsorption and surface treatment: Horse-radish-peroxidase (HRP) (Sigma-Aldrich) was immobilized onto the ZrO_2 substrates via CDI (Sigma-Aldrich), a bioactive linker molecule. The linker was coupled to the oxide surface by immersion in a 25 mmol/l solution in $CHCl_3$, (Sigma-Aldrich, purity >99.8%) at room temperature (RT, 24 °C) for 24 h. Samples were rinsed with chloroform and dried under a nitrogen stream. The CDI-modified surfaces were immersed in a phosphate-buffered saline (PBS) solution {pH 6.4} with a protein concentration of 100 µg/ml for 24 h at 4°C according to Killian. et. al.[27] A separate set of substrate-surface was treated by immersion in 15 ml of concentrated H_3PO_4 (Sigma-Aldrich, purity >99.9%) for 10 min and then air-dried.

Activity Assay: The protein-coated samples were placed in a multi-well plate containing 0.75 ml PBS solution (pH 6.4), 0.3% H_2O_2, and 0.05 mol/l ABTS (Fluka). H_2O_2 was added as a biological substrate for the enzyme (HRP) and consequently oxidizes the ABTS molecule, detectable by the intense green color of the stable ABTS radical, having corresponding absorption maxima at A= 405 nm and A = 747 nm.[27] The intensity of the absorption of the differently treated samples was measured at A = 747 nm on a UV-Vis spectrometer{ Lambda Bio XLS} after 30 min incubation time at room temperature covered from direct illumination. Absorption values were referenced to the absorption of the pure ABTS solution. Reference samples of pure ZrO_2 did not show any activity in the ABTS assays.

Bioactivity analysis*:* (a) Acellular bioactivity was evaluated by immersing the samples in SBF, according to the standard protocol of Kokubo et al., as reported elsewhere.[9] After 3, 7, and 14 days, the samples were removed from the dissolution medium, and the pH of the remaining

medium was recorded after each time interval, (b) In vitro cell tests were performed on samples that were sterilized using 70% Ethanol and direct cell test was performed using cell-line NIH-3T3 cells (Biomedical Technology Center of the Medical Faculty Münster, German). The cells were grown, harvested, and counted as reported previously. A total of 40,000 cells were seeded on each sample and incubated for 2 days. Cell viability was assessed 48 hours after the seeding by MTT assay (Sigma Aldrich, Germany) and to investigate cell morphology, staining with rhodamine-phalloidin and DAPI (ThermoFisher Scientific, Germany) was performed as previously described within the text.

Acknowledgement- Dipl.-Biol Sabine-Wenderhold-Reeb, Physikalische Chemie I, Universitat Siegen.

Nanoindentation: Nanoindentation using a proprietary device capable of nanoindentation at Thomas Magnete GmbH, with a continuous stiffness measurement capability. The nanoindentation experiments were performed using a Berkovich tip with a radius of 20 nm and a force of 10 mN. The indentation was performed in a slow hardness mode and once the maximum prescribed depth {= 2μm) was reached, loading was stopped and the load was held constant for 10 s. The source of variations gathered from five test sites is within the limit for each sample. Indentation experiments were conducted for ten samples per processing conditions.

Acknowledgement- Ms. Nayeli Carrion Saldana, Laboratory Engineer Materials, SU Quality, Thomas Magnete GmbH.

References for section 4.5

[1] S. Zak, C.O.W. Trost, P. Kreiml, M.J. Cordill, Accurate measurement of thin film mechanical properties using nanoindentation, J. Mater. Res. 37 {2022}. https://doi.org/10.1557/s43578-022-00541-1.

[2] S.N.V. Raghu, K. Chuluunbandi, M.S. Killian, Zirconia nanotube coatings - UV-resistant superhydrophobic surfaces, Surfaces and Interfaces. 26 {2021}. https://doi.org/10.1016/J.SURFIN.2021.101357.

[3] H.J. Wenz, J. Bartsch, S. Wolfart, M. Kern, Osseointegration and clinical success of zirconia dental implants: a systematic review., Int. J. Prosthodont. 21 {2008}. http://www.ncbi.nlm.nih.gov/pubmed/18350943.

[4] Y. Ikarashi, K. Toyoda, E. Kobayashi, H. Doi, T. Yoneyama, H. Hamanaka, T. Tsuchiya, Improved biocompatibility of titanium-zirconium {Ti-Zr} alloy: Tssue reaction and sensitization to Ti-Zr alloy compared with pure Ti and Zr in rat implantation study, Mater. Trans. {2005}. https://doi.org/10.2320/matertrans.46.2260.

[5] J.D. Langhoff, K. Voelter, D. Scharnweber, M. Schnabelrauch, F. Schlottig, T. Hefti, K. Kalchofner, K. Nuss, B. von Rechenberg, Comparison of chemically and pharmaceutically modified titanium and zirconia implant surfaces in dentistry: a study in sheep, Int. J. Oral Maxillofac. Surg. 37 {2008}. https://doi.org/10.1016/j.ijom.2008.09.008.

[6] C.J. Whitters, R. Strang, D. Brown, R.L. Clarke, R. V. Curtis, P. V. Hatton, A.J. Ireland, C.H. Lloyd, J.F. McCabe, J.W. Nicholson, S.N. Scrimgeour, J.C. Setcos, M. Sherriff, R. Van Noort, B.C. Watts, D. Wood, Dental materials: 1997 literature review, J. Dent. {1999}. https://doi.org/10.1016/S0300-5712{99}00007-X.

[7] R. Depprich, H. Zipprich, M. Ommerborn, C. Naujoks, H.-P. Wiesmann, S. Kiattavorncharoen, H.-C. Lauer, U. Meyer, N.R. KUbler, J. Handschel, Osseointegration of zirconia implants compared with titanium: an in vivo study, Heaf Face Med. {2008}.

https://doi.org/10.1186/1746-160X-4-30.

[8] M. Andreiotelli, H.J. Wenz, R.J. Kohal, Are ceramic implants a viable alternative to titanium implants? A systematic literature review, Clin. Oral Implants Res. {2009}. https://doi.org/10.1111/j.1600-0501.2009.01785.x.

[9] K. Schuhladen, S.N.V. Raghu, L. Liverani, Z. Nescakova, A.R. Boccaccini, Production of a novel poly{E-caprolactone}-methylcellulose electrospun wound dressing by incorporating bioactive glass and Manuka honey, J. Biomed. Mater. Res. - Part B Appl. Biomater. 109 {2021}. https://doi.org/10.1002/jbm.b.34690.

[10] L. Rimondini, L. Cerroni, A. Carrassi, P. Torricelli, Bacterial colonization of zirconia ceramic surfaces: an in vitro and in vivo study., Int. J. Oral Maxillofac. Implants. 17 {2002}. http://www.ncbi.nlm.nih.gov/pubmed/12507238.

[11] A. Scarano, M. Piattelli, S. Caputi, G.A. Favero, A. Piattelli, Bacterial Adhesion on Commercially Pure Titanium and Zirconium Oxide Disks: An In Vivo Human Study, J. Periodontol. {2004}. https://doi.org/10.1902/jop.2004.75.2.292.

[12] R.H. Doremus, Review Bioceramics, J. Mater. Sci. 27 {1992}. https://link.springer.com/content/pdf/10.1007%2FBF00543915.pdf.

[13] D. Knaack, M.E.P. Goad, M. Aiolova, C. Rey, A. Tofighi, P. Chakravarthy, D.D. Lee, Resorbable calcium phosphate bone substitute, J. Biomed. Mater. Res. 43 {1998}. https://doi.org/10.1002/{SICI}1097-4636{199824}43:4<399::AID-JBM7>3.0.CO;2-J.

[14] J.L. Jainchill, S.A. Aaronson, G.J. Todaro, Murine Sarcoma and Leukemia Viruses: Assay Using Clonal Lines of Contact-Inhibited Mouse Cells, J. Virol. 4 {1969}. https://doi.org/10.1128/jvi.4.5.549-553.1969.

[15] K.M. Kummer, E.N. Taylor, N.G. Durmas, K.M. Tarquinio, B. Ercan, T.J. Webster, Effects of different sterilization techniques and varying anodized TiO_2 nanotube dimensions on bacteria growth, J. Biomed. Mater. Res. - Part B Appl. Biomater. {2013}. https://doi.org/10.1002/jbm.b.32870.

[16] L. Zhao, S. Mei, W. Wang, P.K. Chu, Z. Wu, Y. Zhang, The role of sterilization in the cytocompatibility of titania nanotubes, Biomaterials. {2010}. https://doi.org/10.1016/j.biomaterials.2009.11.103.

[17] W. Att, N. Hori, F. Iwasa, M. Yamada, T. Ueno, T. Ogawa, The effect of UV-photofunctionalization on the time-related bioactivity of titanium and chromium-cobalt alloys, Biomaterials. {2009}. https://doi.org/10.1016/j.biomaterials.2009.04.048.

[18] A.I. Teixeira, G.A. Abrams, P.J. Bertics, C.J. Murphy, P.F. Nealey, Epithelial contact guidance on well-defined micro- and nanostructured substrates., J. Cell Sci. 116 {2003}. https://doi.org/10.1242/jcs.00383.

[19] C.J. Bettinger, R. Langer, J.T. Borenstein, Engineering substrate topography at the Micro- and nanoscale to control cell function, Angew. Chemie - Int. Ed. 48 {2009}. https://doi.org/10.1002/anie.200805179.

[20] A.T. Nguyen, S.R. Sathe, E.K.F. Yim, From nano to micro: topographical scale and its impact on cell adhesion, morphology and contact guidance, J. Phys. Condens. Matter. 28 {2016}. https://doi.org/10.1088/0953-8984/28/18/183001.

[21] M. Henry, P. Bertrand, Surface composition of insulin and albumin adsorbed on polymer substrates as revealed by multivariate analysis of ToF-SIMS data, Surf. Interface Anal. 41 {2009}. https://doi.org/10.1002/sia.2993.

[22] D.S. Mantust, B.D. Ratner, B.A. Carlson, J.F. Moulder, Static Secondary Ion Mass Spectrometry of Adsorbed Proteins, Anal. Chem. 65 {1993}. https://doi.org/10.1021/ac00058a021.

[23] M.S. Wagner, D.G. Castner, Characterization of Adsorbed Protein Films by Time-of-Flight Secondary Ion Mass Spectrometry with Principal Component Analysis, Langmuir. 17 {2001}. https://doi.org/10.1021/la001209t.

[24] K.C. Popat, M. Eltgroth, T.J. LaTempa, C.A. Grimes, T.A. Desai, Titania nanotubes: A novel platform for drug-eluting coatings for medical implants?, Small. 3 {2007}.

https://doi.org/10.1002/smll.200700412.

[25] E.J. Wood, Harper's biochemistry 24th edition, {1996}. https://doi.org/10.1016/s0307-4412{97}80776-5.

[26] A. Maelicke, Biochemistry. Von C. K. Mathews und K. E. van Holde. The Benjamin/Cummings Publishing Co. Inc., Redwood City, CA {USA}, ISBN 0-8053-5015-2, Angew. Chemie. 104 {1992}. https://doi.org/10.1002/ange.19921041041.

[27] M.S. Killian, P. Schmuki, Influence of bioactive linker molecules on protein adsorption, Surf. Interface Anal. 46 {2014}. https://doi.org/10.1002/sia.5497.

[28] E. Gantumur, S. Sakai, M. Nakahata, M. Taya, Horseradish peroxidase-catalyzed hydrogelation consuming enzyme-produced hydrogen peroxide in the presence of reducing sugars, Soft Matter. 15 {2019}. https://doi.org/10.1039/C8SM01839A.

[29] E. Gantumur, S. Sakai, M. Nakahata, M. Taya, Cytocompatible Enzymatic Hydrogelation Mediated by Glucose and Cysteine Residues, ACS Macro Lett. 6 {2017}. https://doi.org/10.1021/acsmacrolett.7b00122.

[30] W.F. Osswald, W. SchUtz, E.F. Elstner, Cysteine and Crocin Oxidation Catalyzed by Horseradish Peroxidase, Free Radic. Res. Commun. 5 {1989}. https://doi.org/10.3109/10715768909074709.

5. CONCLUSION

This thesis primarily discusses the fabrication of zirconia nanotubular structures using electrochemical anodization, their subsequent surface modifications, and their applications as functional coatings.

- ***Role of material chemistry***

The synthesis of zirconia {ZrO_2} nanotubes involved a controlled dissolution of thick oxide films formed on the surface of zirconium metal in a fluoride-containing organic electrolyte during electrochemical passivation. The highlight of this anodization protocol remains the one-pot synthesis in ambient conditions, which without the need for any pre-etching in hazardous mineral acids, like hydrofluoric acid, successfully results in ordered homogeneous nanotubular arrays. A change in the anodization parameters like variation in the operating voltage and duration of an event can result in morphological variations in the subsequently formed oxide structures. To a greater extent, this dissertation focused on the synthesis of nanotubular zirconia. The synthesized ZrNTs are metal-oxides and this nanostructured zirconia is intrinsically different from the starting material zirconium, a metal. The difference in chemical composition and structure strongly influences the surface characteristics of these materials. Most metals show hydrophilic behavior when in contact with wetting agents due to the presence of a thin oxide layer, also known as the native oxide film. This layer consists of surface hydroxyl groups in ambient conditions, acting as condensation reaction sites.[54] A similar response was observed for metal-oxide surfaces synthesized via anodic oxidation, resulting in the formation of a more uniform and thicker oxide layer. In addition to this, the nanotubes are essentially capillaries and have an accessible volumetric capacity. Due to this structural property, nanotubes promote fluid imbibition, and consequently, liquids penetrate the capillaries and demonstrate a superior and ideal wetting response.[57] Another factor influencing wetting is the presence of surface hydroxyl groups. Hydroxyl groups hold a strong relevance in light of surface modifications using organic molecules.

Based on the composition of the organic molecule in question, the interaction chemistry with the underlying substrate is affected. In the case of ZrNTs modified via octadecylphosphonic acid {OPA SAMs, the resulting hydrophobic modification is amplified due to the following aspects: the porous metal-oxide structure leading to the Cassie-Baxter effect, the hydrophilic surface chemistry offering many reaction sites for condensation reactions. Since, zirconium metal intrinsically has a large number of Lewis acid/base elemental reaction sites readily available for bond formation, the overall coverage and stability of any subsequent coating on ZrNTs is influenced. As a result, Zr shows superior stability of the modifications in comparison to the other valve metals investigated. This behavior is especially significant for the performance of OPA-modified ZrNTs, as investigated under outdoor/ambient light exposure, simulated UV exposure, and during storage in water. It is noteworthy to mention the intrinsic insulating behavior of Zr, which helps to preserve the monolayer coating and promotes the stability of the SAM for prolonged periods. The longevity of these SAMs is facilitated in the absence of any catalytic degradation of the organic molecules, as observed for TiO_2. Modified ZrNTs surfaces continued to demonstrate prolonged hydrophobicity when used as coatings, also for outdoor applications.

- ***Nanostructure morphology dependent functionalization extent***

Furthermore, the superhydrophobic response was additionally investigated concerning the dependency on nanotubular morphology by variation in nanotube diameters. Phosphonic acid aliphatic molecules demonstrate higher adsorption to both valve metal oxides, namely titania and zirconia, when compared to other anchoring groups such as silanes, stearic acid, and amines. When modified with octadecylphosphonic acid {OPA} SAMs, both titania nanotubes {TiNTs} and zirconia nanotubes {ZrNTs} exhibited hydrophobic behaviour, i.e., water contact angle {WCA} > 90°. However, the hydrophobicity for TiNTs was dependent on the nanotube diameter, such that, the larger the tube diameter the greater the tendency towards superhydrophobic behaviour, i.e., {WCA} > 140°. Interestingly, a divergence to the results of TiNTs is observed in functionalized ZrNTs, such that superhydrophobicity is achieved even at smaller nanotube diameters.

Since, WCA analysis was at the physical limit of measurement with respect to measured superhydrophobicity, it was hypothesized that ZrNTs were better coated. This implied OPA-SAMs demonstrated preferential adsorption kinetics, and a higher coverage of organic molecules on ZrNTs. Surface modifications of nanotubes were pivotal to this work, highlighting the influence of physical surface modifications, as nanostructuring- on the extent of possible changes to surface behavior. This observation was supplemented by investigating the role of the ZrNT oxide layer thickness, confirming that superhydrophobicity is independent of both; tube diameter and tube length. This independent relationship to tube length invariably reinforces the underlying mechanisms of using organic molecule modification in the form of SAMs, as truly being a surface phenomenon.

- ***Multi-depth modification for drug release applications***

Within this thesis, a clear description of the role of the type of chemical modification technique was formulated in order to develop multi-molecule and multi-depth modification techniques. These techniques were conceptualized based on prevailing diffusion kinetics when functionalized using either bulk-immersion {BI} or micro-contact printing {µCP} technique. The effect of each technique used to render a chemical modification to the nanotubes was analyzed with the help of depth profiling using ToF-SIMS characterization. The semi-quantitative ToF-SIMS analysis provided information on the presence of the molecules inside the nanotubes by variation in characteristic signal intensities as a function of sputter depth. A clear distinction on the penetration depth of the hydrophobic molecules when modified using either method independently was observed. This information highlights the utility of using such physically stamped hydrophobic layers via µCP as capping agents. The µCP technique deposits molecules predominantly onto the top-most layers of the nanotubular openings, were proven to seal the mouth, i.e., the tube tops, such that potentially drug-filled capillaries can be secured-shut for conditional release. These capped capillaries may also be capable of selective drug elution due to the tunable degradation response of a particular type of nanotube capping.

Selective degradation of the capping agent is achievable under triggers such as; type of solvent, pH of the media, temperature, to name a few. Herein, ZrNTs were filled with dye molecules using the BI technique, followed by the deposition of OPA SAM onto nanotube openings via the μCP technique to perform a capping function. The assembly was subjected to wetting in different and appropriate media to promote the localized degradation of the capping, simulating the mechanism of a triggered release from an eluting surface. Thus, the design, deposition, and probing of an active surface capable of volumetric elution were successfully elucidated within this work.

- ***Transferable nanotube coatings***

Considering applications in the biomedical field, biomaterials are often metals, metal-oxides, or compacted ceramics. Arguably in dentistry and orthopedics, it would be beneficial to design nano-surfaced bulk materials. A significant shift towards ceramics in implantation may provide the necessary starting point for hybrid functionalities. In particular, rendering such ceramics with micro/nanoscale functionality may be highly advantageous for developing material systems capable of eliciting varied therapeutic benefits to promote biological acceptance and integration while improving overall and patient compliance. In light of this, we exploit the flexible operational parameters of electrochemical anodization that make it possible to synthesize anodic layers that can readily detach from the underlying metal substrate. Herein, the ZrNT layers are weakened at the interface of the metal/metal-oxide by using particular voltage pulses that initiate the generation of finer pores under the already formed oxide array. This layer was then attached to a strip of office-tape to make way for a facile peel-off from the metal foil. The ZrNTs sticking on the adhesive were seamlessly released by using a favorable wetting solvent, acetone. Thus, the ZrNT layer was transferred from the tape in an acetone bath and directly deposited onto a corresponding preformed ceramic surface, successfully rendering the bulk material with nanostructured facets.

The goal was to render surfaces with ZrNT layers and investigate the transferability and unmediated attachment of ZrNTs onto bulk ceramics. In this work, the fabrication of such a hybrid material was made possible in ambient conditions without using any intermediate fabrication steps. Furthermore, this assembly was evaluated both qualitatively and quantitatively concerning the intrinsic adhesion between the bulk ceramic and the deposited ZrNT. A noteworthy mention is the mechanical robustness of the ZrNT layer itself, which remained intact during the transfer process and post-deposition. The deposited layer remains adhered to the underlying bulk surface with adequate friction to prevent unintentional removal. Furthermore, no sliding-off of the newly transferred layer during; handling, ultrasonic cleaning, and storing were detected. This stability was perhaps due to the inherent chemical similarity between the bulk and the nanolayer, resulting in a 'stick-slip' motion that may inevitably prevent the sliding-off of the ZrNT layer. Consequently, when subjected to mechanical abrasion, the interfacial friction resulted in a coefficient of friction in the range of ideal non-slip interactions, thereby confirming our original hypothesis on the mechanism of intrinsic adhesion of the ZrNT layer to the ceramic.

In conclusion, the work performed within this dissertation reflects on several fundamental reactions utilized towards the design of hybrid materials for a varied set of potential applications. Protocols to synthesize smaller nanotube geometries {diameter ⍰15 nm} using a one-pot synthesis and evaluating SAM-modified ZrNTs for non-stick/wetting or non-catalytic self-cleaning applications as a function of surface superhydrophobicity were successfully proposed. Experiments described in this manuscript were primarily performed to ascertain the merit of such modified oxide nanostructures made from Zr. The evaluation of the performance of such modified ZrNTs and the successfully modified ceramic ZrNT coatings were comparable to previously reported metal-oxide NTs of Ti, Fe, Mg, Nb, etc., to name a few.[84,91,166,167,168] Especially, the OPA-modified ZrNTs were at par with commercially employed superhydrophobic coatings such as Polytetrafluoroethylene {PTFE} and perfluorodecylphosphonic acid {PFDPA}. In addition to outstanding stability, OPA is also

biocompatible and applied as capping agents for drug-filled ZrNTs. In light of biomedical applications, functionalization strategies used on ZrNTs with multi-molecule/depth modifications were successfully exhibited. These assemblies advance the principle of ZrNT layers as coatings capable of behaving as drug-eluting surfaces that may undergo selective release, especially when coupled with an appropriate capping agent. Lastly, a strategy to externally deposit such ZrNT layers on preformed bulk ceramics was made feasible via a facile solvent-mediated transfer strategy. This technique recognizes an alternate way to render nanostructure morphology to many kinds of bulk surfaces without additional manufacturing steps.

References

(1) Kumar Teli, M.; Mutalik, S.; Rajanikant, G. K. Nanotechnology and Nanomedicine: Going Small Means Aiming Big. *Curr. Pharm. Des.* **2010**, *16* (16), 1882–1892. https://doi.org/10.2174/138161210791208992.

(2) Ling Zhang. Applications, Challenges and Development of Nanomaterials and Nanotechnology. *J.Chem.Soc.Pak* **2020**, *42* (5).

(3) Iqbal, P.; Preece, J. A.; Mendes, P. M. Nanotechnology: The "Top-Down" and "Bottom-Up" Approaches. In *Supramolecular Chemistry*; John Wiley & Sons, Ltd: Chichester, UK, 2012. https://doi.org/10.1002/9780470661345.smc195.

(4) Iafisco, M.; Zheng, K.; Yang, F.; Minardi, S.; Lyons, J. G.; Plantz, M. A.; Hsu, W. K.; Hsu, E. L. Nanostructured Biomaterials for Bone Regeneration. **2020**. https://doi.org/10.3389/fbioe.2020.00922.

(5) Mann, S. Life as a Nanoscale Phenomenon. *Angew. Chemie Int. Ed.* **2008**, *47* (29), 5306–5320. https://doi.org/10.1002/anie.200705538.

(6) Chen, L.; Liu, Z.; Guo, Z.; Huang, X.-J. Regulation of Intrinsic Physicochemical Properties of Metal Oxide Nanomaterials for Energy Conversion and Environmental Detection Applications. *J. Mater. Chem. A* **2020**, *8* (34), 17326–17359. https://doi.org/10.1039/D0TA05539E.

(7) Ameta, S. C.; Ameta, R. *The Science of Nanomaterials*; Apple Academic Press: New York, 2022. https://doi.org/10.1201/9781003283126.

(8) Prakash Sharma, V.; Sharma, U.; Chattopadhyay, M.; Shukla, V. N. Advance Applications of Nanomaterials: A Review. *Mater. Today Proc.* **2018**, *5* (2), 6376–6380. https://doi.org/10.1016/j.matpr.2017.12.248.

(9) Garnett, E.; Mai, L.; Yang, P. Introduction: 1D Nanomaterials/Nanowires. *Chem. Rev.* **2019**, *119* (15), 8955–8957. https://doi.org/10.1021/acs.chemrev.9b00423.

(10) Zhai, T.; Fang, X.; Liao, M.; Xu, X.; Zeng, H.; Yoshio, B.; Golberg, D. A Comprehensive Review of One-Dimensional Metal-Oxide Nanostructure Photodetectors. *Sensors* **2009**, *9* (8), 6504–6529. https://doi.org/10.3390/s90806504.

(11) Sanchez-Moreno, P.; Ortega-Vinuesa, J. L.; Peula-Garcia, J. M.; Marchal, J. A.; Boulaiz, H. Smart Drug-Delivery Systems for Cancer Nanotherapy. *Curr. Drug Targets* **2018**, *19* (4), 339–359. https://doi.org/10.2174/1389450117666160527142544.

(12) Rostami, M.; Sobhani Nasab, A.; Fasihi-Ramandi, M.; Badiei, A.; Rahimi-Nasrabadi, M.; Ahmadi, F. The $ZnFe_2O_4$ @mZnO–N/RGO Nano-Composite as a Carrier and an Intelligent Releaser Drug with Dual PH- and Ultrasound-Triggered Control. *New J. Chem.* **2021**, *45* (9), 4280–4291. https://doi.org/10.1039/D0NJ04758A.

(13) Biswas, S.; Bellare, J. Bioactivity, Biocompatibility, and Toxicity of Metal Oxides. In *Metal Oxides for Biomedical and Biosensor Applications, edited by Kunal Mondal*; Elsevier, 2022; pp 3–33. https://doi.org/10.1016/B978-0-12-823033-6.00001-6.

(14) Singer, A.; Markoutsa, E.; Limayem, A.; Mohapatra, S.; Mohapatra, S. S. Nanobiotechnology

Medical Applications: Overcoming Challenges through Innovation. *EuroBiotech J.* **2018**, *2* (3), 146–160. https://doi.org/10.2478/ebtj-2018-0019.

(15) Junker, R.; Dimakis, A.; Thoneick, M.; Jansen, J. A. Effects of Implant Surface Coatings and Composition on Bone Integration: A Systematic Review. *Clinical Oral Implants Research*. 2009. https://doi.org/10.1111/j.1600-0501.2009.01777.x.

(16) Bruschi, M.; Steinmüller-Nethl, D.; Goriwoda, W.; Rasse, M. Composition and Modifications of Dental Implant Surfaces. *J. Oral Implant.* **2015**. https://doi.org/10.1155/2015/527426.

(17) Masuda, H.; Fukuda, K. Ordered Metal Nanohole Arrays Made by a Two-Step Replication of Honeycomb Structures of Anodic Alumina. *Science (80).* **1995**, *268* (5216), 1466–1468. https://doi.org/10.1126/science.268.5216.1466.

(18) Wang, M.; Liu, Y.; Yang, H. A Unified Thermodynamic Theory for the Formation of Anodized Metal Oxide Structures. *Electrochim. Acta* **2012**, *62*, 424–432. https://doi.org/10.1016/j.electacta.2011.12.054.

(19) Sample, C.; Golovin, A. A. Formation of Porous Metal Oxides in the Anodization Process. *Phys. Rev. E* **2006**, *74* (4), 041606. https://doi.org/10.1103/PhysRevE.74.041606.

(20) Losic, D.; Simovic, S. Self-Ordered Nanopore and Nanotube Platforms for Drug Delivery Applications. *Expert Opinion on Drug Delivery*. **2009**. https://doi.org/10.1517/17425240903300857.

(21) Ikarashi, Y.; Toyoda, K.; Kobayashi, E.; Doi, H.; Yoneyama, T.; Hamanaka, H.; Tsuchiya, T. Improved Biocompatibility of Titanium-Zirconium (Ti-Zr) Alloy: Tssue Reaction and Sensitization to Ti-Zr Alloy Compared with Pure Ti and Zr in Rat Implantation Study. *Mater. Trans.* **2005**. https://doi.org/10.2320/matertrans.46.2260.

(22) Farsinezhad, S.; Waghmare, P. R.; Wiltshire, B. D.; Sharma, H.; Amiri, S.; Mitra, S. K.; Shankar, K. Amphiphobic Surfaces from Functionalized TiO_2 Nanotube Arrays. *RSC Adv.* **2014**, *4* (63), 33587–33598. https://doi.org/10.1039/c4ra06402j.

(23) Zhao, H.; Jacob, C.; Stone, H. A.; Hart, A. J. Liquid Imbibition in Ceramic-Coated Carbon Nanotube Films. *Langmuir* **2016**, *32* (48), 12686–12692. https://doi.org/10.1021/acs.langmuir.6b03661.

(24) Delamarche, E.; Donzel, C.; Kamounah, F. S.; Wolf, H.; Geissler, M.; Stutz, R.; Schmidt-Winkel, P.; Michel, B.; Mathieu, H. J.; Schaumburg, K. Microcontact Printing Using Poly(Dimethylsiloxane) Stamps Hydrophilized by Poly(Ethylene Oxide) Silanes. *Langmuir* **2003**, *19* (21), 8749–8758. https://doi.org/10.1021/la034370n.

(25) Maccauro, G.; Rossi, P.; Raffaelli, L.; Francesco, P. Alumina and Zirconia Ceramic for Orthopaedic and Dental Devices. *Biomater. Appl. Nanomedicine* **2011**, No. July. https://doi.org/10.5772/23917.

(26) Zhang, Y.; Gulati, K.; Li, Z.; Di, P.; Liu, Y. Dental Implant Nano-Engineering: Advances, Limitations and Future Directions. *Nanomaterials* **2021**, *11* (10), 2489. https://doi.org/10.3390/nano11102489.

(27) Cohen, D. D.; Bird, R.; Dytlewski, N.; Siegele, R. Ion Beams for Material Analysis. In *Encyclopedia of Physical Science and Technology*; Elsevier, 2003; pp 55–63. https://doi.org/10.1016/B0-12-227410-5/00351-3.

(28) Swab, J. J. Role of Oxide Additives in Stabilizing Zirconia for Coating Applications. **2001**.

(29) Kohorst, P.; Borchers, L.; Strempel, J.; Stiesch, M.; Hassel, T.; Bach, F. W.; Hübsch, C. Low-Temperature Degradation of Different Zirconia Ceramics for Dental Applications. *Acta Biomater.* **2012**, *8* (3), 1213–1220. https://doi.org/10.1016/J.ACTBIO.2011.11.016.

(30) Indira, K.; Kamachi Mudali, U; Nishimura, T; Rajendran, N. A Review on TiO_2 Nanotubes: Influence of Anodization Parameters, Formation Mechanism, Properties, Corrosion Behavior, and Biomedical Applications. *J. Bio- Tribo-Corrosion 1*. https://doi.org/10.1007/s40735-015-0024-x.

(31) Piconi, C.; Maccauro, G. Zirconia as a Ceramic Biomaterial. *Biomaterials*. 1999. https://doi.org/10.1016/S0142-9612(98)00010-6.

(32) Makushok, Y. E.; Parkhutik, V. P.; Martinez-Duart, J. M.; Albella, J. M. Morphology of Passive Films Formed during Electrochemical Anodization of Materials. *J. Phys. D. Appl. Phys.* **1994**, *27* (3), 661–669. https://doi.org/10.1088/0022-3727/27/3/036.

(33) Lee, W.; Park, S.-J. Porous Anodic Aluminum Oxide: Anodization and Templated Synthesis of Functional Nanostructures. *Chem. Rev.* **2014**, *114* (15), 7487–7556. https://doi.org/10.1021/cr500002z.

(34) Muratore, F.; Baron-Wiechec, A.; Hashimoto, T.; Skeldon, P.; Thompson, G. E. Anodic Zirconia Nanotubes: Composition and Growth Mechanism. *Electrochem. commun.* **2010**, *12* (12), 1727–1730. https://doi.org/10.1016/j.elecom.2010.10.007.

(35) Tsuchiya, H.; MacAk, J. M.; Ghicov, A.; Taveira, L.; Schmuki, P. Self-Organized Porous TiO_2 and ZrO_2 Produced by Anodization. *Corros. Sci.* **2005**. https://doi.org/10.1016/j.corsci.2005.05.041.

(36) Li, W.; Huang, H.; Li, H.; Zhang, W.; Liu, H. Facile Synthesis of Pure Monoclinic and Tetragonal Zirconia Nanoparticles and Their Phase Effects on the Behavior of Supported Molybdena Catalysts for Methanol-Selective Oxidation. https://doi.org/10.1021/la800370r.

(37) Amer, A. W.; Mohamed, S. M.; Hafez, A. M.; Alqaradawi, S. Y.; Aljaber, A. S.; Allam, N. K. Self-Assembled Zirconia Nanotube Arrays: Fabrication Mechanism, Energy Consideration and Optical Activity. *RSC Adv.* **2014**. https://doi.org/10.1039/c4ra05115g.

(38) Jiang, W.; He, J.; Zhong, J.; Lu, J.; Yuan, S.; Liang, B. Preparation and Photocatalytic Performance of ZrO_2 Nanotubes Fabricated with Anodization Process. *Appl. Surf. Sci.* **2014**. https://doi.org/10.1016/j.apsusc.2014.04.047.

(39) Pasikhani, J. V.; Gilani, N.; Pirbazari, A. E. The Effect of the Anodization Voltage on the Geometrical Characteristics and Photocatalytic Activity of TiO_2. *Nano-Structures & Nano-Objects* **2016**, *8*, 7–14. https://doi.org/10.1016/j.nanoso.2016.09.001.

(40) Srimuangmak, K.; Niyomwas, S. Effects of Voltage and Addition of Water on Photocatalytic Activity of TiO_2 Nanotubes Prepared by Anodization Method. *Energy Procedia* **2011**, *9*, 435–439. https://doi.org/10.1016/j.egypro.2011.09.048.

(41) Kapusta-Kotodziej, J.; Syrek, K.; Sulka, G. D. Synthesis and Photoelectrochemical Properties of Anodic Oxide Films on Titanium Formed by Pulse Anodization. *J. Electrochem. Soc.* **2018**, *165* (13), H838–H844. https://doi.org/10.1149/2.0561813jes.

(42) Chernozem, R. V; Surmeneva, M. A.; Surmenev, R. A. Influence of Anodization Time and Voltage

on the Parameters of TiO_2 Nanotubes. *IOP Conf. Ser. Mater. Sci. Eng.* **2016**, *116*, 012025. https://doi.org/10.1088/1757-899X/116/1/012025.

(43) Regonini, D.; Clemens, F. J. Anodized TiO_2 Nanotubes: Effect of Anodizing Time on Film Length, Morphology and Photoelectrochemical Properties. *Mater. Lett.* **2015**, *142*, 97–101. https://doi.org/10.1016/j.matlet.2014.11.145.

(44) Grover, V.; Shukla, R.; Tyagi, A. K. Facile Synthesis of ZrO_2 Powders: Control of Morphology. *Scr. Mater.* **2007**. https://doi.org/10.1016/j.scriptamat.2007.06.053.

(45) Garcia, R.; Martinez, R. V.; Martinez, J. Nano-Chemistry and Scanning Probe Nanolithographies. *Chemical Society Reviews*. 2006. https://doi.org/10.1039/b501599p.

(46) Heiroth, S.; Ghisleni, R.; Lippert, T.; Michler, J.; Wokaun, A. Optical and Mechanical Properties of Amorphous and Crystalline Yttria-Stabilized Zirconia Thin Films Prepared by Pulsed Laser Deposition. *Acta Mater.* **2011**. https://doi.org/10.1016/j.actamat.2010.12.029.

(47) Killian, M. S. Organic Modification of TiO_2 and Other Metal Oxides with SAMs and Proteins - a Surface Analytical Investigation. FAU-Erlangen-Nuremberg, Tech. Fak. (2013), https://opus4.kobv.de/opus4-fau/frontdoor/index/index/year/2013/docId/3720*Tech. Fak.* **2013**.

(48) Hofer, R.; Textor, M.; Spencer, N. D. Alkyl Phosphate Monolayers, Self-Assembled from Aqueous Solution onto Metal Oxide Surfaces. *Langmuir* **2001**. https://doi.org/10.1021/la001756e.

(49) He, L.; Karumuri, A.; Mukhopadhyay, S. M. Wettability Tailoring of Nanotube Carpets: Morphology-Chemistry Synergy for Hydrophobic-Hydrophilic Cycling. *RSC Adv.* **2017**. https://doi.org/10.1039/c7ra02745a.

(50) Chaki, N. K.; Aslam, M.; Sharma, J.; Vijayamohanan, K. *Applications of Self-Assembled Monolayers in Materials Chemistry*; Vol. 113.

(51) Margapoti, E.; Li, J.; Ceylan, Ö.; Seifert, M.; Nisic, F.; Le Anh, T.; Meggendorfer, F.; Dragonetti, C.; Palma, C.-A.; Barth, J. V; Finley E Margapoti, J. J.; Ceylan, Ö.; Seifert, M.; Anh, T. L.; Meggendorfer, F.; Finley, J. J.; Li, J.; Palma, C.; Barth, J. V; Nisic, F.; Dragonetti, C. A 2D Semiconductor-Self-Assembled Monolayer Photoswitchable Diode. **2015**. https://doi.org/10.1002/adma.201405110.

(52) Uhlig's Corrosion Handbook (2nd Ed.). *Aircr. Eng. Aerosp. Technol.* **2000**. https://doi.org/10.1108/aeat.2000.12772dae.001.

(53) Wang, R.; Hashimoto, K.; Fujishima, A.; Chikuni, M.; Kojima, E.; Kitamura, A.; Shimohigoshi, M.; Watanabe, T. Light-Induced Amphiphilic Surfaces [4]. *Nature*. 1997. https://doi.org/10.1038/41233.

(54) Tamura, H.; Mita, K.; Tanaka, A.; Ito, M. Mechanism of Hydroxylation of Metal Oxide Surfaces. *J. Colloid Interface Sci.* **2001**. https://doi.org/10.1006/jcis.2001.7864.

(55) Cai, J.; Chen, Y.; Liu, Y.; Li, S.; Sun, C. Capillary Imbibition and Flow of Wetting Liquid in Irregular Capillaries: A 100-Year Review. *Adv. Colloid Interface Sci.* **2022**, *304*, 102654. https://doi.org/10.1016/j.cis.2022.102654.

(56) Lai, Y.; Huang, J.; Cui, Z.; Ge, M.; Zhang, K.-Q.; Chen, Z.; Chi, L. Recent Advances in TiO_2 -Based Nanostructured Surfaces with Controllable Wettability and Adhesion. *Small* **2016**, *12* (16), 2203–2224. https://doi.org/10.1002/smll.201501837.

(57) Vakamulla Raghu, S. N.; Killian, M. S. Wetting Behavior of Zirconia Nanotubes. *RSC Adv.* **2021**, *11* (47), 29585–29589. https://doi.org/10.1039/D1RA04751E.

(58) Avramescu, M.-L.; Rasmussen, P. E.; Chénier, M.; Gardner, H. D. Influence of PH, Particle Size and Crystal Form on Dissolution Behaviour of Engineered Nanomaterials. *Environ. Sci. Pollut. Res.* **2017**, *24* (2), 1553–1564. https://doi.org/10.1007/s11356-016-7932-2.

(59) Karakoti, A. S.; Tsigkou, O.; Yue, S.; Lee, P. D.; Stevens, M. M.; Jones, J. R.; Seal, S. Rare Earth Oxides as Nanoadditives in 3-D Nanocomposite Scaffolds for Bone Regeneration. *J. Mater. Chem.* **2010**, *20* (40), 8912. https://doi.org/10.1039/c0jm01072c.

(60) Utembe, W.; Potgieter, K.; Stefaniak, A. B.; Gulumian, M. Dissolution and Biodurability: Important Parameters Needed for Risk Assessment of Nanomaterials. *Part. Fibre Toxicol.* **2015**, *12* (1), 11. https://doi.org/10.1186/s12989-015-0088-2.

(61) Balaur, E.; Macak, J. M.; Tsuchiya, H.; Schmuki, P. Wetting Behaviour of Layers of TiO_2 Nanotubes with Different Diameters. *J. Mater. Chem.* **2005**. https://doi.org/10.1039/b509672c.

(62) Nawrocki, J.; Rigney, M.; McCormick, A.; Carr, P. W. Chemistry of Zirconia and Its Use in Chromatography. *J. Chromatogr. A* **1993**, *657* (2), 229–282. https://doi.org/10.1016/0021-9673(93)80284-F.

(63) Trammell, B. C.; Hillmyer, M. A.; Carr, P. W. A Study of the Lewis Acid-Base Interactions of Vinylphosphonic Acid-Modified Polybutadiene-Coated Zirconia. *Anal. Chem.* **2001**, *73* (14), 3323–3331. https://doi.org/10.1021/ac010032k.

(64) Salavati-fard, T.; Vasiliadou, E. S.; Jenness, G. R.; Lobo, R. F.; Caratzoulas, S.; Doren, D. J. Lewis Acid Site and Hydrogen-Bond-Mediated Polarization Synergy in the Catalysis of Diels–Alder Cycloaddition by Band-Gap Transition-Metal Oxides. *ACS Catal.* **2019**, *9* (1), 701–715. https://doi.org/10.1021/acscatal.8b03664.

(65) Komanoya, T.; Nakajima, K.; Kitano, M.; Hara, M. Synergistic Catalysis by Lewis Acid and Base Sites on ZrO_2 for Meerwein–Ponndorf–Verley Reduction. *J. Phys. Chem. C* **2015**, *119* (47), 26540–26546. https://doi.org/10.1021/acs.jpcc.5b08355.

(66) Schreiber, F. Structure and Growth of Self-Assembling Monolayers. *Prog. Surf. Sci.* **2000**. https://doi.org/10.1016/S0079-6816(00)00024-1.

(67) Han, X.; Sun, S.; He, T. Preparation and Photolithography of Self-Assembled Monolayers of 10-Mercaptodecanylphosphonic Acid on Glass Mediated by Zirconium for Protein Patterning. *Colloids Surfaces B Biointerfaces* **2013**, *108*, 66–71. https://doi.org/10.1016/j.colsurfb.2013.02.030.

(68) Smith, R. K.; Lewis, P. A.; Weiss, P. S. Patterning Self-Assembled Monolayers. *Progress in Surface Science*. 2004. https://doi.org/10.1016/j.progsurf.2003.12.001.

(69) Gawalt, E. S.; Avaltroni, M. J.; Koch, N.; Schwartz, J. Self-Assembly and Bonding of Alkanephosphonic Acids on the Native Oxide Surface of Titanium. *Langmuir* **2001**. https://doi.org/10.1021/la010649x.

(70) Magnus, L. Thermodynamics of Self-Assembly. In *Application of Thermodynamics to Biological and Materials Science*; InTech, 2011. https://doi.org/10.5772/13711.

(71) Wei, H.; Huang, K.; Zhang, L.; Ge, B.; Wang, D.; Lang, J.; Ma, J.; Wang, D.; Zhang, S.; Li, Q.; Zhang, R.; Hussain, N.; Lei, M.; Liu, L.-M.; Wu, H. Ice Melting to Release Reactants in Solution Syntheses. *Angew. Chemie Int. Ed.* **2018**, *57* (13), 3354–3359. https://doi.org/10.1002/anie.201711128.

(72) Varga, M. Self-Assembly of Nanobiomaterials. *Fabr. Self-Assembly Nanobiomaterials Appl. Nanobiomaterials* **2016**, 57–90. https://doi.org/10.1016/B978-0-323-41533-0.00003-9.

(73) Mirzajanzadeh, M.; Deshpande, V. S.; Fleck, N. A. Water Rise in a Cellulose Foam: By Capillary or Diffusional Flow? *J. Mech. Phys. Solids* **2019**, *124*, 206–219. https://doi.org/10.1016/j.jmps.2018.10.009.

(74) Nanis, L.; Richards, S. R.; Bockris, J. O. The 11 l Effect in Capillary-Reservoir Diffusion Measurements. *Rev. Sci. Instrum.* **1965**, *36* (5), 673–677. https://doi.org/10.1063/1.1719662.

(75) Hall, K. R.; Eagleton, L. C.; Acrivos, A.; Vermeulen, T. Pore- and Solid-Diffusion Kinetics in Fixed-Bed Adsorption under Constant-Pattern Conditions. *Ind. Eng. Chem. Fundam.* **1966**, *5* (2), 212–223. https://doi.org/10.1021/i160018a011.

(76) Taylor, G. I. Diffusion and Mass Transport in Tubes. *Proc. Phys. Soc. Sect. B* **1954**, *67* (12), 857–869. https://doi.org/10.1088/0370-1301/67/12/301.

(77) De Souza, R. A.; Martin, M. Probing Diffusion Kinetics with Secondary Ion Mass Spectrometry. *MRS Bull.* **2009**, *34* (12), 907–914. https://doi.org/10.1557/mrs2009.212.

(78) Rosei, F. Nanostructured Surfaces: Challenges and Frontiers in Nanotechnology. *J. Phys. Condens. Matter* **2004**, *16* (17), S1373–S1436. https://doi.org/10.1088/0953-8984/16/17/001.

(79) Negrescu, A. M.; Killian, M. S.; Raghu, S. N. V.; Schmuki, P.; Mazare, A.; Cimpean, A. Metal Oxide Nanoparticles: Review of Synthesis, Characterization and Biological Effects. *J. Funct. Biomater.* **2022**, *13* (4), 274. https://doi.org/10.3390/jfb13040274.

(80) Miracle, D. B.; Donaldson, S. L. Introduction to Composites. In *Composites*; ASM International, 2001; pp 3–17. https://doi.org/10.31399/asm.hb.v21.a0003350.

(81) Yay, you found the easter egg! Email. me for your reward before 08.2024.

(82) Rajak, D. K.; Pagar, D. D.; Kumar, R.; Pruncu, C. I. Recent Progress of Reinforcement Materials: A Comprehensive Overview of Composite Materials. *J. Mater. Res. Technol.* **2019**, *8* (6), 6354–6374. https://doi.org/10.1016/j.jmrt.2019.09.068.

(83) Zazpe, R.; Knaut, M.; Sopha, H.; Hromadko, L.; Albert, M.; Prikryl, J.; Gä Rtnerová,Rtnerová, V.; Bartha, J. W.; Macak, J. M. Laboratory of Nanostructures and Nanomaterials, Institute of Physics of the CAS, v.v.i., Na Slovance 2, 182 21 Prague 8. **2016**. https://doi.org/10.1021/acs.langmuir.6b03119.

(84) Chopra, D.; Gulati, K.; Ivanovski, S. Towards Clinical Translation: Optimized Fabrication of Controlled Nanostructures on Implant-Relevant Curved Zirconium Surfaces. *Nanomaterials* **2021**, *11* (4). https://doi.org/10.3390/nano11040868.

(85) Piszczek, P.; Lewandowska, Z.; Radtke, A.; Kozak, W.; Sadowska, B.; Szubka, M.; Talik, E.; Fiori, F. Biocompatibility of Titania Nanotube Coatings Enriched with Silver Nanograins by Chemical Vapor Deposition. https://doi.org/10.3390/nano7090274.

(86) Gent, A.N. and Lin, C. . Model Studies of the Effect of Surface Roughness D T Ic. *J. Adhes.* **1990**,

32(2-3), 113–125.

(87) Lee, K.; Mazare, A.; Schmuki, P. One-Dimensional Titanium Dioxide Nanomaterials: Nanotubes. *Chemical Reviews*. 2014. https://doi.org/10.1021/cr500061m.

(88) Pujari, S. P.; Scheres, L.; Marcelis, A. T. M.; Zuilhof, H. Covalent Surface Modification of Oxide Surfaces. *Angew. Chemie Int. Ed.* **2014**, *53* (25), 6322–6356. https://doi.org/10.1002/anie.201306709.

(89) Taveira, L. V.; Macák, J. M.; Tsuchiya, H.; Dick, L. F. P.; Schmuki, P. Initiation and Growth of Self-Organized TiO_2 Nanotubes Anodically Formed in NH_4F $(NH_4)_2SO_4$ Electrolytes. *J. Electrochem. Soc.* **2005**, *152* (10), B405. https://doi.org/10.1149/1.2008980.

(90) Roy, P.; Berger, S.; Schmuki, P. TiO_2 Nanotubes: Synthesis and Applications. *Angew. Chemie Int. Ed.* **2011**, *50* (13), 2904–2939. https://doi.org/10.1002/anie.201001374.

(91) Minagar, S.; Berndt, C.; Wen, C. Fabrication and Characterization of Nanoporous Niobia, and Nanotubular Tantala, Titania and Zirconia via Anodization. *J. Funct. Biomater.* **2015**, *6* (2), 153–170. https://doi.org/10.3390/jfb6020153.

(92) Berger, S.; Faltenbacher, J.; Bauer, S.; Schmuki, P. Enhanced Self-Ordering of Anodic ZrO_2 Nanotubes in Inorganic and Organic Electrolytes Using Two-Step Anodization. *Phys. Status Solidi - Rapid Res. Lett.* **2008**. https://doi.org/10.1002/pssr.200802019.

(93) Paz Martínez-Viademonte, M.; Abrahami, S. T.; Hack, T.; Burchardt, M.; Terryn, H. A Review on Anodizing of Aerospace Aluminum Alloys for Corrosion Protection. *Coatings* **2020**, *10* (11), 1106. https://doi.org/10.3390/coatings10111106.

(94) Macdonald, D. D. The History of the Point Defect Model for the Passive State: A Brief Review of Film Growth Aspects. *Electrochim. Acta* **2011**, *56* (4), 1761–1772. https://doi.org/10.1016/j.electacta.2010.11.005.

(95) Sulka, G. D. Highly Ordered Anodic Porous Alumina Formation by Self-Organized Anodizing. In *Nanostructured Materials in Electrochemistry*; Wiley-VCH Verlag GmbH & Co. KGaA: Weinheim, Germany; pp 1–116. https://doi.org/10.1002/9783527621507.ch1.

(96) Thompson, G. . Porous Anodic Alumina: Fabrication, Characterization and Applications. *Thin Solid Films* **1997**, *297* (1–2), 192–201. https://doi.org/10.1016/S0040-6090(96)09440-0.

(97) Berger, S.; Jakubka, F.; Schmuki, P. Self-Ordered Hexagonal Nanoporous Hafnium Oxide and Transition to Aligned HfO[Sub 2] Nanotube Layers. *Electrochem. Solid-State Lett.* **2009**, *12* (7), K45. https://doi.org/10.1149/1.3117253.

(98) Ismail, S.; Lockman, Z.; Ahmad, Z. A.; Berenov, A. Formation and Mechanistic Study of Self-Ordering ZrO_2 Nanotubes by Anodic Oxidation. In *Advanced Materials Research*; 2011. https://doi.org/10.4028/www.scientific.net/AMR.173.173.

(99) Kim, D.; Lee, K.; Roy, P.; Birajdar, B. I.; Spiecker, E.; Schmuki, P. Formation of a Non-Thickness-Limited Titanium Dioxide Mesosponge and Its Use in Dye-Sensitized Solar Cells. *Angew. Chemie Int. Ed.* **2009**, *48* (49), 9326–9329. https://doi.org/10.1002/anie.200904455.

(100) Allam, N. K.; Feng, X. J.; Grimes, C. A. Self-Assembled Fabrication of Vertically Oriented Ta_2O_5 Nanotube Arrays, and Membranes Thereof, by One-Step Tantalum Anodization. *Chem. Mater.*

2008, *20* (20), 6477–6481. https://doi.org/10.1021/cm801472y.

(101) Chen, Q.; Xu, D. Large-Scale, Noncurling, and Free-Standing Crystallized TiO_2 Nanotube Arrays for Dye-Sensitized Solar Cells. *J. Phys. Chem. C* **2009**, *113* (15), 6310–6314. https://doi.org/10.1021/jp900336e.

(102) Kant, K.; Losic, D. A Simple Approach for Synthesis of TiO_2 Nanotubes with Through-Hole Morphology. *Phys. status solidi - Rapid Res. Lett.* **2009**, *3* (5), 139–141. https://doi.org/10.1002/pssr.200903087.

(103) Fang, D.; Liu, S.; Luo, Z.; Xiong, C.; Xu, W. Facile Fabrication of Freestanding Through-Hole ZrO_2 Nanotube Membranes via Two-Step Anodization Methods. *Appl. Surf. Sci.* **2012**, *258* (17), 6217–6223. https://doi.org/10.1016/j.apsusc.2012.02.140.

(104) Kanta, A.; Sedev, R.; Ralston, J. The Formation and Stability of Self-Assembled Monolayers of Octadecylphosphonic Acid on Titania. *Colloids Surfaces A Physicochem. Eng. Asp.* **2006**. https://doi.org/10.1016/j.colsurfa.2005.12.057.

(105) Buehler, L. *Cell Membranes*; Garland Science, 2015. https://doi.org/10.1201/9780429258671.

(106) Fang, D.; Luo, Z.; Liu, S.; Zeng, T.; Liu, L.; Xu, J.; Bai, Z.; Xu, W. Photoluminescence Properties and Photocatalytic Activities of Zirconia Nanotube Arrays Fabricated by Anodization. *Opt. Mater. (Amst).* **2013**. https://doi.org/10.1016/j.optmat.2013.03.002.

(107) Lin, J.; Chen, J.; Chen, X. Facile Fabrication of Free-Standing TiO_2 Nanotube Membranes with Both Ends Open via Self-Detaching Anodization. *Electrochem. commun.* **2010**, *12* (8), 1062–1065. https://doi.org/10.1016/j.elecom.2010.05.027.

(108) Wang, D.; Liu, Y.; Yu, B.; Zhou, F.; Liu, W. TiO_2 Nanotubes with Tunable Morphology, Diameter, and Length: Synthesis and Photo-Electrical/Catalytic Performance. *Chem. Mater.* **2009**, *21* (7), 1198–1206. https://doi.org/10.1021/cm802384y.

(109) Çaykara, T.; Sande, M. G.; Azoia, N.; Rodrigues, L. R.; Silva, C. J. Exploring the Potential of Polyethylene Terephthalate in the Design of Antibacterial Surfaces. *Med. Microbiol. Immunol.* **2020**, *209* (3), 363–372. https://doi.org/10.1007/s00430-020-00660-8.

(110) Killian, M. S.; Seiler, S.; Wagener, V.; Hahn, R.; Ebensperger, C.; Meyer, B.; Schmuki, P. Interface Chemistry and Molecular Bonding of Functional Ethoxysilane-Based Self-Assembled Monolayers on Magnesium Surfaces. *ACS Appl. Mater. Interfaces* **2015**. https://doi.org/10.1021/am5075634.

(111) Morimoto, T.; Nagao, M.; Tokuda, F. Relation between the Amounts of Chemisorbed and Physisorbed Water on Metal Oxides. *J. Phys. Chem.* **1969**, *73* (1), 243–248. https://doi.org/10.1021/j100721a039.

(112) Butt, H.-J.; Graf, K.; Kappl, M.; GmbH, W.; KGaA, C. Physics and Chemistry of Interfaces.

(113) Guerrero, G.; Alauzun, J. G.; Granier, M.; Laurencin, D.; Mutin, P. H. Phosphonate Coupling Molecules for the Control of Surface/Interface Properties and the Synthesis of Nanomaterials. *Dalt. Trans.* **2013**, *42* (35), 12569. https://doi.org/10.1039/c3dt51193f.

(114) Helmy, R.; Fadeev, A. Y. Self-Assembled Monolayers Supported on TiO_2 : Comparison of $C_{18}H_{37}SiX_3$ (X = H, Cl, OCH_3), $C_{18}H_{37}Si(CH_3)_2Cl$, and $C_{18}H_{37}PO(OH)_2$. *Langmuir* **2002**, *18* (23), 8924–8928. https://doi.org/10.1021/la0262506.

(115) Chen, X.; Lenhert, S.; Hirtz, M.; Lu, N.; Fuchs, H.; Chi, L. Langmuir–Blodgett Patterning: A Bottom–Up Way To Build Mesostructures over Large Areas. *Acc. Chem. Res.* **2007**, *40* (6), 393–401. https://doi.org/10.1021/ar600019r.

(116) Osvaldo, N.; Oliveira, J. Langmuir-Blodgett Films - Properties and Possible Applications. *Brazilian J. Phys.* **1992**, *22* (2), 60–69.

(117) Etellion, surface coverage adsorption kinetics, (2016).; Https://commons.wikimedia.org/wiki/File:Surface_coverage_plot.gif. No Title.

(118) Randon, J.; Blanc, P.; Paterson, R. Modification of Ceramic Membrane Surfaces Using Phosphoric Acid and Alkyl Phosphonic Acids and Its Effects on Ultrafiltration of BSA Protein. *J. Memb. Sci.* **1995**. https://doi.org/10.1016/0376-7388(94)00183-Y.

(119) Gawalt, E. S.; Lu, G.; Bernasek, S. L.; Schwartz, J. Enhanced Bonding of Alkanephosphonic Acids to Oxidized Titanium Using Surface-Bound Alkoxyzirconium Complex Interfaces. *Langmuir* **1999**. https://doi.org/10.1021/la990906m.

(120) Ahmad, Z.; Rahman, A. M. N. A. A. Plastics in Waveguide Application. In *Encyclopedia of Materials: Plastics and Polymers*; Elsevier, **2022**; pp 295–315. https://doi.org/10.1016/B978-0-12-820352-1.00163-2.

(121) Bhave, G.; Gopal, A.; Hoshino, K.; Zhang, J. X. Microcontact Printing. In *Encyclopedia of Nanotechnology*; Springer Netherlands: Dordrecht, **2015**; pp 1–12. https://doi.org/10.1007/978-94-007-6178-0_337-2.

(122) Vladsinger, Self-assembled monolayer of molecules on a substrate, (2018). https://commons.wikimedia.org/wiki/File:Self-assembled_monolayer.svg.

(123) Ebnesajjad, S. Surface and Material Characterization Techniques. In *Surface Treatment of Materials for Adhesive Bonding*; Elsevier, **2014**; pp 39–75. https://doi.org/10.1016/B978-0-323-26435-8.00004-6.

(124) Killian, M. S.; Gnichwitz, J. F.; Hirsch, A.; Schmuki, P.; Kunze, J. ToF-SIMS and XPS Studies of the Adsorption Characteristics of a Zn-Porphyrin on TiO_2. *Langmuir* **2010**, *26* (5), 3531–3538. https://doi.org/10.1021/la9032139.

(125) Theory and Practice of Contemporary Pharmaceutics; Ghosh, T. K., Jasti, B. R., Eds.; CRC Press, 2021. https://doi.org/10.1201/9780203644478.

(126) Waigh, T. A. *The Physics of Living Processes*; John Wiley & Sons, Ltd: Chichester, UK, 2014. https://doi.org/10.1002/9781118698310.

(127) W.C. Ponor, Electron-matter interaction volume, CC BY-SA 4.0, (2011). https://creativecommons.org/licenses/by-sa/4.0>.

(128) Viacheslav Kazmiruk. *Scanning Electron Microscopy*; Kazmiruk, V., Ed.; InTech, 2012. https://doi.org/10.5772/1973.

(129) Gillen, G.; Bennett, J.; Tarlov, M. J.; Burgess, D. R. F. Molecular Imaging Secondary Ion Mass Spectrometry for the Characterization of Patterned Self-Assembled Monolayers on Silver and Gold. *Anal. Chem.* **1994**, *66* (13), 2170–2174. https://doi.org/10.1021/ac00085a036.

(130) Vickerman, J. C.; Winograd, N. SIMS—A Precursor and Partner to Contemporary Mass

Spectrometry. *Int. J. Mass Spectrom.* **2015**, *377*, 568–579. https://doi.org/10.1016/j.ijms.2014.06.021.

(131) Hofmann, J. P.; Rohnke, M.; Weckhuysen, B. M. Recent Advances in Secondary Ion Mass Spectrometry of Solid Acid Catalysts: Large Zeolite Crystals under Bombardment. *Phys. Chem. Chem. Phys.* **2014**, *16* (12), 5465–5474. https://doi.org/10.1039/C3CP54337D.

(132) Fearn, S. *An Introduction to Time-of-Flight Secondary Ion Mass Spectrometry (ToF-SIMS) and Its Application to Materials Science*; IOP Publishing, **2015**. https://doi.org/10.1088/978-1-6817-4088-1.

(133) Brison, J.; Muramoto, S.; Castner, D. G. ToF-SIMS Depth Profiling of Organic Films: A Comparison between Single-Beam and Dual-Beam Analysis. *J. Phys. Chem. C* **2010**, *114* (12), 5565–5573. https://doi.org/10.1021/jp9066179.

(134) McPhail, D.; Dowsett, M. Dynamic SIMS. In *Surface Analysis– The Principal Techniques*; John Wiley & Sons, Ltd: Chichester, UK; pp 207–268. https://doi.org/10.1002/9780470721582.ch5.

(135) Sultan, U.; Ahmadloo, F.; Cha, G.; Gökcan, B.; Hejazi, S.; Yoo, J.-E.; Nguyen, N. T.; Altomare, M.; Schmuki, P.; Killian, M. S. A High-Field Anodic NiO Nanosponge with Tunable Thickness for Application in p-Type Dye-Sensitized Solar Cells. *ACS Appl. Energy Mater.* **2020**, *3* (8), 7865–7872. https://doi.org/10.1021/acsaem.0c01249.

(136) McLafferty, F. W. Mass Spectrometric Analysis. Molecular Rearrangements. *Anal. Chem.* **1959**, *31* (1), 82–87. https://doi.org/10.1021/ac60145a015.

(137) Shard, A. G.; Spencer, S. J.; Smith, S. A.; Havelund, R.; Gilmore, I. S. The Matrix Effect in Organic Secondary Ion Mass Spectrometry. *Int. J. Mass Spectrom.* **2015**, *377*, 599–609. https://doi.org/10.1016/j.ijms.2014.06.027.

(138) Depth Profile via ToF-SIMS. No Title https://www.nist.gov/programs-projects/secondary-ion-mass-spectrometry-ion-source-development.

(139) Mahoney, C. M. Cluster Secondary Ion Mass Spectrometry of Polymers and Related Materials. *Mass Spectrom. Rev.* **2010**, *29* (2), 247–293. https://doi.org/10.1002/mas.20233.

(140) Hoffmann, F. Kristallformen Und Bravais-Gitter. In *Faszination Kristalle und Symmetrie*; Springer Fachmedien Wiesbaden: Wiesbaden, 2016; pp 33–91. https://doi.org/10.1007/978-3-658-09581-9_2.

(141) Offermann, W.; Vögtle, F. Book Review: Molecular and Crystal Structure Models. A. Walton. *Angew. Chemie Int. Ed. English* **1980**, *19* (3), 229–229. https://doi.org/10.1002/anie.198002292.

(142) J. F. Watts, J. Wolstenholme, An Introduction To Surface Analysis By XPS And AES, e-pdf,(2003).http://202.38.64.11/~mams/escalab/An.Introduction.To.Surface.Analysis.By.XPS.And.AES.pdf.

(143) Ortner, H. M. D. J. O'Connor, B. A. Sexton, R. St. C. Smart (Eds.): Surface Analysis Methods in Materials Science, Vol. 23 Aus Der Reihe: Springer Series in Surface Sciences, Springer Verlag, Berlin, Heidelberg 1992, ISBN 3-540-53611-6, 453 Seiten, Preis: DM 114,-. *Berichte der Bunsengesellschaft für Phys. Chemie* **1992**, *96* (11), 1796–1796. https://doi.org/10.1002/bbpc.19920961161.

(144) Adolphi, B.; Jahne, E.; Busch, G.; Cai, X. Characterization of the Adsorption of w-(Thiophene-3-Yl Alkyl) Phosphonic Acid on Metal Oxides with AR-XPS. In *Analytical and Bioanalytical Chemistry*; 2004. https://doi.org/10.1007/s00216-004-2634-x.

(145) F. O. B. Mawr, Schematic- Optical microscope, Liscnse-CC BY-SA 3.0 (2013). https://en.wikipedia.org/wiki/Optical_microscope#/media/File:Microscope_compound_diagram.png.

(146) Poon, C. Y.; Bhushan, B. Comparison of Surface Roughness Measurements by Stylus Profiler, AFM and Non-Contact Optical Profiler. *Wear* **1995**, *190* (1), 76–88. https://doi.org/10.1016/0043-1648(95)06697-7.

(147) Bakhtazad, A.; Chowdhury, S. An Evaluation of Optical Profilometry Techniques for CMUT Characterization. *Microsyst. Technol.* **2019**, *25* (9), 3627–3642. https://doi.org/10.1007/s00542-019-04377-4.

(148) Bridgman, P. W. Crystal Structure: The Crystalline State . Edited by Sir W. H. Bragg and W. L. Bragg. Vol. I. A General Survey, by W. L. Bragg, Xiv + 352 Pages, 23 × 14.5 Cm, with 186 Figures and 6 Appendices. Published by Macmillan and Company, 60 Fifth Ave., New York C. *Science (80-.).* **1934**, *80* (2074), 290–291. https://doi.org/10.1126/science.80.2074.290.b.

(149) Sherwood, P. M. A. Carbons and Graphites: Surface Properties Of. In *Encyclopedia of Materials: Science and Technology*; Elsevier, 2001; pp 985–995. https://doi.org/10.1016/B0-08-043152-6/00183-2.

(150) Seibt, S.; Ryan, T. Microfluidics for Time-Resolved Small-Angle X-Ray Scattering. In *Advances in Microfluidics and Nanofluids*; IntechOpen, 2021. https://doi.org/10.5772/intechopen.95059.

(151) Cassie, A. B. D.; Baxter, S. Wettability of Porous Surfaces. *Trans. Faraday Soc.* **1944**. https://doi.org/10.1039/tf9444000546.

(152) Huhtamäki, T.; Tian, X.; Korhonen, J. T.; Ras, R. H. A. Surface-Wetting Characterization Using Contact-Angle Measurements. *Nat. Protoc.* **2018**, *13* (7), 1521–1538. https://doi.org/10.1038/s41596-018-0003-z.

(153) Wenzel, R. N. Resistance of Solid Surfaces to Wetting by Water. *Ind. Eng. Chem.* **1936**. https://doi.org/10.1021/ie50320a024.

(154) *Contact Angle, Wettability and Adhesion, Volume 6*; Mittal, K. L., Ed.; CRC Press, 2009. https://doi.org/10.1201/b12247.

(155) David, R.; Neumann, A. W. Energy Barriers between the Cassie and Wenzel States on Random, Superhydrophobic Surfaces. *Colloids Surfaces A Physicochem. Eng. Asp.* **2013**. https://doi.org/10.1016/j.colsurfa.2013.02.049.

(156) Shafrin, E. G.; Zisman, W. A. CONSTITUTIVE RELATIONS IN THE WETTING OF LOW ENERGY SURFACES AND THE THEORY OF THE RETRACTION METHOD OF PREPARING MONOLAYERS 1. *J. Phys. Chem.* **1960**, *64* (5), 519–524. https://doi.org/10.1021/j100834a002.

(157) Jothi Prakash, C. G.; Prasanth, R. Approaches to Design a Surface with Tunable Wettability: A Review on Surface Properties. *J. Mater. Sci.* **2021**, *56* (1), 108–135. https://doi.org/10.1007/s10853-020-05116-1.

{158} Swinehart, D. F. The Beer-Lambert Law. *J. Chem. Educ.* **1962**, *39* (7), 333. https://doi.org/10.1021/ed039p333.

{159} Braga, M. S.; Gomes, O. F.; Jaimes, R. F. V. V.; Braga, E. R.; Borysow, W.; Salcedo, W. J. Multispectral Colorimetric Portable System for Detecting Metal Ions in Liquid Media. In *2019 4th International Symposium on Instrumentation Systems, Circuits and Transducers (INSCIT)*; IEEE, 2019; pp 1–6. https://doi.org/10.1109/INSCIT.2019.8868861.

{160} UCalgary. UV-Vis-Basic Principles. (2010), https://www.chem.ucalgary.ca/courses/353/Carey5th/Ch13/ch13-uvvis.html.

{161} UV-VIS Spektroskopie. In *Laborpraxis Band 4: Analytische Methoden*; Springer International Publishing: Cham, 2017; pp 125–156. https://doi.org/10.1007/978-3-0348-0972-6_11.

{162} Lenard, J. G. Tribology. In *Primer on Flat Rolling*; Elsevier, 2014; pp 193–266. https://doi.org/10.1016/B978-0-08-099418-5.00009-3.

{163} Leroux, P. Scratch and Wear Evaluation Prepared by Duanjie Li , PhD & Andrea Herrmann. **2015**, No. May. https://doi.org/10.13140/RG.2.1.3283.8562.

{164} Feng, B. Tribology Behavior on Scratch Tests: Effects of Yield Strength. *Friction* **2017**, *5* (1), 108–114. https://doi.org/10.1007/s40544-017-0148-8.

{165} Barnes, D.; Johnson, S.; Snell, R.; Best, S. Using Scratch Testing to Measure the Adhesion Strength of Calcium Phosphate Coatings Applied to Poly(Carbonate Urethane) Substrates. *J. Mech. Behav. Biomed. Mater.* **2012**, *6*, 128–138. https://doi.org/10.1016/j.jmbbm.2011.10.010.

{166} Wang, K.; Liu, G.; Hoivik, N.; Johannessen, E.; Jakobsen, H. Electrochemical Engineering of Hollow Nanoarchitectures: Pulse/Step Anodization (Si, Al, Ti) and Their Applications. *Chem. Soc. Rev.* **2014**, *43* (5), 1476–1500. https://doi.org/10.1039/C3CS60150A.

{167} Zalnezhad, E.; Hamouda, A. M. S.; Jaworski, J.; Kim, Y. Do. From Zirconium Nanograins to Zirconia Nanoneedles OPEN. *Nat. Publ. Gr.* **2016**. https://doi.org/10.1038/srep33282.

{168} Kummer, K. M.; Taylor, E. N.; Durmas, N. G.; Tarquinio, K. M.; Ercan, B.; Webster, T. J. Effects of Different Sterilization Techniques and Varying Anodized TiO_2 Nanotube Dimensions on Bacteria Growth. *J. Biomed. Mater. Res. - Part B Appl. Biomater.* **2013**. https://doi.org/10.1002/jbm.b.32870.